ELECTRIC FEED SYSTEMS FOR LIQUID PROPELLANT ROCKET ENGINES.

Pablo Rachov, Hernán Tacca y Diego Lentini.

ELECTRIC FEED SYSTEMS FOR LIQUID PROPELLANT ROCKET ENGINES

Pablo RACHOV

LABORATORIO DE CONTROL DE ACCIONAMIENTOS, TRACCIÓN Y POTENCIA (LABCATYP)
Departamento de Electrónica
Facultad de Ingeniería
UNIVERSIDAD DE BUENOS AIRES

Directors:

Prof. Hernán TACCA, University of Buenos Aires, Argentina

Prof. Diego LENTINI, University of Roma "La Sapienza", Italy

REPORT Nº 1

COMPARISON OF LIQUID PROPELLANT ROCKET ENGINE FEED SYSTEMS

Pablo RACHOV

LABORATORIO DE CONTROL DE ACCIONAMIENTOS, TRACCIÓN Y POTENCIA
(LABCATYP)
Departamento de Electrónica
Facultad de Ingeniería
UNIVERSIDAD DE BUENOS AIRES

Directors:
>   Prof. Hernán TACCA, University of Buenos Aires, Argentine
>   Prof. Diego LENTINI, University of Roma "La Sapienza", Italy

Buenos Aires, December 6th, 2010.

<u>CONTENTS</u>

I. INTRODUCTION

Since several decades the systems to impel propellants inside the combustion chamber are based on the employment of turbo-pumps or a pressurized gas. However, in virtue of the technological advances of the last 10 years in matter of electric engines and batteries, is possible to think about the viability of development electric-pumps feed systems.

One of the most difficult requirements to achieve when designing a rocket engine is to keep the weight as low as possible, because generally the payload is a small fraction of the total weight. For this reason, this requirement turns out to be a basic parameter to compare the three systems.

Beginning with a brief description of the parts that compose each feed system, the conceptual diagrams of each system are presented in figure 1.
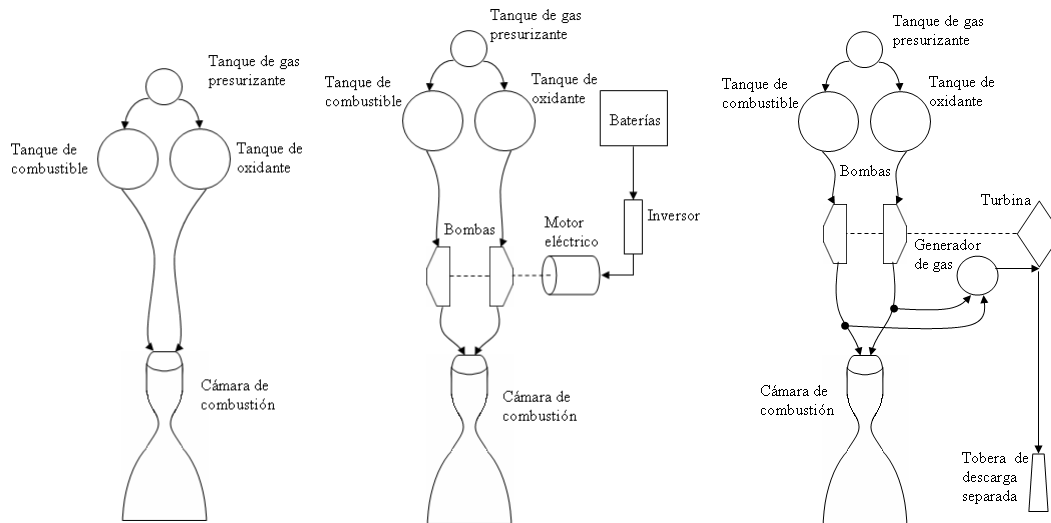

Figure 1: Schemes of the 3 feed systems to analyzing.

The figure 1 shows that all the three systems have fuel and oxidizer tanks, and also a third tank containing a pressurized gas.

In the first system, that gas makes the work of displacing the propellant's masses inside the combustion chamber. Hereby, the stored gas in the above mentioned tank is under high pressure with typical values ranging from 6.9MPa to 69MPa [1].

For the other two systems, the pumps make the work of displacing the propellants while the gas function is only to prevent cavitation in the pumps. Therefore, the gas mass necessary in such systems is much lower.

The two pumps systems differ from each other by the pump drive method. In the turbo-pump system, the device that provides power to the pumps is a gas turbine (sometimes one by pump).

The available methods to drive the turbine can be found detailed in [2]. Here the gas generator method will be evaluated. Such a gas generator takes a fraction of the tank stored propellants and, by a separated combustion process (usually fuel rich), provides the gas that drives the turbine. The gas generator is fed usually with propellants that are taken from the feed lines located after the pumps to improve the efficiency. This requires the use of some start method, being usual to use a solid fuel cartridge.

In the case here depicted, the turbine gas discharge is done through a separated nozzle direct on the atmosphere (which is named as open cycle turbopump system).

Otherwise, the electric pump system is driven by a brushless synchronous electric motor (also can have one by each pump). Each motor is fed by an inverter which converts the direct

current from the battery to alternative current with a frequency suitable enough to drive the electric motor at the required speed.

II.   ANALYTICAL DEVELOPMENT

To realize comparisons it is necessary to estimate the total mass of each feed system described in the previous section. To simplify this analysis, only the mass of the principal components of each system will be considered. That is, the masses of the plumbing system, the mounting system, the valves and the electronics controls will be assumed as negligible.

Hence, giving denominations to the diverse masses of the components of each feed system yields:

m_{tp}: total mass of the turbo-pump feed system.
m_{ep}: total mass of the electric-pump feed system.
m_{pg}: total mass of the pressurized-gas feed system.
m_g: pressurizing gas mass.
m_{tg}: pressurizing gas propellant tank mass.
m_{to}: oxidizer tank mass.
m_{tf}: fuel tank mass.
m_{pu}: pumps mass.
m_{tu}: turbine mass.
m_{gg}: gas generator mass.
m_{ee}: electric engine mass.
m_{inv}: inverters mass.
m_{bat}: batteries mass.
m_o: oxidizer mass.
m_f: fuel mass.
$m_p = m_o + m_f$: propellant total mass.
m_{ptu}: turbine driven propellant mass.

Thereby, and taking into account the figure 1 schemes, the total masses of each feed system respond to the following equations:

$$m_{tp} = m_g + m_{tg} + m_{to} + m_{tf} + m_{pu} + m_{tu} + m_{gg} + m_{ptu}$$

$$m_{ep} = m_g + m_{tg} + m_{to} + m_{tf} + m_{pu} + m_{ee} + m_{inv} + m_{bat}$$

$$m_{pg} = m_g + m_{tg} + m_{to} + m_{tf}$$

The comparisons presented in this report, deal with engines primarily intended to be applied in vehicles operating far above of the sea level, where the atmospheric pressure is very low. Therefore, in the following calculations the atmospheric pressure will be neglected.

2.1. Pressurizing gas mass

From the analysis done in [1], about the propellant tank pressurization, using the energy conservation principle, the next expression can be obtained:

$$m_g = \frac{p_p V_p}{R_g T_0} \left(\frac{\gamma_g}{1 - \dfrac{p_g}{p_o}} \right) \tag{2.1.1}$$

where, m_g: Pressurizing gas mass (kg).
p_p: Propellant tank instantaneous pressure (Pa).
p_g: Gas tank instantaneous pressure (Pa).
p_o: Pressurizing gas initial pressure (Pa).
T_o: Pressurizing gas initial temperature (K).
V_p: Propellant volume (m^3).
R_g: Pressurizing gas constant (J/kgK).
γ_g: Pressurizing gas specific heat ratio.

To foresee the scope of this analysis, the assumptions that allow deriving the previous equation will be enunciated:

- Adiabatic process.
- Ideal gas.
- Negligible initial mass inside the pipes and propellant tanks.

It will be assumed that the instantaneous pressure in the gas and propellants tanks is the same, that is, there are no losses in the pipes connecting them. Also, it is interesting to refer all feed system pressures to the combustion chamber pressure, which is a project parameter [3]. Based on this criterion, the following constant is defined:

$$k_p = \frac{p_p}{p_C} = \frac{p_g}{p_C} \qquad (2.1.2)$$

where p_C is the combustión chamber pressure (Pa).

Not all the volume of a propellant tank is occupied by this one. A small part is occupied by gas and that portion of the total volume of the tank is denominated *ullage*. This is the necessary space to allow the propellant thermal expansion, the accumulation of gases that were originally dissolved in the propellants and to contain the reaction products of the slow reactions, which occurs during storage [1]. To assess this quantity in the analysis, an additional constant relating both volumes will be introduced, also assuming that it is the same for both tanks:

$$k_u = \frac{V_{tf}}{V_f} = \frac{V_{to}}{V_o} \qquad (2.1.3)$$

where, V_{tf}: Fuel tank volume (m^3).
V_{to}: Oxidizer tank volume (m^3).
V_f: Fuel volume (m^3).
V_o: Oxidizer volume (m^3).

Besides, the gas constant should be expressed in terms of their molar mass, thus:

$$R_g = \frac{R_u}{M_g} \qquad (2.1.4)$$

where, R_u: Universal gas constant (8314.41J/kmolK).
M_g: Pressurizing gas molar mass (kg/kmol).

Furthermore, volume and mass will be related through the following expressions:

$$O/F = \frac{\overset{*}{m}_o}{\overset{*}{m}_f} = \frac{\rho_o \overset{*}{v}_o}{\rho_f \overset{*}{v}_f} \tag{2.1.5}$$

$$\overset{*}{v}_o = \frac{O/F}{\rho_o}\left(\frac{1}{1+O/F}\right)\overset{*}{m}_p = \alpha_o \overset{*}{m}_p \tag{2.1.6}$$

$$\overset{*}{v}_f = \frac{1}{\rho_f}\left(\frac{1}{1+O/F}\right)\overset{*}{m}_p = \alpha_f \overset{*}{m}_p \tag{2.1.7}$$

where, $\overset{*}{v}_o \,\&\, v_f$: Oxidizer or fuel volumetric flow as designated with "o" or "f" (m^3/s).

$\overset{*}{m}_o \,\&\, \overset{*}{m}_f$: Oxidizer or fuel mass flow as designated with "o" or "f" (kg/s).

$\rho_o \,\&\, \rho_f$: Oxidizer or fuel density (kg/m^3).

O/F: Propellant mixture ratio.

m_p: Propellant total mass (kg).

Note that once defined the α_o and α_f constants is possible to write:

$$\alpha_o + \alpha_f = \alpha \tag{2.1.8}$$

$$V_p = V_o + V_f = \alpha_o m_p + \alpha_f m_p = \alpha\, m_p \tag{2.1.9}$$

Finally, a safety constant k_g is defined, which provides a margin to account the gas mass that, at the end of the operation cycle, will stay inside the gas tank and in the feed system pipes. Thus, the equation 2.1.1 becomes:

$$m_g = k_g k_p\, k_u\, \gamma_g\, \alpha\, \frac{M_g}{R_u T_0}\left(\frac{m_p\, p_C}{1 - k_p\dfrac{p_C}{p_o}}\right) \tag{2.1.10}$$

2.2. Tanks mass

The tanks' masses can be estimated multiplying each tank volume by its constituting material density. Thus, the next expression is obtained:

$$m_t = \rho_t S_t\, e_t \tag{2.2.1}$$

donde, m_t: Tank mass (kg).

S_t: Tank surface (m^2).

e_t: Tank wall thickness (m).

ρ_t: Tank material density (kg/m^3).

Using the *Laplace's Law* is possible to relate the wall stress of a body, under the effect of a determined pressure, whit their physical dimensions. In particular, if a spherical tank is considered, the next relationship is derived:

$$\Delta p = \frac{2T}{r} \tag{2.2.2}$$

where, Δp: Sphere outside to inside pressure fall.
   T: Sphere wall stress.
   r: Sphere radius

In turn, the maximum stress that the wall supports is proportional to their thickness. The maximum allowable stress for a rigid material can be obtained using the UTS parameter (Ultimate Tensile Strength) which is temperature dependent. Thus:

$$T_{MAX} = \sigma\, e \tag{2.2.3}$$

where, T_{MAX}: Maximum allowable material stress.
   σ: UTS (Pa).
   e: material thickness (m).

Assuming a spherical tank, the next expressions turn out:

$$V_t = \frac{4}{3}\pi\, r_t^3 \tag{2.2.4}$$

$$S_t = 4\pi\, r_t^2 \tag{2.2.5}$$

2.2.1. Pressurizing gas tank mass

Now this mass estimation can be faced, assuming that the tank volume is completely filled by the gas:

$$V_t = V_g = \frac{m_g R_u T_o}{p_o M_g} \tag{2.2.6}$$

Then, combining the expressions 2.2.2, 2.2.3, 2.2.4 and 2.2.6:

$$e_t = \frac{p_o}{2\sigma_t}\left(\frac{3 m_g R_u T_o}{4\pi p_o M_g}\right)^{1/3} \tag{2.2.7}$$

Finally, an equation to estimate the mass of the spherical tank can be obtained combining the expressions 2.1.10, 2.2.1, 2.2.5 y 2.2.7:

$$m_{tg} = \frac{3\rho_t}{2\sigma_t} k_{tg}\, k_g k_p\, k_u\, \gamma_g\, \alpha \left(\frac{m_p\, p_C}{1 - k_p \dfrac{p_C}{p_o}} \right) \tag{2.2.8}$$

where k_{tg} is a constant that provides a safety margin to the estimated mass.

2.2.2. Propellant tank mass

In a similar way, an expression can be developed for these tanks, combining the expressions 2.2.1 to 2.2.5:

$$m_{tp} = \rho_{tp} 4\pi \left(\frac{3V_{tp}}{4\pi}\right)^{2/3} \frac{p_{tp}}{2\sigma_{tp}} \left(\frac{3V_{tp}}{4\pi}\right)^{1/3} \tag{2.2.9}$$

This expression is combined with 2.1.2 and 2.1.3 to express it in function of the adequate parameter to make the comparison:

$$m_{tp} = \frac{3\rho_{tp}}{2\sigma_{tp}} k_{tp} k_p k_u \alpha_p m_p p_C \tag{2.2.10}$$

where k_{tp} is a constant that provides a safety margin with respect of the estimated mass.

The suffixes "p" must be replaced by *"o"* or *"f"* as correspond to the oxidizer or fuel tank, except in case of k_p and m_p variables.
In the case of the propellant tanks of the systems that use pumps, the tanks walls are thin. The thickness estimated by the Laplace's Law application, might be too thin to withstand the loads that could appear during the vehicle acceleration [3]. Therefore, a minimum thickness is established as a limit from which the previous equations are valid. In the case where the thickness estimated by the Laplace's Law, be less than the minimum established, the estimation must be made directly using the following expression:

$$m_{tp} = (4\pi)^{1/3} \rho_{tp} \left(3k_u \alpha_p m_p\right)^{2/3} e_{min} \tag{2.2.11}$$

being e_{min} the minimum thickness of the propellant tank wall (m).

2.3. Propellant pumps mass

To estimate the pump mass, one should start remembering that the pumping power is proportional to the propellant volume and the pressure raise in the pump, while it is inversely proportional to the operation time [4]. This means:

$$P_{opu} = \Delta p_{pu} \frac{V_p}{t_b} \tag{2.3.1}$$

where, P_{opu}: Pumping power (W)
Δp_{pu}: Pump imposed pressure raise (Pa).
t_b: Engine burning time (s)

In turn, watching the figure 1 schemes, for the three systems the pressure raise can be write in this way:

$$\Delta p_{pu} = p_C + \Delta p_i - p_p \tag{2.3.2}$$

where Δp_i is the pressure fall in the injector (Pa).

At this point, is convenient to refer the above defined pressure fall, to the combustion chamber pressure. For this purpose the following constant is introduced:

$$k_{pi} = \frac{\Delta p_i}{p_C}$$

(2.3.3)

Now, a pump merit factor named *power density*, is defined by relating the pumping power with the total mass:

$$\delta_{pu} = \frac{P_{opu}}{m_{pu}}$$

(2.3.4)

where, δ_{pu}: Propellant power density (W/kg).
m_{pu}: Propellant mass (kg).

From equations 2.3.1 to 2.3.4 and 2.1.10 two expressions are derived for the fuel and oxidizer pumps masses, both valid for the electric-pump and the turbo-pump systems:

$$m_{puf} = (1 + k_{pi} - k_p)\frac{\alpha_f p_C m_p}{\delta_{puf} t_b}$$

(2.3.5)

$$m_{puo} = (1 + k_{pi} - k_p)\frac{\alpha_o p_C m_p}{\delta_{puo} t_b}$$

(2.3.6)

2.4. Electric engine mass

It is begun by relating the inlet pump power (taken from the electric engine) with the output pumping power. This is necessary because the pumps dissipates energy as heat, due to the frictions on their moving parts, and not all the electric motor power is transformed in pumping power. These losses are taken into acount defining a merit factor called *efficiency*, as:

$$\eta_{pu} = \frac{P_{opu}}{P_{oee}}$$

(2.4.1)

where, P_{oee}: Electric engine mechanical output power (W).
η_{pu}: Propellant pump efficiency.

The power to be supplied by the electrical motor will be the sum of the power that each pump requires to do their work. Furthermore, a motor merit factor (similar to the one defined for the pumps) is introduced for convenience, the motor power density:

$$\delta_{ee} = \frac{P_{oee}}{m_{ee}}$$

(2.4.2)

With the prior expressions the engine mass can be obtained:

$$m_{ee} = \left(\frac{P_{opuf}}{\eta_{puf}} + \frac{P_{opuo}}{\eta_{puo}} \right) \frac{1}{\delta_{ee}} \tag{2.4.3}$$

Replacing the powers, with the help of preceding equations, finally yields:

$$m_{ee} = (1 + k_{pi} - k_p) \frac{p_C m_p}{t_b} \left(\frac{\alpha_f}{\eta_{puf}} + \frac{\alpha_o}{\eta_{puo}} \right) \frac{1}{\delta_{ee}} \tag{2.4.4}$$

It is necessary to denote that a similar expression can be obtained by the same procedure, considering a system where each pump is driven by individual motors.

2.5. Inverter mass

As above, beginning with defining the electric motor efficiency, with the same approach applied for the pumps case, will allow relating the inverter output power with the power consumed by the pumps:

$$\eta_{ee} = \frac{P_{oee}}{P_{oinv}} \tag{2.5.1}$$

In the same way, the inverter power density relates its output power with its mass:

$$\delta_{inv} = \frac{P_{oinv}}{m_{inv}} \tag{2.5.2}$$

In this way, from the two above equations, from 2.4.1 and with the same arguments that in the preceding paragraph the inverter mass is estimated in the following way:

$$m_{inv} = (1 + k_{pi} - k_p) \frac{p_C m_p}{t_b} \left(\frac{\alpha_f}{\eta_{puf}} + \frac{\alpha_o}{\eta_{puo}} \right) \frac{1}{\eta_{ee} \delta_{inv}} \tag{2.5.3}$$

2.6. Batteries mass

The batteries are limited in both their energy and power capacity; therefore, the mass must be estimated accordingly with the most restricting factor. Then, two batteries merit factors are defined:

$$\delta_{bap} = \frac{P_{bat}}{m_{ba}} \tag{2.6.1}$$

$$\delta_{baw} = \frac{t_b P_{bat}}{m_{ba}} \tag{2.6.2}$$

where, δ_{bap}: Batteries power density (W/kg).
δ_{baw}: Batteries energy density (J/kg).

According to the previously exposed, the batteries mass must be estimated with both factors, and it must be chosen as best estimator the one yielding the greatest value. That is why the mass can be determined with the next equation set:

$$m_{bap} = (1 + k_{pi} - k_p) \frac{p_C m_p}{t_b} \left(\frac{\alpha_f}{\eta_{puf}} + \frac{\alpha_o}{\eta_{puo}} \right) \frac{k_b}{\eta_{ee} \eta_{inv} \delta_{bap}} \tag{2.6.3}$$

$$m_{baw} = (1 + k_{pi} - k_p) p_C m_p \left(\frac{\alpha_f}{\eta_{puf}} + \frac{\alpha_o}{\eta_{puo}} \right) \frac{k_b}{\eta_{ee} \eta_{inv} \delta_{baw}} \tag{2.6.4}$$

$$m_{ba} = \max(m_{bap}, m_{baw}) \tag{2.6.5}$$

where k_b is a safety factor to consider during the system sizing.

2.7. Gas generator mass

The parameters derived from combustion chamber design approaches usually result too small, because the combustion characteristics inside a gas generator (GG) are quite different [5]. To get a good volume estimation the guidelines proposed in [5] were followed. A GG with spherical shape was adopted and the *stay time* method was used. The GG chamber volume was estimated using the next expression:

$$V_{gg} = \frac{t_s m_{ptu}}{t_b \rho_{gg}} \tag{2.7.1}$$

where, t_s: Stay time (s).
m_{ptu}: GG propellant burning mass (kg).
ρ_{gg}: GG exhaut gases density (kg/m³).
V_{gg}: GG chamber volume (m³).

From the obtained volume and accepting a spherical GG, their surface can be calculated. In addition, utilizing the Laplace's Law is possible to calculate the GG wall thickness. The formulas to do those calculations are presented below:

$$V_{gg} = \frac{4}{3} \pi r_{gg}^3 \tag{2.7.2}$$

$$S_{gg} = 4\pi r_{gg}^2 \tag{2.7.3}$$

$$e_{gg} = k_{gg} \frac{p_{gg} r_{gg}}{2\sigma_{gg}} \tag{2.7.4}$$

where, S_{gg}: GG chamber surface (m²).
r_{gg}: GG chamber radius (m).
e_{gg}: GG chamber wall thickness (m).
k_{gg}: GG chamber wall thickness safety factor.
p_{gg}: GG chamber pressure (Pa).
σ_{gg}: GG chamber wall material UTS (Pa).

Finally, combining the above expressions with 2.2.1 the gas generator mass can be obtained:

$$m_{gg} = \frac{\rho_{tgg}}{2\sigma_{gg}} k_{gg}\, p_{gg}\, r_{gg}\, 4\pi \left(\frac{3V_{gg}}{4\pi} \right)^{2/3} \tag{2.7.5}$$

where ρ_{tgg} is the gas generador wall material density (kg/m³).

2.8. Turbine mass

To estimate this mass, it is followed the same argumentation as for the electric motor, changing only for the right values. So, the final expression becomes:

$$m_{tu} = (1 + k_{pi} - k_p) \frac{p_C m_p}{t_b} \left(\frac{\alpha_f}{\eta_{puf}} + \frac{\alpha_o}{\eta_{puo}} \right) \frac{1}{\delta_{tu}} \tag{2.8.1}$$

where δ_{tu} is the turbine power density (W/kg).

As for the electric motor case, a similar expression can be obtained in the case when separated turbines for each pump are considered.

2.9. Propellant mass consumed by the turbine

The propellant burned by the gas generator is used to drive the turbine, and consequently, it must be included in the estimation of the turbo-pump total mass.

The pump power can be related to the one required by the turbine, through the pump and turbine efficiencies, as shown in the following expressions:

$$\eta_{pu} = \frac{P_{opu}}{P_{otu}} \tag{2.9.1}$$

$$\eta_{tu} = \frac{P_{otu}}{P_{itu}} \tag{2.9.2}$$

where, η_{tu}: Turbine efficiency.
P_{itu}: Turbine inlet power (W).
P_{otu}: Turbine outlet power (W).

As the power consumed by the turbine is due to the thermal expansion of the GG gases inside the turbine, the following expression may be proposed:

$$P_{itu} = \frac{m_{ptu}}{2 t_b} v_{gg}^2 \tag{2.9.3}$$

being v_{gg} the velocity of the gases that impels the turbine (m/s).

Assuming an isentropic gas expansion inside the turbine, the velocity of the gases passing through can be expressed as:

$$v_{gg}^2 = \frac{2\gamma_{gg}}{\gamma_{gg}-1} R_{gg} T_{itu} \left(1 - \left(\frac{p_{dtu}}{p_{itu}} \right)^{\frac{\gamma_{gg}-1}{\gamma_{gg}}} \right) \tag{2.9.4}$$

where, R_{gg}: Turbine drive gas constant (J/kgK).

γ_{gg}: Turbine drive gas specific heat ratio.

T_{itu}: Turbine drive gas temperature (K).

p_{dtu}: Turbine discharge pressure (Pa).

p_{itu}: Turbine inlet pressure (Pa).

Thus, from equations 2.9.2 to 2.9.4 and 2.1.4, the required propellant pump power can be found as function of the gas generator hot gas parameters (This expression can be verified both in [1] and [2]):

$$P_{otu} = \eta_{tu} \frac{m_{ptu}}{t_b} \frac{\gamma_{gg}}{(\gamma_{gg}-1)} \frac{R_u}{M_{gg}} T_{itu} \left(1 - \left(\frac{p_{dtu}}{p_{itu}} \right)^{\frac{\gamma_{gg}-1}{\gamma_{gg}}} \right) \tag{2.9.5}$$

being, M_{gg} the turbine impels gasses molar mass (kg/kmol).

Finally, the propellant total mass that impels the turbine can be estimated combining the previous expression with 2.9.1 and 2.3.1, giving:

$$m_{ptu} = (1 + k_{pi} - k_p) \frac{p_C m_p}{\eta_{tu}} \left(\frac{\alpha_f}{\eta_{puf}} + \frac{\alpha_o}{\eta_{puo}} \right) \frac{M_{gg}(\gamma_{gg}-1)}{R_u \gamma_{gg}} \left(T_{itu} \left(1 - \left(\frac{p_{dtu}}{p_{itu}} \right)^{\frac{\gamma_{gg}-1}{\gamma_{gg}}} \right) \right)^{-1} \tag{2.9.6}$$

III. DATA ESTIMATION

To trace the results curves it is necessary to assume some data values. In this section the methods and the sources of such estimations are detailed.

3.1. Combustion parameters

First, a propellant combination for the rocket engine is adopted. In this case, the comparisons will be performed using:

- Fuel: Mono-methyl Hydrazine (MMH)
- Oxidizer: Nitrogen Tetroxide (NTO)

From which the following data are transcribed [2]:

Table 1: Characteristics of chosen propellants.			
Propellant	Composition	Density [kg/m³]	Material compatibility
MMH	CH_3NH-NH_2	878	Al, SS, Teflon, Kel-F, Polyethylene
NTO	N_2O_4	1440	Al, SS, Ni, Teflon

For each calculation routine, it will be necessary to adopt a combustion chamber pressure value and a propellants mixture ratio value. With this parameters established, both the specific heat ratio and the molar mass of the combustion gasses can be estimated from the data presented in [2].

3.2. Pressurizing gas

Helium is chosen as pressurizing gas and the necessary data are obtained from [3]:

Table 2: Characteristics of the pressurizing gas.

Gas	Temperature [K]	Specific heat ratio	Molar Mass [kg/kmol]
Helium	288.15	1.667	4.0026

The gas is initially pressurized (unless the calculation routine suggests another thing) to:

$$p_o = 200 \, Bar$$

3.3. Propellants and gas tanks

The propellant tanks are pressurized to a higher or lower pressure depending on the employed feed system. In that way, is convenient to number the systems as follows:

1. Pressure-gas feed system.
2. Electric-pump feed system.
3. Turbo-pump feed system.

It is assumed that both fuel and oxidizer pressures are the same.

3.4. Propellant pumps

From the mass estimation done in section 2.3 it is evident that two parameters are necessary: the pump power density and the pump efficiency. It is assumed identical fuel and oxidizer pumps. In this way, the following values are adopted for the parameters of the two propellant pumps [14]:

$$\delta_{pf} = \delta_{po} = 40 \, {kW}/{kg} \qquad \eta_{pf} = \eta_{po} = 0.8$$

3.5. Turbine

It is assumed that a single one-stage impulse turbine will be employed. The inlet gas temperature should not be too higher to avoid complicating the turbine blades design. However, it must be as higher as possible to increase the turbine efficiency. Depending on the material from the blades are made the maximum temperature should vary between 850K and 900K (Stated that no exotic alloys will be employed). So, the following optimistic limit is adopted:

$$T_{itu} = 900^\circ K$$

The turbine inlet gases are to a very similar pressure to the one inside the gas generator. To make and optimistic estimation, it will be neglected any pressure fall that can occur in the heat exchanger and in the piping sections between the turbine and the gas generator. In such a way:

$$p_{itu} = p_{gg}$$

The ratio between the inlet and outlet turbine gas pressure affects its efficiency. A higher value of this ratio is desirable but, however, very high values can cause pressure distribution problems in other parts of the engine [2].

It will be assumed that the rocket engine is vacuum operated, because this assumption was adopted for the other two feed systems, and identical operation conditions are required in order to make valid comparisons between the three systems. In consequence, an optimistic value of 20 is adopted for such ratio, taking into account that this is an open cycle engine, and thereby, the turbine discharge pressure is defined as:

$$p_{dtu} = \frac{p_{itu}}{20}$$

An optimistic value is taken for the turbine efficiency according to the recommended values in the references [1] and [2] for an impulse turbine

$$\eta_{tu} = 0.7$$

Finally, the turbine power density is estimated from [14] as:

$$\delta_{tu} = 20\,{kW}\!\big/\!{kg}$$

3.6. Gas generator

With the objective of maximizing the efficiency, a chamber pressure as higher as possible is preferable. As the gas generator is fed from the propellants pumps, the same pressure than the one at the main combustion chamber will be adopted (which implies that the injector pressure fall in both combustion chambers will be the same), that is:

$$p_{gg} = p_C$$

In this case, the gas generator will work with the same propellants as the main engine. A strongly fuel rich mixture is required to ensure a low combustion temperature, thus eliminating the use of some type of cooling system and, at the same time, limiting the turbine blade erosion [1]. So, it is adopted:

$$O/F_{gg} = 0.01$$

From the above parameters, the gas generator molar mass, the specific heat ratio and the gas density can be estimated.

Finally, the stay time, for a gas generator like the one considered in this analysis, is established, according to [5]:

$$t_s = 10ms$$

3.7. Materials

It is necessary to dispose both the density and the maximum tensile strengh, of the materials employed to manufacture all tanks and the gas generator. For this purpose, the table 6 is presented, where also the oversizing factors chosen for the analysis were included:

Table 3: Proposed materials for the feed systems manufacturing				
Component	Material	Density [kg/m^3]	UTS [MPa]	Oversizing factor
Gas tank	Kevlar	1700	3300	2.5
Oxidazer tank	Aluminium Alloy	2800	455	2.5
Fuel tank	Aluminium Alloy	2800	455	2.5
Gas generator	Hastelloy C	8890	524 (1033K)	2.5
	CRES 347	7960	180 (1090K)	

Clearly, although there are many other materials options available, they were discarded because both, the material itself or the tank manufacturing methods, are quite expensive. From the two options available for the gas generator manufacturing, one may conclude that being not an element that limits the turbo-pumps total mass, whatever be the material adoption it will not have major influence. Therefore, all the graphics were made adopting "Hastelloy C" alloy as the gas generator material.

3.7. Motor, Inverter and Batteries

As was mentioned in the introduction brushless DC electric motors are employed. Two merit figures of these motors are relevant for the comparison: the power density and the efficiency. Next, a table with some data examples of these motors is presented:

Table 4: Candidates DC-Brushless Motors					
Model	Nominal Power [W]	Power Density [W/kg]	Efficiency	Speed [rpm]	Reference
AXi4120/14	865	2700	85%	29000	[12]
AXi5320/18	1600	3300	93%	16000	[12]
Hacker A60-14L	2100	2800	-	7100	[15]
Predator 37	15000	7890	-	5900	[16]
Predator 30	12500	7100	88%	5600	[16]
Himax HC 5030-390	1500	3800	-	12000	[18]
Hyperion ZS4045-10	3000	4800	-	10800	[19]
Yuneec Power Drive 60	60000(*)	2000	92%	2400	[20]

(*) The power density of an electric motor decreases with power and efficiency but increases with speed. The typical specific mass vs. speed curves for electric motors are depicted below:
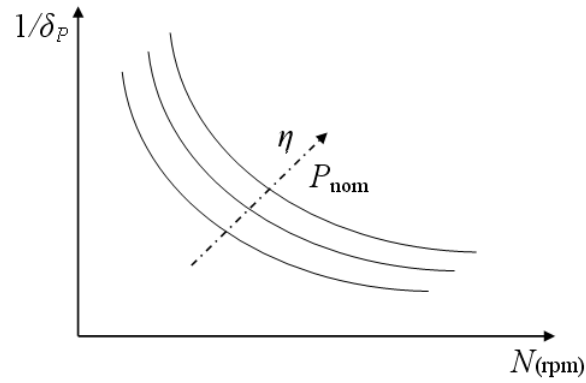
Figure 2: Synchronous motor specific mass in function of their rotational speed. In dotted line, the dependency with the efficiency and the nominal power is denoted.

Therefore, for the expected pumps operation speed range (from 10,000 rpm to 40,000 rpm) a 3.8 kW/kg power density is considered feasible within the power range required (5 to 60 kW).

Hence, the following values for such parameters are adopted:

$$\delta_{ee} = 3.8\,{kW}/{kg} \qquad \eta_{ee} = 0.8$$

The inverter is characterized with the same motor parameters. In addition to the above mentioned denominations, these devices are often called *Electronic Speed Controls* (ESC) because they perform this function in scale radio-controlled vehicles.

Next, a table with some examples of these devices is presented:

Table 5: DC-Brushless Motors Inverters.			
Model	Power Density [kW/kg]	Efficiency	Reference
Jeti Advance 70 Pro	41	-	[13]
Jeti Advance 90 Pro	37	-	[13]
Phoenix ICE HV 80	70.5	85%	[17]
Phoenix ICE HV 160	61.8	85%	[17]

Finally, the power density and efficiency values adopted are:

$$\delta_{inv} = 60\,{kW}/{kg} \qquad \eta_{inv} = 0.85$$

Regarding batteries, there are various manufacturing tecnologies that should be considered. There are two parameters that relate both their efficiency and their mass. In one hand, is the power density while in the other hand is the energy density. The last one becomes very important as the operation time increases. It becomes a limiting factor for long operation times. Therefore, a technology offering both higher power and energy densities should be chosen, being one a more important factor than the other according to the total engine burning time.

Among the most promising technologies there are:

- Lithium-Ion (Li-Ion)
- Lithium-Ion Polymer (Li-Po)
- Lithium-Sulfur (Li-S)

In the following table some typical data of these technologies are presented:

Table 6: Proposed batteries technologies data.				
Battery type	Power Density [W/kg]	Energy Density [Wh/kg]	Cell Nominal Voltage [V]	References
Li-Ion	3000	100 – 180	3.6	[8] [10] [11]
Li-Po	6000	130	3.7	[6]
Li-S	670	350	2.15	[7]
Li-S (under development)	2000	220	2.15	[9]

The values presented for the first three cases are estimations made over currently marketed products. Worth to mention that the battery developments are continously evolving and the tabulated values can be enhanced in short term. The fourth case presented is a good example of this, which is an improvement on the Lithim-Sulfur technology. It is actually in development but it could be available as a commercial product in short term.

Finally, is necessary to foresee a battery sizing margin. In this case, it is assumed that a margin in the battery mass of 20% will be adequate. Hence:

$$k_b = 1.2$$

IV. RESULTS

Next, the results of the calculations are presented. Such calculations were done with the data estimated in the previous section. The curves parameters are shown with legends in each graphic. An important remark valid for all the following sections is that (unless otherwise specified) the electric systems are powered by Li-Po batteries.

4.1. Comparison with the work done in [3]

In this firt estimation the same original work data are used. For more detail, below are listed all those parameters which were changed respect to the ones from the previous section:

$$p_C = 30 Bar$$
$$\gamma_C = 1.225$$
$$p_{tp1} = 1.8 * p_C$$
$$k_{tg} = 2.4$$

$$M_C = 22 kg$$
$$p_{tp2} = 0.3 * p_C$$
$$k_{tp2} = 1.25$$

$$O/F = 1.64$$
$$\Delta p_{in} = 0.8 * p_C$$
$$p_{tp3} = 0.3 * p_C$$
$$k_{tp3} = 1.25$$

Also, it is mentioned that, for the electric feed system, Li-Po batteries are adopted. It is interesting, also, to trace a curve that was not included in the original work, to analyze what happens if the propellants mass is taken as calculation parameter. The results obtained are shown below:
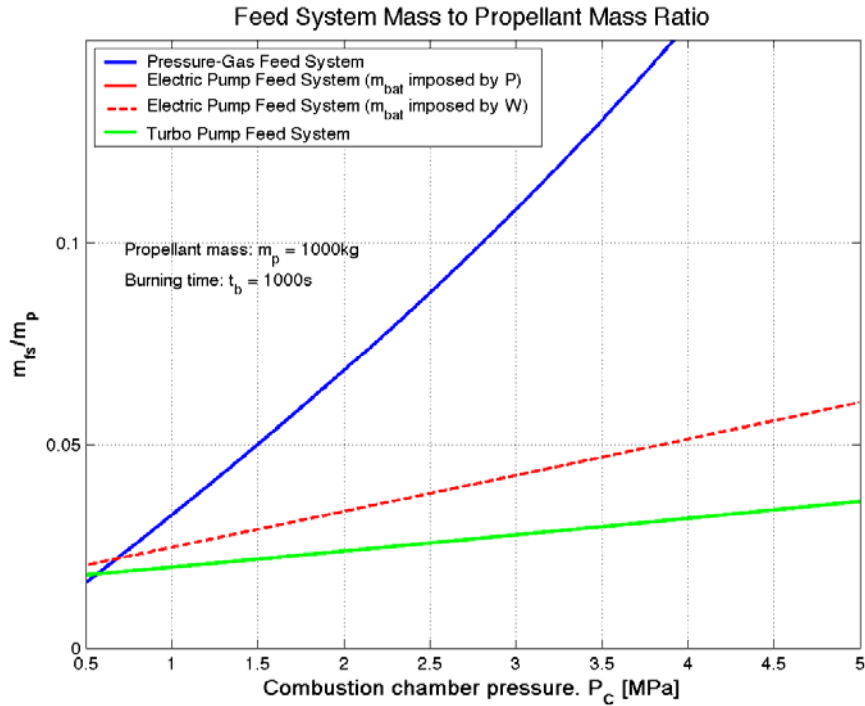
Figure 3: Ratio between the feed system mass and the total propellant mass for the three analized systems in function of the combustión chamber pressure, propellant mass of 1000 kg and burning time of 1000 s.
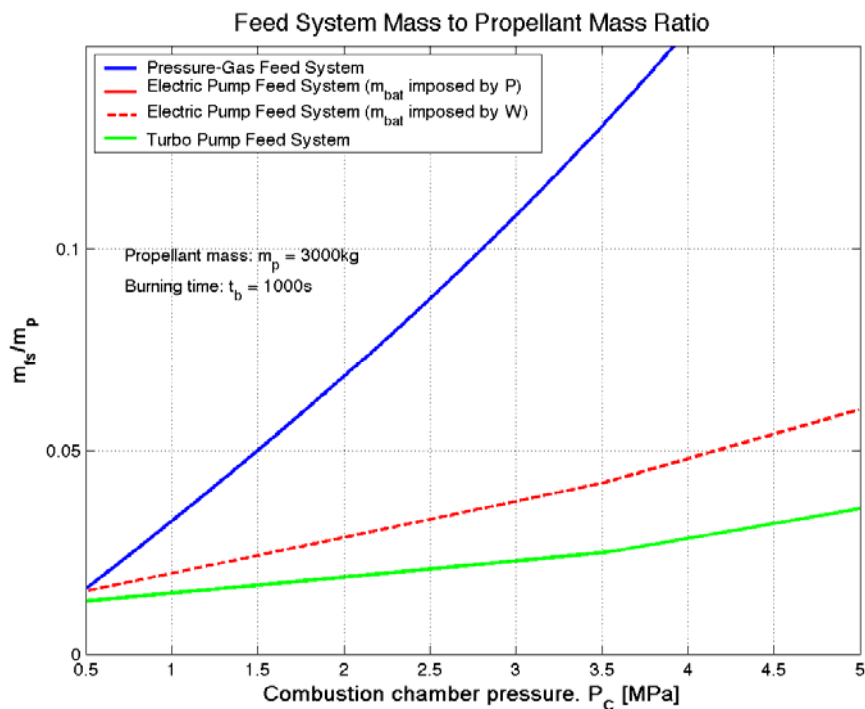
Figure 4: Ratio between the feed system mass and the total propellant mass for the three analized systems in function of the combustión chamber pressure, propellant mass of 3000 kg and burning time of 1000 s.
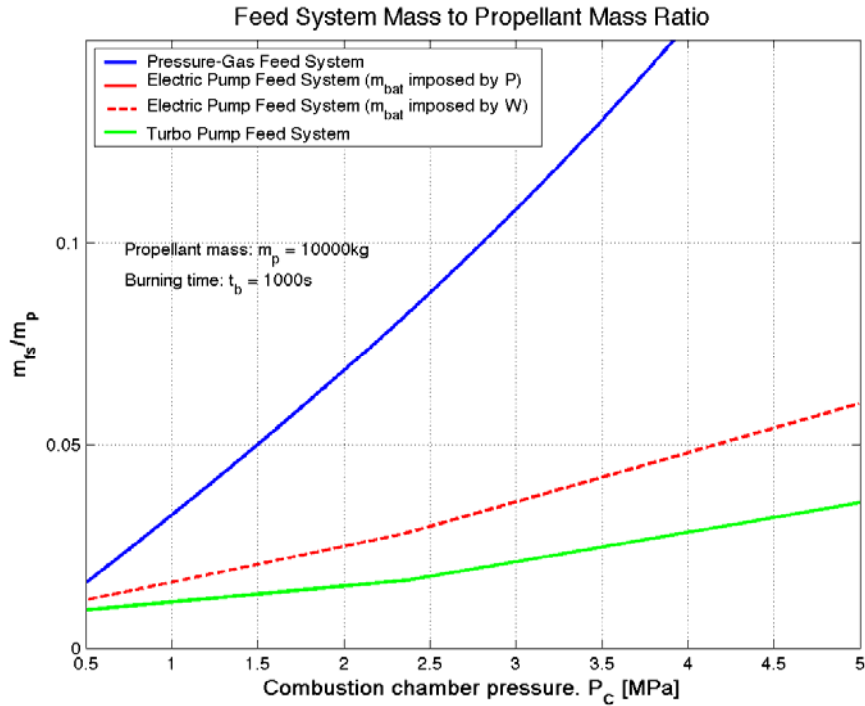
Figure 5: Ratio between the feed system mass and the total propellant mass for the three analized systems in function of the combustión chamber pressure, propellant mass of 10000 kg and burning time of 1000 s.
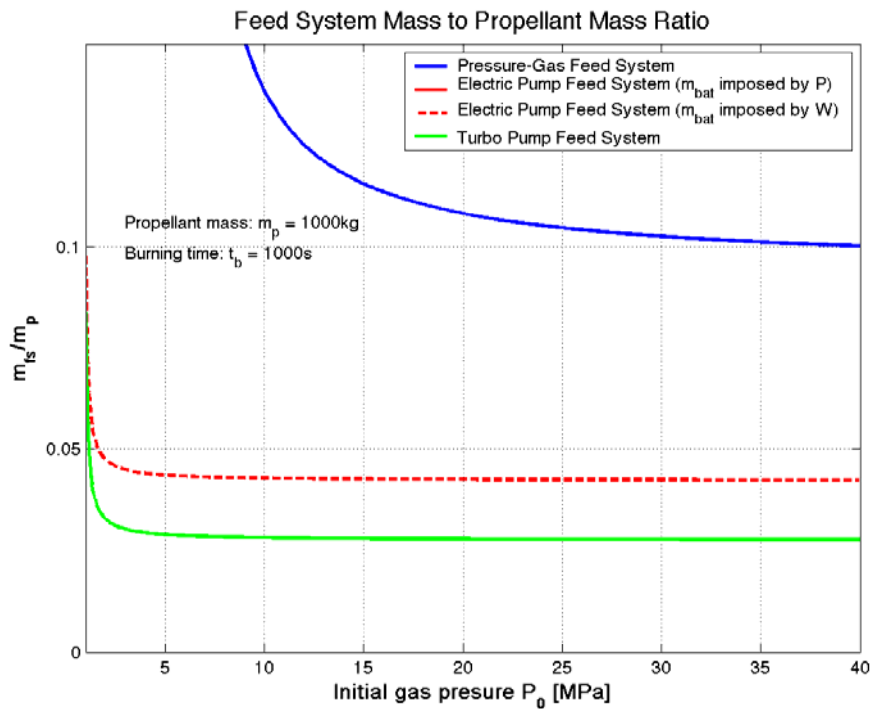

Figure 6: Ratio between the feed system mass and the total propellant mass for the three analized systems in function of the initial gas pressure, propellant mass of 1000 kg and burning time of 1000 s.
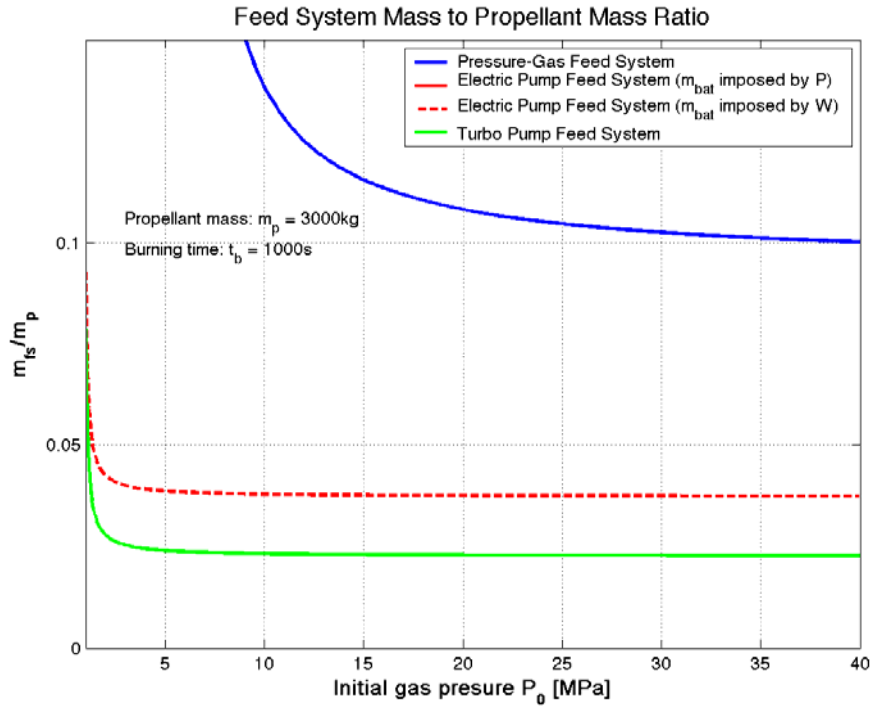
Figure 7: Ratio between the feed system mass and the total propellant mass for the three analized systems in function of the initial gas pressure, propellant mass of 3000 kg and burning time of 1000 s.
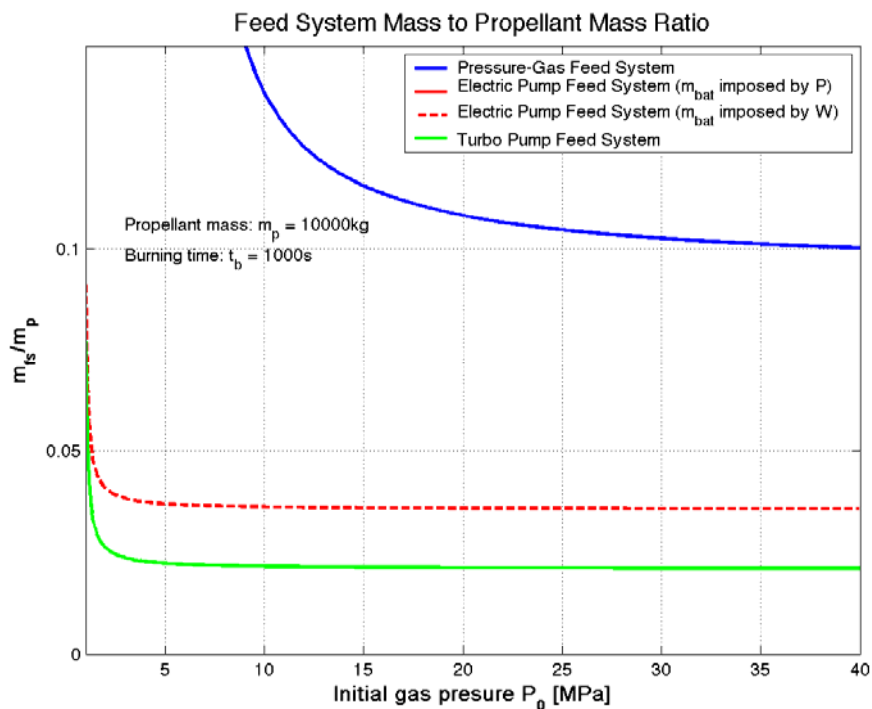
Figure 8: Ratio between the feed system mass and the total propellant mass for the three analized systems in function of the initial gas pressure, propellant mass of 10000 kg and burning time of 1000 s.
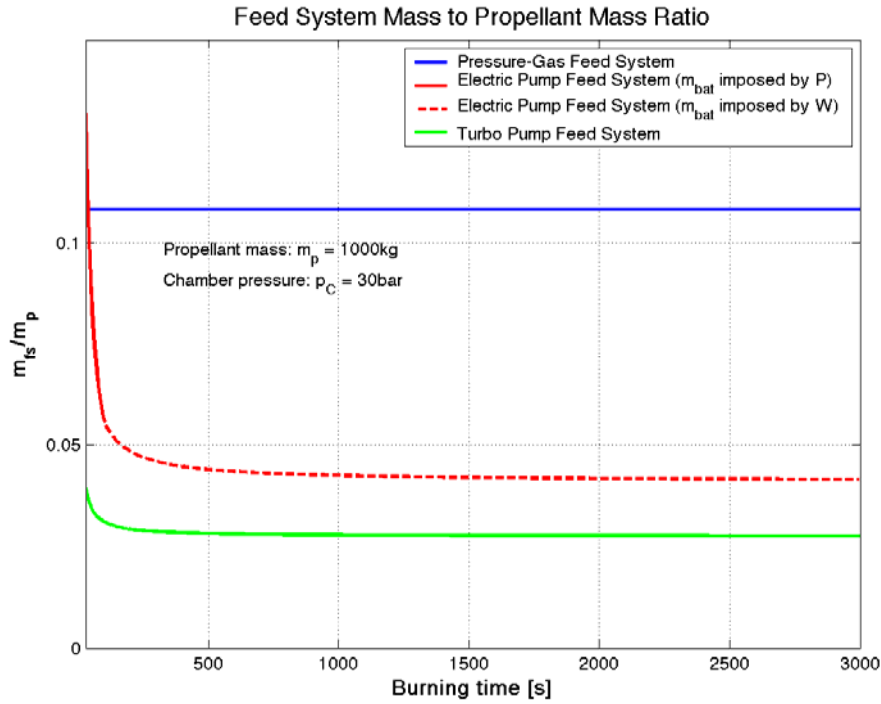
Figure 9: Ratio between the feed system mass and the total propellant mass for the three analized systems in function of the burning time, propellant mass of 1000 kg and chamber pressure of 30 bar.
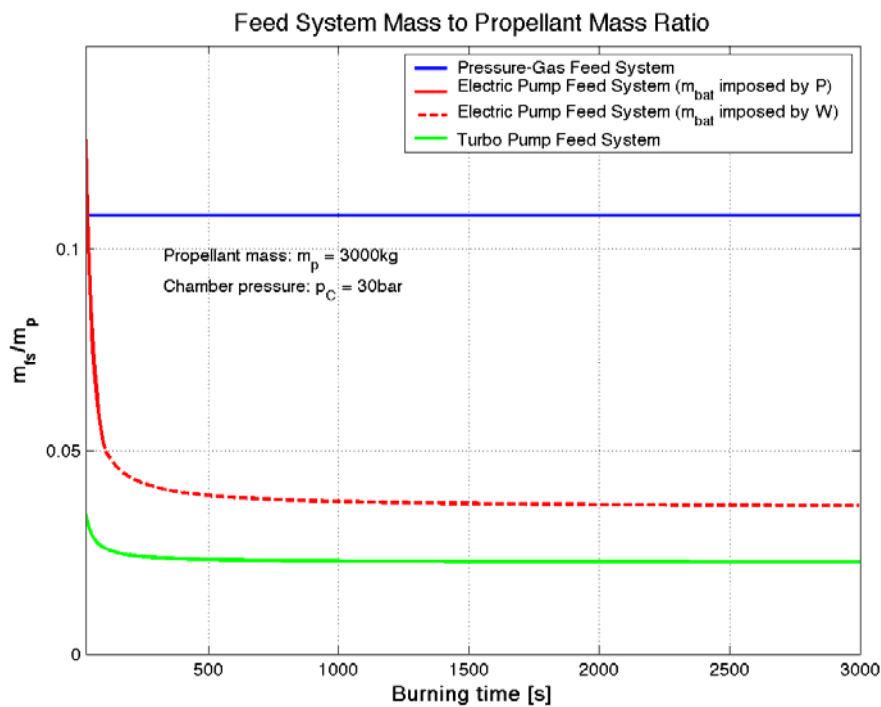

Figure 10: Ratio between the feed system mass and the total propellant mass for the three analized systems in function of the burning time, propellant mass of 3000 kg and chamber pressure of 30 bar.
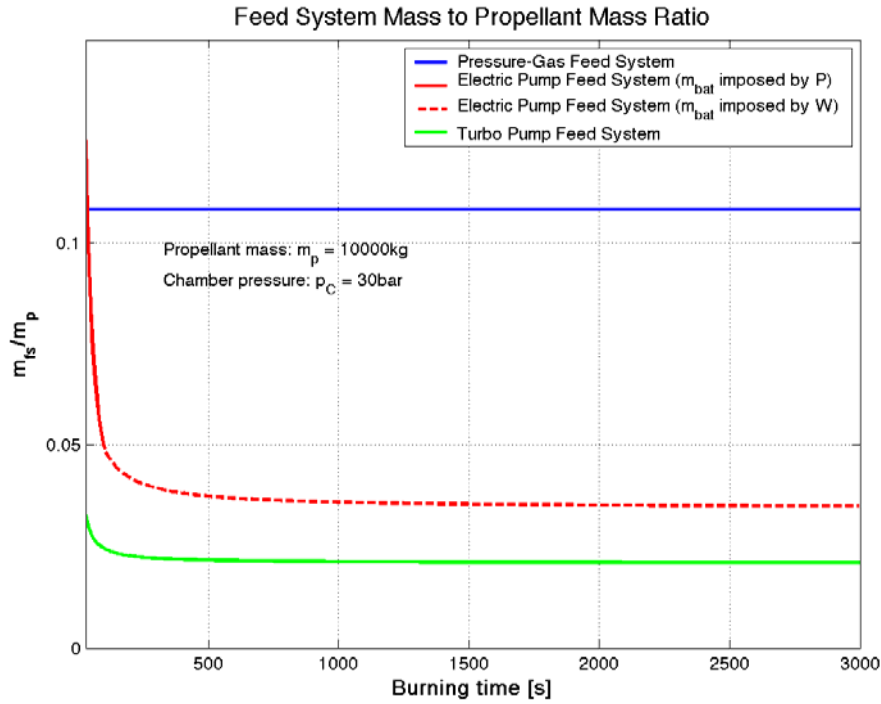
Figure 11: Ratio between the feed system mass and the total propellant mass for the three analized systems in function of the burning time, propellant mass of 10000 kg and chamber pressure of 30 bar.
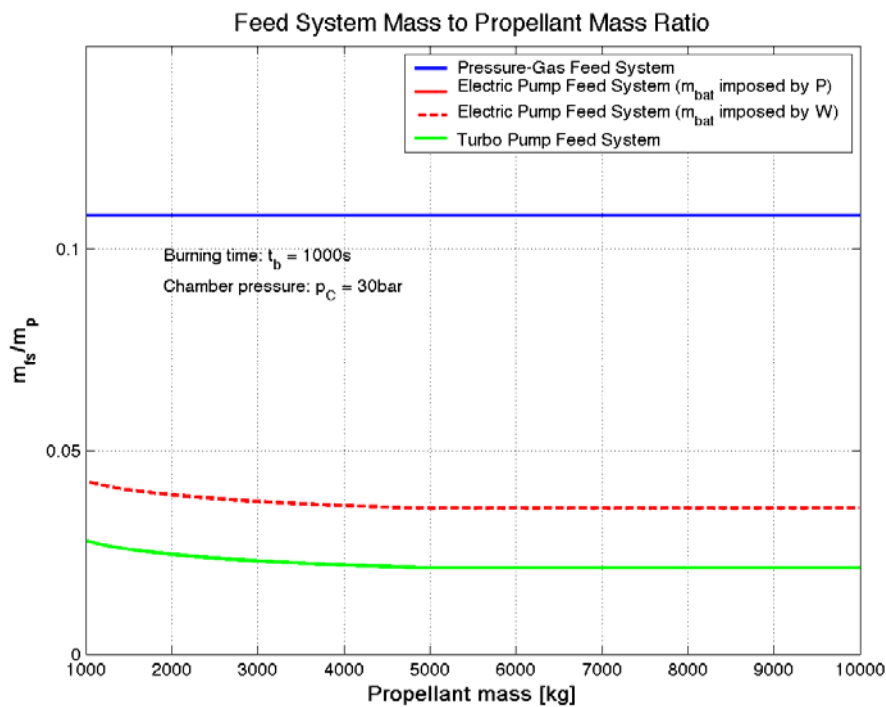

Figure 12: Ratio between the feed system mass and the total propellant mass for the three analized systems in function of the propellant mass, burning time of 1000 s and chamber pressure of 30 bar.

In addition, it is interesting to evaluate the systems mass in the same conditions as above but for a lower burning time, which is usual for orbital launcher upper stages. Then, it is repeated the above graphic for a burning time of 90 seconds.
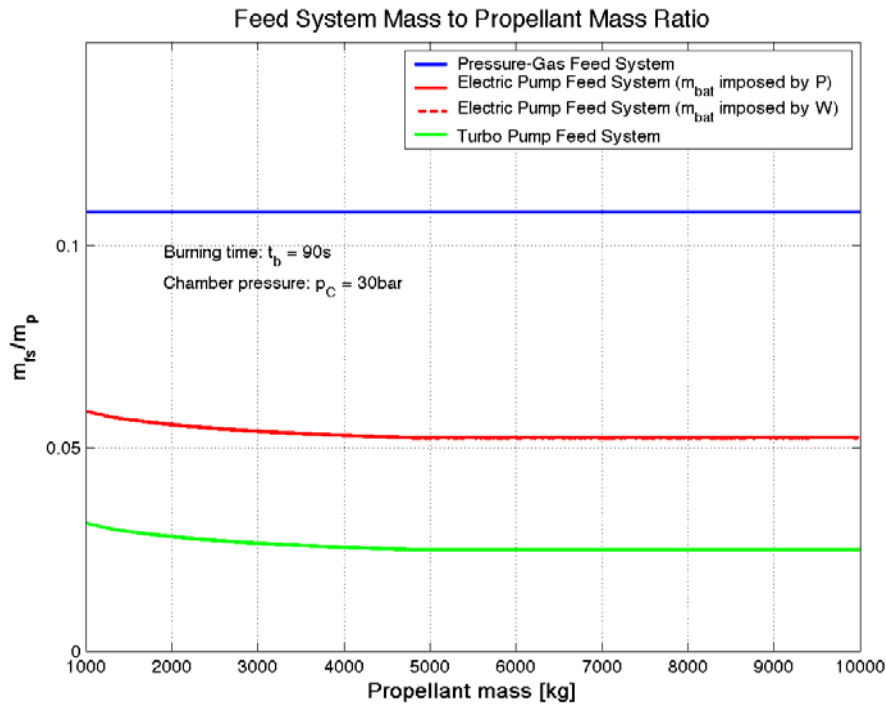
Figure 13: Ratio between the feed system mass and the total propellant mass for the three analized systems in function of the propellant mass, burning time of 90 s and chamber pressure of 30 bar.

4.2. Battery technologies comparison

In this section, the results of the evaluation of the electric-pumps feed system mass, which is obtained by using the various battery technologies cited in the previous section, are presented. As reference, also the curves of the pressurized gas and turbo-pumps feed systems masses were traced. The parameters of the turbo-pumps feed system remain unchanged from the above section.

From the figure 14 is derived that there would be an optimal burning time from the battery use point of view. This optimal time would correspond to the limit between the continuos and dotted traces. In the limit point, the battery is being used so that the required power density is equal to which the battery can supply and also the required energy density matches the battery own.
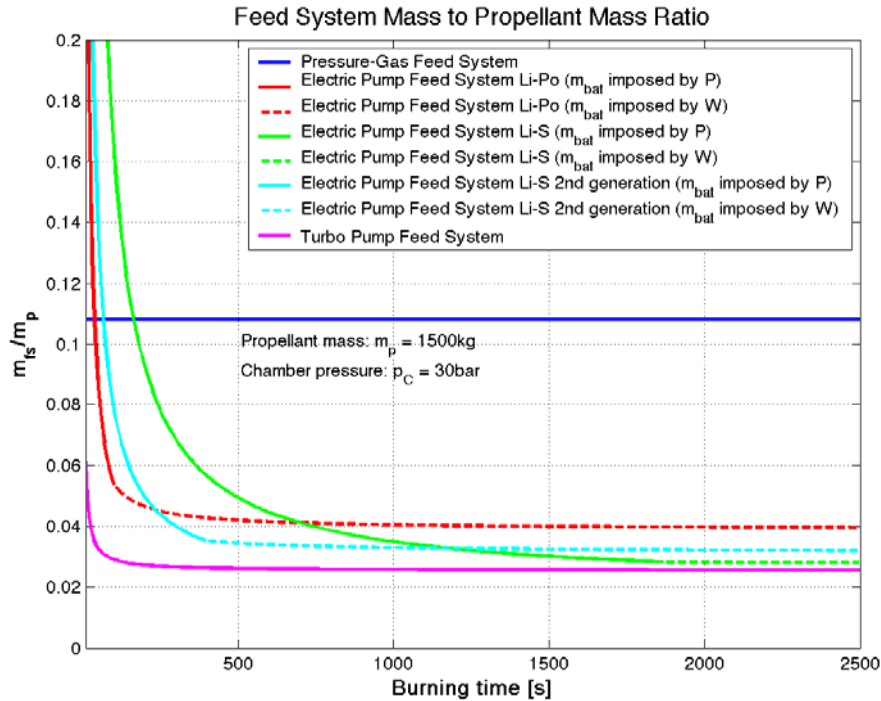
Figure 14: Ratio between the feed system mass and the total propellant mass for the three analized systems in function of the burning time, propellant mass of 1500 kg and chamber pressure of 30 bar.

From the battery point of view the optimal burning times are characteristics from each technology. It can be seen from the equations 2.6.3 and 2.6.4, forcing the mass estimated from both expressions to be the same. With this condition, the burning time which optimally profits both battery densities, results from dividing the energy by the power density. Below, in a table, the optimal values of the proposed technologies are presented:

Table 7: Burning times that optimizes the batteries mass.			
Tecnology	Power density [W/kg]	Energy Density [Wh/kg]	Optimal time [s]
Li-Po	3000	100 – 180	120 - 216
Li-Ion	6000	130	78
Li-S	670	350	1881
Li-S (under development)	2000	220	396

4.3. Comparison with short burning times and high chamber pressures

In this section the results obtained when employing short burning times are presented. Also the curves corresponding to high chamber pressures are traced to evaluate the impact of this parameter in the system mass.

Let start by drawing a curve set in function of the chamber pressure. The varying parameter is the burning time, which take values of 60s, 90s y 240s. All other parameters values are keep as in the 4.1 section. Then, the curves corresponding to the combustion chamber pressure shift are traced. These ones were traced as function of the burning time, taking values of 15Bar, 30Bar and 60Bar.
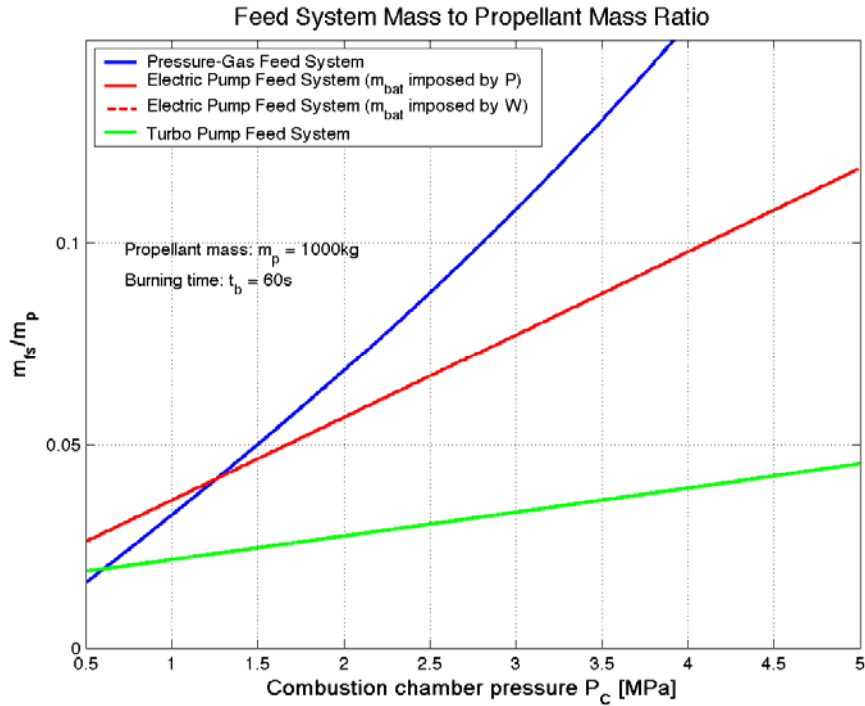
**Figure 15: Ratio between the feed system mass and the total propellant mass for the three analized systems in function of the combustión chamber pressure, propellant mass of 1000 kg and burning time of 60 s.**
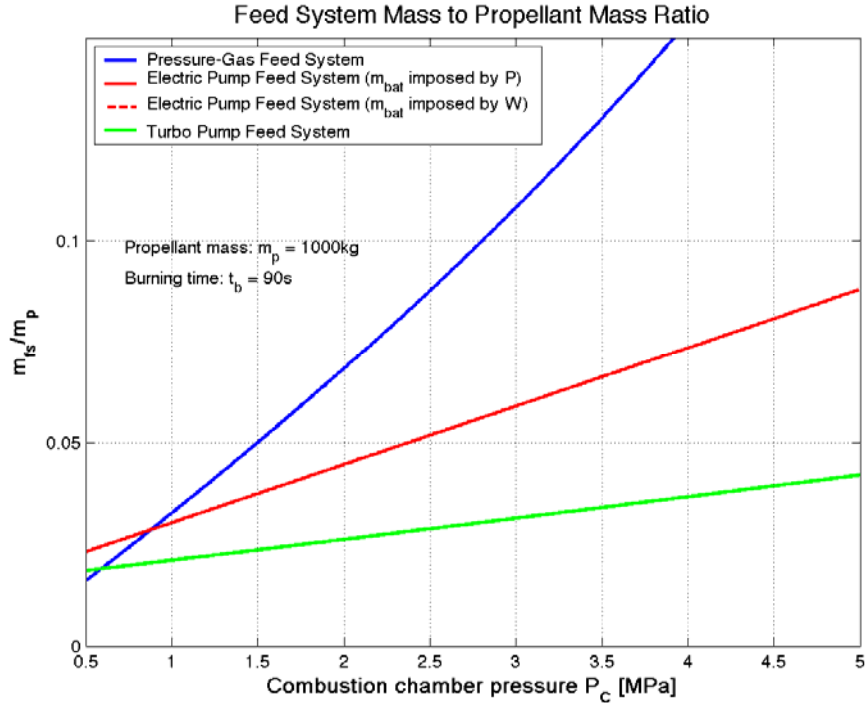
Figure 16: Ratio between the feed system mass and the total propellant mass for the three analized systems in function of the combustión chamber pressure, propellant mass of 1000 kg and burning time of 90 s.
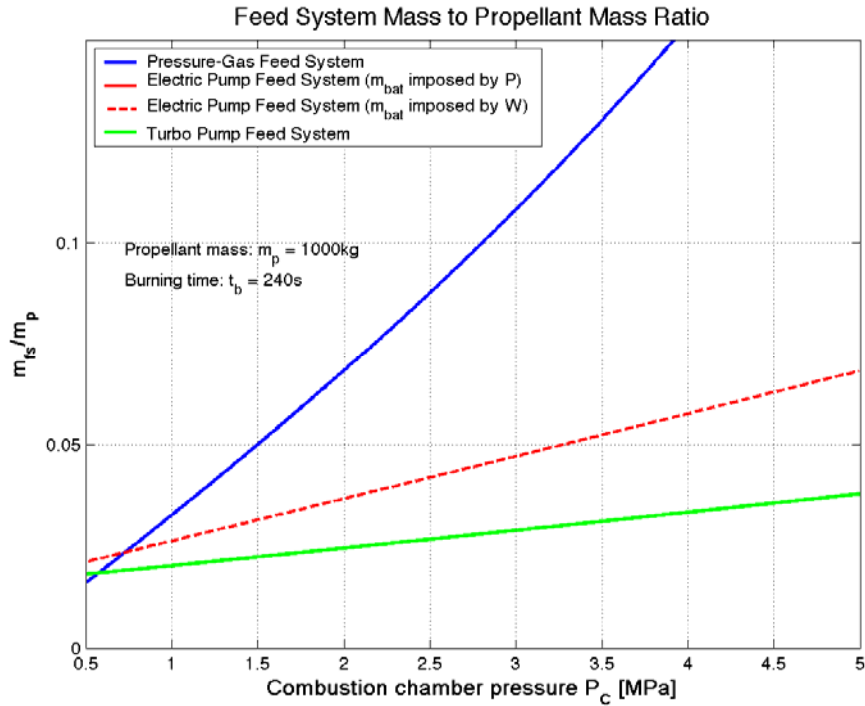
Figure 17: Ratio between the feed system mass and the total propellant mass for the three analized systems in function of the combustión chamber pressure, propellant mass of 1000 kg and burning time of 240 s.
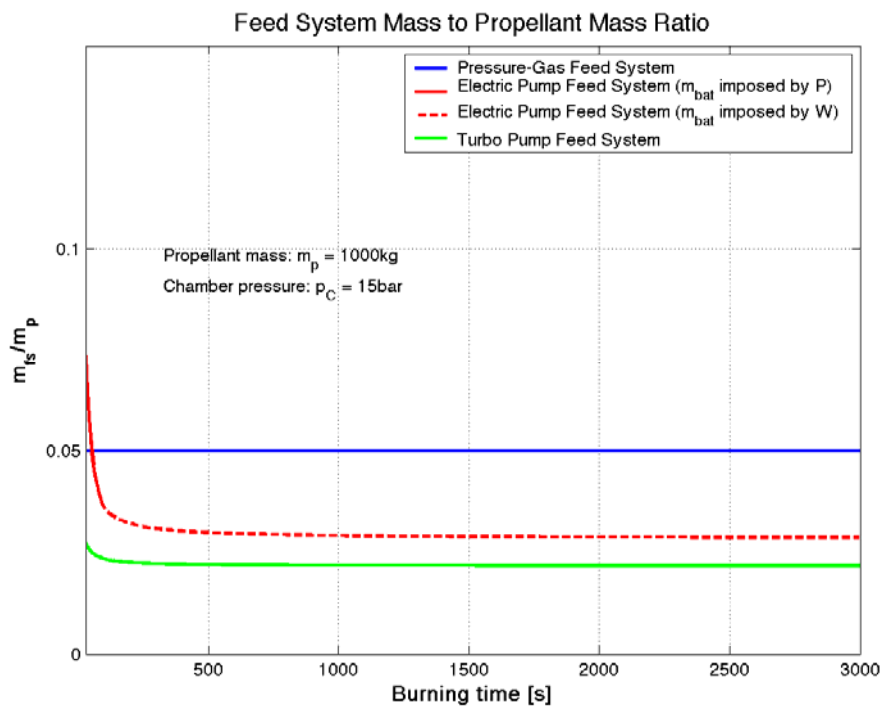
Figure 18: Ratio between the feed system mass and the total propellant mass for the three analized systems in function of the burning time, propellant mass of 1000 kg and chamber pressure of 15 bar.
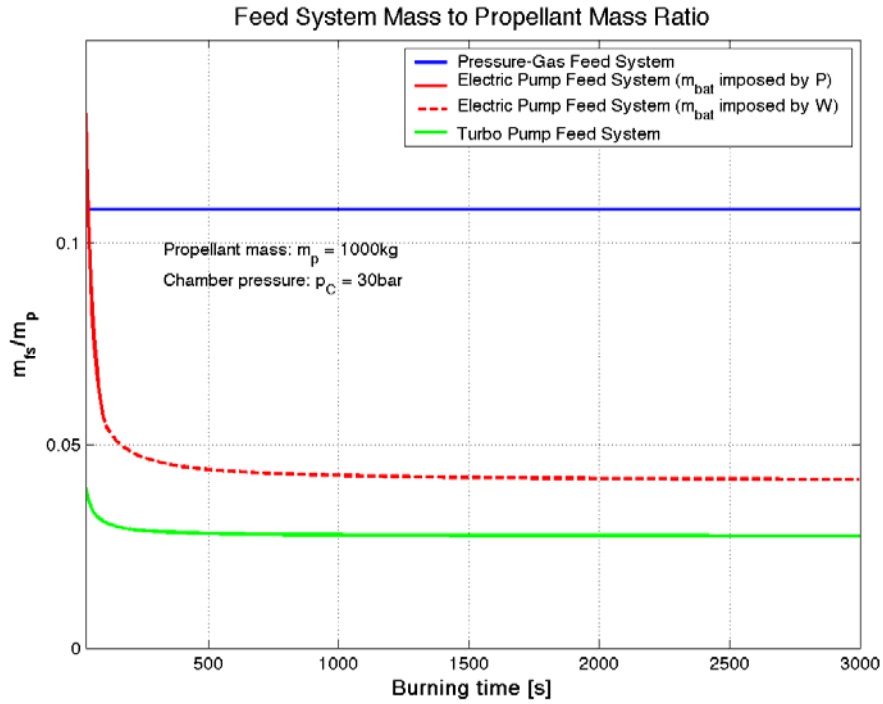
Figure 19: Ratio between the feed system mass and the total propellant mass for the three analized systems in function of the burning time, propellant mass of 1000 kg and chamber pressure of 30 bar.
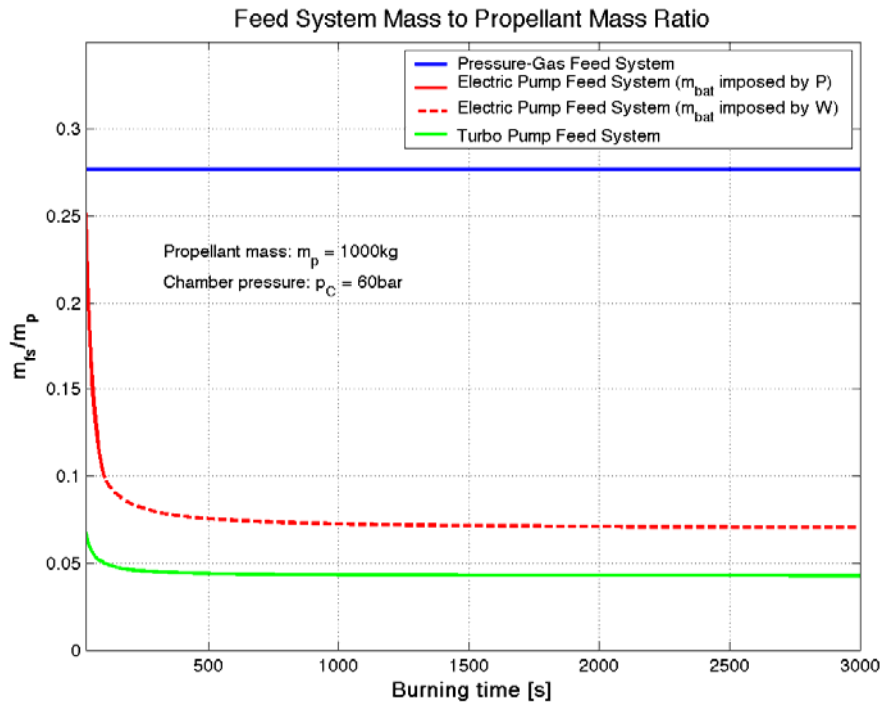
Figure 20: Ratio between the feed system mass and the total propellant mass for the three analized systems in function of the burning time, propellant mass of 1000 kg and chamber pressure of 60 bar.

4.4. Comparison with an orbital launcher third stage

It is interesting to compare the results obtained using the estimated data from a third stage of an orbital launcher. Such orbital launcher is intented to locate a 200kg payload into a LEO (and it was originally designed with a pressurized gas feed system).

Below are listed all parameters used to perform these estimations:

$$p_C = 15 Bar$$

$$\gamma_C = 1.23$$

$$p_{tp1} = 21 Bar$$

$$k_{tg} = 2.5$$

$$M_C = 23 kg$$

$$p_{tp2} = 6 Bar$$

$$k_{tp2} = 2.5$$

$$O/F = 1.9$$

$$\Delta p_{in} = 0.3 * p_C$$

$$p_{tp3} = 6 Bar$$

$$k_{tp3} = 2.5$$

Thus, the following graphics are obtained:
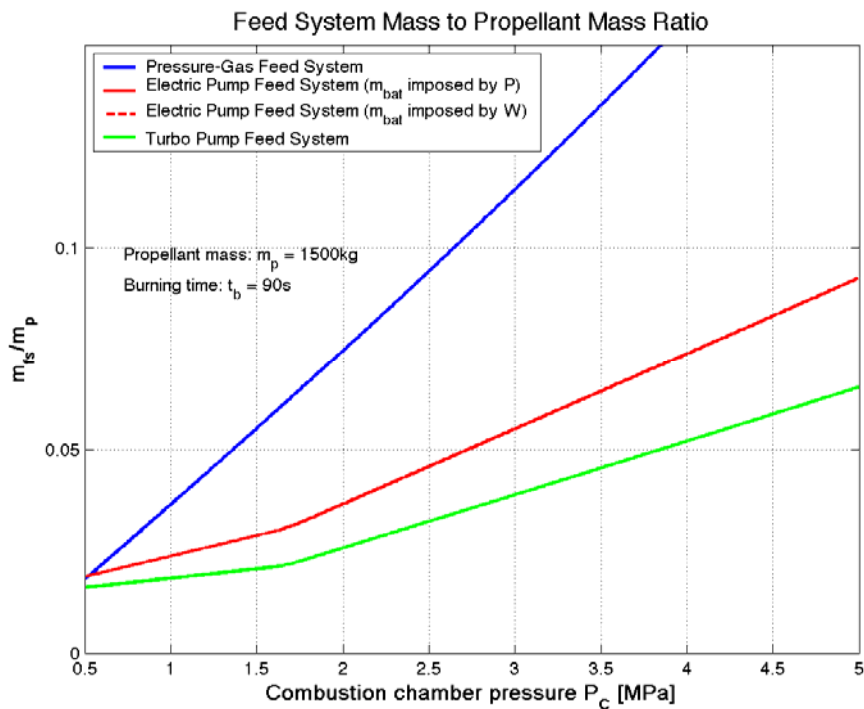
Figure 21: Ratio between the feed system mass and the total propellant mass for the three analized systems in function of the combustión chamber pressure, propellant mass of 1500 kg and burning time of 90 s.
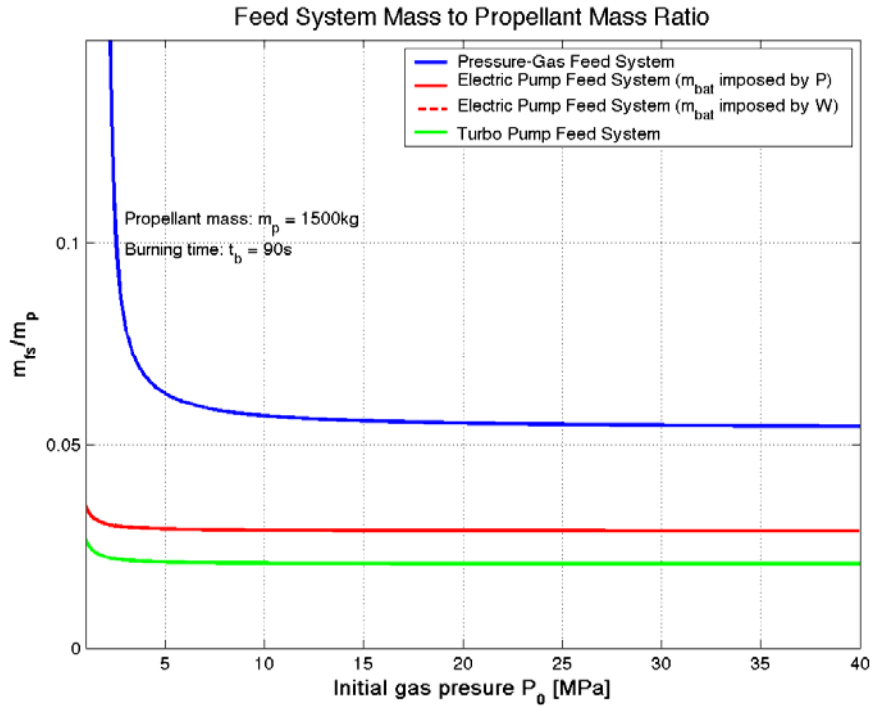
Figure 22: Ratio between the feed system mass and the total propellant mass for the three analized systems in function of the initial gas pressure, propellant mass of 1500 kg and burning time of 90 s.
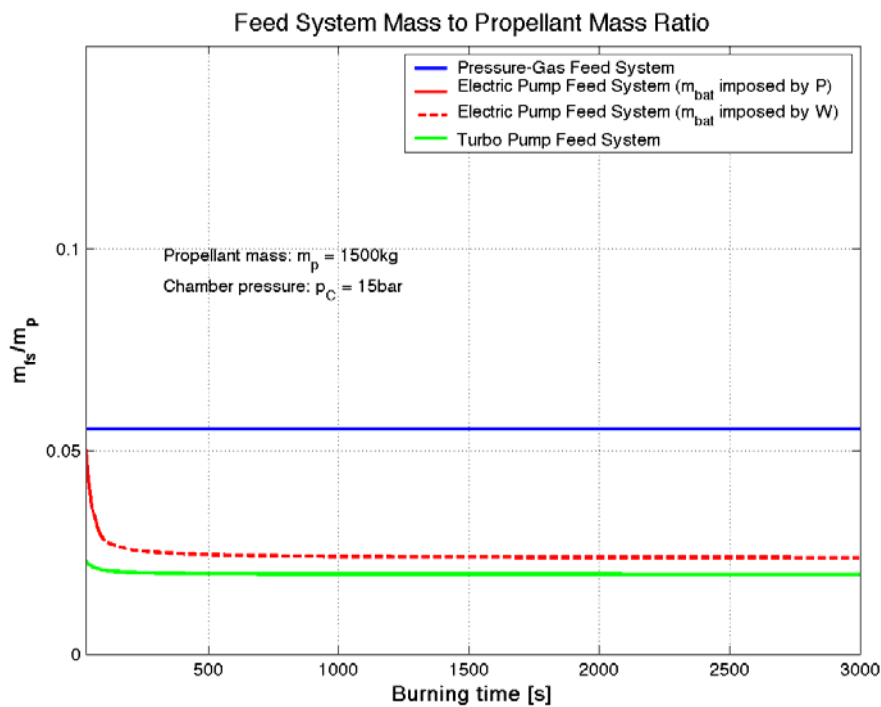
Figure 23: Ratio between the feed system mass and the total propellant mass for the three analized systems in function of the burning time, propellant mass of 1500 kg and chamber pressure of 15 bar.
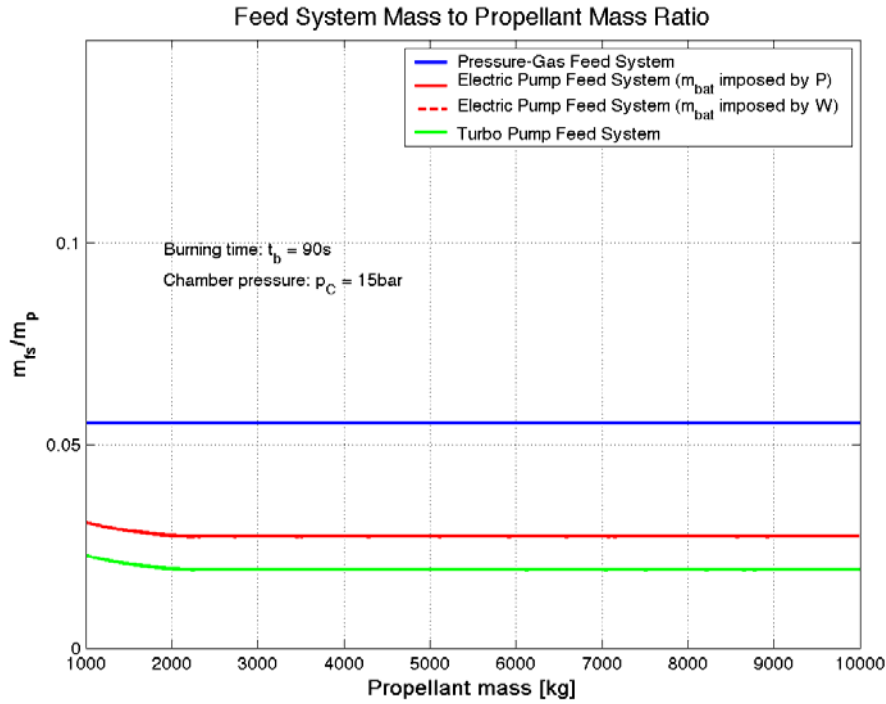
Figure 24: Ratio between the feed system mass and the total propellant mass for the three analized systems in function of the propellant mass, burning time of 90 s and chamber pressure of 15 bar.

4.5. Electric feed system masses analysis

In this section curve sets are presented showing the relative contribution of each main component mass to the total system mass. In this case, batteries with LiPo technology are employed. Then, a graphic is presented showing the required power and energy densities to obtain an electric feed system with a total mass equivalent to the one of the turbo-pump feed system.
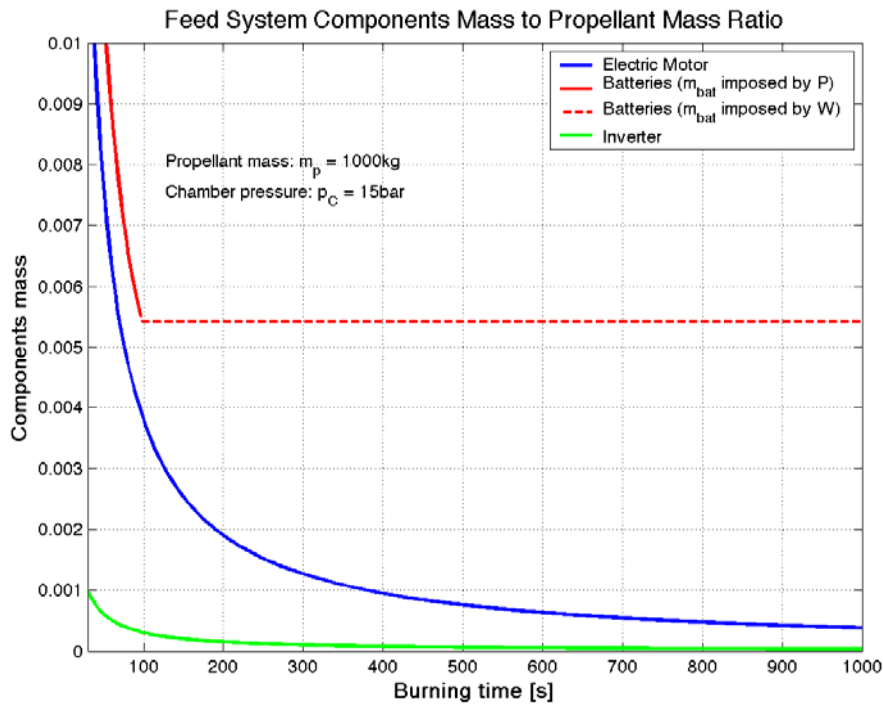
Figure 25: Ratio between the various main components masses of the electric feed system and the total propellant mass in function of the burning time, propellant mass of 1000 kg and chamber pressure of 15 bar.
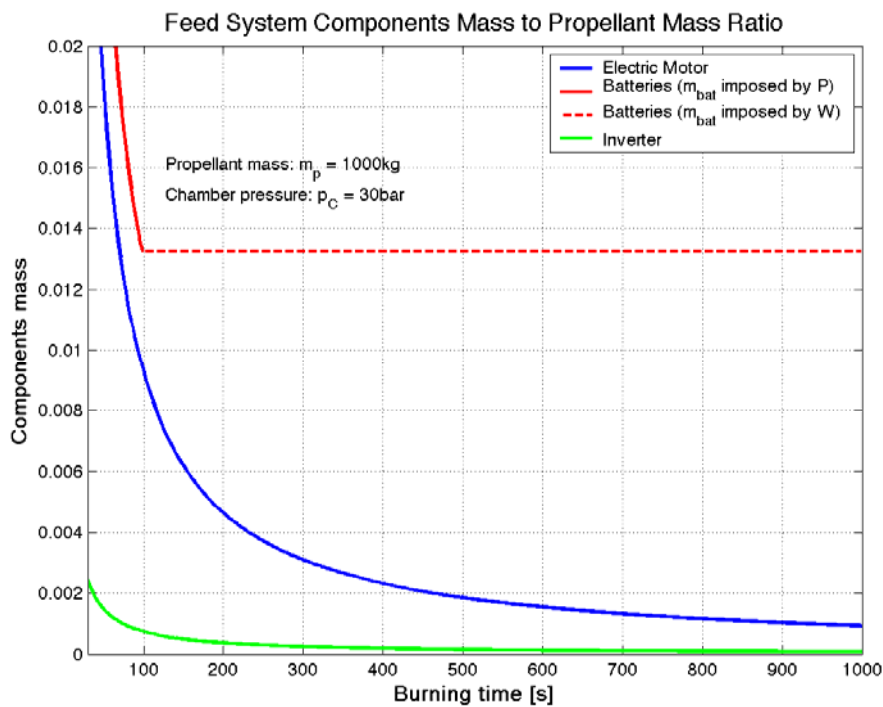
Figure 26: Ratio between the various main components masses of the electric feed system and the total propellant mass in function of the burning time, propellant mass of 1000 kg and chamber pressure of 30 bar.
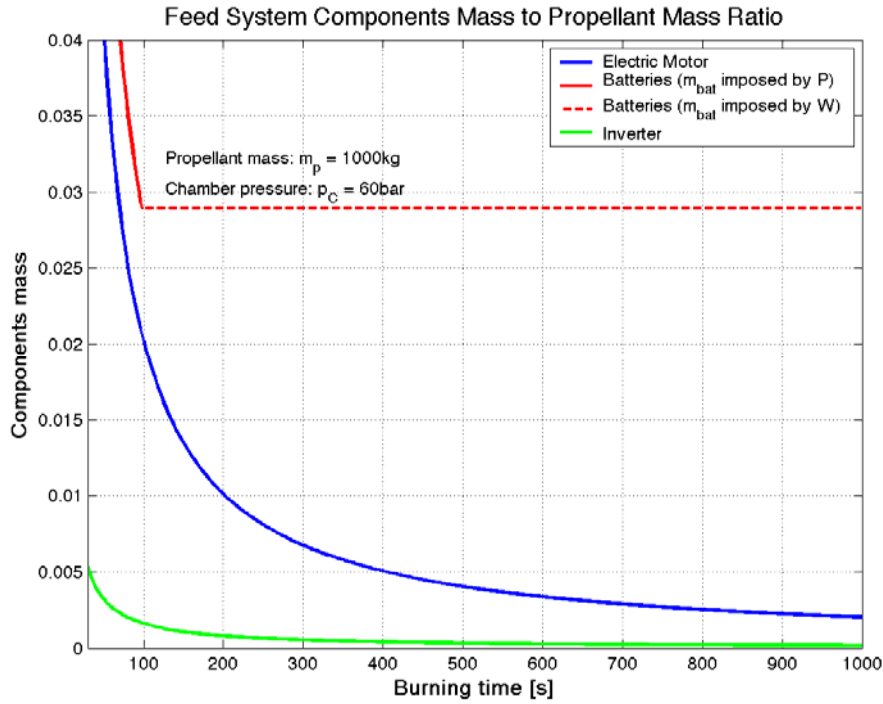
**Figure 27: Ratio between the various main components masses of the electric feed system and the total propellant mass in function of the burning time, propellant mass of 1000 kg and chamber pressure of 60 bar.**
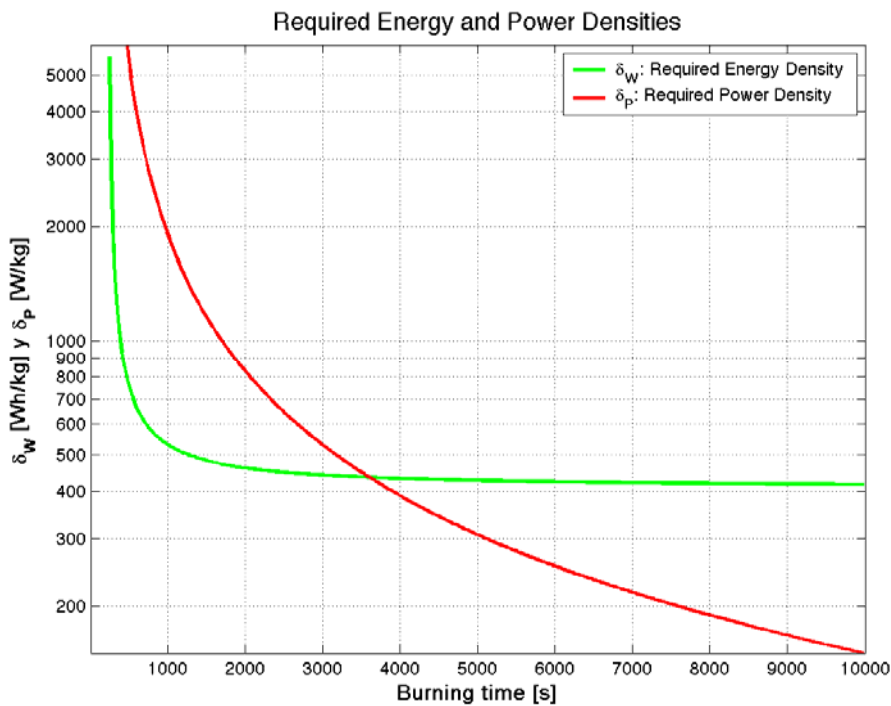
**Figure 28: Required power and energy densities to match the electric-pumps feed system total mass to the turbo-pumps feed system total mass. In this case, the curves are not dependent of either the combustion chamber pressure or the total propellant mass.**

V.   CONCLUSIONS

The first conclusions that emerge from the elaboration of this report are extracted from figures 3, 4 and 5. It is observed as the proposed system results lighter than the pressurized gas system according as the combustion chamber pressure increases. This feature was already observed in the original work [3]. Further, the difference is accentuated as the total propellant mass increases. This causes that the electric-pump feed system become advantageous over the pressurized gas feed system, in applications where higher chamber pressures be required.

From figures 6, 7 and 8 one may conclude that a high gas initial pressure is desirable for a pressurized gas system, however, for the other two feed system this preference is almost irrelevant. Such trend was exposed in [3], explaining that in the pumping systems case, only a moderate pressure in the propellant tanks is required, to avoid the pump cavitation. As above, the improvement with the propellant mass increment of the proposed system is verified, while no difference was noted for the pressurized feed system.

It is interesting to see the burning time effect in the total mass of all analyzed systems. That can be appreciated from figures 9, 10 and 11. It is evident that, while there is not influence of burning time in the mass fraction of the pressurized gas feed system; it does influence in the other two. This is because, once set the propellant mass, the greater the burning time the lower the propellant flow through the pumps and, as consecuence, a lower power is required by the pumps. In the turbo-pump feed system this implies lighter turbines and smaller gas generators, while in the electric pump feed system this save motor and battery wheight.

Moreover, from the graphics it is evident that the electric system battery mass become imposed by the power density when short combustion times are used (continuos trace), while it is imposed by the energy density when long burning times are considered (dotted line). The crossing point depends on the particular battery technology adopted (as below is mentioned).

Even if it is not observed from the figures, it is convenient to say that each graphic is limited, to the lower time values, by the battery minimum discharge time. This means that all the traced curves for the electric feed system becomes valid starting from a minimum value defined by such discharge time.

From figures 12 and 13 one may conclude that the proposed electrical feed system progresively improves whereas greater be the propellant mass (until some point) while the pressurized gas system is not sensitive to that. This improvement in the electric feed system is due to the fact that for small values of propellant mass, the tank wall tickness is determinated by the minimum tickness, defined to withstand the acceleration loads. While the tickness is defined in such way, the greater the propellant mass the better the electric feed system mass fraction.

This happens until the point when the tank mass start to be defined by the Laplace Law. Notice, that for long burning times (figure 12) the electric feed system mass is imposed by the energy density (dotted line) while for short burning times (figure 13) the mass is imposed by the power density (continuous line).

From figure 14 it is concluded that the choice of one kind of battery technology over another depends on the burning time. If short operation times are required by the mission, the Li-Po batteries techonology shows better results. That is because their power density is notoriously higher to the Li-S batteries ones. However, if the burning time becomes longer the trend is reverted and using Li-S batteries (with higher energy density) becomes a better option.

On the other hand, it is denoted that the Li-S batteries new generation widely excels to the first one, rivaling with Li-Po batteries even when not too longer combustion times are required. In fact, they become a better option when the combustion time is greater than 240s.

Another important conclusion from that section is obtained from the table 7. It is observed that, depending on the adopted technology, a burning time exists which optimizes the batteries characteristics exploitation. Below this optimal burning time, is necessary to include greater batteries quantity (Even when from the energy point of view it being well sized) because the electric power required for the motor operation exceeds the battery maximum power capability. The more the power extracted from the battery, more important becomes the cooling

requirements. This must to be taking into account because it would be necessary to dispose of some mechanism to dissipate the generated heat.

It is interesting to remark how the proposed system was improved from the original estimations from [3]. The weight saving is due to the use of high power density DC Brushless motors. This notorious gain makes that, although the electric pumps system is always heavier than the turbo pumps based ones, for slightly high chamber pressures (see figures 3, 4 and 5) the difference makes reasonable to think that the proposed system can be preferred in some applications, because their many advantages over the turbo-pumps feed system [4]. At this point, it is convenient to denote some of these advantages. On one hand, with an electric pump feed system is very easy to adjust the propellant mixture ratio (O/F) during the engine operation. This will allow, first, to facilitate the engine start, and second, makes soft starts that minimize the stress over the payload and the electronic fly controls. Furthermore, the electric feed system design is simpler than the turbo-pump feed system.

From the graphics presented in the figures 15, 16 and 17 it can be extracted some interesting conclusions. It is denoted that, with the exception of the pressurized gas feed system, both the turbo-pumps and the electric-pumps feed systems are sensible to the burning time. Decreasing such time, increases the required pump power and this has negative consequences over the pumping components weight. However, from the figure 16 is shown that for burning times greater or equals to 90s, if chamber pressures of 10Bar or higher are adopted, the proposed system result lighter than the gas pressurized one. Thanks to modern batteries, the electric feed system results more advantageous than the pressurized gas one for a great quantity of applications.

On the other hand, from the analysis of figures 18, 19 and 20, one may verify that the mass fractions corresponding to the pumping systems converge to stable values, being almost irrelevant their burning time dependence for values above the 300s.

However, if the burning time exceeds the 100s the pumping systems results significantly lighters. Furthermore, the difference between the mass ratios of the pumping based and pressurized gas systems becomes notoriously greater according as the combustion chamber pressure increases. Both features make that the proposed system results particulary advantageous respect of the pressurized gas feed system when the chamber pressure is higher than 15Bar and the burning time is higher than 100s. It must be mentioned that, this advantage over the pressurized gas feed system is obtained without employing expensive materials in the propellant tanks manufacturing. Consequently, that a superior electric feed system can be manufactured using less expensive materials or parts.

In the section 4.5 some curves were traced to allow analysing the electric feed system performance. In first place, the grapohics of the relative weight of each electric feed system key component are presented (figures 25, 26 and 27). It is evident that nowadays the weight limiting components are the battery packs. It is interesting then to question how much it must be improved the current technology to make both systems comparable (the electric-pump fed and the turbo-pump based one).

To do that, it is interesting to estimate which would be the power density and energy density values that make both the total feed systems masses equal. Such densities are show in figure 28. Notice that such required densities do not depend on either the combustion chamber pressure or the total propellant mass. The reason of this fact may be understood checking the battery equations from Section 2, verifying that both the battery mass and the required pumping power depend on these parameters in the same way. Thus, the effects of such dependence cancel each other when both the power and the energy densities are computed. Note that, for burning times greater than 5,000 s both required densities would be reachable by the current technologies, while for burning times between 1,000 s and 5,000 s the required densities might be presumably feasible in a near future.

In conclusion this implies that, by virtue of the electric feed system inherent advantages over the turbo-pumps feed system, one may think on applying these ones in engines for first stages of microsatellite launchers.

VI.   REFERENCES

[1] Sutton, G. P. and Biblarz, O.: *Rocket Propulsion Elements*, 7th ed., Wiley, New York.

[2] Humble R. W. Henry, G.N. and Larson, W. J.: Space Propulsion Analysis and Design, 1st ed., McGraw-Hill, New York, 1995.

[3] Lentini, D. and Soldà, N.: *Opportunities for a Liquid Rocket Feed System Based on Electric Pumps*, Journal of Propulsion and Power, vol. 24, No 6 Nov-Dec 2008.

[4] Tacca, H. E.: *Aplicación de Bombas Eléctricas para Sistemas de Alimentación de Motores Cohete con Propulsantes Líquidos*, LABCATYP – Fac. de Ingeniería – U.B.A.

[5] NASA SP-8081, *Liquid Propellants Gas Generators*, March 1972.

[6] Thunder Power Li-Po Battery Data Sheet, 2250mAh, 5-Cell/5S (18.5V 30C/60C).

[7] Sion Power, Lithium Sulfur Rechargeable Battery Data Sheet, SION Power Inc., 2900E. Elvira Rd., Tucson, AZ 85756, (www.sionpower.com).

[8] High Power Lithium Ion ANR26650M1A, Battery Data Sheet, A123Systems Inc., 321 Arsenal Street, Watertown, MA 02472, (www.a123systems.com).

[9] Yu Mikhaylik, I. Kovalev, J. Xu, R. Schock, (Sion Power, Tucson, AZ, USA), "Rechargeable Li-S battery with Specific Energy 350 Wh/kg and Specific Power 3000 W/kg", 213th ECS Meeting, The Electrochemical Society, Abstract #112.

[10] NASA CR-2003-212350, *Comparison of Mars Aircraft Propulsion Systems*, May 2003.

[11] Panasonic Technical Data, *Overview of Lithium Ion Batteries*, January 2007 (http://www.panasonic.com/industrial/batteries-oem/oem/lithium-ion.aspx).

[12] DC-Brushless Motor Datasheets, Electricwingman Inc., Chester England (UK) (www.electricwingman.com).

[13] Electronic Speed Control Datasheets, Electricwingman Inc., Chester England (UK) (www.electricwingman.com).

[14] NASA SP-8107, *Turbopump Systems forLiquid Rocket Engines*, August 1974.

[15] Hacker Brushless Motors, Catalog 2010, (www.hacker-motor.com).

[16] Plettenberg Electromotoren, Predator 37 y Predator 30 datasheet, (www.plettenberg-motoren.com).

[17] Castle Creations Inc., Phoenix ICE HV ESC data sheets, (www.castlecreations.com).

[18] Maxx Products International Inc., Himax HC5030-390 datasheet, (www.maxxprod.com).

[19] Hyperion HK Ltd., Hyperion ZS 4045-10 datasheet, (www.hyperion-world.com).

VII.   APPENDIX

7.1.- MATLAB Code

```
%%%%%%%% RUTINA DE COMPARACION I %%%%%%%%%%%%%%%%%%%%%%
% Descripcion: Esta rutina compara la fraccion de masa del sistema
% de alimentacion (m_fs) respecto de la masa total de propelente (m_p).
%
% Comentarios:
%1.- La variable para la comparacion es la presion de camara de combustion.

clear all
close all

% 1.- VARIABLES DE
ENTRADA %%%%%%%%%%%%%%%%%%%%%%%%%%%%%%%%%%%%%%%%%%%%%%%%%%%%%%%%%%%%

% 1.1.- Presiones:

%Aclaraciones:

% Sistema 1: alimentado por gas presurizado
```

% Sistema 2: alimentado por electrobombas
% Sistema 3: alimentado por turbobombas
% Se asume que la presion en el tanque de combustible y en el tanque de
% oxidante son iguales entre si. Para cada sistema entonces se define una
% presion en el tanque de propelente.

p_c = 6.0e6;	%Presion de la camara de combustion [Pa]
p_0 = 20e6;	%Presion inicial del tanque de gas [Pa]
p_irat = 0.3;	%Relacion entre la presion de camara y la del inyector
p_tp1 = (1+p_irat)*p_c;	%Presion del tanque de propelente p/ el sist. 1 [Pa]
p_tp2 = 0.6e6;	%Presion del tanque de propelente p/ el sist. 2 [Pa]
p_tp3 = 0.6e6;	%Presion del tanque de propelente p/ el sist. 3 [Pa]
p_in = p_irat*p_c;	%Presion en el inyector [Pa]
p_gg = p_c;	%Presion de la camara del generador [Pa]
p_itu = p_gg;	%Presion de ingreso de la turbina [Pa]
p_trat = 20;	%Relacion de presiones de la turbina
p_dtu = p_itu/p_trat;	%Presion de descarga de la turbina [Pa]

% 1.2.- Temperaturas:

T_itu = 900;	%Temperatura de los gases q ingresan en la turbina [ºK]
T_g = 288.15;	%Temperatura del gas presurizante [ºK]
T_gg = 1100;	%Temperatura de la camara del generador de gas [ºK]

% 1.3.- Variables Quimicas (Masas, masas molares y const. isentropicas):

gamma_c = 1.23;	%Parametro isentropico de los gases de la camara
gamma_g = 1.667;	%Parametro isentropico del gas presurizante
gamma_gg = 1.196;	%Parametro isentropico de los gases del gen. de gas
M_c = 23;	%Masa molar de los gases de la camara [kg/kmol]
M_gg = 14.2;	%Masa molar de los gases de la gen. de gas [kg/kmol]
M_g = 4.0026;	%Masa molar del gas presurizante [kg/kmol]
OF = 1.9;	%Relacion oxidante/combustible
R_u = 8314.41;	%Constante Universal de los gases [J/kmolºK]
t_s = 10e-3;	%stay time

% 1.4.- Densidades:

rho_f = 874;	%Densidad del combustible [kg/m3]
rho_o = 1431;	%Densidad del oxidante [kg/m3]
rho_gg = 0.8774;	%Densidad de los gases de escape [kg/m3]
rho_tg = 1700;	%Densidad del tanque de gas [kg/m3]
rho_to = 2800;	%Densidad del tanque de oxidante [kg/m3]
rho_tf = 2800;	%Densidad del tanque de combustible [kg/m3]
rho_tgg = 8890;	%Densidad del material de la camara del GG [kg/m3]
	%rho_tgg = 8890 <- Hastelloy C
	%rho_tgg = 7960kg/m3 <- CRES 347
	%rho_tgg = 8800 <- Cu-Ni-Si-Cr Alloy

delta_pf = 40e3;	%Densidad de potencia de la bomba de comb. [W/kg]
delta_po = 40e3;	%Densidad de potencia de la bomba de ox. [W/kg]
delta_e = 3.8e3;	%Densidad de potencia del motor [W/kg]
delta_ef = 3.8e3;	%Densidad de potencia del motor de comb. [W/kg]
delta_eo = 3.8e3;	%Densidad de potencia del motor de ox. [W/kg]
delta_tu = 20e3;	%Densidad de potencia de la turbina [W/kg]
delta_tf = 20e3;	%Densidad de potencia de la turbina de comb. [W/kg]
delta_to = 20e3;	%Densidad de potencia de la turbina de ox. [W/kg]
delta_inv = 60e3;	%Densidad de potencia del inversor [W/kg]
delta_bap = 4.8e3;	%Densidad de potencia de las baterias [W/kg]
delta_baw = 130;	%Densidad de energia de las baterias [Wh/kg]
delta_baw = delta_baw*3600;	%Densidad de energia de las baterias [J/kg]

% 1.5.- Rendimientos:

eta_pf = 0.8;	%Rendimiento de la bomba de comb.

```
eta_po = 0.8;              %Rendimiento de la bomba de ox.
eta_e = 0.8;               %Rendimiento del motor electrico
eta_ef = 0.8;              %Rendimiento del motor de comb.
eta_eo = 0.8;              %Rendimiento del motor de ox.
eta_inv = 0.85;            %Rendimiento del inversor
eta_tu = 0.8;              %Rendimiento de la turbina


% 2.- CONSTANTES %%%%%%%%%%%%%%%%%%%%%%%%%%%%%%%%%%%%%%%%%%%%%%%%%%%%%

kappa_p1 = p_tp1/p_c;      %para el sistema de alimentacion por gas pres.
kappa_p2 = p_tp2/p_c;      %para el sist. de alim. por electrobombas
kappa_p3 = p_tp3/p_c;      %para el sist. de alim. por turbobombas
kappa_pi = p_in/p_c;       %razon de la caida en el inyector respecto de p_c
kappa_u = 1.05;            %factor de seguridad para preveer el "ullage"
kappa_g = 1.3;             %factor de seguridad para la masa de gas
kappa_tg = 2.5;            %factor de seguridad para el espesor del tanque de gas
kappa_tf = 2.5;            %factor de seguridad para el espesor del tanque de comb.
kappa_to = 2.5;            %factor de seguridad para el espesor del tanque de ox.
kappa_b = 1.2;             %margen de diseño para la masa de las baterias
kappa_gg = 2.5;            %factor de seguridad para el espesor de la pared del GG

alfa_f = 1/(rho_f*(1+OF)); %permite relacionar el volumen de comb. con m_p
alfa_o = OF/(rho_o*(1+OF)); %permite relacionar el volumen de ox. con m_p
alfa = alfa_f + alfa_o;    %permite relacionar el volumen de propelente con m_p

sigma_tg = 3.3e9;          %Resistencia max a la tension del tanque de gas [Pa]
sigma_tf = 455e6;          %Resistencia max a la tension del tanque de comb. [Pa]
sigma_to = 455e6;          %Resistencia max a la tension del tanque de ox. [Pa]
sigma_gg = 524e6;          %Resistencia max a la tension del GG (UTS)[Pa]
                           %sigma_gg = 524MPa  <- Hastelloy C (1033ºK)
                           %sigma_gg = 180MPa  <- CRES 347 (1090ºK)
                           %sigma_gg = 413.7MPa <- Cu-Ni-Si-Cr Alloy


emin = 0.001;              %espesor minimo de la pared de los tanques [m]


% 3.- PARAMETROS DE CALCULO %%%%%%%%%%%%%%%%%%%%%%%%%%%%%%%%%%%%%%%%%%

FLAG_SIST = 'A';           %A: Un solo motor/turbina
                           %B: Un motor/turbina por bomba

COTA = 0.1;                %Cota para detectar que los vectores son iguales

fp_LIM = 0.99;             %Valor limite en la razon p_c/p_0

t_bVALOR = 90;             %Valor de tiempo de combustion de interes [s]
t_b = t_bVALOR             %Tiempo de combustion del cohete [s]

m_pVALOR = 1500;           %Valor puntual de masa de propelente de interes [kg]
m_p = m_pVALOR             %Cambio un valor del vector por el valor de interes

p_cMAX = 5e6;              %Presion maxima de la camara [Pa]
p_cMIN = 0.5e6;            %Presion minima de la camara [Pa]
p_cN = 500;                %Longitud del vector p_c
p_cPASO = (p_cMAX-p_cMIN)/(p_cN-1);        %Paso de presion [Pa]

p_c = (p_cMIN:p_cPASO:p_cMAX);             %Vector de Presion de la camara [Pa]


% 4.- RUTINA DE CALCULO %%%%%%%%%%%%%%%%%%%%%%%%%%%%%%%%%%%%%%%%%%%%%%

%%% COMENTARIOS
%1.- La masa de propelente es un parametro de los graficos
%2.- La presion de la camara de combustion (para ambos sistemas) es un
%    parametro
%3.- El tiempo de combustion es un parametro
%4.- La presion inicial del gas presurizante es la variable
```

```
for i=1:size(p_c,2)

% 4.1.- CALCULO DE LA MASA DE GAS
   if p_0>(kappa_p3*p_c(i))
      %la expresion tiene sentido si p_tf<p_tg entonces se evalua esa
      %condicion
      m_g3(i) = kappa_g*kappa_u*kappa_p3*alfa*gamma_g*M_g*p_c(i)*m_p/(R_u*T_g*(1-kappa_p3*p_c(i)/p_0));
   else
      m_g3(i) = kappa_g*kappa_u*kappa_p3*alfa*gamma_g*M_g*p_c(i)*m_p/(R_u*T_g*(1-fp_LIM));
   end
   if p_0>(kappa_p2*p_c(i))
      %la expresion tiene sentido si p_tf<p_tg entonces se evalua esa
      %condicion
      m_g2(i) = kappa_g*kappa_u*kappa_p2*alfa*gamma_g*M_g*p_c(i)*m_p/(R_u*T_g*(1-kappa_p2*p_c(i)/p_0));
   else
      m_g2(i) = kappa_g*kappa_u*kappa_p2*alfa*gamma_g*M_g*p_c(i)*m_p/(R_u*T_g*(1-fp_LIM));
   end
   if p_0>(kappa_p1*p_c(i))
      %la expresion tiene sentido si p_tf<p_tg entonces se evalua esa
      %condicion
      m_g1(i) = kappa_g*kappa_u*kappa_p1*alfa*gamma_g*M_g*p_c(i)*m_p/(R_u*T_g*(1-kappa_p1*p_c(i)/p_0));
   else
      m_g1(i) = kappa_g*kappa_u*kappa_p1*alfa*gamma_g*M_g*p_c(i)*m_p/(R_u*T_g*(1-fp_LIM));
   end

% 4.2.- CALCULO DE LA MASA DE LOS TANQUES DE GAS
   if p_0>(kappa_p2*p_c(i))
      %la expresion tiene sentido si p_tf<p_tg entonces se evalua esa
      %condicion
      m_tg2(i) = 1.5*rho_tg*kappa_tg*kappa_g*kappa_u*kappa_p2*alfa*gamma_g*p_c(i)*m_p/(sigma_tg*(1-
kappa_p2*p_c(i)/p_0));
   else
      m_tg2(i) = 1.5*rho_tg*kappa_tg*kappa_g*kappa_u*kappa_p2*alfa*gamma_g*p_c(i)*m_p/(sigma_tg*(1-
fp_LIM));
   end
   if p_0>(kappa_p3*p_c(i))
      %la expresion tiene sentido si p_tf<p_tg entonces se evalua esa
      %condicion
      m_tg3(i) = 1.5*rho_tg*kappa_tg*kappa_g*kappa_u*kappa_p3*alfa*gamma_g*p_c(i)*m_p/(sigma_tg*(1-
kappa_p3*p_c(i)/p_0));
   else
      m_tg3(i) = 1.5*rho_tg*kappa_tg*kappa_g*kappa_u*kappa_p3*alfa*gamma_g*p_c(i)*m_p/(sigma_tg*(1-
fp_LIM));
   end
   if p_0>(kappa_p1*p_c(i))
      %la expresion tiene sentido si p_tf<p_tg entonces se evalua esa
      %condicion
      m_tg1(i) = 1.5*rho_tg*kappa_tg*kappa_g*kappa_u*kappa_p1*alfa*gamma_g*p_c(i)*m_p/(sigma_tg*(1-
kappa_p1*p_c(i)/p_0));
   else
      m_tg1(i) = 1.5*rho_tg*kappa_tg*kappa_g*kappa_u*kappa_p1*alfa*gamma_g*p_c(i)*m_p/(sigma_tg*(1-
fp_LIM));
   end

% 4.3.- CALCULO DE LA MASA DE LOS TANQUES DE PROPELENTE
   %Masa del tanque de combustible para el sistema de gas presurizado
   m_tf11(i) = 1.5*rho_tf*kappa_u*kappa_p1*kappa_tf*alfa_f*m_p*p_c(i)/sigma_tf;
%   m_tf12(i) = ((4*pi)^(1/3))*rho_tf*((3*kappa_u*alfa_f*m_p)^(2/3))*emin;
%   m_tf1(i) = max(m_tf11(i),m_tf12(i));
   m_tf1(i) = m_tf11(i);

   %Masa del tanque de oxidante para el sistema de gas presurizado
   m_to11(i) = 1.5*rho_to*kappa_u*kappa_p1*kappa_to*alfa_o*m_p*p_c(i)/sigma_to;
%   m_to12(i) = ((4*pi)^(1/3))*rho_to*((3*kappa_u*alfa_o*m_p)^(2/3))*emin;
%   m_to1(i) = max(m_to11(i),m_to12(i));
```

```
    m_to1(i) = m_to11(i);

    %Masa del tanque de combustible para el sistema de electrobombas
    m_tf21(i) = 1.5*rho_tf*kappa_u*kappa_p2*kappa_tf*alfa_f*m_p*p_c(i)/sigma_tf;
    m_tf22(i) = ((4*pi)^(1/3))*rho_tf*((3*kappa_u*alfa_f*m_p)^(2/3))*emin;
    m_tf2(i) = max(m_tf21(i),m_tf22(i));

    %Masa del tanque de oxidante para el sistema de electrobombas
    m_to21(i) = 1.5*rho_to*kappa_u*kappa_p2*kappa_to*alfa_o*m_p*p_c(i)/sigma_to;
    m_to22(i) = ((4*pi)^(1/3))*rho_to*((3*kappa_u*alfa_o*m_p)^(2/3))*emin;
    m_to2(i) = max(m_to21(i),m_to22(i));

    %Masa del tanque de combustible para el sistema de turbobombas
    m_tf31(i) = 1.5*rho_tf*kappa_u*kappa_p3*kappa_tf*alfa_f*m_p*p_c(i)/sigma_tf;
    m_tf32(i) = ((4*pi)^(1/3))*rho_tf*((3*kappa_u*alfa_f*m_p)^(2/3))*emin;
    m_tf3(i) = max(m_tf31(i),m_tf32(i));

    %Masa del tanque de oxidante para el sistema de turbobombas
    m_to31(i) = 1.5*rho_to*kappa_u*kappa_p3*kappa_to*alfa_o*m_p*p_c(i)/sigma_to;
    m_to32(i) = ((4*pi)^(1/3))*rho_to*((3*kappa_u*alfa_o*m_p)^(2/3))*emin;
    m_to3(i) = max(m_to31(i),m_to32(i));

% 4.4.- CALCULO DE LA MASA DE LAS BOMBAS
    m_puf(i) = (1+kappa_pi-kappa_p2)*alfa_f*p_c(i)*m_p/(delta_pf*t_b);
    m_puo(i) = (1+kappa_pi-kappa_p2)*alfa_o*p_c(i)*m_p/(delta_po*t_b);
    m_pu(i) = m_puf(i) + m_puo(i);

% 4.5.- CALCULO DE LA MASA DEL MOTOR
    switch(FLAG_SIST)
        case 'A'    %Masa con un solo motor
            m_ee(i) = (1+kappa_pi-kappa_p2)*p_c(i)*m_p*(alfa_f/eta_pf+alfa_o/eta_po)/(delta_e*t_b);
        case 'B'    %Masa con un motor por bomba
            m_ef(i) = (1+kappa_pi-kappa_p2)*alfa_f*p_c(i)*m_p/(eta_pf*delta_e*t_b);
            m_eo(i) = (1+kappa_pi-kappa_p2)*alfa_o*p_c(i)*m_p/(eta_po*delta_e*t_b);
            m_ee(i) = m_ef(i) + m_eo(i);
        otherwise
            ERROR(i) = 1;
    end

% 4.6.- CALCULO DE LA MASA DE LA TURBINA
    switch(FLAG_SIST)
        case 'A'    %Masa con una sola turbina
            m_tu(i) = (1+kappa_pi-kappa_p3)*p_c(i)*m_p*(alfa_f/eta_pf+alfa_o/eta_po)/(delta_tu*t_b);
        case 'B'    %Masa con una turbina por bomba
            m_tf(i) = (1+kappa_pi-kappa_p3)*alfa_f*p_c(i)*m_p/(eta_pf*delta_tf*t_b);
            m_to(i) = (1+kappa_pi-kappa_p3)*alfa_o*p_c(i)*m_p/(eta_po*delta_to*t_b);
            m_tu(i) = m_tf(i) + m_to(i);
        otherwise
            ERROR(i) = 1;
    end

% 4.7.- CALCULO DE LA MASA DEL INVERSOR
    switch(FLAG_SIST)
        case 'A'    %Masa del inversor con un solo motor
            m_inv(i) = (1+kappa_pi-kappa_p2)*p_c(i)*m_p*(alfa_f/eta_pf+alfa_o/eta_po)/(eta_e*delta_inv*t_b);
        case 'B'    %Masa de los inversores con un motor por bomba
            m_inf(i) = (1+kappa_pi-kappa_p2)*alfa_f*p_c(i)*m_p/(eta_pf*eta_ef*delta_inv*t_b);
            m_ino(i) = (1+kappa_pi-kappa_p2)*alfa_o*p_c(i)*m_p/(eta_po*eta_eo*delta_inv*t_b);
            m_inv(i) = m_inf(i) + m_ino(i);
        otherwise
            ERROR(i) = 1;
    end

% 4.8.- CALCULO DE LA MASA DE LAS BATERIAS
    switch(FLAG_SIST)
        case 'A'    %Masa de las baterias con un solo motor
```

```
        m_bap(i) = (1+kappa_pi-
kappa_p2)*p_c(i)*m_p*kappa_b*(alfa_f/eta_pf+alfa_o/eta_po)/(eta_e*eta_inv*delta_bap*t_b);
        m_baw(i) = (1+kappa_pi-
kappa_p2)*p_c(i)*m_p*kappa_b*(alfa_f/eta_pf+alfa_o/eta_po)/(eta_e*eta_inv*delta_baw);
        m_bat(i) = max(m_bap(i),m_baw(i));
      case 'B'    %Masa de las baterias con un motor por bomba
        m_bap(i) = (1+kappa_pi-
kappa_p2)*p_c(i)*m_p*kappa_b*(alfa_f/(eta_pf*eta_ef*eta_inv)+alfa_o/(eta_po*eta_eo*eta_inv))/(delta_bap*t_b);
        m_baw(i) = (1+kappa_pi-
kappa_p2)*p_c(i)*m_p*kappa_b*(alfa_f/(eta_pf*eta_ef*eta_inv)+alfa_o/(eta_po*eta_eo*eta_inv))/delta_baw;
        m_bat(i) = max(m_bap(i),m_baw(i));
      otherwise
        ERROR(i) = 1;
    end

% 4.9.- CALCULO DE PROPELENTE PARA ACCIONAR LA TURBINA
    m_ptu(i) = (1+kappa_pi-kappa_p3)*p_c(i)*m_p*M_gg*(gamma_gg-
1)*(alfa_f/eta_pf+alfa_o/eta_po)/(eta_tu*T_itu*gamma_gg*R_u*(1-(p_dtu/p_itu)^((gamma_gg-1)/gamma_gg)));

% 4.10.- CALCULO DE LA MASA DEL GENERADOR DE GAS
    V_g(i) = t_s*m_ptu(i)/(t_b*rho_gg);
    r_g(i) = (0.75*V_g(i))^(1/3);
    S_g(i) = 4*pi*(0.75*V_g(i)/pi)^(2/3);
    m_gg(i) = rho_tgg*kappa_gg*p_gg*r_g(i)*S_g(i)/(2*sigma_gg);

end


% Se detecta el punto a partir del cual la masa de las baterias pasa de ser
% impuesta por la potencia a ser impuesta por la energia

Indices = find((m_bat-m_baw)<COTA);
if length(Indices)>0
    LIMITE = Indices(1);
else
    LIMITE = p_cN-1;
end


% Se calcula la masa total de cada sistema

m_pg = m_g1 + m_tg1 + m_tf1 + m_to1;
m_tp = m_g3 + m_tg3 + m_tf3 + m_to3 + m_pu + m_tu + m_gg + m_ptu;

% Para el sistema electrico se separa la curva en dos (una si la masa de
% las baterias esta impuesta por potencia y la otra por energia) de modo
% que luego se las pueda diferenciar con el trazo

 for k=1:LIMITE
    p_cA(k) = p_c(k);
    m_epA(k) = m_g2(k) + m_tg2(k) + m_tf2(k) + m_to2(k) + m_pu(k) + m_ee(k) + m_inv(k) +
max(m_bap(k),m_baw(k));
 end

 for j=1:(length(p_c)-LIMITE)
    p_cB(j) = p_c(j+LIMITE-1);
    m_epB(j) = m_g2(j+LIMITE-1) + m_tg2(j+LIMITE-1) + m_tf2(j+LIMITE-1) + m_to2(j+LIMITE-1) +
m_pu(j+LIMITE-1) + m_ee(j+LIMITE-1) + m_inv(j+LIMITE-1) + max(m_bap(j+LIMITE-1),m_baw(j+LIMITE-1));
 end


% Se calculan las fracciones de masa de los tres sistemas

fm_pg = m_pg/m_p;           %Fraccion de masas: gas presurizado/masa propelente
fm_epA = m_epA/m_p;         %Fraccion de masas: electrobombas/masa propelente
fm_epB = m_epB/m_p;         %Fraccion de masas: electrobombas/masa propelente
fm_tp = m_tp/m_p;           %Fraccion de masas: turbobombas/masa propelente
```

```
% 4.- RUTINA DE GENERACION DE GRAFICOS %%%%%%%%%%%%%%%%%%%%%%%%%%%%%%%%%%%

p_c = p_c/1e6;              %Se convierte de Pa a MPa
p_cA = p_cA/1e6;            %Se convierte de Pa a MPa
p_cB = p_cB/1e6;            %Se convierte de Pa a MPa

x_MIN = p_cMIN/1e6;
x_MAX = p_cMAX/1e6;
y_MIN = 0;
y_MAX = 0.15;
x_COOR = x_MIN+0.05*(x_MAX-x_MIN);
y_COOR = y_MIN+0.65*(y_MAX-y_MIN);
RENGLON = 0.05*(y_MAX-y_MIN);

figure
plot(p_c,fm_pg,'b','linewidth',2)
axis([x_MIN x_MAX y_MIN y_MAX])
xlabel('Presion de la camara de comb. P_C [MPa]','FontSize',12,'FontWeight','demi')
ylabel('m_f_s/m_p','FontSize',12,'FontWeight','demi')
title('Relacion Masa del Sist. de Alimentacion vs Masa de Propelente','FontSize',14)
text(x_COOR,y_COOR,['Masa de propelente: m_p = ' num2str(m_pVALOR) 'kg'])
text(x_COOR,y_COOR-RENGLON,['Tiempo de combustion: t_b = ' num2str(t_bVALOR) 's'])
grid on
hold on
plot(p_cA,fm_epA,'r','linewidth',2)
hold on
plot(p_cB,fm_epB,'r--','linewidth',2)
hold on
plot(p_c,fm_tp,'g','linewidth',2)
legend('Sist. Gas Presurizado','Sist. de Electrobombas (m_b_a_t impuesta por P)','Sist. de Electrobombas (m_b_a_t
impuesta por W)','Sist. de Turbobombas',2)

saveas(gcf,['masa_vs_PC_ver05_mp_' num2str(m_pVALOR) '_tb_' num2str(t_bVALOR) '.png'])




%%%%%%%% RUTINA DE COMPARACION II %%%%%%%%%%%%%%%%%%%%%%%%%%%
% Descripcion: Esta rutina compara la fraccion de masa del sistema
% de alimentacion (m_fs) respecto de la masa total de propelente (m_p).
%
% Comentarios:
%1.- La variable para la comparacion es la presion inicial de gas.

clear all
close all

% 1.- VARIABLES DE ENTRADA %%%%%%%%%%%%%%%%%%%%%%%%%%%%%%%%%%%%%%%%%%%%

% 1.1.- Presiones:

%Aclaraciones:

% Sistema 1: alimentado por gas presurizado
% Sistema 2: alimentado por electrobombas
% Sistema 3: alimentado por turbobombas
% Se asume que la presion en el tanque de combustible y en el tanque de
% oxidante son iguales entre si. Para cada sistema entonces se define una
% presion en el tanque de propelente.


p_c = 6.0e6;               %Presion de la camara de combustion [Pa]
p_0 = 20e6;                %Presion inicial del tanque de gas [Pa]
p_irat = 0.3;              %Relacion entre la presion de camara y la del inyector
p_tp1 = (1+p_irat)*p_c;    %Presion del tanque de propelente p/ el sist. 1 [Pa]
p_tp2 = 0.6e6;             %Presion del tanque de propelente p/ el sist. 2 [Pa]
p_tp3 = 0.6e6;             %Presion del tanque de propelente p/ el sist. 3 [Pa]
```

```
p_in = p_irat*p_c;              %Presion en el inyector [Pa]
p_gg = p_c;                     %Presion de la camara del generador [Pa]
p_itu = p_gg;                   %Presion de ingreso de la turbina [Pa]
p_trat = 20;                    %Relacion de presiones de la turbina
p_dtu = p_itu/p_trat;           %Presion de descarga de la turbina [Pa]
```

% 1.2.- Temperaturas:

```
T_itu = 900;                    %Temperatura de los gases q ingresan en la turbina [ºK]
T_g = 288.15;                   %Temperatura del gas presurizante [ºK]
T_gg = 1100;                    %Temperatura de la camara del generador de gas [ºK]
```

% 1.3.- Variables Quimicas (Masas, masas molares y const. isentropicas):

```
gamma_c = 1.23;                 %Parametro isentropico de los gases de la camara
gamma_g = 1.667;                %Parametro isentropico del gas presurizante
gamma_gg = 1.196;               %Parametro isentropico de los gases del gen. de gas
M_c = 23;                       %Masa molar de los gases de la camara [kg/kmol]
M_gg = 14.2;                    %Masa molar de los gases de la gen. de gas [kg/kmol]
M_g = 4.0026;                   %Masa molar del gas presurizante [kg/kmol]
OF = 1.9;                       %Relacion oxidante/combustible
R_u = 8314.41;                  %Constante Universal de los gases [J/kmolºK]
t_s = 10e-3;                    %stay time
```

% 1.4.- Densidades:

```
rho_f = 874;                    %Densidad del combustible [kg/m3]
rho_o = 1431;                   %Densidad del oxidante [kg/m3]
rho_gg = 0.8774;                %Densidad de los gases de escape [kg/m3]
rho_tg = 1700;                  %Densidad del tanque de gas [kg/m3]
rho_to = 2800;                  %Densidad del tanque de oxidante [kg/m3]
rho_tf = 2800;                  %Densidad del tanque de combustible [kg/m3]
rho_tgg = 8890;                 %Densidad del material de la camara del GG [kg/m3]
                                %rho_tgg = 8890 <- Hastelloy C
                                %rho_tgg = 7960kg/m3 <- CRES 347
                                %rho_tgg = 8800 <- Cu-Ni-Si-Cr Alloy


delta_pf = 40e3;                %Densidad de potencia de la bomba de comb. [W/kg]
delta_po = 40e3;                %Densidad de potencia de la bomba de ox. [W/kg]
delta_e = 3.8e3;                %Densidad de potencia del motor [W/kg]
delta_ef = 3.8e3;               %Densidad de potencia del motor de comb. [W/kg]
delta_eo = 3.8e3;               %Densidad de potencia del motor de ox. [W/kg]
delta_tu = 20e3;                %Densidad de potencia de la turbina [W/kg]
delta_tf = 20e3;                %Densidad de potencia de la turbina de comb. [W/kg]
delta_to = 20e3;                %Densidad de potencia de la turbina de ox. [W/kg]
delta_inv = 60e3;               %Densidad de potencia del inversor [W/kg]
delta_bap = 4.8e3;              %Densidad de potencia de las baterias [W/kg]
delta_baw = 130;                %Densidad de energia de las baterias [Wh/kg]
delta_baw = delta_baw*3600;     %Densidad de energia de las baterias [J/kg]
```

% 1.5.- Rendimientos:

```
eta_pf = 0.8;                   %Rendimiento de la bomba de comb.
eta_po = 0.8;                   %Rendimiento de la bomba de ox.
eta_e = 0.8;                    %Rendimiento del motor electrico
eta_ef = 0.8;                   %Rendimiento del motor de comb.
eta_eo = 0.8;                   %Rendimiento del motor de ox.
eta_inv = 0.85;                 %Rendimiento del inversor
eta_tu = 0.8;                   %Rendimiento de la turbina
```

% 2.- CONSTANTES %%%

```
kappa_p1 = p_tp1/p_c;           %para el sistema de alimentacion por gas pres.
kappa_p2 = p_tp2/p_c;           %para el sist. de alim. por electrobombas
kappa_p3 = p_tp3/p_c;           %para el sist. de alim. por turbobombas
kappa_pi = p_in/p_c;            %razon de la caida en el inyector respecto de p_c
```

```
kappa_u = 1.05;          %factor de seguridad para preveer el "ullage"
kappa_g = 1.3;           %factor de seguridad para la masa de gas
kappa_tg = 2.5;          %factor de seguridad para el espesor del tanque de gas
kappa_tf = 2.5;          %factor de seguridad para el espesor del tanque de comb.
kappa_to = 2.5;          %factor de seguridad para el espesor del tanque de ox.
kappa_b = 1.2;           %margen de diseño para la masa de las baterias
kappa_gg = 2.5;          %factor de seguridad para el espesor de la pared del GG

alfa_f = 1/(rho_f*(1+OF));   %permite relacionar el volumen de comb. con m_p
alfa_o = OF/(rho_o*(1+OF)); %permite relacionar el volumen de ox. con m_p
alfa = alfa_f + alfa_o;      %permite relacionar el volumen de propelente con m_p

sigma_tg = 3.3e9;        %Resistencia max a la tension del tanque de gas [Pa]
sigma_tf = 455e6;        %Resistencia max a la tension del tanque de comb. [Pa]
sigma_to = 455e6;        %Resistencia max a la tension del tanque de ox. [Pa]
sigma_gg = 524e6;        %Resistencia max a la tension del GG (UTS)[Pa]
                         %sigma_gg = 524MPa   <- Hastelloy C (1033ºK)
                         %sigma_gg = 180MPa   <- CRES 347 (1090ºK)
                         %sigma_gg = 413.7MPa <- Cu-Ni-Si-Cr Alloy

emin = 0.001;            %espesor minimo de la pared de los tanques [m]

% 3.- PARAMETROS DE CALCULO %%%%%%%%%%%%%%%%%%%%%%%%%%%%%%%%%%%%%%%%%%%%%

FLAG_SIST = 'A';         %A: Un solo motor/turbina
                         %B: Un motor/turbina por bomba

COTA = 0.1;             %Cota para detectar que los vectores son iguales

fp_LIM = 0.99;          %Valor limite en la razon p_c/p_0

t_bVALOR = 90;          %Valor de tiempo de combustion de interes [s]
t_b = t_bVALOR          %Tiempo de combustion del cohete [s]

m_pVALOR = 1500;        %Valor puntual de masa de propelente de interes [kg]
m_p = m_pVALOR          %Cambio un valor del vector por el valor de interes

p_iMAX = 40e6;          %Presion maxima del tanque de gas [Pa]
p_iMIN = 1e6;           %Presion minima del tanque de gas [Pa]
p_iN = 500;             %Longitud del vector p_i
p_iPASO = (p_iMAX-p_iMIN)/(p_iN-1);      %Paso de presion [Pa]

p_i = (p_iMIN:p_iPASO:p_iMAX);           %Vector de Presion del tanque de gas [Pa]


% 4.- RUTINA DE CALCULO %%%%%%%%%%%%%%%%%%%%%%%%%%%%%%%%%%%%%%%%%%%%%%%%%

%%% COMENTARIOS
%1.- La masa de propelente es un parametro de los graficos
%2.- La presion de la camara de combustion (para ambos sistemas) es un
%    parametro
%3.- El tiempo de combustion es un parametro
%4.- La presion inicial del gas presurizante es la variable


for i=1:size(p_i,2)

% 4.1.- CALCULO DE LA MASA DE GAS
   if p_i(i)>(kappa_p3*p_c)
      %la expresion tiene sentido si p_tf<p_tg entonces se evalua esa
      %condicion
      m_g3(i) = kappa_g*kappa_u*kappa_p3*alfa*gamma_g*M_g*p_c*m_p/(R_u*T_g*(1-kappa_p3*p_c/p_i(i)));
   else
      m_g3(i) = kappa_g*kappa_u*kappa_p3*alfa*gamma_g*M_g*p_c*m_p/(R_u*T_g*(1-fp_LIM));
   end
   if p_i(i)>(kappa_p2*p_c)
      %la expresion tiene sentido si p_tf<p_tg entonces se evalua esa
```

```
    %condicion
    m_g2(i) = kappa_g*kappa_u*kappa_p2*alfa*gamma_g*M_g*p_c*m_p/(R_u*T_g*(1-kappa_p2*p_c/p_i(i)));
  else
    m_g2(i) = kappa_g*kappa_u*kappa_p2*alfa*gamma_g*M_g*p_c*m_p/(R_u*T_g*(1-fp_LIM));
  end
  if p_i(i)>(kappa_p1*p_c)
    %la expresion tiene sentido si p_tf<p_tg entonces se evalua esa
    %condicion
    m_g1(i) = kappa_g*kappa_u*kappa_p1*alfa*gamma_g*M_g*p_c*m_p/(R_u*T_g*(1-kappa_p1*p_c/p_i(i)));
  else
    m_g1(i) = kappa_g*kappa_u*kappa_p1*alfa*gamma_g*M_g*p_c*m_p/(R_u*T_g*(1-fp_LIM));
  end

% 4.2.- CALCULO DE LA MASA DE LOS TANQUES DE GAS
  if p_i(i)>(kappa_p2*p_c)
    %la expresion tiene sentido si p_tf<p_tg entonces se evalua esa
    %condicion
    m_tg2(i) = 1.5*rho_tg*kappa_tg*kappa_g*kappa_u*kappa_p2*alfa*gamma_g*p_c*m_p/(sigma_tg*(1-
kappa_p2*p_c/p_i(i)));
  else
    m_tg2(i) = 1.5*rho_tg*kappa_tg*kappa_g*kappa_u*kappa_p2*alfa*gamma_g*p_c*m_p/(sigma_tg*(1-
fp_LIM));
  end
  if p_i(i)>(kappa_p3*p_c)
    %la expresion tiene sentido si p_tf<p_tg entonces se evalua esa
    %condicion
    m_tg3(i) = 1.5*rho_tg*kappa_tg*kappa_g*kappa_u*kappa_p3*alfa*gamma_g*p_c*m_p/(sigma_tg*(1-
kappa_p3*p_c/p_i(i)));
  else
    m_tg3(i) = 1.5*rho_tg*kappa_tg*kappa_g*kappa_u*kappa_p3*alfa*gamma_g*p_c*m_p/(sigma_tg*(1-
fp_LIM));
  end
  if p_i(i)>(kappa_p1*p_c)
    %la expresion tiene sentido si p_tf<p_tg entonces se evalua esa
    %condicion
    m_tg1(i) = 1.5*rho_tg*kappa_tg*kappa_g*kappa_u*kappa_p1*alfa*gamma_g*p_c*m_p/(sigma_tg*(1-
kappa_p1*p_c/p_i(i)));
  else
    m_tg1(i) = 1.5*rho_tg*kappa_tg*kappa_g*kappa_u*kappa_p1*alfa*gamma_g*p_c*m_p/(sigma_tg*(1-
fp_LIM));
  end

% 4.3.- CALCULO DE LA MASA DE LOS TANQUES DE PROPELENTE
  %Masa del tanque de combustible para el sistema de gas presurizado
  m_tf11(i) = 1.5*rho_tf*kappa_u*kappa_p1*kappa_tf*alfa_f*m_p*p_c/sigma_tf;
  m_tf12(i) = ((4*pi)^(1/3))*rho_tf*((3*kappa_u*alfa_f*m_p)^(2/3))*emin;
  m_tf1(i) = max(m_tf11(i),m_tf12(i));

  %Masa del tanque de oxidante para el sistema de gas presurizado
  m_to11(i) = 1.5*rho_to*kappa_u*kappa_p1*kappa_to*alfa_o*m_p*p_c/sigma_to;
  m_to12(i) = ((4*pi)^(1/3))*rho_to*((3*kappa_u*alfa_o*m_p)^(2/3))*emin;
  m_to1(i) = max(m_to11(i),m_to12(i));

  %Masa del tanque de combustible para el sistema de electrobombas
  m_tf21(i) = 1.5*rho_tf*kappa_u*kappa_p2*kappa_tf*alfa_f*m_p*p_c/sigma_tf;
  m_tf22(i) = ((4*pi)^(1/3))*rho_tf*((3*kappa_u*alfa_f*m_p)^(2/3))*emin;
  m_tf2(i) = max(m_tf21(i),m_tf22(i));

  %Masa del tanque de oxidante para el sistema de electrobombas
  m_to21(i) = 1.5*rho_to*kappa_u*kappa_p2*kappa_to*alfa_o*m_p*p_c/sigma_to;
  m_to22(i) = ((4*pi)^(1/3))*rho_to*((3*kappa_u*alfa_o*m_p)^(2/3))*emin;
  m_to2(i) = max(m_to21(i),m_to22(i));

  %Masa del tanque de combustible para el sistema de turbobombas
  m_tf31(i) = 1.5*rho_tf*kappa_u*kappa_p3*kappa_tf*alfa_f*m_p*p_c/sigma_tf;
  m_tf32(i) = ((4*pi)^(1/3))*rho_tf*((3*kappa_u*alfa_f*m_p)^(2/3))*emin;
  m_tf3(i) = max(m_tf31(i),m_tf32(i));
```

```
   %Masa del tanque de oxidante para el sistema de turbobombas
   m_to31(i) = 1.5*rho_to*kappa_u*kappa_p3*kappa_to*alfa_o*m_p*p_c/sigma_to;
   m_to32(i) = ((4*pi)^(1/3))*rho_to*((3*kappa_u*alfa_o*m_p)^(2/3))*emin;
   m_to3(i) = max(m_to31(i),m_to32(i));

% 4.4.- CALCULO DE LA MASA DE LAS BOMBAS
   m_puf(i) = (1+kappa_pi-kappa_p2)*alfa_f*p_c*m_p/(delta_pf*t_b);
   m_puo(i) = (1+kappa_pi-kappa_p2)*alfa_o*p_c*m_p/(delta_po*t_b);
   m_pu(i) = m_puf(i) + m_puo(i);

% 4.5.- CALCULO DE LA MASA DEL MOTOR
   switch(FLAG_SIST)
      case 'A'    %Masa con un solo motor
        m_ee(i) = (1+kappa_pi-kappa_p2)*p_c*m_p*(alfa_f/eta_pf+alfa_o/eta_po)/(delta_e*t_b);
      case 'B'    %Masa con un motor por bomba
        m_ef(i) = (1+kappa_pi-kappa_p2)*alfa_f*p_c*m_p/(eta_pf*delta_e*t_b);
        m_eo(i) = (1+kappa_pi-kappa_p2)*alfa_o*p_c*m_p/(eta_po*delta_e*t_b);
        m_ee(i) = m_ef(i) + m_eo(i);
      otherwise
        ERROR(i) = 1;
   end

% 4.6.- CALCULO DE LA MASA DE LA TURBINA
   switch(FLAG_SIST)
      case 'A'    %Masa con una sola turbina
        m_tu(i) = (1+kappa_pi-kappa_p3)*p_c*m_p*(alfa_f/eta_pf+alfa_o/eta_po)/(delta_tu*t_b);
      case 'B'    %Masa con una turbina por bomba
        m_tf(i) = (1+kappa_pi-kappa_p3)*alfa_f*p_c*m_p/(eta_pf*delta_tf*t_b);
        m_to(i) = (1+kappa_pi-kappa_p3)*alfa_o*p_c*m_p/(eta_po*delta_to*t_b);
        m_tu(i) = m_tf(i) + m_to(i);
      otherwise
        ERROR(i) = 1;
   end

% 4.7.- CALCULO DE LA MASA DEL INVERSOR
   switch(FLAG_SIST)
      case 'A'    %Masa del inversor con un solo motor
        m_inv(i) = (1+kappa_pi-kappa_p2)*p_c*m_p*(alfa_f/eta_pf+alfa_o/eta_po)/(eta_e*delta_inv*t_b);
      case 'B'    %Masa de los inversores con un motor por bomba
        m_inf(i) = (1+kappa_pi-kappa_p2)*alfa_f*p_c*m_p/(eta_pf*eta_ef*delta_inv*t_b);
        m_ino(i) = (1+kappa_pi-kappa_p2)*alfa_o*p_c*m_p/(eta_po*eta_eo*delta_inv*t_b);
        m_inv(i) = m_inf(i) + m_ino(i);
      otherwise
        ERROR(i) = 1;
   end

% 4.8.- CALCULO DE LA MASA DE LAS BATERIAS
   switch(FLAG_SIST)
      case 'A'    %Masa de las baterias con un solo motor
        m_bap(i) = (1+kappa_pi-
kappa_p2)*p_c*m_p*kappa_b*(alfa_f/eta_pf+alfa_o/eta_po)/(eta_e*eta_inv*delta_bap*t_b);
        m_baw(i) = (1+kappa_pi-
kappa_p2)*p_c*m_p*kappa_b*(alfa_f/eta_pf+alfa_o/eta_po)/(eta_e*eta_inv*delta_baw);
        m_bat(i) = max(m_bap(i),m_baw(i));
      case 'B'    %Masa de las baterias con un motor por bomba
        m_bap(i) = (1+kappa_pi-
kappa_p2)*p_c*m_p*kappa_b*(alfa_f/(eta_pf*eta_ef*eta_inv)+alfa_o/(eta_po*eta_eo*eta_inv))/(delta_bap*t_b);
        m_baw(i) = (1+kappa_pi-
kappa_p2)*p_c*m_p*kappa_b*(alfa_f/(eta_pf*eta_ef*eta_inv)+alfa_o/(eta_po*eta_eo*eta_inv))/delta_baw;
        m_bat(i) = max(m_bap(i),m_baw(i));
      otherwise
        ERROR(i) = 1;
   end

% 4.9.- CALCULO DE PROPELENTE PARA ACCIONAR LA TURBINA
```

```
    m_ptu(i) = (1+kappa_pi-kappa_p3)*p_c*m_p*M_gg*(gamma_gg-
1)*(alfa_f/eta_pf+alfa_o/eta_po)/(eta_tu*T_itu*gamma_gg*R_u*(1-(p_dtu/p_itu)^((gamma_gg-1)/gamma_gg)));

% 4.10.- CALCULO DE LA MASA DEL GENERADOR DE GAS
    V_g(i) = t_s*m_ptu(i)/(t_b*rho_gg);
    r_g(i) = (0.75*V_g(i))^(1/3);
    S_g(i) = 4*pi*(0.75*V_g(i)/pi)^(2/3);
    m_gg(i) = rho_tgg*kappa_gg*p_gg*r_g(i)*S_g(i)/(2*sigma_gg);

end


Indices = find((m_bat-m_baw)<COTA);
if length(Indices)>0
    LIMITE = Indices(1);
else
    LIMITE = p_iN-1;
end

m_pg = m_g1 + m_tg1 + m_tf1 + m_to1;
m_tp = m_g3 + m_tg3 + m_tf3 + m_to3 + m_pu + m_tu + m_gg + m_ptu;

 for k=1:LIMITE
    p_iA(k) = p_i(k);
    m_epA(k) = m_g2(k) + m_tg2(k) + m_tf2(k) + m_to2(k) + m_pu(k) + m_ee(k) + m_inv(k) +
max(m_bap(k),m_baw(k));
 end

 for j=1:(length(p_i)-LIMITE)
    p_iB(j) = p_i(j+LIMITE-1);
    m_epB(j) = m_g2(j+LIMITE-1) + m_tg2(j+LIMITE-1) + m_tf2(j+LIMITE-1) + m_to2(j+LIMITE-1) +
m_pu(j+LIMITE-1) + m_ee(j+LIMITE-1) + m_inv(j+LIMITE-1) + max(m_bap(j+LIMITE-1),m_baw(j+LIMITE-1));
 end


fm_pg = m_pg/m_p;              %Fraccion de masas: gas presurizado/masa propelente
fm_epA = m_epA/m_p;            %Fraccion de masas: electrobombas/masa propelente
fm_epB = m_epB/m_p;            %Fraccion de masas: electrobombas/masa propelente
fm_tp = m_tp/m_p;              %Fraccion de masas: turbobombas/masa propelente

% 4.- RUTINA DE GENERACION DE GRAFICOS %%%%%%%%%%%%%%%%%%%%%%%%%%%%%%%%%%%%%%

p_i = p_i/1e6;                 %Paso de Pa a MPa
p_iA = p_iA/1e6;               %Paso de Pa a MPa
p_iB = p_iB/1e6;               %Paso de Pa a MPa

x_MIN = p_iMIN/1e6;
x_MAX = p_iMAX/1e6;
y_MIN = 0;
y_MAX = 0.15;
x_COOR = x_MIN+0.05*(x_MAX-x_MIN);
y_COOR = y_MIN+0.7*(y_MAX-y_MIN);
RENGLON = 0.05*(y_MAX-y_MIN);

figure
plot(p_i,fm_pg,'b','linewidth',2)
axis([x_MIN x_MAX y_MIN y_MAX])
xlabel('Presion inicial del gas P_0 [MPa]','FontSize',12,'FontWeight','demi')
ylabel('m_f_s/m_p','FontSize',12,'FontWeight','demi')
title('Relacion Masa del Sist. de Alimentacion vs Masa de Propelente','FontSize',14)
text(x_COOR,y_COOR,['Masa de propelente: m_p = ' num2str(m_pVALOR) 'kg'])
text(x_COOR,y_COOR-RENGLON,['Tiempo de combustion: t_b = ' num2str(t_bVALOR) 's'])
grid on
hold on
plot(p_iA,fm_epA,'r','linewidth',2)
hold on
plot(p_iB,fm_epB,'r--','linewidth',2)
```

```
hold on
plot(p_i,fm_tp,'g','linewidth',2)
legend('Sist. Gas Presurizado','Sist. de Electrobombas (m_b_a_t impuesta por P)','Sist. de Electrobombas (m_b_a_t
impuesta por W)','Sist. de Turbobombas',1)

saveas(gcf,['masa_vs_P0_ver05_mp_' num2str(m_pVALOR) '_tb_' num2str(t_bVALOR) '_PC_' num2str(p_c/1e5)
'.png'])
```

```
%%%%%%% RUTINA DE COMPARACION III %%%%%%%%%%%%%%%%%%%%%%%
% Descripcion: Esta rutina compara la fraccion de masa del sistema
% de alimentacion (m_fs) respecto de la masa total de propelente (m_p).
%
% Comentarios:
%1.- La variable para la comparacion es el tiempo de combustion.

clear all
close all

% 1.- VARIABLES DE ENTRADA %%%%%%%%%%%%%%%%%%%%%%%%%%%%%%%%%%%%%%%%%%%%%%

% 1.1.- Presiones:

%Aclaraciones:

% Sistema 1: alimentado por gas presurizado
% Sistema 2: alimentado por electrobombas
% Sistema 3: alimentado por turbobombas
% Se asume que la presion en el tanque de combustible y en el tanque de
% oxidante son iguales entre si. Para cada sistema entonces se define una
% presion en el tanque de propelente.


p_c = 6.0e6;                    %Presion de la camara de combustion [Pa]
p_0 = 20e6;                     %Presion inicial del tanque de gas [Pa]
p_irat = 0.3;                   %Relacion entre la presion de camara y la del inyector
p_tp1 = (1+p_irat)*p_c;         %Presion del tanque de propelente p/ el sist. 1 [Pa]
p_tp2 = 0.6e6;                  %Presion del tanque de propelente p/ el sist. 2 [Pa]
p_tp3 = 0.6e6;                  %Presion del tanque de propelente p/ el sist. 3 [Pa]
p_in = p_irat*p_c;              %Presion en el inyector [Pa]
p_gg = p_c;                     %Presion de la camara del generador [Pa]
p_itu = p_gg;                   %Presion de ingreso de la turbina [Pa]
p_trat = 20;                    %Relacion de presiones de la turbina
p_dtu = p_itu/p_trat;           %Presion de descarga de la turbina [Pa]

% 1.2.- Temperaturas:

T_itu = 900;                    %Temperatura de los gases q ingresan en la turbina [ºK]
T_g = 288.15;                   %Temperatura del gas presurizante [ºK]
T_gg = 1100;                    %Temperatura de la camara del generador de gas [ºK]

% 1.3.- Variables Quimicas (Masas, masas molares y const. isentropicas):

gamma_c = 1.23;                 %Parametro isentropico de los gases de la camara
gamma_g = 1.667;                %Parametro isentropico del gas presurizante
gamma_gg = 1.196;               %Parametro isentropico de los gases del gen. de gas
M_c = 23;                       %Masa molar de los gases de la camara [kg/kmol]
M_gg = 14.2;                    %Masa molar de los gases de la gen. de gas [kg/kmol]
M_g = 4.0026;                   %Masa molar del gas presurizante [kg/kmol]
OF = 1.9;                       %Relacion oxidante/combustible
R_u = 8314.41;                  %Constante Universal de los gases [J/kmolºK]
t_s = 10e-3;                    %stay time

% 1.4.- Densidades:

rho_f = 874;                    %Densidad del combustible [kg/m3]
rho_o = 1431;                   %Densidad del oxidante [kg/m3]
```

```
rho_gg = 0.8774;              %Densidad de los gases de escape [kg/m3]
rho_tg = 1700;                %Densidad del tanque de gas [kg/m3]
rho_to = 2800;                %Densidad del tanque de oxidante [kg/m3]
rho_tf = 2800;                %Densidad del tanque de combustible [kg/m3]
rho_tgg = 8890;               %Densidad del material de la camara del GG [kg/m3]
                             %rho_tgg = 8890 <- Hastelloy C
                             %rho_tgg = 7960kg/m3 <- CRES 347
                             %rho_tgg = 8800 <- Cu-Ni-Si-Cr Alloy


delta_pf = 40e3;             %Densidad de potencia de la bomba de comb. [W/kg]
delta_po = 40e3;             %Densidad de potencia de la bomba de ox. [W/kg]
delta_e = 3.8e3;             %Densidad de potencia del motor [W/kg]
delta_ef = 3.8e3;            %Densidad de potencia del motor de comb. [W/kg]
delta_eo = 3.8e3;            %Densidad de potencia del motor de ox. [W/kg]
delta_tu = 20e3;             %Densidad de potencia de la turbina [W/kg]
delta_tf = 20e3;             %Densidad de potencia de la turbina de comb. [W/kg]
delta_to = 20e3;             %Densidad de potencia de la turbina de ox. [W/kg]
delta_inv = 60e3;            %Densidad de potencia del inversor [W/kg]
delta_bap = 4.8e3;           %Densidad de potencia de las baterias [W/kg]
delta_baw = 130;             %Densidad de energia de las baterias [Wh/kg]
delta_baw = delta_baw*3600;  %Densidad de energia de las baterias [J/kg]
```

% 1.5.- Rendimientos:

```
eta_pf = 0.8;                %Rendimiento de la bomba de comb.
eta_po = 0.8;                %Rendimiento de la bomba de ox.
eta_e = 0.8;                 %Rendimiento del motor electrico
eta_ef = 0.8;                %Rendimiento del motor de comb.
eta_eo = 0.8;                %Rendimiento del motor de ox.
eta_inv = 0.85;              %Rendimiento del inversor
eta_tu = 0.8;                %Rendimiento de la turbina
```

% 2.- CONSTANTES %%%

```
kappa_p1 = p_tp1/p_c;        %para el sistema de alimentacion por gas pres.
kappa_p2 = p_tp2/p_c;        %para el sist. de alim. por electrobombas
kappa_p3 = p_tp3/p_c;        %para el sist. de alim. por turbobombas
kappa_pi = p_in/p_c;         %razon de la caida en el inyector respecto de p_c
kappa_u = 1.05;              %factor de seguridad para preveer el "ullage"
kappa_g = 1.3;               %factor de seguridad para la masa de gas
kappa_tg = 2.5;              %factor de seguridad para el espesor del tanque de gas
kappa_tf = 2.5;              %factor de seguridad para el espesor del tanque de comb.
kappa_to = 2.5;              %factor de seguridad para el espesor del tanque de ox.
kappa_b = 1.2;               %margen de diseño para la masa de las baterias
kappa_gg = 2.5;              %factor de seguridad para el espesor de la pared del GG

alfa_f = 1/(rho_f*(1+OF));   %permite relacionar el volumen de comb. con m_p
alfa_o = OF/(rho_o*(1+OF));  %permite relacionar el volumen de ox. con m_p
alfa = alfa_f + alfa_o;      %permite relacionar el volumen de propelente con m_p

sigma_tg = 3.3e9;            %Resistencia max a la tension del tanque de gas [Pa]
sigma_tf = 455e6;            %Resistencia max a la tension del tanque de comb. [Pa]
sigma_to = 455e6;            %Resistencia max a la tension del tanque de ox. [Pa]
sigma_gg = 524e6;            %Resistencia max a la tension del GG (UTS)[Pa]
                             %sigma_gg = 524MPa   <- Hastelloy C (1033ºK)
                             %sigma_gg = 180MPa   <- CRES 347 (1090ºK)
                             %sigma_gg = 413.7MPa <- Cu-Ni-Si-Cr Alloy

emin = 0.001;                %espesor minimo de la pared de los tanques [m]
```

% 3.- PARAMETROS DE CALCULO %%

```
FLAG_SIST = 'A';             %A: Un solo motor/turbina
                             %B: Un motor/turbina por bomba


COTA = 0.1;                  %Cota para detectar que los vectores son iguales
```

```
fp_LIM = 0.99;              %Valor limite en la razon p_c/p_0

t_bVALOR = 90;             %Valor de tiempo de combustion de interes [s]
t_b = t_bVALOR             %Tiempo de combustion del cohete [s]

m_pVALOR = 1000;           %Valor puntual de masa de propelente de interes [kg]
m_p = m_pVALOR             %Cambio un valor del vector por el valor de interes

t_bMAX = 3.0e3;            %Tiempo maximo decombustion [s]
t_bMIN = 30;               %Tiempo minimo decombustion [s]
t_bN = 500;                %Longitud del vector t_b
t_bPASO = (t_bMAX-t_bMIN)/(t_bN-1);      %Paso de tiempo de combustion [s]

t_b = (t_bMIN:t_bPASO:t_bMAX);           %Vector de tiempo de combustion [s]


% 4.- RUTINA DE CALCULO %%%%%%%%%%%%%%%%%%%%%%%%%%%%%%%%%%%%%%%%%%%%%%%%%

%%% COMENTARIOS
%1.- La masa de propelente es un parametro de los graficos
%2.- La presion de la camara de combustion (para ambos sistemas) es un
%    parametro
%3.- El tiempo de combustion es un parametro
%4.- La presion inicial del gas presurizante es la variable


for i=1:size(t_b,2)

% 4.1.- CALCULO DE LA MASA DE GAS
    if p_0>(kappa_p3*p_c)
        %la expresion tiene sentido si p_tf<p_tg entonces se evalua esa
        %condicion
        m_g3(i) = kappa_g*kappa_u*kappa_p3*alfa*gamma_g*M_g*p_c*m_p/(R_u*T_g*(1-kappa_p3*p_c/p_0));
    else
        m_g3(i) = kappa_g*kappa_u*kappa_p3*alfa*gamma_g*M_g*p_c*m_p/(R_u*T_g*(1-fp_LIM));
    end
    if p_0>(kappa_p2*p_c)
        %la expresion tiene sentido si p_tf<p_tg entonces se evalua esa
        %condicion
        m_g2(i) = kappa_g*kappa_u*kappa_p2*alfa*gamma_g*M_g*p_c*m_p/(R_u*T_g*(1-kappa_p2*p_c/p_0));
    else
        m_g2(i) = kappa_g*kappa_u*kappa_p2*alfa*gamma_g*M_g*p_c*m_p/(R_u*T_g*(1-fp_LIM));
    end
    if p_0>(kappa_p1*p_c)
        %la expresion tiene sentido si p_tf<p_tg entonces se evalua esa
        %condicion
        m_g1(i) = kappa_g*kappa_u*kappa_p1*alfa*gamma_g*M_g*p_c*m_p/(R_u*T_g*(1-kappa_p1*p_c/p_0));
    else
        m_g1(i) = kappa_g*kappa_u*kappa_p1*alfa*gamma_g*M_g*p_c*m_p/(R_u*T_g*(1-fp_LIM));
    end

% 4.2.- CALCULO DE LA MASA DE LOS TANQUES DE GAS
    if p_0>(kappa_p2*p_c)
        %la expresion tiene sentido si p_tf<p_tg entonces se evalua esa
        %condicion
        m_tg2(i) = 1.5*rho_tg*kappa_tg*kappa_g*kappa_u*kappa_p2*alfa*gamma_g*p_c*m_p/(sigma_tg*(1-kappa_p2*p_c/p_0));
    else
        m_tg2(i) = 1.5*rho_tg*kappa_tg*kappa_g*kappa_u*kappa_p2*alfa*gamma_g*p_c*m_p/(sigma_tg*(1-fp_LIM));
    end
    if p_0>(kappa_p3*p_c)
        %la expresion tiene sentido si p_tf<p_tg entonces se evalua esa
        %condicion
        m_tg3(i) = 1.5*rho_tg*kappa_tg*kappa_g*kappa_u*kappa_p3*alfa*gamma_g*p_c*m_p/(sigma_tg*(1-kappa_p3*p_c/p_0));
```

```
      else
          m_tg3(i) = 1.5*rho_tg*kappa_tg*kappa_g*kappa_u*kappa_p3*alfa*gamma_g*p_c*m_p/(sigma_tg*(1-
fp_LIM));
      end
      if p_0>(kappa_p1*p_c)
          %la expresion tiene sentido si p_tf<p_tg entonces se evalua esa
          %condicion
          m_tg1(i) = 1.5*rho_tg*kappa_tg*kappa_g*kappa_u*kappa_p1*alfa*gamma_g*p_c*m_p/(sigma_tg*(1-
kappa_p1*p_c/p_0));
      else
          m_tg1(i) = 1.5*rho_tg*kappa_tg*kappa_g*kappa_u*kappa_p1*alfa*gamma_g*p_c*m_p/(sigma_tg*(1-
fp_LIM));
      end

% 4.3.- CALCULO DE LA MASA DE LOS TANQUES DE PROPELENTE
   %Masa del tanque de combustible para el sistema de gas presurizado
   m_tf11(i) = 1.5*rho_tf*kappa_u*kappa_p1*kappa_tf*alfa_f*m_p*p_c/sigma_tf;
   m_tf12(i) = ((4*pi)^(1/3))*rho_tf*((3*kappa_u*alfa_f*m_p)^(2/3))*emin;
   m_tf1(i) = max(m_tf11(i),m_tf12(i));

   %Masa del tanque de oxidante para el sistema de gas presurizado
   m_to11(i) = 1.5*rho_to*kappa_u*kappa_p1*kappa_to*alfa_o*m_p*p_c/sigma_to;
   m_to12(i) = ((4*pi)^(1/3))*rho_to*((3*kappa_u*alfa_o*m_p)^(2/3))*emin;
   m_to1(i) = max(m_to11(i),m_to12(i));

   %Masa del tanque de combustible para el sistema de electrobombas
   m_tf21(i) = 1.5*rho_tf*kappa_u*kappa_p2*kappa_tf*alfa_f*m_p*p_c/sigma_tf;
   m_tf22(i) = ((4*pi)^(1/3))*rho_tf*((3*kappa_u*alfa_f*m_p)^(2/3))*emin;
   m_tf2(i) = max(m_tf21(i),m_tf22(i));

   %Masa del tanque de oxidante para el sistema de electrobombas
   m_to21(i) = 1.5*rho_to*kappa_u*kappa_p2*kappa_to*alfa_o*m_p*p_c/sigma_to;
   m_to22(i) = ((4*pi)^(1/3))*rho_to*((3*kappa_u*alfa_o*m_p)^(2/3))*emin;
   m_to2(i) = max(m_to21(i),m_to22(i));

   %Masa del tanque de combustible para el sistema de turbobombas
   m_tf31(i) = 1.5*rho_tf*kappa_u*kappa_p3*kappa_tf*alfa_f*m_p*p_c/sigma_tf;
   m_tf32(i) = ((4*pi)^(1/3))*rho_tf*((3*kappa_u*alfa_f*m_p)^(2/3))*emin;
   m_tf3(i) = max(m_tf31(i),m_tf32(i));

   %Masa del tanque de oxidante para el sistema de turbobombas
   m_to31(i) = 1.5*rho_to*kappa_u*kappa_p3*kappa_to*alfa_o*m_p*p_c/sigma_to;
   m_to32(i) = ((4*pi)^(1/3))*rho_to*((3*kappa_u*alfa_o*m_p)^(2/3))*emin;
   m_to3(i) = max(m_to31(i),m_to32(i));

% 4.4.- CALCULO DE LA MASA DE LAS BOMBAS
   m_puf(i) = (1+kappa_pi-kappa_p2)*alfa_f*p_c*m_p/(delta_pf*t_b(i));
   m_puo(i) = (1+kappa_pi-kappa_p2)*alfa_o*p_c*m_p/(delta_po*t_b(i));
   m_pu(i) = m_puf(i) + m_puo(i);

% 4.5.- CALCULO DE LA MASA DEL MOTOR
   switch(FLAG_SIST)
      case 'A'    %Masa con un solo motor
          m_ee(i) = (1+kappa_pi-kappa_p2)*p_c*m_p*(alfa_f/eta_pf+alfa_o/eta_po)/(delta_e*t_b(i));
      case 'B'    %Masa con un motor por bomba
          m_ef(i) = (1+kappa_pi-kappa_p2)*alfa_f*p_c*m_p/(eta_pf*delta_e*t_b(i));
          m_eo(i) = (1+kappa_pi-kappa_p2)*alfa_o*p_c*m_p/(eta_po*delta_e*t_b(i));
          m_ee(i) = m_ef(i) + m_eo(i);
      otherwise
          ERROR(i) = 1;
   end

% 4.6.- CALCULO DE LA MASA DE LA TURBINA
   switch(FLAG_SIST)
      case 'A'    %Masa con una sola turbina
          m_tu(i) = (1+kappa_pi-kappa_p3)*p_c*m_p*(alfa_f/eta_pf+alfa_o/eta_po)/(delta_tu*t_b(i));
      case 'B'    %Masa con una turbina por bomba
```

```
            m_tf(i) = (1+kappa_pi-kappa_p3)*alfa_f*p_c*m_p/(eta_pf*delta_tf*t_b(i));
            m_to(i) = (1+kappa_pi-kappa_p3)*alfa_o*p_c*m_p/(eta_po*delta_to*t_b(i));
            m_tu(i) = m_tf(i) + m_to(i);
        otherwise
            ERROR(i) = 1;
    end

% 4.7.- CALCULO DE LA MASA DEL INVERSOR
    switch(FLAG_SIST)
        case 'A'    %Masa del inversor con un solo motor
            m_inv(i) = (1+kappa_pi-kappa_p2)*p_c*m_p*(alfa_f/eta_pf+alfa_o/eta_po)/(eta_e*delta_inv*t_b(i));
        case 'B'    %Masa de los inversores con un motor por bomba
            m_inf(i) = (1+kappa_pi-kappa_p2)*alfa_f*p_c*m_p/(eta_pf*eta_ef*delta_inv*t_b(i));
            m_ino(i) = (1+kappa_pi-kappa_p2)*alfa_o*p_c*m_p/(eta_po*eta_eo*delta_inv*t_b(i));
            m_inv(i) = m_inf(i) + m_ino(i);
        otherwise
            ERROR(i) = 1;
    end

% 4.8.- CALCULO DE LA MASA DE LAS BATERIAS
    switch(FLAG_SIST)
        case 'A'    %Masa de las baterias con un solo motor
            m_bap(i) = (1+kappa_pi-
kappa_p2)*p_c*m_p*kappa_b*(alfa_f/eta_pf+alfa_o/eta_po)/(eta_e*eta_inv*delta_bap*t_b(i));
            m_baw(i) = (1+kappa_pi-
kappa_p2)*p_c*m_p*kappa_b*(alfa_f/eta_pf+alfa_o/eta_po)/(eta_e*eta_inv*delta_baw);
            m_bat(i) = max(m_bap(i),m_baw(i));
        case 'B'    %Masa de las baterias con un motor por bomba
            m_bap(i) = (1+kappa_pi-
kappa_p2)*p_c*m_p*kappa_b*(alfa_f/(eta_pf*eta_ef*eta_inv)+alfa_o/(eta_po*eta_eo*eta_inv))/(delta_bap*t_b(i));
            m_baw(i) = (1+kappa_pi-
kappa_p2)*p_c*m_p*kappa_b*(alfa_f/(eta_pf*eta_ef*eta_inv)+alfa_o/(eta_po*eta_eo*eta_inv))/delta_baw;
            m_bat(i) = max(m_bap(i),m_baw(i));
        otherwise
            ERROR(i) = 1;
    end

% 4.9.- CALCULO DE PROPELENTE PARA ACCIONAR LA TURBINA
    m_ptu(i) = (1+kappa_pi-kappa_p3)*p_c*m_p*M_gg*(gamma_gg-
1)*(alfa_f/eta_pf+alfa_o/eta_po)/(eta_tu*T_itu*gamma_gg*R_u*(1-(p_dtu/p_itu)^((gamma_gg-1)/gamma_gg)));

% 4.10.- CALCULO DE LA MASA DEL GENERADOR DE GAS
    V_g(i) = t_s*m_ptu(i)/(t_b(i)*rho_gg);
    r_g(i) = (0.75*V_g(i))^(1/3);
    S_g(i) = 4*pi*(0.75*V_g(i)/pi)^(2/3);
    m_gg(i) = rho_tgg*kappa_gg*p_gg*r_g(i)*S_g(i)/(2*sigma_gg);

end

Indices = find((m_bat-m_baw)<COTA);
if length(Indices)>0
    LIMITE = Indices(1);
else
    LIMITE = 1;
end

m_pg = m_g1 + m_tg1 + m_tf1 + m_to1;
m_tp = m_g3 + m_tg3 + m_tf3 + m_to3 + m_pu + m_tu + m_gg + m_ptu;

 for k=1:LIMITE
    t_bA(k) = t_b(k);
    m_epA(k) = m_g2(k) + m_tg2(k) + m_tf2(k) + m_to2(k) + m_pu(k) + m_ee(k) + m_inv(k) +
max(m_bap(k),m_baw(k));
 end

 for j=1:(length(t_b)-LIMITE)
    t_bB(j) = t_b(j+LIMITE-1);
```

```
    m_epB(j) = m_g2(j+LIMITE-1) + m_tg2(j+LIMITE-1) + m_tf2(j+LIMITE-1) + m_to2(j+LIMITE-1) +
m_pu(j+LIMITE-1) + m_ee(j+LIMITE-1) + m_inv(j+LIMITE-1) + max(m_bap(j+LIMITE-1),m_baw(j+LIMITE-1));
 end


fm_pg = m_pg/m_p;           %Fraccion de masas: gas presurizado/masa propelente
fm_epA = m_epA/m_p;         %Fraccion de masas: electrobombas/masa propelente
fm_epB = m_epB/m_p;         %Fraccion de masas: electrobombas/masa propelente
fm_tp = m_tp/m_p;           %Fraccion de masas: turbobombas/masa propelente


% 4.- RUTINA DE GENERACION DE GRAFICOS %%%%%%%%%%%%%%%%%%%%%%%%%%%%%%%%%%%%%


x_MIN = t_bMIN;
x_MAX = t_bMAX;
y_MIN = 0;
y_MAX = 0.1;
x_COOR = x_MIN+0.1*(x_MAX-x_MIN);
y_COOR = y_MIN+0.65*(y_MAX-y_MIN);
RENGLON = 0.05*(y_MAX-y_MIN);


figure
plot(t_b,fm_pg,'b','linewidth',2)
axis([x_MIN x_MAX y_MIN y_MAX])
xlabel('Tiempo de combustion [s]','FontSize',12,'FontWeight','demi')
ylabel('m_f_s/m_p','FontSize',12,'FontWeight','demi')
title('Relacion Masa del Sist. de Alimentacion vs Masa de Propelente','FontSize',14)
text(x_COOR,y_COOR,['Masa de propelente: m_p = ' num2str(m_pVALOR) 'kg'])
text(x_COOR,y_COOR-RENGLON,['Presion de camara: p_C = ' num2str(p_c/1e5) 'bar'])
grid on
hold on
plot(t_bA,fm_epA,'r','linewidth',2)
hold on
plot(t_bB,fm_epB,'r--','linewidth',2)
hold on
plot(t_b,fm_tp,'g','linewidth',2)
legend('Sist. Gas Presurizado','Sist. de Electrobombas (m_b_a_t impuesta por P)','Sist. de Electrobombas (m_b_a_t
impuesta por W)','Sist. de Turbobombas',1)

saveas(gcf,['masa_vs_tb_ver05_mp_' num2str(m_pVALOR) '_PC_' num2str(p_c/1e5) '.png'])



%%%%%%% RUTINA DE COMPARACION IV %%%%%%%%%%%%%%%%%%%%%%%%%
% Descripcion: Esta rutina compara la fraccion de masa del sistema
% de alimentacion (m_fs) respecto de la masa total de propelente (m_p).
%
% Comentarios:
%1.- La variable para la comparacion es la masa de propelente.

clear all
close all

% 1.- VARIABLES DE
ENTRADA %%%%%%%%%%%%%%%%%%%%%%%%%%%%%%%%%%%%%%%%%%%%%%%%%%%%%%%%%%%%%%

% 1.1.- Presiones:

%Aclaraciones:

% Sistema 1: alimentado por gas presurizado
% Sistema 2: alimentado por electrobombas
% Sistema 3: alimentado por turbobombas
% Se asume que la presion en el tanque de combustible y en el tanque de
% oxidante son iguales entre si. Para cada sistema entonces se define una
% presion en el tanque de propelente.
```

```
p_c = 6.0e6;                          %Presion de la camara de combustion [Pa]
p_0 = 20e6;                           %Presion inicial del tanque de gas [Pa]
p_irat = 0.3;                         %Relacion entre la presion de camara y la del inyector
p_tp1 = (1+p_irat)*p_c;               %Presion del tanque de propelente p/ el sist. 1 [Pa]
p_tp2 = 0.6e6;                        %Presion del tanque de propelente p/ el sist. 2 [Pa]
p_tp3 = 0.6e6;                        %Presion del tanque de propelente p/ el sist. 3 [Pa]
p_in = p_irat*p_c;                    %Presion en el inyector [Pa]
p_gg = p_c;                           %Presion de la camara del generador [Pa]
p_itu = p_gg;                         %Presion de ingreso de la turbina [Pa]
p_trat = 20;                          %Relacion de presiones de la turbina
p_dtu = p_itu/p_trat;                 %Presion de descarga de la turbina [Pa]
```

% 1.2.- Temperaturas:

```
T_itu = 900;                          %Temperatura de los gases q ingresan en la turbina [ºK]
T_g = 288.15;                         %Temperatura del gas presurizante [ºK]
T_gg = 1100;                          %Temperatura de la camara del generador de gas [ºK]
```

% 1.3.- Variables Quimicas (Masas, masas molares y const. isentropicas):

```
gamma_c = 1.23;                       %Parametro isentropico de los gases de la camara
gamma_g = 1.667;                      %Parametro isentropico del gas presurizante
gamma_gg = 1.196;                     %Parametro isentropico de los gases del gen. de gas
M_c = 23;                             %Masa molar de los gases de la camara [kg/kmol]
M_gg = 14.2;                          %Masa molar de los gases de la gen. de gas [kg/kmol]
M_g = 4.0026;                         %Masa molar del gas presurizante [kg/kmol]
OF = 1.9;                             %Relacion oxidante/combustible
R_u = 8314.41;                        %Constante Universal de los gases [J/kmolºK]
t_s = 10e-3;                          %stay time
```

% 1.4.- Densidades:

```
rho_f = 874;                          %Densidad del combustible [kg/m3]
rho_o = 1431;                         %Densidad del oxidante [kg/m3]
rho_gg = 0.8774;                      %Densidad de los gases de escape [kg/m3]
rho_tg = 1700;                        %Densidad del tanque de gas [kg/m3]
rho_to = 2800;                        %Densidad del tanque de oxidante [kg/m3]
rho_tf = 2800;                        %Densidad del tanque de combustible [kg/m3]
rho_tgg = 8890;                       %Densidad del material de la camara del GG [kg/m3]
                                      %rho_tgg = 8890 <- Hastelloy C
                                      %rho_tgg = 7960kg/m3 <- CRES 347
                                      %rho_tgg = 8800 <- Cu-Ni-Si-Cr Alloy


delta_pf = 40e3;                      %Densidad de potencia de la bomba de comb. [W/kg]
delta_po = 40e3;                      %Densidad de potencia de la bomba de ox. [W/kg]
delta_e = 3.8e3;                      %Densidad de potencia del motor [W/kg]
delta_ef = 3.8e3;                     %Densidad de potencia del motor de comb. [W/kg]
delta_eo = 3.8e3;                     %Densidad de potencia del motor de ox. [W/kg]
delta_tu = 20e3;                      %Densidad de potencia de la turbina [W/kg]
delta_tf = 20e3;                      %Densidad de potencia de la turbina de comb. [W/kg]
delta_to = 20e3;                      %Densidad de potencia de la turbina de ox. [W/kg]
delta_inv = 60e3;                     %Densidad de potencia del inversor [W/kg]
delta_bap = 4.8e3;                    %Densidad de potencia de las baterias [W/kg]
delta_baw = 130;                      %Densidad de energia de las baterias [Wh/kg]
delta_baw = delta_baw*3600;           %Densidad de energia de las baterias [J/kg]
```

% 1.5.- Rendimientos:

```
eta_pf = 0.8;                         %Rendimiento de la bomba de comb.
eta_po = 0.8;                         %Rendimiento de la bomba de ox.
eta_e = 0.8;                          %Rendimiento del motor electrico
eta_ef = 0.8;                         %Rendimiento del motor de comb.
eta_eo = 0.8;                         %Rendimiento del motor de ox.
eta_inv = 0.85;                       %Rendimiento del inversor
eta_tu = 0.8;                         %Rendimiento de la turbina
```

% 2.- CONSTANTES %%%

```
kappa_p1 = p_tp1/p_c;        %para el sistema de alimentacion por gas pres.
kappa_p2 = p_tp2/p_c;        %para el sist. de alim. por electrobombas
kappa_p3 = p_tp3/p_c;        %para el sist. de alim. por turbobombas
kappa_pi = p_in/p_c;         %razon de la caida en el inyector respecto de p_c
kappa_u = 1.05;             %factor de seguridad para preveer el "ullage"
kappa_g = 1.3;             %factor de seguridad para la masa de gas
kappa_tg = 2.5;            %factor de seguridad para el espesor del tanque de gas
kappa_tf = 2.5;            %factor de seguridad para el espesor del tanque de comb.
kappa_to = 2.5;           %factor de seguridad para el espesor del tanque de ox.
kappa_b = 1.2;            %margen de diseño para la masa de las baterias
kappa_gg = 2.5;          %factor de seguridad para el espesor de la pared del GG

alfa_f = 1/(rho_f*(1+OF));    %permite relacionar el volumen de comb. con m_p
alfa_o = OF/(rho_o*(1+OF));   %permite relacionar el volumen de ox. con m_p
alfa = alfa_f + alfa_o;       %permite relacionar el volumen de propelente con m_p

sigma_tg = 3.3e9;           %Resistencia max a la tension del tanque de gas [Pa]
sigma_tf = 455e6;          %Resistencia max a la tension del tanque de comb. [Pa]
sigma_to = 455e6;          %Resistencia max a la tension del tanque de ox. [Pa]
sigma_gg = 524e6;          %Resistencia max a la tension del GG (UTS)[Pa]
                            %sigma_gg = 524MPa   <- Hastelloy C (1033ºK)
                            %sigma_gg = 180MPa   <- CRES 347 (1090ºK)
                            %sigma_gg = 413.7MPa <- Cu-Ni-Si-Cr Alloy

emin = 0.001;              %espesor minimo de la pared de los tanques [m]
```

% 3.- PARAMETROS DE CALCULO %%%

```
FLAG_SIST = 'A';           %A: Un solo motor/turbina
                           %B: Un motor/turbina por bomba

COTA = 0.1;                %Cota para detectar que los vectores son iguales

fp_LIM = 0.99;             %Valor limite en la razon p_c/p_0

t_bVALOR = 90;             %Valor de tiempo de combustion de interes [s]
t_b = t_bVALOR             %Tiempo de combustion del cohete [s]

m_pMIN = 1000;             %Masa de propelente minima [kg]
m_pMAX = 10000;            %Masa de propelente maxima [kg]
m_pN = 500;                %Longitud del vector m_p
m_pPASO = (m_pMAX-m_pMIN)/(m_pN-1);   %Paso de Masa de propelente [kg]
m_p = (m_pMIN:m_pPASO:m_pMAX);         %Vector Masa de propelente [kg]
```

% 4.- RUTINA DE CALCULO %%%

```
%%% COMENTARIOS
%1.- La masa de propelente es un parametro de los graficos
%2.- La presion de la camara de combustion (para ambos sistemas) es un
%    parametro
%3.- El tiempo de combustion es un parametro
%4.- La presion inicial del gas presurizante es la variable


for i=1:size(m_p,2)

% 4.1.- CALCULO DE LA MASA DE GAS
  if p_0>(kappa_p3*p_c)
    %la expresion tiene sentido si p_tf<p_tg entonces se evalua esa
    %condicion
    m_g3(i) = kappa_g*kappa_u*kappa_p3*alfa*gamma_g*M_g*p_c*m_p(i)/(R_u*T_g*(1-kappa_p3*p_c/p_0));
  else
    m_g3(i) = kappa_g*kappa_u*kappa_p3*alfa*gamma_g*M_g*p_c*m_p(i)/(R_u*T_g*(1-fp_LIM));
```

```
    end
    if p_0>(kappa_p2*p_c)
        %la expresion tiene sentido si p_tf<p_tg entonces se evalua esa
        %condicion
        m_g2(i) = kappa_g*kappa_u*kappa_p2*alfa*gamma_g*M_g*p_c*m_p(i)/(R_u*T_g*(1-kappa_p2*p_c/p_0));
    else
        m_g2(i) = kappa_g*kappa_u*kappa_p2*alfa*gamma_g*M_g*p_c*m_p(i)/(R_u*T_g*(1-fp_LIM));
    end
    if p_0>(kappa_p1*p_c)
        %la expresion tiene sentido si p_tf<p_tg entonces se evalua esa
        %condicion
        m_g1(i) = kappa_g*kappa_u*kappa_p1*alfa*gamma_g*M_g*p_c*m_p(i)/(R_u*T_g*(1-kappa_p1*p_c/p_0));
    else
        m_g1(i) = kappa_g*kappa_u*kappa_p1*alfa*gamma_g*M_g*p_c*m_p(i)/(R_u*T_g*(1-fp_LIM));
    end
```

% 4.2.- CALCULO DE LA MASA DE LOS TANQUES DE GAS
```
    if p_0>(kappa_p2*p_c)
        %la expresion tiene sentido si p_tf<p_tg entonces se evalua esa
        %condicion
        m_tg2(i) = 1.5*rho_tg*kappa_tg*kappa_g*kappa_u*kappa_p2*alfa*gamma_g*p_c*m_p(i)/(sigma_tg*(1-kappa_p2*p_c/p_0));
    else
        m_tg2(i) = 1.5*rho_tg*kappa_tg*kappa_g*kappa_u*kappa_p2*alfa*gamma_g*p_c*m_p(i)/(sigma_tg*(1-fp_LIM));
    end
    if p_0>(kappa_p3*p_c)
        %la expresion tiene sentido si p_tf<p_tg entonces se evalua esa
        %condicion
        m_tg3(i) = 1.5*rho_tg*kappa_tg*kappa_g*kappa_u*kappa_p3*alfa*gamma_g*p_c*m_p(i)/(sigma_tg*(1-kappa_p3*p_c/p_0));
    else
        m_tg3(i) = 1.5*rho_tg*kappa_tg*kappa_g*kappa_u*kappa_p3*alfa*gamma_g*p_c*m_p(i)/(sigma_tg*(1-fp_LIM));
    end
    if p_0>(kappa_p1*p_c)
        %la expresion tiene sentido si p_tf<p_tg entonces se evalua esa
        %condicion
        m_tg1(i) = 1.5*rho_tg*kappa_tg*kappa_g*kappa_u*kappa_p1*alfa*gamma_g*p_c*m_p(i)/(sigma_tg*(1-kappa_p1*p_c/p_0));
    else
        m_tg1(i) = 1.5*rho_tg*kappa_tg*kappa_g*kappa_u*kappa_p1*alfa*gamma_g*p_c*m_p(i)/(sigma_tg*(1-fp_LIM));
    end
```

% 4.3.- CALCULO DE LA MASA DE LOS TANQUES DE PROPELENTE
```
    %Masa del tanque de combustible para el sistema de gas presurizado
    m_tf11(i) = 1.5*rho_tf*kappa_u*kappa_p1*kappa_tf*alfa_f*m_p(i)*p_c/sigma_tf;
    m_tf12(i) = ((4*pi)^(1/3))*rho_tf*((3*kappa_u*alfa_f*m_p(i))^(2/3))*emin;
    m_tf1(i) = max(m_tf11(i),m_tf12(i));

    %Masa del tanque de oxidante para el sistema de gas presurizado
    m_to11(i) = 1.5*rho_to*kappa_u*kappa_p1*kappa_to*alfa_o*m_p(i)*p_c/sigma_to;
    m_to12(i) = ((4*pi)^(1/3))*rho_to*((3*kappa_u*alfa_o*m_p(i))^(2/3))*emin;
    m_to1(i) = max(m_to11(i),m_to12(i));

    %Masa del tanque de combustible para el sistema de electrobombas
    m_tf21(i) = 1.5*rho_tf*kappa_u*kappa_p2*kappa_tf*alfa_f*m_p(i)*p_c/sigma_tf;
    m_tf22(i) = ((4*pi)^(1/3))*rho_tf*((3*kappa_u*alfa_f*m_p(i))^(2/3))*emin;
    m_tf2(i) = max(m_tf21(i),m_tf22(i));

    %Masa del tanque de oxidante para el sistema de electrobombas
    m_to21(i) = 1.5*rho_to*kappa_u*kappa_p2*kappa_to*alfa_o*m_p(i)*p_c/sigma_to;
    m_to22(i) = ((4*pi)^(1/3))*rho_to*((3*kappa_u*alfa_o*m_p(i))^(2/3))*emin;
    m_to2(i) = max(m_to21(i),m_to22(i));

    %Masa del tanque de combustible para el sistema de turbobombas
```

```
    m_tf31(i) = 1.5*rho_tf*kappa_u*kappa_p3*kappa_tf*alfa_f*m_p(i)*p_c/sigma_tf;
    m_tf32(i) = ((4*pi)^(1/3))*rho_tf*((3*kappa_u*alfa_f*m_p(i))^(2/3))*emin;
    m_tf3(i) = max(m_tf31(i),m_tf32(i));

    %Masa del tanque de oxidante para el sistema de turbobombas
    m_to31(i) = 1.5*rho_to*kappa_u*kappa_p3*kappa_to*alfa_o*m_p(i)*p_c/sigma_to;
    m_to32(i) = ((4*pi)^(1/3))*rho_to*((3*kappa_u*alfa_o*m_p(i))^(2/3))*emin;
    m_to3(i) = max(m_to31(i),m_to32(i));

% 4.4.- CALCULO DE LA MASA DE LAS BOMBAS
    m_puf(i) = (1+kappa_pi-kappa_p2)*alfa_f*p_c*m_p(i)/(delta_pf*t_b);
    m_puo(i) = (1+kappa_pi-kappa_p2)*alfa_o*p_c*m_p(i)/(delta_po*t_b);
    m_pu(i) = m_puf(i) + m_puo(i);

% 4.5.- CALCULO DE LA MASA DEL MOTOR
    switch(FLAG_SIST)
        case 'A'    %Masa con un solo motor
          m_ee(i) = (1+kappa_pi-kappa_p2)*p_c*m_p(i)*(alfa_f/eta_pf+alfa_o/eta_po)/(delta_e*t_b);
        case 'B'    %Masa con un motor por bomba
          m_ef(i) = (1+kappa_pi-kappa_p2)*alfa_f*p_c*m_p(i)/(eta_pf*delta_e*t_b);
          m_eo(i) = (1+kappa_pi-kappa_p2)*alfa_o*p_c*m_p(i)/(eta_po*delta_e*t_b);
          m_ee(i) = m_ef(i) + m_eo(i);
        otherwise
          ERROR(i) = 1;
    end

% 4.6.- CALCULO DE LA MASA DE LA TURBINA
    switch(FLAG_SIST)
        case 'A'    %Masa con una sola turbina
          m_tu(i) = (1+kappa_pi-kappa_p3)*p_c*m_p(i)*(alfa_f/eta_pf+alfa_o/eta_po)/(delta_tu*t_b);
        case 'B'    %Masa con una turbina por bomba
          m_tf(i) = (1+kappa_pi-kappa_p3)*alfa_f*p_c*m_p(i)/(eta_pf*delta_tf*t_b);
          m_to(i) = (1+kappa_pi-kappa_p3)*alfa_o*p_c*m_p(i)/(eta_po*delta_to*t_b);
          m_tu(i) = m_tf(i) + m_to(i);
        otherwise
          ERROR(i) = 1;
    end

% 4.7.- CALCULO DE LA MASA DEL INVERSOR
    switch(FLAG_SIST)
        case 'A'    %Masa del inversor con un solo motor
          m_inv(i) = (1+kappa_pi-kappa_p2)*p_c*m_p(i)*(alfa_f/eta_pf+alfa_o/eta_po)/(eta_e*delta_inv*t_b);
        case 'B'    %Masa de los inversores con un motor por bomba
          m_inf(i) = (1+kappa_pi-kappa_p2)*alfa_f*p_c*m_p(i)/(eta_pf*eta_ef*delta_inv*t_b);
          m_ino(i) = (1+kappa_pi-kappa_p2)*alfa_o*p_c*m_p(i)/(eta_po*eta_eo*delta_inv*t_b);
          m_inv(i) = m_inf(i) + m_ino(i);
        otherwise
          ERROR(i) = 1;
    end

% 4.8.- CALCULO DE LA MASA DE LAS BATERIAS
    switch(FLAG_SIST)
        case 'A'    %Masa de las baterias con un solo motor
          m_bap(i) = (1+kappa_pi-
kappa_p2)*p_c*m_p(i)*kappa_b*(alfa_f/eta_pf+alfa_o/eta_po)/(eta_e*eta_inv*delta_bap*t_b);
          m_baw(i) = (1+kappa_pi-
kappa_p2)*p_c*m_p(i)*kappa_b*(alfa_f/eta_pf+alfa_o/eta_po)/(eta_e*eta_inv*delta_baw);
          m_bat(i) = max(m_bap(i),m_baw(i));
        case 'B'    %Masa de las baterias con un motor por bomba
          m_bap(i) = (1+kappa_pi-
kappa_p2)*p_c*m_p(i)*kappa_b*(alfa_f/(eta_pf*eta_ef*eta_inv)+alfa_o/(eta_po*eta_eo*eta_inv))/(delta_bap*t_b);
          m_baw(i) = (1+kappa_pi-
kappa_p2)*p_c*m_p(i)*kappa_b*(alfa_f/(eta_pf*eta_ef*eta_inv)+alfa_o/(eta_po*eta_eo*eta_inv))/delta_baw;
          m_bat(i) = max(m_bap(i),m_baw(i));
        otherwise
          ERROR(i) = 1;
    end
```

```
% 4.9.- CALCULO DE PROPELENTE PARA ACCIONAR LA TURBINA
   m_ptu(i) = (1+kappa_pi-kappa_p3)*p_c*m_p(i)*M_gg*(gamma_gg-
1)*(alfa_f/eta_pf+alfa_o/eta_po)/(eta_tu*T_itu*gamma_gg*R_u*(1-(p_dtu/p_itu)^((gamma_gg-1)/gamma_gg)));

% 4.10.- CALCULO DE LA MASA DEL GENERADOR DE GAS
   V_g(i) = t_s*m_ptu(i)/(t_b*rho_gg);
   r_g(i) = (0.75*V_g(i))^(1/3);
   S_g(i) = 4*pi*(0.75*V_g(i)/pi)^(2/3);
   m_gg(i) = rho_tgg*kappa_gg*p_gg*r_g(i)*S_g(i)/(2*sigma_gg);

end

Indices = find((m_bat-m_baw)<COTA);
if length(Indices)>0
   LIMITE = Indices(1);
else
   LIMITE = m_pN-1;
end

m_pg = m_g1 + m_tg1 + m_tf1 + m_to1;
m_tp = m_g3 + m_tg3 + m_tf3 + m_to3 + m_pu + m_tu + m_gg + m_ptu;

 for k=1:LIMITE
    m_pA(k) = m_p(k);
    m_epA(k) = m_g2(k) + m_tg2(k) + m_tf2(k) + m_to2(k) + m_pu(k) + m_ee(k) + m_inv(k) +
max(m_bap(k),m_baw(k));
 end

 for j=1:(length(m_p)-LIMITE)
    m_pB(j) = m_p(j+LIMITE-1);
    m_epB(j) = m_g2(j+LIMITE-1) + m_tg2(j+LIMITE-1) + m_tf2(j+LIMITE-1) + m_to2(j+LIMITE-1) +
m_pu(j+LIMITE-1) + m_ee(j+LIMITE-1) + m_inv(j+LIMITE-1) + max(m_bap(j+LIMITE-1),m_baw(j+LIMITE-1));
 end


fm_pg = m_pg./m_p;        %Fraccion de masas: gas presurizado/masa propelente
fm_epA = m_epA./m_pA;     %Fraccion de masas: electrobombas/masa propelente
fm_epB = m_epB./m_pB;     %Fraccion de masas: electrobombas/masa propelente
fm_tp = m_tp./m_p;        %Fraccion de masas: turbobombas/masa propelente

% 4.- RUTINA DE GENERACION DE
GRAFICOS %%%%%%%%%%%%%%%%%%%%%%%%%%%%%%%%%%%%%%%%%%%%%%%%

x_MIN = m_pMIN;
x_MAX = m_pMAX;
y_MIN = 0;
y_MAX = 0.15;
x_COOR = x_MIN+0.1*(x_MAX-x_MIN);
y_COOR = y_MIN+0.65*(y_MAX-y_MIN);
RENGLON = 0.05*(y_MAX-y_MIN);

figure
plot(m_p,fm_pg,'b','linewidth',2)
axis([x_MIN x_MAX y_MIN y_MAX])
xlabel('Masa de propelente [kg]','FontSize',12,'FontWeight','demi')
ylabel('m_f_s/m_p','FontSize',12,'FontWeight','demi')
title('Relacion Masa del Sist. de Alimentacion vs Masa de Propelente','FontSize',14)
text(x_COOR,y_COOR,['Tiempo de combustion: t_b = ' num2str(t_bVALOR) 's'])
text(x_COOR,y_COOR-RENGLON,['Presion de camara: p_C = ' num2str(p_c/1e5) 'bar'])
grid on
hold on
plot(m_pA,fm_epA,'r','linewidth',2)
hold on
plot(m_pB,fm_epB,'r--','linewidth',2)
```

```
hold on
plot(m_p,fm_tp,'g','linewidth',2)
legend('Sist. Gas Presurizado','Sist. de Electrobombas (m_b_a_t impuesta por P)','Sist. de Electrobombas (m_b_a_t
impuesta por W)','Sist. de Turbobombas',0)

saveas(gcf,['masa_vs_mp_ver05_PC_' num2str(p_c/1e5) '_tb_' num2str(t_bVALOR) '.png'])



%%%%%%% RUTINA DE COMPARACION V %%%%%%%%%%%%%%%%%%%%%%%%%
% Descripcion: Esta rutina compara la fraccion de masa del sistema
% de alimentacion (m_fs) respecto de la masa total de propelente (m_p).
%
% Comentarios:
%1.- La variable para la comparacion es el tiempo de combustion.
%2.- Esta rutina sirve para comparar distintas tecnologias entre si.

clear all
close all

% 1.- VARIABLES DE E NTRADA %%%%%%%%%%%%%%%%%%%%%%%%%%%%%%%%%%%%%%%%%%%%%%%

% 1.1.- Presiones:

%Aclaraciones:

% Sistema 1: alimentado por gas presurizado
% Sistema 2: alimentado por electrobombas
% Sistema 3: alimentado por turbobombas
% Se asume que la presion en el tanque de combustible y en el tanque de
% oxidante son iguales entre si. Para cada sistema entonces se define una
% presion en el tanque de propelente.


p_c = 6.0e6;                    %Presion de la camara de combustion [Pa]
p_0 = 20e6;                     %Presion inicial del tanque de gas [Pa]
p_irat = 0.3;                   %Relacion entre la presion de camara y la del inyector
p_tp1 = (1+p_irat)*p_c;         %Presion del tanque de propelente p/ el sist. 1 [Pa]
p_tp2 = 0.6e6;                  %Presion del tanque de propelente p/ el sist. 2 [Pa]
p_tp3 = 0.6e6;                  %Presion del tanque de propelente p/ el sist. 3 [Pa]
p_in = p_irat*p_c;              %Presion en el inyector [Pa]
p_gg = p_c;                     %Presion de la camara del generador [Pa]
p_itu = p_gg;                   %Presion de ingreso de la turbina [Pa]
p_trat = 20;                    %Relacion de presiones de la turbina
p_dtu = p_itu/p_trat;           %Presion de descarga de la turbina [Pa]

% 1.2.- Temperaturas:

T_itu = 900;                    %Temperatura de los gases q ingresan en la turbina [ºK]
T_g = 288.15;                   %Temperatura del gas presurizante [ºK]
T_gg = 1100;                    %Temperatura de la camara del generador de gas [ºK]

% 1.3.- Variables Quimicas (Masas, masas molares y const. isentropicas):

gamma_c = 1.23;                 %Parametro isentropico de los gases de la camara
gamma_g = 1.667;                %Parametro isentropico del gas presurizante
gamma_gg = 1.196;               %Parametro isentropico de los gases del gen. de gas
M_c = 23;                       %Masa molar de los gases de la camara [kg/kmol]
M_gg = 14.2;                    %Masa molar de los gases de la gen. de gas [kg/kmol]
M_g = 4.0026;                   %Masa molar del gas presurizante [kg/kmol]
OF = 1.9;                       %Relacion oxidante/combustible
R_u = 8314.41;                  %Constante Universal de los gases [J/kmolºK]
t_s = 10e-3;                    %stay time

% 1.4.- Densidades:

rho_f = 874;                    %Densidad del combustible [kg/m3]
rho_o = 1431;                   %Densidad del oxidante [kg/m3]
```

```
rho_gg = 0.8774;            %Densidad de los gases de escape [kg/m3]
rho_tg = 1700;             %Densidad del tanque de gas [kg/m3]
rho_to = 2800;             %Densidad del tanque de oxidante [kg/m3]
rho_tf = 2800;             %Densidad del tanque de combustible [kg/m3]
rho_tgg = 8890;            %Densidad del material de la camara del GG [kg/m3]
                           %rho_tgg = 8890 <- Hastelloy C
                           %rho_tgg = 7960kg/m3 <- CRES 347
                           %rho_tgg = 8800 <- Cu-Ni-Si-Cr Alloy


delta_pf = 40e3;           %Densidad de potencia de la bomba de comb. [W/kg]
delta_po = 40e3;           %Densidad de potencia de la bomba de ox. [W/kg]
delta_e = 3.8e3;           %Densidad de potencia del motor [W/kg]
delta_ef = 3.8e3;          %Densidad de potencia del motor de comb. [W/kg]
delta_eo = 3.8e3;          %Densidad de potencia del motor de ox. [W/kg]
delta_tu = 20e3;           %Densidad de potencia de la turbina [W/kg]
delta_tf = 20e3;           %Densidad de potencia de la turbina de comb. [W/kg]
delta_to = 20e3;           %Densidad de potencia de la turbina de ox. [W/kg]
delta_inv = 60e3;          %Densidad de potencia del inversor [W/kg]
delta_bap = 4.8e3;         %Densidad de potencia de las baterias [W/kg]
delta_baw = 130;           %Densidad de energia de las baterias [Wh/kg]
delta_baw = delta_baw*3600; %Densidad de energia de las baterias [J/kg]

% 1.5.- Rendimientos:

eta_pf = 0.8;              %Rendimiento de la bomba de comb.
eta_po = 0.8;              %Rendimiento de la bomba de ox.
eta_e = 0.8;               %Rendimiento del motor electrico
eta_ef = 0.8;              %Rendimiento del motor de comb.
eta_eo = 0.8;              %Rendimiento del motor de ox.
eta_inv = 0.85;            %Rendimiento del inversor
eta_tu = 0.8;              %Rendimiento de la turbina

% 2.- CONSTANTES %%%%%%%%%%%%%%%%%%%%%%%%%%%%%%%%%%%%%%%%%%%%%%%%%%%%

kappa_p1 = p_tp1/p_c;      %para el sistema de alimentacion por gas pres.
kappa_p2 = p_tp2/p_c;      %para el sist. de alim. por electrobombas
kappa_p3 = p_tp3/p_c;      %para el sist. de alim. por turbobombas
kappa_pi = p_in/p_c;       %razon de la caida en el inyector respecto de p_c
kappa_u = 1.05;            %factor de seguridad para preveer el "ullage"
kappa_g = 1.3;             %factor de seguridad para la masa de gas
kappa_tg = 2.5;            %factor de seguridad para el espesor del tanque de gas
kappa_tf = 2.5;            %factor de seguridad para el espesor del tanque de comb.
kappa_to = 2.5;            %factor de seguridad para el espesor del tanque de ox.
kappa_b = 1.2;             %margen de diseño para la masa de las baterias
kappa_gg = 2.5;            %factor de seguridad para el espesor de la pared del GG

alfa_f = 1/(rho_f*(1+OF));    %permite relacionar el volumen de comb. con m_p
alfa_o = OF/(rho_o*(1+OF)); %permite relacionar el volumen de ox. con m_p
alfa = alfa_f + alfa_o;      %permite relacionar el volumen de propelente con m_p

sigma_tg = 3.3e9;          %Resistencia max a la tension del tanque de gas [Pa]
sigma_tf = 455e6;          %Resistencia max a la tension del tanque de comb. [Pa]
sigma_to = 455e6;          %Resistencia max a la tension del tanque de ox. [Pa]
sigma_gg = 524e6;          %Resistencia max a la tension del GG (UTS)[Pa]
                           %sigma_gg = 524MPa   <- Hastelloy C (1033ºK)
                           %sigma_gg = 180MPa   <- CRES 347 (1090ºK)
                           %sigma_gg = 413.7MPa <- Cu-Ni-Si-Cr Alloy

emin = 0.001;              %espesor minimo de la pared de los tanques [m]

% 3.- PARAMETROS DE CALCULO %%%%%%%%%%%%%%%%%%%%%%%%%%%%%%%%%%%%%%%%%

FLAG_SIST = 'A';           %A: Un solo motor/turbina
                           %B: Un motor/turbina por bomba

COTA = 0.1;                %Cota para detectar que los vectores son iguales
```

```
fp_LIM = 0.99;                    %Valor limite en la razon p_c/p_0

t_bVALOR = 90;                    %Valor de tiempo de combustion de interes [s]
t_b = t_bVALOR                    %Tiempo de combustion del cohete [s]

m_pVALOR = 1500;                  %Valor puntual de masa de propelente de interes [kg]
m_p = m_pVALOR                    %Cambio un valor del vector por el valor de interes

t_bMAX = 2.5e3;                   %Tiempo maximo decombustion [s]
t_bMIN = 10;                      %Tiempo minimo decombustion [s]
t_bN = 500;                       %Longitud del vector t_b
t_bPASO = (t_bMAX-t_bMIN)/(t_bN-1);        %Paso de tiempo de combustion [s]

t_b = (t_bMIN:t_bPASO:t_bMAX);             %Vector de tiempo de combustion [s]


% 4.- RUTINA DE CALCULO %%%%%%%%%%%%%%%%%%%%%%%%%%%%%%%%%%%%%%%%%%%%%%%%%

%%% COMENTARIOS
%1.- La masa de propelente es un parametro de los graficos
%2.- La presion de la camara de combustion (para ambos sistemas) es un
%    parametro
%3.- El tiempo de combustion es un parametro
%4.- La presion inicial del gas presurizante es la variable


for i=1:size(t_b,2)

% 4.1.- CALCULO DE LA MASA DE GAS
    if p_0>(kappa_p3*p_c)
        %la expresion tiene sentido si p_tf<p_tg entonces se evalua esa
        %condicion
        m_g3(i) = kappa_g*kappa_u*kappa_p3*alfa*gamma_g*M_g*p_c*m_p/(R_u*T_g*(1-kappa_p3*p_c/p_0));
    else
        m_g3(i) = kappa_g*kappa_u*kappa_p3*alfa*gamma_g*M_g*p_c*m_p/(R_u*T_g*(1-fp_LIM));
    end
    if p_0>(kappa_p2*p_c)
        %la expresion tiene sentido si p_tf<p_tg entonces se evalua esa
        %condicion
        m_g2(i) = kappa_g*kappa_u*kappa_p2*alfa*gamma_g*M_g*p_c*m_p/(R_u*T_g*(1-kappa_p2*p_c/p_0));
    else
        m_g2(i) = kappa_g*kappa_u*kappa_p2*alfa*gamma_g*M_g*p_c*m_p/(R_u*T_g*(1-fp_LIM));
    end
    if p_0>(kappa_p1*p_c)
        %la expresion tiene sentido si p_tf<p_tg entonces se evalua esa
        %condicion
        m_g1(i) = kappa_g*kappa_u*kappa_p1*alfa*gamma_g*M_g*p_c*m_p/(R_u*T_g*(1-kappa_p1*p_c/p_0));
    else
        m_g1(i) = kappa_g*kappa_u*kappa_p1*alfa*gamma_g*M_g*p_c*m_p/(R_u*T_g*(1-fp_LIM));
    end

% 4.2.- CALCULO DE LA MASA DE LOS TANQUES DE GAS
    if p_0>(kappa_p3*p_c)
        %la expresion tiene sentido si p_tf<p_tg entonces se evalua esa
        %condicion
        m_tg3(i) = 1.5*rho_tg*kappa_tg*kappa_g*kappa_u*kappa_p3*alfa*gamma_g*p_c*m_p/(sigma_tg*(1-
kappa_p3*p_c/p_0));
    else
        m_tg3(i) = 1.5*rho_tg*kappa_tg*kappa_g*kappa_u*kappa_p3*alfa*gamma_g*p_c*m_p/(sigma_tg*(1-
fp_LIM));
    end
    if p_0>(kappa_p2*p_c)
        %la expresion tiene sentido si p_tf<p_tg entonces se evalua esa
        %condicion
        m_tg2(i) = 1.5*rho_tg*kappa_tg*kappa_g*kappa_u*kappa_p2*alfa*gamma_g*p_c*m_p/(sigma_tg*(1-
kappa_p2*p_c/p_0));
```

```
    else
        m_tg2(i) = 1.5*rho_tg*kappa_tg*kappa_g*kappa_u*kappa_p2*alfa*gamma_g*p_c*m_p/(sigma_tg*(1-
fp_LIM));
    end
    if p_0>(kappa_p1*p_c)
        %la expresion tiene sentido si p_tf<p_tg entonces se evalua esa
        %condicion
        m_tg1(i) = 1.5*rho_tg*kappa_tg*kappa_g*kappa_u*kappa_p1*alfa*gamma_g*p_c*m_p/(sigma_tg*(1-
kappa_p1*p_c/p_0));
    else
        m_tg1(i) = 1.5*rho_tg*kappa_tg*kappa_g*kappa_u*kappa_p1*alfa*gamma_g*p_c*m_p/(sigma_tg*(1-
fp_LIM));
    end
```

% 4.3.- CALCULO DE LA MASA DE LOS TANQUES DE PROPELENTE

```
    %Masa del tanque de combustible para el sistema de gas presurizado
    m_tf11(i) = 1.5*rho_tf*kappa_u*kappa_p1*kappa_tf*alfa_f*m_p*p_c/sigma_tf;
    m_tf12(i) = ((4*pi)^(1/3))*rho_tf*((3*kappa_u*alfa_f*m_p)^(2/3))*emin;
    m_tf1(i) = max(m_tf11(i),m_tf12(i));

    %Masa del tanque de oxidante para el sistema de gas presurizado
    m_to11(i) = 1.5*rho_to*kappa_u*kappa_p1*kappa_to*alfa_o*m_p*p_c/sigma_to;
    m_to12(i) = ((4*pi)^(1/3))*rho_to*((3*kappa_u*alfa_o*m_p)^(2/3))*emin;
    m_to1(i) = max(m_to11(i),m_to12(i));

    %Masa del tanque de combustible para el sistema de electrobombas
    m_tf21(i) = 1.5*rho_tf*kappa_u*kappa_p2*kappa_tf*alfa_f*m_p*p_c/sigma_tf;
    m_tf22(i) = ((4*pi)^(1/3))*rho_tf*((3*kappa_u*alfa_f*m_p)^(2/3))*emin;
    m_tf2(i) = max(m_tf21(i),m_tf22(i));

    %Masa del tanque de oxidante para el sistema de electrobombas
    m_to21(i) = 1.5*rho_to*kappa_u*kappa_p2*kappa_to*alfa_o*m_p*p_c/sigma_to;
    m_to22(i) = ((4*pi)^(1/3))*rho_to*((3*kappa_u*alfa_o*m_p)^(2/3))*emin;
    m_to2(i) = max(m_to21(i),m_to22(i));

    %Masa del tanque de combustible para el sistema de turbobombas
    m_tf31(i) = 1.5*rho_tf*kappa_u*kappa_p3*kappa_tf*alfa_f*m_p*p_c/sigma_tf;
    m_tf32(i) = ((4*pi)^(1/3))*rho_tf*((3*kappa_u*alfa_f*m_p)^(2/3))*emin;
    m_tf3(i) = max(m_tf31(i),m_tf32(i));

    %Masa del tanque de oxidante para el sistema de turbobombas
    m_to31(i) = 1.5*rho_to*kappa_u*kappa_p3*kappa_to*alfa_o*m_p*p_c/sigma_to;
    m_to32(i) = ((4*pi)^(1/3))*rho_to*((3*kappa_u*alfa_o*m_p)^(2/3))*emin;
    m_to3(i) = max(m_to31(i),m_to32(i));
```

% 4.4.- CALCULO DE LA MASA DE LAS BOMBAS

```
    m_puf(i) = (1+kappa_pi-kappa_p2)*alfa_f*p_c*m_p/(delta_pf*t_b(i));
    m_puo(i) = (1+kappa_pi-kappa_p2)*alfa_o*p_c*m_p/(delta_po*t_b(i));
    m_pu(i) = m_puf(i) + m_puo(i);
```

% 4.5.- CALCULO DE LA MASA DEL MOTOR

```
    switch(FLAG_SIST)
        case 'A'    %Masa con un solo motor
            m_ee(i) = (1+kappa_pi-kappa_p2)*p_c*m_p*(alfa_f/eta_pf+alfa_o/eta_po)/(delta_e*t_b(i));
        case 'B'    %Masa con un motor por bomba
            m_ef(i) = (1+kappa_pi-kappa_p2)*alfa_f*p_c*m_p/(eta_pf*delta_e*t_b(i));
            m_eo(i) = (1+kappa_pi-kappa_p2)*alfa_o*p_c*m_p/(eta_po*delta_e*t_b(i));
            m_ee(i) = m_ef(i) + m_eo(i);
        otherwise
            ERROR(i) = 1;
    end
```

% 4.6.- CALCULO DE LA MASA DE LA TURBINA

```
    switch(FLAG_SIST)
        case 'A'    %Masa con una sola turbina
            m_tu(i) = (1+kappa_pi-kappa_p3)*p_c*m_p*(alfa_f/eta_pf+alfa_o/eta_po)/(delta_tu*t_b(i));
        case 'B'    %Masa con una turbina por bomba
```

```
        m_tf(i) = (1+kappa_pi-kappa_p3)*alfa_f*p_c*m_p/(eta_pf*delta_tf*t_b(i));
        m_to(i) = (1+kappa_pi-kappa_p3)*alfa_o*p_c*m_p/(eta_po*delta_to*t_b(i));
        m_tu(i) = m_tf(i) + m_to(i);
    otherwise
        ERROR(i) = 1;
    end

% 4.7.- CALCULO DE LA MASA DEL INVERSOR
    switch(FLAG_SIST)
        case 'A'    %Masa del inversor con un solo motor
          m_inv(i) = (1+kappa_pi-kappa_p2)*p_c*m_p*(alfa_f/eta_pf+alfa_o/eta_po)/(eta_e*delta_inv*t_b(i));
        case 'B'    %Masa de los inversores con un motor por bomba
          m_inf(i) = (1+kappa_pi-kappa_p2)*alfa_f*p_c*m_p/(eta_pf*eta_ef*delta_inv*t_b(i));
          m_ino(i) = (1+kappa_pi-kappa_p2)*alfa_o*p_c*m_p/(eta_po*eta_eo*delta_inv*t_b(i));
          m_inv(i) = m_inf(i) + m_ino(i);
        otherwise
          ERROR(i) = 1;
    end

% 4.8.- CALCULO DE LA MASA DE LAS BATERIAS
% Primera tecnologia de baterias:
    switch(FLAG_SIST)
        case 'A'    %Masa de las baterias con un solo motor
          m_bap1(i) = (1+kappa_pi-
kappa_p2)*p_c*m_p*kappa_b*(alfa_f/eta_pf+alfa_o/eta_po)/(eta_e*eta_inv*delta_bap1*t_b(i));
          m_baw1(i) = (1+kappa_pi-
kappa_p2)*p_c*m_p*kappa_b*(alfa_f/eta_pf+alfa_o/eta_po)/(eta_e*eta_inv*delta_baw1);
          m_bat1(i) = max(m_bap1(i),m_baw1(i));
        case 'B'    %Masa de las baterias con un motor por bomba
          m_bap1(i) = (1+kappa_pi-
kappa_p2)*p_c*m_p*kappa_b*(alfa_f/(eta_pf*eta_ef*eta_inv)+alfa_o/(eta_po*eta_eo*eta_inv))/(delta_bap1*t_b(i));
          m_baw1(i) = (1+kappa_pi-
kappa_p2)*p_c*m_p*kappa_b*(alfa_f/(eta_pf*eta_ef*eta_inv)+alfa_o/(eta_po*eta_eo*eta_inv))/delta_baw1;
          m_bat1(i) = max(m_bap1(i),m_baw1(i));
        otherwise
          ERROR(i) = 1;
    end

% Segunda tecnologia de baterias:
    switch(FLAG_SIST)
        case 'A'    %Masa de las baterias con un solo motor
          m_bap2(i) = (1+kappa_pi-
kappa_p2)*p_c*m_p*kappa_b*(alfa_f/eta_pf+alfa_o/eta_po)/(eta_e*eta_inv*delta_bap2*t_b(i));
          m_baw2(i) = (1+kappa_pi-
kappa_p2)*p_c*m_p*kappa_b*(alfa_f/eta_pf+alfa_o/eta_po)/(eta_e*eta_inv*delta_baw2);
          m_bat2(i) = max(m_bap2(i),m_baw2(i));
        case 'B'    %Masa de las baterias con un motor por bomba
          m_bap2(i) = (1+kappa_pi-
kappa_p2)*p_c*m_p*kappa_b*(alfa_f/(eta_pf*eta_ef*eta_inv)+alfa_o/(eta_po*eta_eo*eta_inv))/(delta_bap2*t_b(i));
          m_baw2(i) = (1+kappa_pi-
kappa_p2)*p_c*m_p*kappa_b*(alfa_f/(eta_pf*eta_ef*eta_inv)+alfa_o/(eta_po*eta_eo*eta_inv))/delta_baw2;
          m_bat2(i) = max(m_bap2(i),m_baw2(i));
        otherwise
          ERROR(i) = 1;
    end

% Tercera tecnologia de baterias:
    switch(FLAG_SIST)
        case 'A'    %Masa de las baterias con un solo motor
          m_bap3(i) = (1+kappa_pi-
kappa_p2)*p_c*m_p*kappa_b*(alfa_f/eta_pf+alfa_o/eta_po)/(eta_e*eta_inv*delta_bap3*t_b(i));
          m_baw3(i) = (1+kappa_pi-
kappa_p2)*p_c*m_p*kappa_b*(alfa_f/eta_pf+alfa_o/eta_po)/(eta_e*eta_inv*delta_baw3);
          m_bat3(i) = max(m_bap3(i),m_baw3(i));
        case 'B'    %Masa de las baterias con un motor por bomba
          m_bap3(i) = (1+kappa_pi-
kappa_p2)*p_c*m_p*kappa_b*(alfa_f/(eta_pf*eta_ef*eta_inv)+alfa_o/(eta_po*eta_eo*eta_inv))/(delta_bap3*t_b(i));
```

```
        m_baw3(i) = (1+kappa_pi-
kappa_p2)*p_c*m_p*kappa_b*(alfa_f/(eta_pf*eta_ef*eta_inv)+alfa_o/(eta_po*eta_eo*eta_inv))/delta_baw3;
        m_bat3(i) = max(m_bap3(i),m_baw3(i));
      otherwise
        ERROR(i) = 1;
   end

% 4.9.- CALCULO DE PROPELENTE PARA ACCIONAR LA TURBINA
   m_ptu(i) = (1+kappa_pi-kappa_p3)*p_c*m_p*M_gg*(gamma_gg-
1)*(alfa_f/eta_pf+alfa_o/eta_po)/(eta_tu*T_itu*gamma_gg*R_u*(1-(p_dtu/p_itu)^((gamma_gg-1)/gamma_gg)));

% 4.10.- CALCULO DE LA MASA DEL GENERADOR DE GAS
   V_g(i) = t_s*m_ptu(i)/(t_b(i)*rho_gg);
   r_g(i) = (0.75*V_g(i))^(1/3);
   S_g(i) = 4*pi*(0.75*V_g(i)/pi)^(2/3);
   m_gg(i) = rho_tgg*kappa_gg*p_gg*r_g(i)*S_g(i)/(2*sigma_gg);
end

%Busco el punto donde la masa pasa de estar impuesta por potencia a estar
%impuesta por energia para la tecnologia 1

Indices1 = find((m_bat1-m_baw1)<COTA);
if length(Indices1)>0
   LIMITE1 = Indices1(1);
else
   LIMITE1 = 1;
end

%Busco el punto donde la masa pasa de estar impuesta por potencia a estar
%impuesta por energia para la tecnologia 2

Indices2 = find((m_bat2-m_baw2)<COTA);
if length(Indices2)>0
   LIMITE2 = Indices2(1);
else
   LIMITE2 = t_bN-1;
end

%Busco el punto donde la masa pasa de estar impuesta por potencia a estar
%impuesta por energia para la tecnologia 3

Indices3 = find((m_bat3-m_baw3)<COTA);
if length(Indices3)>0
   LIMITE3 = Indices3(1);
else
   LIMITE3 = t_bN-1;
end

m_pg = m_g1 + m_tg1 + m_tf1 + m_to1;
m_tp = m_g3 + m_tg3 + m_tf3 + m_to3 + m_pu + m_tu + m_gg + m_ptu;

%Genero dos vectores, uno con los valores correspondientes a la masa
%impuesta por la potencia y el otro con los valores de la masa impuesta por
%la energia para cada tecnologia

 for k=1:LIMITE1
   t_b1A(k) = t_b(k);
   m_ep1A(k) = m_g2(k) + m_tg2(k) + m_tf2(k) + m_to2(k) + m_pu(k) + m_ee(k) + m_inv(k) +
max(m_bap1(k),m_baw1(k));
 end

 for j=1:(length(t_b)-LIMITE1)
   t_b1B(j) = t_b(j+LIMITE1-1);
   m_ep1B(j) = m_g2(j+LIMITE1-1) + m_tg2(j+LIMITE1-1) + m_tf2(j+LIMITE1-1) + m_to2(j+LIMITE1-1) +
m_pu(j+LIMITE1-1) + m_ee(j+LIMITE1-1) + m_inv(j+LIMITE1-1) + max(m_bap1(j+LIMITE1-
1),m_baw1(j+LIMITE1-1));
 end
```

```
 for k=1:LIMITE2
    t_b2A(k) = t_b(k);
    m_ep2A(k) = m_g2(k) + m_tg2(k) + m_tf2(k) + m_to2(k) + m_pu(k) + m_ee(k) + m_inv(k) +
max(m_bap2(k),m_baw2(k));
 end

 for j=1:(length(t_b)-LIMITE2)
    t_b2B(j) = t_b(j+LIMITE2-1);
    m_ep2B(j) = m_g2(j+LIMITE2-1) + m_tg2(j+LIMITE2-1) + m_tf2(j+LIMITE2-1) + m_to2(j+LIMITE2-1) +
m_pu(j+LIMITE2-1) + m_ee(j+LIMITE2-1) + m_inv(j+LIMITE2-1) + max(m_bap2(j+LIMITE2-
1),m_baw2(j+LIMITE2-1));
 end

 for k=1:LIMITE3
    t_b3A(k) = t_b(k);
    m_ep3A(k) = m_g2(k) + m_tg2(k) + m_tf2(k) + m_to2(k) + m_pu(k) + m_ee(k) + m_inv(k) +
max(m_bap3(k),m_baw3(k));
 end

 for j=1:(length(t_b)-LIMITE3)
    t_b3B(j) = t_b(j+LIMITE3-1);
    m_ep3B(j) = m_g2(j+LIMITE3-1) + m_tg2(j+LIMITE3-1) + m_tf2(j+LIMITE3-1) + m_to2(j+LIMITE3-1) +
m_pu(j+LIMITE3-1) + m_ee(j+LIMITE3-1) + m_inv(j+LIMITE3-1) + max(m_bap3(j+LIMITE3-
1),m_baw3(j+LIMITE3-1));
 end


fm_pg = m_pg/m_p;          %Fraccion de masas: gas presurizado/masa propelente
fm_ep1A = m_ep1A/m_p;      %Fraccion de masas: electrobombas/masa propelente
fm_ep1B = m_ep1B/m_p;      %Fraccion de masas: electrobombas/masa propelente
fm_ep2A = m_ep2A/m_p;      %Fraccion de masas: electrobombas/masa propelente
fm_ep2B = m_ep2B/m_p;      %Fraccion de masas: electrobombas/masa propelente
fm_ep3A = m_ep3A/m_p;      %Fraccion de masas: electrobombas/masa propelente
fm_ep3B = m_ep3B/m_p;      %Fraccion de masas: electrobombas/masa propelente
fm_tp = m_tp/m_p;          %Fraccion de masas: turbobombas/masa propelente

% 4.- RUTINA DE GENERACION DE GRAFICOS %%%%%%%%%%%%%%%%%%%%%%%%%%%%%%%%%%%%%


x_MIN = t_bMIN;
x_MAX = t_bMAX;
y_MIN = 0;
y_MAX = 0.2;
x_COOR = x_MIN+0.2*(x_MAX-x_MIN);
y_COOR = y_MIN+0.5*(y_MAX-y_MIN);
RENGLON = 0.05*(y_MAX-y_MIN);

figure
plot(t_b,fm_pg,'b','linewidth',2)
axis([x_MIN x_MAX y_MIN y_MAX])
xlabel('Tiempo de combustion [s]','FontSize',12,'FontWeight','demi')
ylabel('m_f_s/m_p','FontSize',12,'FontWeight','demi')
title('Relacion Masa del Sist. de Alimentacion vs Masa de Propelente','FontSize',14)
text(x_COOR,y_COOR,['Masa de propelente: m_p = ' num2str(m_pVALOR) 'kg'])
text(x_COOR,y_COOR-RENGLON,['Presion de camara: p_C = ' num2str(p_c/1e5) 'bar'])
grid on
hold on
plot(t_b1A,fm_ep1A,'r','linewidth',2)
hold on
plot(t_b1B,fm_ep1B,'r--','linewidth',2)
hold on
plot(t_b2A,fm_ep2A,'g','linewidth',2)
hold on
plot(t_b2B,fm_ep2B,'g--','linewidth',2)
hold on
```

```
plot(t_b3A,fm_ep3A,'c','linewidth',2)
hold on
plot(t_b3B,fm_ep3B,'c--','linewidth',2)
hold on
plot(t_b,fm_tp,'m','linewidth',2)
legend('Sist. Gas Presurizado','Electrico Li-Po(m_b_a_t impuesta por P)','Electrico Li-Po(m_b_a_t impuesta por
W)','Electrico Li-S(m_b_a_t impuesta por P)','Electrico Li-S(m_b_a_t impuesta por W)','Electrico Li-S 2da
generacion (m_b_a_t impuesta por P)','Electrico Li-S 2da generacion (m_b_a_t impuesta por W)','Sist. de
Turbobombas',0)

saveas(gcf,['masa_vs_bat_ver03_mp_' num2str(m_pVALOR) '_PC_' num2str(p_c/1e5) '.png'])


%%%%%%% RUTINA DE COMPARACION VI %%%%%%%%%%%%%%%%%%%%%%
% Descripcion: Esta rutina compara la fraccion de masa de cada
% componente que forma parte del sistema electrico.
%
% Comentarios:
%1.- La variable para la comparacion es el tiempo de combustion.

clear all
close all

% 1.- VARIABLES DE ENTRADA %%%%%%%%%%%%%%%%%%%%%%%%%%%%%%%%%%%%%%%%%%%%%

% 1.1.- Presiones:

%Aclaraciones:

% Sistema 1: alimentado por gas presurizado
% Sistema 2: alimentado por electrobombas
% Sistema 3: alimentado por turbobombas
% Se asume que la presion en el tanque de combustible y en el tanque de
% oxidante son iguales entre si. Para cada sistema entonces se define una
% presion en el tanque de propelente.


p_c = 6.0e6;                 %Presion de la camara de combustion [Pa]
p_0 = 20e6;                  %Presion inicial del tanque de gas [Pa]
p_irat = 0.3;                %Relacion entre la presion de camara y la del inyector
p_tp1 = (1+p_irat)*p_c;      %Presion del tanque de propelente p/ el sist. 1 [Pa]
p_tp2 = 0.6e6;               %Presion del tanque de propelente p/ el sist. 2 [Pa]
p_tp3 = 0.6e6;               %Presion del tanque de propelente p/ el sist. 3 [Pa]
p_in = p_irat*p_c;           %Presion en el inyector [Pa]
p_gg = p_c;                  %Presion de la camara del generador [Pa]
p_itu = p_gg;                %Presion de ingreso de la turbina [Pa]
p_trat = 20;                 %Relacion de presiones de la turbina
p_dtu = p_itu/p_trat;        %Presion de descarga de la turbina [Pa]

% 1.2.- Temperaturas:

T_itu = 900;                 %Temperatura de los gases q ingresan en la turbina [ºK]
T_g = 288.15;                %Temperatura del gas presurizante [ºK]
T_gg = 1100;                 %Temperatura de la camara del generador de gas [ºK]

% 1.3.- Variables Quimicas (Masas, masas molares y const. isentropicas):

gamma_c = 1.23;              %Parametro isentropico de los gases de la camara
gamma_g = 1.667;             %Parametro isentropico del gas presurizante
gamma_gg = 1.196;            %Parametro isentropico de los gases del gen. de gas
M_c = 23;                    %Masa molar de los gases de la camara [kg/kmol]
M_gg = 14.2;                 %Masa molar de los gases de la gen. de gas [kg/kmol]
M_g = 4.0026;                %Masa molar del gas presurizante [kg/kmol]
OF = 1.9;                    %Relacion oxidante/combustible
R_u = 8314.41;               %Constante Universal de los gases [J/kmolºK]
t_s = 10e-3;                 %stay time

% 1.4.- Densidades:
```

```
rho_f = 874;              %Densidad del combustible [kg/m3]
rho_o = 1431;             %Densidad del oxidante [kg/m3]
rho_gg = 0.8774;          %Densidad de los gases de escape [kg/m3]
rho_tg = 1700;            %Densidad del tanque de gas [kg/m3]
rho_to = 2800;            %Densidad del tanque de oxidante [kg/m3]
rho_tf = 2800;            %Densidad del tanque de combustible [kg/m3]
rho_tgg = 8890;           %Densidad del material de la camara del GG [kg/m3]
                          %rho_tgg = 8890 <- Hastelloy C
                          %rho_tgg = 7960kg/m3 <- CRES 347
                          %rho_tgg = 8800 <- Cu-Ni-Si-Cr Alloy


delta_pf = 40e3;          %Densidad de potencia de la bomba de comb. [W/kg]
delta_po = 40e3;          %Densidad de potencia de la bomba de ox. [W/kg]
delta_e = 3.8e3;          %Densidad de potencia del motor [W/kg]
delta_ef = 3.8e3;         %Densidad de potencia del motor de comb. [W/kg]
delta_eo = 3.8e3;         %Densidad de potencia del motor de ox. [W/kg]
delta_tu = 20e3;          %Densidad de potencia de la turbina [W/kg]
delta_tf = 20e3;          %Densidad de potencia de la turbina de comb. [W/kg]
delta_to = 20e3;          %Densidad de potencia de la turbina de ox. [W/kg]
delta_inv = 60e3;         %Densidad de potencia del inversor [W/kg]
delta_bap = 4.8e3;        %Densidad de potencia de las baterias [W/kg]
delta_baw = 130;          %Densidad de energia de las baterias [Wh/kg]
delta_baw = delta_baw*3600; %Densidad de energia de las baterias [J/kg]

% 1.5.- Rendimientos:

eta_pf = 0.8;             %Rendimiento de la bomba de comb.
eta_po = 0.8;             %Rendimiento de la bomba de ox.
eta_e = 0.8;              %Rendimiento del motor electrico
eta_ef = 0.8;             %Rendimiento del motor de comb.
eta_eo = 0.8;             %Rendimiento del motor de ox.
eta_inv = 0.85;           %Rendimiento del inversor
eta_tu = 0.8;             %Rendimiento de la turbina

% 2.- CONSTANTES %%%%%%%%%%%%%%%%%%%%%%%%%%%%%%%%%%%%%%%%%%%%%%%%%%%%%%

kappa_p1 = p_tp1/p_c;     %para el sistema de alimentacion por gas pres.
kappa_p2 = p_tp2/p_c;     %para el sist. de alim. por electrobombas
kappa_p3 = p_tp3/p_c;     %para el sist. de alim. por turbobombas
kappa_pi = p_in/p_c;      %razon de la caida en el inyector respecto de p_c
kappa_u = 1.05;           %factor de seguridad para preveer el "ullage"
kappa_g = 1.3;            %factor de seguridad para la masa de gas
kappa_tg = 2.5;           %factor de seguridad para el espesor del tanque de gas
kappa_tf = 2.5;           %factor de seguridad para el espesor del tanque de comb.
kappa_to = 2.5;           %factor de seguridad para el espesor del tanque de ox.
kappa_b = 1.2;            %margen de diseño para la masa de las baterias
kappa_gg = 2.5;           %factor de seguridad para el espesor de la pared del GG

alfa_f = 1/(rho_f*(1+OF));   %permite relacionar el volumen de comb. con m_p
alfa_o = OF/(rho_o*(1+OF)); %permite relacionar el volumen de ox. con m_p
alfa = alfa_f + alfa_o;      %permite relacionar el volumen de propelente con m_p

sigma_tg = 3.3e9;         %Resistencia max a la tension del tanque de gas [Pa]
sigma_tf = 455e6;         %Resistencia max a la tension del tanque de comb. [Pa]
sigma_to = 455e6;         %Resistencia max a la tension del tanque de ox. [Pa]
sigma_gg = 524e6;         %Resistencia max a la tension del GG (UTS)[Pa]
                          %sigma_gg = 524MPa   <- Hastelloy C (1033ºK)
                          %sigma_gg = 180MPa   <- CRES 347 (1090ºK)
                          %sigma_gg = 413.7MPa <- Cu-Ni-Si-Cr Alloy

emin = 0.001;             %espesor minimo de la pared de los tanques [m]


% 3.- PARAMETROS DE CALCULO %%%%%%%%%%%%%%%%%%%%%%%%%%%%%%%%%%%%%%%%%%%%
```

```
FLAG_SIST = 'A';              %A: Un solo motor/turbina
                              %B: Un motor/turbina por bomba

COTA = 0.1;                   %Cota para detectar que los vectores son iguales

fp_LIM = 0.99;                %Valor limite en la razon p_c/p_0

t_bVALOR = 90;                %Valor de tiempo de combustion de interes [s]
t_b = t_bVALOR                %Tiempo de combustion del cohete [s]

m_pVALOR = 1000;              %Valor puntual de masa de propelente de interes [kg]
m_p = m_pVALOR                %Cambio un valor del vector por el valor de interes

t_bMAX = 1.0e3;               %Tiempo maximo decombustion [s]
t_bMIN = 30;                  %Tiempo minimo decombustion [s]
t_bN = 500;                   %Longitud del vector t_b
t_bPASO = (t_bMAX-t_bMIN)/(t_bN-1);      %Paso de tiempo de combustion [s]

t_b = (t_bMIN:t_bPASO:t_bMAX);           %Vector de tiempo de combustion [s]


% 4.- RUTINA DE CALCULO %%%%%%%%%%%%%%%%%%%%%%%%%%%%%%%%%%%%%%%%%%%%%%%%

%%% COMENTARIOS
%1.- La masa de propelente es un parametro de los graficos
%2.- La presion de la camara de combustion (para ambos sistemas) es un
%    parametro
%3.- El tiempo de combustion es un parametro
%4.- La presion inicial del gas presurizante es la variable


for i=1:size(t_b,2)

% 4.1.- CALCULO DE LA MASA DE GAS
   if p_0>(kappa_p3*p_c)
      %la expresion tiene sentido si p_tf<p_tg entonces se evalua esa
      %condicion
      m_g3(i) = kappa_g*kappa_u*kappa_p3*alfa*gamma_g*M_g*p_c*m_p/(R_u*T_g*(1-kappa_p3*p_c/p_0));
   else
      m_g3(i) = kappa_g*kappa_u*kappa_p3*alfa*gamma_g*M_g*p_c*m_p/(R_u*T_g*(1-fp_LIM));
   end
   if p_0>(kappa_p2*p_c)
      %la expresion tiene sentido si p_tf<p_tg entonces se evalua esa
      %condicion
      m_g2(i) = kappa_g*kappa_u*kappa_p2*alfa*gamma_g*M_g*p_c*m_p/(R_u*T_g*(1-kappa_p2*p_c/p_0));
   else
      m_g2(i) = kappa_g*kappa_u*kappa_p2*alfa*gamma_g*M_g*p_c*m_p/(R_u*T_g*(1-fp_LIM));
   end
   if p_0>(kappa_p1*p_c)
      %la expresion tiene sentido si p_tf<p_tg entonces se evalua esa
      %condicion
      m_g1(i) = kappa_g*kappa_u*kappa_p1*alfa*gamma_g*M_g*p_c*m_p/(R_u*T_g*(1-kappa_p1*p_c/p_0));
   else
      m_g1(i) = kappa_g*kappa_u*kappa_p1*alfa*gamma_g*M_g*p_c*m_p/(R_u*T_g*(1-fp_LIM));
   end

% 4.2.- CALCULO DE LA MASA DE LOS TANQUES DE GAS
   if p_0>(kappa_p2*p_c)
      %la expresion tiene sentido si p_tf<p_tg entonces se evalua esa
      %condicion
      m_tg2(i) = 1.5*rho_tg*kappa_tg*kappa_g*kappa_u*kappa_p2*alfa*gamma_g*p_c*m_p/(sigma_tg*(1-kappa_p2*p_c/p_0));
   else
      m_tg2(i) = 1.5*rho_tg*kappa_tg*kappa_g*kappa_u*kappa_p2*alfa*gamma_g*p_c*m_p/(sigma_tg*(1-fp_LIM));
   end
   if p_0>(kappa_p3*p_c)
```

```matlab
        %la expresion tiene sentido si p_tf<p_tg entonces se evalua esa
        %condicion
        m_tg3(i) = 1.5*rho_tg*kappa_tg*kappa_g*kappa_u*kappa_p3*alfa*gamma_g*p_c*m_p/(sigma_tg*(1-
kappa_p3*p_c/p_0));
    else
        m_tg3(i) = 1.5*rho_tg*kappa_tg*kappa_g*kappa_u*kappa_p3*alfa*gamma_g*p_c*m_p/(sigma_tg*(1-
fp_LIM));
    end
    if p_0>(kappa_p1*p_c)
        %la expresion tiene sentido si p_tf<p_tg entonces se evalua esa
        %condicion
        m_tg1(i) = 1.5*rho_tg*kappa_tg*kappa_g*kappa_u*kappa_p1*alfa*gamma_g*p_c*m_p/(sigma_tg*(1-
kappa_p1*p_c/p_0));
    else
        m_tg1(i) = 1.5*rho_tg*kappa_tg*kappa_g*kappa_u*kappa_p1*alfa*gamma_g*p_c*m_p/(sigma_tg*(1-
fp_LIM));
    end

% 4.3.- CALCULO DE LA MASA DE LOS TANQUES DE PROPELENTE
    %Masa del tanque de combustible para el sistema de gas presurizado
    m_tf11(i) = 1.5*rho_tf*kappa_u*kappa_p1*kappa_tf*alfa_f*m_p*p_c/sigma_tf;
    m_tf12(i) = ((4*pi)^(1/3))*rho_tf*((3*kappa_u*alfa_f*m_p)^(2/3))*emin;
    m_tf1(i) = max(m_tf11(i),m_tf12(i));

    %Masa del tanque de oxidante para el sistema de gas presurizado
    m_to11(i) = 1.5*rho_to*kappa_u*kappa_p1*kappa_to*alfa_o*m_p*p_c/sigma_to;
    m_to12(i) = ((4*pi)^(1/3))*rho_to*((3*kappa_u*alfa_o*m_p)^(2/3))*emin;
    m_to1(i) = max(m_to11(i),m_to12(i));

    %Masa del tanque de combustible para el sistema de electrobombas
    m_tf21(i) = 1.5*rho_tf*kappa_u*kappa_p2*kappa_tf*alfa_f*m_p*p_c/sigma_tf;
    m_tf22(i) = ((4*pi)^(1/3))*rho_tf*((3*kappa_u*alfa_f*m_p)^(2/3))*emin;
    m_tf2(i) = max(m_tf21(i),m_tf22(i));

    %Masa del tanque de oxidante para el sistema de electrobombas
    m_to21(i) = 1.5*rho_to*kappa_u*kappa_p2*kappa_to*alfa_o*m_p*p_c/sigma_to;
    m_to22(i) = ((4*pi)^(1/3))*rho_to*((3*kappa_u*alfa_o*m_p)^(2/3))*emin;
    m_to2(i) = max(m_to21(i),m_to22(i));

    %Masa del tanque de combustible para el sistema de turbobombas
    m_tf31(i) = 1.5*rho_tf*kappa_u*kappa_p3*kappa_tf*alfa_f*m_p*p_c/sigma_tf;
    m_tf32(i) = ((4*pi)^(1/3))*rho_tf*((3*kappa_u*alfa_f*m_p)^(2/3))*emin;
    m_tf3(i) = max(m_tf31(i),m_tf32(i));

    %Masa del tanque de oxidante para el sistema de turbobombas
    m_to31(i) = 1.5*rho_to*kappa_u*kappa_p3*kappa_to*alfa_o*m_p*p_c/sigma_to;
    m_to32(i) = ((4*pi)^(1/3))*rho_to*((3*kappa_u*alfa_o*m_p)^(2/3))*emin;
    m_to3(i) = max(m_to31(i),m_to32(i));

% 4.4.- CALCULO DE LA MASA DE LAS BOMBAS
    m_puf(i) = (1+kappa_pi-kappa_p2)*alfa_f*p_c*m_p/(delta_pf*t_b(i));
    m_puo(i) = (1+kappa_pi-kappa_p2)*alfa_o*p_c*m_p/(delta_po*t_b(i));
    m_pu(i) = m_puf(i) + m_puo(i);

% 4.5.- CALCULO DE LA MASA DEL MOTOR
    switch(FLAG_SIST)
        case 'A'    %Masa con un solo motor
            m_ee(i) = (1+kappa_pi-kappa_p2)*p_c*m_p*(alfa_f/eta_pf+alfa_o/eta_po)/(delta_e*t_b(i));
        case 'B'    %Masa con un motor por bomba
            m_ef(i) = (1+kappa_pi-kappa_p2)*alfa_f*p_c*m_p/(eta_pf*delta_e*t_b(i));
            m_eo(i) = (1+kappa_pi-kappa_p2)*alfa_o*p_c*m_p/(eta_po*delta_e*t_b(i));
            m_ee(i) = m_ef(i) + m_eo(i);
        otherwise
            ERROR(i) = 1;
    end

% 4.6.- CALCULO DE LA MASA DE LA TURBINA
```

```
    switch(FLAG_SIST)
       case 'A'    %Masa con una sola turbina
          m_tu(i) = (1+kappa_pi-kappa_p3)*p_c*m_p*(alfa_f/eta_pf+alfa_o/eta_po)/(delta_tu*t_b(i));
       case 'B'    %Masa con una turbina por bomba
          m_tf(i) = (1+kappa_pi-kappa_p3)*alfa_f*p_c*m_p/(eta_pf*delta_tf*t_b(i));
          m_to(i) = (1+kappa_pi-kappa_p3)*alfa_o*p_c*m_p/(eta_po*delta_to*t_b(i));
          m_tu(i) = m_tf(i) + m_to(i);
       otherwise
          ERROR(i) = 1;
    end

% 4.7.- CALCULO DE LA MASA DEL INVERSOR
    switch(FLAG_SIST)
       case 'A'    %Masa del inversor con un solo motor
          m_inv(i) = (1+kappa_pi-kappa_p2)*p_c*m_p*(alfa_f/eta_pf+alfa_o/eta_po)/(eta_e*delta_inv*t_b(i));
       case 'B'    %Masa de los inversores con un motor por bomba
          m_inf(i) = (1+kappa_pi-kappa_p2)*alfa_f*p_c*m_p/(eta_pf*eta_ef*delta_inv*t_b(i));
          m_ino(i) = (1+kappa_pi-kappa_p2)*alfa_o*p_c*m_p/(eta_po*eta_eo*delta_inv*t_b(i));
          m_inv(i) = m_inf(i) + m_ino(i);
       otherwise
          ERROR(i) = 1;
    end

% 4.8.- CALCULO DE LA MASA DE LAS BATERIAS
    switch(FLAG_SIST)
       case 'A'    %Masa de las baterias con un solo motor
          m_bap(i) = (1+kappa_pi-
kappa_p2)*p_c*m_p*kappa_b*(alfa_f/eta_pf+alfa_o/eta_po)/(eta_e*eta_inv*delta_bap*t_b(i));
          m_baw(i) = (1+kappa_pi-
kappa_p2)*p_c*m_p*kappa_b*(alfa_f/eta_pf+alfa_o/eta_po)/(eta_e*eta_inv*delta_baw);
          m_bat(i) = max(m_bap(i),m_baw(i));
       case 'B'    %Masa de las baterias con un motor por bomba
          m_bap(i) = (1+kappa_pi-
kappa_p2)*p_c*m_p*kappa_b*(alfa_f/(eta_pf*eta_ef*eta_inv)+alfa_o/(eta_po*eta_eo*eta_inv))/(delta_bap*t_b(i));
          m_baw(i) = (1+kappa_pi-
kappa_p2)*p_c*m_p*kappa_b*(alfa_f/(eta_pf*eta_ef*eta_inv)+alfa_o/(eta_po*eta_eo*eta_inv))/delta_baw;
          m_bat(i) = max(m_bap(i),m_baw(i));
       otherwise
          ERROR(i) = 1;
    end

% 4.9.- CALCULO DE PROPELENTE PARA ACCIONAR LA TURBINA
    m_ptu(i) = (1+kappa_pi-kappa_p3)*p_c*m_p*M_gg*(gamma_gg-
1)*(alfa_f/eta_pf+alfa_o/eta_po)/(eta_tu*T_itu*gamma_gg*R_u*(1-(p_dtu/p_itu)^((gamma_gg-1)/gamma_gg)));

% 4.10.- CALCULO DE LA MASA DEL GENERADOR DE GAS
    V_g(i) = t_s*m_ptu(i)/(t_b(i)*rho_gg);
    r_g(i) = (0.75*V_g(i))^(1/3);
    S_g(i) = 4*pi*(0.75*V_g(i)/pi)^(2/3);
    m_gg(i) = rho_tgg*kappa_gg*p_gg*r_g(i)*S_g(i)/(2*sigma_gg);

end

Indices = find((m_bat-m_baw)<COTA);
if length(Indices)>0
    LIMITE = Indices(1);
else
    LIMITE = 1;
end

%
% for k=1:LIMITE
%    p_iA(k) = p_i(k);
%    m_batA(k) = m_bat(k);
% end
%
% for k=1:(length(p_i)-LIMITE)
```

```
%    p_iB(k) = p_i(k+LIMITE-1);
%    m_batB(k) = m_bat(k+LIMITE-1);
% end
%Tengo que partir el vector m_ep en dos vectores uno sumando m_bap hasta
%LIMITE y otro sumando m_baw desde LIMITE + 1 hasta el final

m_pg = m_g1 + m_tg1 + m_tf1 + m_to1;
m_tp = m_g3 + m_tg3 + m_tf3 + m_to3 + m_pu + m_tu + m_gg + m_ptu;

 for k=1:LIMITE
    t_bA(k) = t_b(k);
    m_batA(k) = max(m_bap(k),m_baw(k));
 end

 for j=1:(length(t_b)-LIMITE)
    t_bB(j) = t_b(j+LIMITE-1);
    m_batB(j) = max(m_bap(j+LIMITE-1),m_baw(j+LIMITE-1));
 end


fm_pg = m_pg/m_p;          %Fraccion de masas: gas presurizado/masa propelente
fm_tp = m_tp/m_p;          %Fraccion de masas: turbobombas/masa propelente

fm_ee = m_ee/m_p;          %Fraccion de masas: motor electrico/masa propelente
fm_inv = m_inv/m_p;        %Fraccion de masas: inversor/masa propelente
fm_batA = m_batA/m_p;      %Fraccion de masas: baterias/masa propelente
fm_batB = m_batB/m_p;      %Fraccion de masas: baterias/masa propelente


% 4.- RUTINA DE GENERACION DE GRAFICOS %%%%%%%%%%%%%%%%%%%%%%%%%%%%%%%%%%%%


x_MIN = t_bMIN;
x_MAX = t_bMAX;
y_MIN = 0;
y_MAX = 0.04;
x_COOR = x_MIN+0.1*(x_MAX-x_MIN);
y_COOR = y_MIN+0.8*(y_MAX-y_MIN);
RENGLON = 0.05*(y_MAX-y_MIN);

figure
plot(t_b,fm_ee,'b','linewidth',2)
axis([x_MIN x_MAX y_MIN y_MAX])
xlabel('Tiempo de combustion [s]','FontSize',12,'FontWeight','demi')
ylabel('masa de los componentes','FontSize',12,'FontWeight','demi')
title('Relacion Masa de los Componentes del Sist. Electrico vs Masa de Propelente','FontSize',14)
text(x_COOR,y_COOR,['Masa de propelente: m_p = ' num2str(m_pVALOR) 'kg'])
text(x_COOR,y_COOR-RENGLON,['Presion de camara: p_C = ' num2str(p_c/1e5) 'bar'])
grid on
hold on
plot(t_bA,fm_batA,'r','linewidth',2)
hold on
plot(t_bB,fm_batB,'r--','linewidth',2)
hold on
plot(t_b,fm_inv,'g','linewidth',2)
legend('Motor Electrico','Baterias (m_b_a_t impuesta por P)','Baterias (m_b_a_t impuesta por W)','Inversor',1)

saveas(gcf,['masaSisElec_vs_tb_ver00_mp_' num2str(m_pVALOR) '_PC_' num2str(p_c/1e5) '.png'])


%%%%%%% RUTINA DE COMPARACION VII %%%%%%%%%%%%%%%%%%%%%%%%%%%%%%%%%%%%%%%%%
% Descripcion: Esta rutina determina las densidades de energia y potencia
% necesarias para que la fraccion de masa del sistema electrico sea igual a
% la del sistema con turbobombas.
%
% Comentarios:
%1.- La variable para la comparacion es el tiempo de combustion.
```

```
clear all
close all

% 1.- VARIABLES DE ENTRADA %%%%%%%%%%%%%%%%%%%%%%%%%%%%%%%%%%%%%%%%%%%%%%

% 1.1.- Presiones:

%Aclaraciones:

% Sistema 1: alimentado por gas presurizado
% Sistema 2: alimentado por electrobombas
% Sistema 3: alimentado por turbobombas
% Se asume que la presion en el tanque de combustible y en el tanque de
% oxidante son iguales entre si. Para cada sistema entonces se define una
% presion en el tanque de propelente.

p_c = 1.5e6;                    %Presion de la camara de combustion [Pa]
p_0 = 20e6;                     %Presion inicial del tanque de gas [Pa]
p_irat = 0.3;                   %Relacion entre la presion de camara y la del inyector
p_tp1 = (1+p_irat)*p_c;         %Presion del tanque de propelente p/ el sist. 1 [Pa]
p_tp2 = 0.6e6;                  %Presion del tanque de propelente p/ el sist. 2 [Pa]
p_tp3 = 0.6e6;                  %Presion del tanque de propelente p/ el sist. 3 [Pa]
p_in = p_irat*p_c;              %Presion en el inyector [Pa]
p_gg = p_c;                     %Presion de la camara del generador [Pa]
p_itu = p_gg;                   %Presion de ingreso de la turbina [Pa]
p_trat = 20;                    %Relacion de presiones de la turbina
p_dtu = p_itu/p_trat;           %Presion de descarga de la turbina [Pa]

% 1.2.- Temperaturas:

T_itu = 900;                    %Temperatura de los gases q ingresan en la turbina [ºK]
T_g = 288.15;                   %Temperatura del gas presurizante [ºK]
T_gg = 1100;                    %Temperatura de la camara del generador de gas [ºK]

% 1.3.- Variables Quimicas (Masas, masas molares y const. isentropicas):

gamma_c = 1.23;                 %Parametro isentropico de los gases de la camara
gamma_g = 1.667;                %Parametro isentropico del gas presurizante
gamma_gg = 1.196;               %Parametro isentropico de los gases del gen. de gas
M_c = 23;                       %Masa molar de los gases de la camara [kg/kmol]
M_gg = 14.2;                    %Masa molar de los gases de la gen. de gas [kg/kmol]
M_g = 4.0026;                   %Masa molar del gas presurizante [kg/kmol]
OF = 1.9;                       %Relacion oxidante/combustible
R_u = 8314.41;                  %Constante Universal de los gases [J/kmolºK]
t_s = 10e-3;                    %stay time

% 1.4.- Densidades:

rho_f = 874;                    %Densidad del combustible [kg/m3]
rho_o = 1431;                   %Densidad del oxidante [kg/m3]
rho_gg = 0.8774;                %Densidad de los gases de escape [kg/m3]
rho_tg = 1700;                  %Densidad del tanque de gas [kg/m3]
rho_to = 2800;                  %Densidad del tanque de oxidante [kg/m3]
rho_tf = 2800;                  %Densidad del tanque de combustible [kg/m3]
rho_tgg = 8890;                 %Densidad del material de la camara del GG [kg/m3]
                                %rho_tgg = 8890 <- Hastelloy C
                                %rho_tgg = 7960kg/m3 <- CRES 347
                                %rho_tgg = 8800 <- Cu-Ni-Si-Cr Alloy


delta_pf = 40e3;                %Densidad de potencia de la bomba de comb. [W/kg]
delta_po = 40e3;                %Densidad de potencia de la bomba de ox. [W/kg]
delta_e = 3.8e3;                %Densidad de potencia del motor [W/kg]
delta_ef = 3.8e3;               %Densidad de potencia del motor de comb. [W/kg]
delta_eo = 3.8e3;               %Densidad de potencia del motor de ox. [W/kg]
delta_tu = 20e3;                %Densidad de potencia de la turbina [W/kg]
```

```
delta_tf = 20e3;              %Densidad de potencia de la turbina de comb. [W/kg]
delta_to = 20e3;              %Densidad de potencia de la turbina de ox. [W/kg]
delta_inv = 60e3;             %Densidad de potencia del inversor [W/kg]
delta_bap = 1.5e3;            %Densidad de potencia de las baterias [W/kg]
delta_baw = 2500;             %Densidad de energia de las baterias [Wh/kg]
delta_baw = delta_baw*3600;   %Densidad de energia de las baterias [J/kg]
```

% 1.5.- Rendimientos:

```
eta_pf = 0.8;                 %Rendimiento de la bomba de comb.
eta_po = 0.8;                 %Rendimiento de la bomba de ox.
eta_e = 0.8;                  %Rendimiento del motor electrico
eta_ef = 0.8;                 %Rendimiento del motor de comb.
eta_eo = 0.8;                 %Rendimiento del motor de ox.
eta_inv = 0.85;               %Rendimiento del inversor
eta_tu = 0.8;                 %Rendimiento de la turbina
```

% 2.- CONSTANTES %%

```
kappa_p1 = p_tp1/p_c;         %para el sistema de alimentacion por gas pres.
kappa_p2 = p_tp2/p_c;         %para el sist. de alim. por electrobombas
kappa_p3 = p_tp3/p_c;         %para el sist. de alim. por turbobombas
kappa_pi = p_in/p_c;          %razon de la caida en el inyector respecto de p_c
kappa_u = 1.05;               %factor de seguridad para preveer el "ullage"
kappa_g = 1.3;                %factor de seguridad para la masa de gas
kappa_tg = 2.5;               %factor de seguridad para el espesor del tanque de gas
kappa_tf = 2.5;               %factor de seguridad para el espesor del tanque de comb.
kappa_to = 2.5;               %factor de seguridad para el espesor del tanque de ox.
kappa_b = 1.2;                %margen de diseño para la masa de las baterias
kappa_gg = 2.5;               %factor de seguridad para el espesor de la pared del GG
```

```
alfa_f = 1/(rho_f*(1+OF));    %permite relacionar el volumen de comb. con m_p
alfa_o = OF/(rho_o*(1+OF));   %permite relacionar el volumen de ox. con m_p
alfa = alfa_f + alfa_o;       %permite relacionar el volumen de propelente con m_p
```

```
sigma_tg = 3.3e9;             %Resistencia max a la tension del tanque de gas [Pa]
sigma_tf = 455e6;             %Resistencia max a la tension del tanque de comb. [Pa]
sigma_to = 455e6;             %Resistencia max a la tension del tanque de ox. [Pa]
sigma_gg = 524e6;             %Resistencia max a la tension del GG (UTS)[Pa]
                              %sigma_gg = 524MPa   <- Hastelloy C (1033ºK)
                              %sigma_gg = 180MPa   <- CRES 347 (1090ºK)
                              %sigma_gg = 413.7MPa <- Cu-Ni-Si-Cr Alloy
```

```
emin = 0.001;                 %espesor minimo de la pared de los tanques [m]
```

% 3.- PARAMETROS DE CALCULO %%%

```
FLAG_SIST = 'A';              %A: Un solo motor/turbina
                              %B: Un motor/turbina por bomba
```

```
COTA = 0.1;                   %Cota para detectar que los vectores son iguales
CERO = 0;
fp_LIM = 0.99;                %Valor limite en la razon p_c/p_0
```

```
t_bVALOR = 90;                %Valor de tiempo de combustion de interes [s]
t_b = t_bVALOR                %Tiempo de combustion del cohete [s]
```

```
m_pVALOR = 1000;              %Valor puntual de masa de propelente de interes [kg]
m_p = m_pVALOR                %Cambio un valor del vector por el valor de interes
```

```
t_bMAX = 10.0e3;              %Tiempo maximo decombustion [s]
t_bMIN = 10;                  %Tiempo minimo decombustion [s]
t_bN = 500;                   %Longitud del vector t_b
t_bPASO = (t_bMAX-t_bMIN)/(t_bN-1);      %Paso de tiempo de combustion [s]
```

```
t_b = (t_bMIN:t_bPASO:t_bMAX);           %Vector de tiempo de combustion [s]
```

% 4.- RUTINA DE CALCULO %%%

%%% COMENTARIOS
%1.- La masa de propelente es un parametro de los graficos
%2.- La presion de la camara de combustion (para ambos sistemas) es un
%   parametro
%3.- El tiempo de combustion es un parametro
%4.- La presion inicial del gas presurizante es la variable

for i=1:size(t_b,2)

% 4.1.- CALCULO DE LA MASA DE GAS
   if p_0>(kappa_p3*p_c)
      %la expresion tiene sentido si p_tf<p_tg entonces se evalua esa
      %condicion
      m_g3(i) = kappa_g*kappa_u*kappa_p3*alfa*gamma_g*M_g*p_c*m_p/(R_u*T_g*(1-kappa_p3*p_c/p_0));
   else
      m_g3(i) = kappa_g*kappa_u*kappa_p3*alfa*gamma_g*M_g*p_c*m_p/(R_u*T_g*(1-fp_LIM));
   end
   if p_0>(kappa_p2*p_c)
      %la expresion tiene sentido si p_tf<p_tg entonces se evalua esa
      %condicion
      m_g2(i) = kappa_g*kappa_u*kappa_p2*alfa*gamma_g*M_g*p_c*m_p/(R_u*T_g*(1-kappa_p2*p_c/p_0));
   else
      m_g2(i) = kappa_g*kappa_u*kappa_p2*alfa*gamma_g*M_g*p_c*m_p/(R_u*T_g*(1-fp_LIM));
   end
   if p_0>(kappa_p1*p_c)
      %la expresion tiene sentido si p_tf<p_tg entonces se evalua esa
      %condicion
      m_g1(i) = kappa_g*kappa_u*kappa_p1*alfa*gamma_g*M_g*p_c*m_p/(R_u*T_g*(1-kappa_p1*p_c/p_0));
   else
      m_g1(i) = kappa_g*kappa_u*kappa_p1*alfa*gamma_g*M_g*p_c*m_p/(R_u*T_g*(1-fp_LIM));
   end

% 4.2.- CALCULO DE LA MASA DE LOS TANQUES DE GAS
   if p_0>(kappa_p2*p_c)
      %la expresion tiene sentido si p_tf<p_tg entonces se evalua esa
      %condicion
      m_tg2(i) = 1.5*rho_tg*kappa_tg*kappa_g*kappa_u*kappa_p2*alfa*gamma_g*p_c*m_p/(sigma_tg*(1-kappa_p2*p_c/p_0));
   else
      m_tg2(i) = 1.5*rho_tg*kappa_tg*kappa_g*kappa_u*kappa_p2*alfa*gamma_g*p_c*m_p/(sigma_tg*(1-fp_LIM));
   end
   if p_0>(kappa_p3*p_c)
      %la expresion tiene sentido si p_tf<p_tg entonces se evalua esa
      %condicion
      m_tg3(i) = 1.5*rho_tg*kappa_tg*kappa_g*kappa_u*kappa_p3*alfa*gamma_g*p_c*m_p/(sigma_tg*(1-kappa_p3*p_c/p_0));
   else
      m_tg3(i) = 1.5*rho_tg*kappa_tg*kappa_g*kappa_u*kappa_p3*alfa*gamma_g*p_c*m_p/(sigma_tg*(1-fp_LIM));
   end
   if p_0>(kappa_p1*p_c)
      %la expresion tiene sentido si p_tf<p_tg entonces se evalua esa
      %condicion
      m_tg1(i) = 1.5*rho_tg*kappa_tg*kappa_g*kappa_u*kappa_p1*alfa*gamma_g*p_c*m_p/(sigma_tg*(1-kappa_p1*p_c/p_0));
   else
      m_tg1(i) = 1.5*rho_tg*kappa_tg*kappa_g*kappa_u*kappa_p1*alfa*gamma_g*p_c*m_p/(sigma_tg*(1-fp_LIM));
   end

% 4.3.- CALCULO DE LA MASA DE LOS TANQUES DE PROPELENTE

```
%Masa del tanque de combustible para el sistema de gas presurizado
m_tf11(i) = 1.5*rho_tf*kappa_u*kappa_p1*kappa_tf*alfa_f*m_p*p_c/sigma_tf;
m_tf12(i) = ((4*pi)^(1/3))*rho_tf*((3*kappa_u*alfa_f*m_p)^(2/3))*emin;
m_tf1(i) = max(m_tf11(i),m_tf12(i));

%Masa del tanque de oxidante para el sistema de gas presurizado
m_to11(i) = 1.5*rho_to*kappa_u*kappa_p1*kappa_to*alfa_o*m_p*p_c/sigma_to;
m_to12(i) = ((4*pi)^(1/3))*rho_to*((3*kappa_u*alfa_o*m_p)^(2/3))*emin;
m_to1(i) = max(m_to11(i),m_to12(i));

%Masa del tanque de combustible para el sistema de electrobombas
m_tf21(i) = 1.5*rho_tf*kappa_u*kappa_p2*kappa_tf*alfa_f*m_p*p_c/sigma_tf;
m_tf22(i) = ((4*pi)^(1/3))*rho_tf*((3*kappa_u*alfa_f*m_p)^(2/3))*emin;
m_tf2(i) = max(m_tf21(i),m_tf22(i));

%Masa del tanque de oxidante para el sistema de electrobombas
m_to21(i) = 1.5*rho_to*kappa_u*kappa_p2*kappa_to*alfa_o*m_p*p_c/sigma_to;
m_to22(i) = ((4*pi)^(1/3))*rho_to*((3*kappa_u*alfa_o*m_p)^(2/3))*emin;
m_to2(i) = max(m_to21(i),m_to22(i));

%Masa del tanque de combustible para el sistema de turbobombas
m_tf31(i) = 1.5*rho_tf*kappa_u*kappa_p3*kappa_tf*alfa_f*m_p*p_c/sigma_tf;
m_tf32(i) = ((4*pi)^(1/3))*rho_tf*((3*kappa_u*alfa_f*m_p)^(2/3))*emin;
m_tf3(i) = max(m_tf31(i),m_tf32(i));

%Masa del tanque de oxidante para el sistema de turbobombas
m_to31(i) = 1.5*rho_to*kappa_u*kappa_p3*kappa_to*alfa_o*m_p*p_c/sigma_to;
m_to32(i) = ((4*pi)^(1/3))*rho_to*((3*kappa_u*alfa_o*m_p)^(2/3))*emin;
m_to3(i) = max(m_to31(i),m_to32(i));

% 4.4.- CALCULO DE LA MASA DE LAS BOMBAS
m_puf(i) = (1+kappa_pi-kappa_p2)*alfa_f*p_c*m_p/(delta_pf*t_b(i));
m_puo(i) = (1+kappa_pi-kappa_p2)*alfa_o*p_c*m_p/(delta_po*t_b(i));
m_pu(i) = m_puf(i) + m_puo(i);

% 4.5.- CALCULO DE LA MASA DEL MOTOR
switch(FLAG_SIST)
    case 'A'    %Masa con un solo motor
        m_ee(i) = (1+kappa_pi-kappa_p2)*p_c*m_p*(alfa_f/eta_pf+alfa_o/eta_po)/(delta_e*t_b(i));
    case 'B'    %Masa con un motor por bomba
        m_ef(i) = (1+kappa_pi-kappa_p2)*alfa_f*p_c*m_p/(eta_pf*delta_e*t_b(i));
        m_eo(i) = (1+kappa_pi-kappa_p2)*alfa_o*p_c*m_p/(eta_po*delta_e*t_b(i));
        m_ee(i) = m_ef(i) + m_eo(i);
    otherwise
        ERROR(i) = 1;
end

% 4.6.- CALCULO DE LA MASA DE LA TURBINA
switch(FLAG_SIST)
    case 'A'    %Masa con una sola turbina
        m_tu(i) = (1+kappa_pi-kappa_p3)*p_c*m_p*(alfa_f/eta_pf+alfa_o/eta_po)/(delta_tu*t_b(i));
    case 'B'    %Masa con una turbina por bomba
        m_tf(i) = (1+kappa_pi-kappa_p3)*alfa_f*p_c*m_p/(eta_pf*delta_tf*t_b(i));
        m_to(i) = (1+kappa_pi-kappa_p3)*alfa_o*p_c*m_p/(eta_po*delta_to*t_b(i));
        m_tu(i) = m_tf(i) + m_to(i);
    otherwise
        ERROR(i) = 1;
end

% 4.7.- CALCULO DE LA MASA DEL INVERSOR
switch(FLAG_SIST)
    case 'A'    %Masa del inversor con un solo motor
        m_inv(i) = (1+kappa_pi-kappa_p2)*p_c*m_p*(alfa_f/eta_pf+alfa_o/eta_po)/(eta_e*delta_inv*t_b(i));
    case 'B'    %Masa de los inversores con un motor por bomba
        m_inf(i) = (1+kappa_pi-kappa_p2)*alfa_f*p_c*m_p/(eta_pf*eta_ef*delta_inv*t_b(i));
        m_ino(i) = (1+kappa_pi-kappa_p2)*alfa_o*p_c*m_p/(eta_po*eta_eo*delta_inv*t_b(i));
        m_inv(i) = m_inf(i) + m_ino(i);
```

```
        otherwise
            ERROR(i) = 1;
    end

% 4.9.- CALCULO DE PROPELENTE PARA ACCIONAR LA TURBINA
    m_ptu(i) = (1+kappa_pi-kappa_p3)*p_c*m_p*M_gg*(gamma_gg-
1)*(alfa_f/eta_pf+alfa_o/eta_po)/(eta_tu*T_itu*gamma_gg*R_u*(1-(p_dtu/p_itu)^((gamma_gg-1)/gamma_gg)));

% 4.10.- CALCULO DE LA MASA DEL GENERADOR DE GAS
    V_g(i) = t_s*m_ptu(i)/(t_b(i)*rho_gg);
    r_g(i) = (0.75*V_g(i))^(1/3);
    S_g(i) = 4*pi*(0.75*V_g(i)/pi)^(2/3);
    m_gg(i) = rho_tgg*kappa_gg*p_gg*r_g(i)*S_g(i)/(2*sigma_gg);

end


m_tp = m_g3 + m_tg3 + m_tf3 + m_to3 + m_pu + m_tu + m_gg + m_ptu;
m_ep = m_tp;
m_bat = m_ep - (m_g2 + m_tg2 + m_tf2 + m_to2 + m_pu + m_ee + m_inv);

% Para ciertos valores de tiempo de quemado, la masa del motor mas la del
% inversor resultan mas pesadas que el conjunto de turbina, propelente para
% impulsarla y generador de gas. De este modo, la masa de las baterias en
% tales condiciones resulta negativa. A los efectos de lograr buenos
% graficos se recortan esos valores ya que la estimacion realizada no es
% valida en tales condiciones.

for j=1:length(t_b)
    delta_bap(j) = (1+kappa_pi-kappa_p2)*p_c*m_p*(alfa_f/eta_pf+alfa_o/eta_po)/(m_bat(j)*t_b(j)*eta_e*eta_inv);
    delta_baw(j) = (1+kappa_pi-kappa_p2)*p_c*m_p*(alfa_f/eta_pf+alfa_o/eta_po)/(m_bat(j)*eta_e*eta_inv*3600);
end

Indices = find(m_bat>CERO);
if length(Indices)>0
    LIMITE = Indices(1);
else
    LIMITE = 1;
end

for n=1:(length(t_b)-LIMITE)
    t_bA(n) = t_b(n+LIMITE-1);
    delta_bapA(n) = delta_bap(n+LIMITE-1);
    delta_bawA(n) = delta_baw(n+LIMITE-1);
end


% 4.- RUTINA DE GENERACION DE GRAFICOS %%%%%%%%%%%%%%%%%%%%%%%%%%%%%%%%%%%%%

x_MIN = t_bMIN;
x_MAX = t_bMAX;
y_MIN = 0;
y_MAX = 0.6e4;
x_COOR = x_MIN+0.45*(x_MAX-x_MIN);
y_COOR = y_MIN+0.75*(y_MAX-y_MIN);
RENGLON = 0.05*(y_MAX-y_MIN);

figure
semilogy(t_bA,delta_bawA,'g','linewidth',2)
axis([x_MIN x_MAX y_MIN y_MAX])
set(gca, 'YTick',[100 200 300 400 500 600 700 800 900 1000 2000 3000 4000 5000])
set(gca, 'YTickLabel',{'100','200','300','400','500','600','700','800','900','1000','2000','3000','4000','5000'})
xlabel('Tiempo de combustion [s]','FontSize',12,'FontWeight','demi')
ylabel('\delta_W [Wh/kg] y \delta_P [W/kg]','FontSize',12,'FontWeight','demi')
title('Densidades de Energia y Potencia requeridas','FontSize',14)
grid on
hold on
```

```
semilogy(t_bA,delta_bapA,'r','linewidth',2)
legend('\delta_W: Densidad de Energia requerida','\delta_P: Densidad de Potencia requerida',1)

saveas(gcf,['densidad_vs_tb_ver01_mp_' num2str(m_pVALOR) '_PC_' num2str(p_c/1e5) '.png'])
```

REPORT Nº 2

PROPELLANTS SELECTION

Pablo RACHOV

LABORATORIO DE CONTROL DE ACCIONAMIENTOS, TRACCIÓN Y POTENCIA
(LABCATYP)
Departamento de Electrónica
Facultad de Ingeniería
UNIVERSIDAD DE BUENOS AIRES

Directors:

Prof. Hernán TACCA, University of Buenos Aires, Argentine
Prof. Diego LENTINI, University of Roma "La Sapienza", Italy

Buenos Aires, March 6th, 2011.

CONTENTS

I.   LIQUID PROPELLANTS PROPERTIES

The rocket engine development requires understanding the propellants properties and characteristics. On the one hand, the propellants properties define some design issues in all rocket systems (i.e. propellant storage system and feed system). On the other hand, the properties of the propellants combustion products have impact on the engine performance. Furthermore, the elected propellants can carry many types of health hazards and handling problems which might increase the project costs. These facts make necessary to have knowledge of the propellants characteristics in the conceptual design phase. For the estimation of combustion gases properties, specific purpose software is employed. These software routines implement iterative calculus algorithms to solve the chemical and thermodynamic equilibrium problem. In this work one of these programs is employed to estimate the combustion products properties and, consequently, the rocket performance. But first, in this initial section, a brief description of some of the key properties is presented.

1.1. Propellant thermochemical desirable characteristics

To achieve high performance in a rocket engine, there are some key thermochemical parameters that should be optimized. The rocket engine performance is strongly affected by the characteristics of the combustion process. In the followings paragraphs a short analysis of such dependence will be introduced.

In a very simple way, it can be said that a rocket engine is propelled forward by the reaction effect of the burned propellant mass expelled backward. Hence, the thrust force can be evaluated by applying the Newton's Motion Second Law, yielding:

$$F = \frac{dm_p}{dt} v_e \tag{1.2.1}$$

where, *F:* Thrust force (N).
   m_p: Propellant mass (kg).
   v_e: Exhaust velocity (m/s).

From the above equation it follows that for a given propellant mass flow rate, the thrust force can be increased if the speed of the hot exhaust gases (products of propellants combustion) are increased too. Further, from [1] the exhaust gases speed is:

$$v_e = \sqrt{\frac{2\gamma_g}{\gamma_g - 1} \frac{R_u T_C}{M_g} \left[1 - \frac{p_e}{p_C} \right]^{\frac{\gamma_g - 1}{\gamma_g}}} \tag{1.2.2}$$

where, R_u: Universal gas constant (J/kgK).
   M_g: Hot gas molar mass (kg/mol).
   γ_g: Hot gas specific heat ratio.
   T_C: Combustion temperature (K).
   p_C: Combustion chamber pressure (Pa).
   p_e: Nozzle exit pressure (Pa).

Both the previous equations show that the rocket performance is closely related to some thermochemical parameters that characterize the combustion process.

On the one hand, it is apparent that the higher the combustion temperature, the higher the thrust force. Hence, a propellant combination that delivers the highest flame temperature is desirable. However, the design of a combustion chamber that could withstand this high

temperature becomes hard, because the temperatures involved in the combustion process become usually close to the typical materials limits. Moreover, the cooling system design becomes more complex with high combustion temperatures because the heat that must be extracted from the thrust chamber is also increased with the flame temperature. According to the previously mentioned, a highest flame temperature should be achieved but always within the limits imposed for a given chamber material and cooling system.

Also, the thrust force is inversely proportional to the combustion gases molar weight. Therefore, a propellant combination that minimizes this quantity is wanted. This is one of the reasons why the hydrogenated compounds in fuel-rich proportions results a very attractive choice as rocket fuel.

1.2. Propellant physical properties

Besides the propellants characteristics discussed in the previous section, there are other physical properties that, while not having direct impact in the rocket engine performance, are also very important in the rocket engine design process.

The first property to take into account is the freezing point. It must be as low as possible because it is expected that the rocket engine operates at very low environment temperatures, near to the atmosphere boundaries or beyond. In some cases, chemical additives are incorporated to reduce the freezing point.

Another important property is the vapor pressure, for which low values are preferred. If the vapor pressure becomes too high for a given temperature, some problems arise: First, there are handling problems, because vapors can escape more easily when the propellant is manipulated. The consequences of such escapes become more dangerous if the propellant is a toxic substance. Moreover, a high vapor pressure can carry cavitation problems in the pumps. This leads to pressure oscillations over the injector plate and may trigger combustion instabilities.

When a regenerative cooling approach is adopted, the cooling propellant (usually the fuel) must have good heat transfer characteristics. A high specific heat, high thermal conductivity and high boiling point are properties that become crucial in the regenerative cooling design.

The viscosity is a property not less important than the others. The more viscous the propellant, the more difficult is to pump it. So, more pumping power is required for a given propellant flow rate. Further, if a regenerative cooling is selected, a high viscosity propellant complicates the flow through the cooling channels. In addition, a fluid with low viscosity is preferred because the pressure drop through the feed system pipeline and injector is minimized.

When the propellants are stored for long time periods, its chemical properties can be affected by chemical reactions that take place inside the storage tanks. Some propellants may react slowly with the tank inner wall material and also with impurities dissolved or suspended inside. Other factors that may affect a propellant stored are the temperature and the pressure. Some propellants can be stored for long time periods under a large range of temperature and pressure and can remain without reacting with the tank materials. The capacity of a propellant to remains unalterable in stored conditions is defined as chemical stability. The longer the time that the propellant can be stored without chemical degradation, the more stable it is.

There is a propellant property of particular interest in this work: the density. It is a key property in the propellants tanks design. Basically, the denser the propellant, the smaller the tank needed to store a given propellant mass. The smaller tank volume means first of all lighter tanks leaving more mass for payload. Additionally, the propellants tanks volume imposes the vehicle size, especially in launch vehicles, where the propellant mass is very large. Therefore, a high propellant density is desirable in the first stage of multistage vehicles, because minimizing the propellant tanks volume involves minimizing too the aerodynamic drag forces.

One of the problems that must be resolved in the development of a rocket engine is the ignition. Usually, an ignition device is employed to start the engine, unless hypergolic propellants are used. This property is defined as the capability of auto-ignition when fuel and

oxidizer join. One of the most popular combinations of hypergolic propellants has Nitrogen Tetroxide (NTO) as oxidizer and Mono-Methyl Hydrazine (MMH) as fuel. A complete properties description of this propellant can be found in [1].

Unfortunately, there are some inherent hazards associated to the hypergolic propellants. It is evident that, if a failure in the engine hardware occurs and the propellants are accidentally mixed, a great explosion is the obvious accident. The same scenario can occur in the storage facilities, so if propellants of this class are employed, the safety precautions must be enhanced (increasing operation cost). The Table 1 shows several features of some of the most common hypergolic propellants combinations:

Table 1: Performance of selected hypergolic propellants combinations.						
Fuel	*Oxidizer*	C_{ryo}	$O/F_{(op)}$	I_{sp} [s]	T_C [K]	δ [kg/m^3]
Hydrazine	Nitrogen tetroxide	No	1.36	292.0	3265	1210
	Hydrogen Peroxide	No	2.05	286.7	2924	1240
	Liquid Fluorine	Ox.	2.32	365.3	4734	1310
MMH	Hydrogen Peroxide	No	3.46	284.7	2993	1240
	IRFNA III	C	2.59	274.5	3122	1290
	Liquid Fluorine	Ox.	2.39	348.3	4347	1240
	Nitrogen tetroxide	No	2.17	288.5	3395	1190
RP-1	FLOX	Ox.	3.84	344.6	4634	1200
	Hydrogen Peroxide [1]	No	7.00	297	2760	1290

Notes: The data compiled in this table was extracted from [2].
The 90% Hydrogen peroxide and RP-1 are no hypergolic itself but spontaneously ignite if oxidizer is previously decomposed.

Abbreviations: C_{ryo}: Cryogenic propellant.
$O/F_{(op)}$: Mass mixture ratio for I_{sp}.
I_{sp}: Specific Impulse for optimal nozzle expansion.
T_C: Combustion temperature.
δ: Exhaust gas density.

Conditions: Combustion chamber pressure: 6.89MPa – Nozzle exit pressure: 1atm – optimum expansion.
It's assumed adiabatic combustion and isentropic expansion of ideal gas.
Mixture ratios are for approximate maximum value of specific impulse.
Frozen flow approach values are given.

The cryogenic propellants category involves those ones that are in gaseous state at ambient temperature but are liquefied (cooled below their boiling point) for storage into tanks. Liquid fluorine (F_2) and oxygen difluoride (OF_2) are examples of cryogenics propellants. These two substances are used as oxidizer and allow achieving high performance. Although, both propellants are very toxic, thereby leading to the use of other cryogenics non-toxics propellants. One of the most popular combinations is the one that employ liquid oxygen (LOX) as oxidizer and liquid hydrogen (LH2) as fuel. The key property of this combination is the high efficiency, which implies specific impulse increments of above 25% respect to other fuels combinations [1]. This type of propellants has storage and handling problems. The mayor problem with cryogenics propellants involves the increment in complexity of tanks, valves and piping system to maintain the low storage temperature. Heavy insulating systems must be employed in order to minimize the boil off losses. Further, an adequate venting system must be employed to expel the

gaseous propellant leakages. The Table 2 brings brief technical data of some cryogenics propellants:

Table 2: Technical data of selected cryogenics propellants.						
Propellant	*Chemical Formula*	*Use*	*Freezing point [K]*	*Boiling point [K]*	*Density [kg/m³]*	*Hazard*
Fluorine	F_2	Oxidizer	53	85	1509	Very toxic Flammable
Oxygen difluoride	F_2O	Oxidizer	49	89	1521	Very toxic Flammable
Oxygen	O_2	Oxidizer	54	90	1141	Good
Hydrogen	H_2	Fuel	14	20	71	Flammable

Note: The data compiled in this table was extracted from [2].

Moreover, the LOX can be combined with a non-cryogenic fuel. A usual example of this case is the combination of LOX with a hydrocarbon fuel like kerosene. The kerosene has some advantage over the LH2. First, the kerosene is cheaper than LH2. Also, as it is denser, the risk of explosion is lower and can be stored at ambient temperature which implies a storage system simpler and cheaper.

Finally, another of the most important requirements in the development and the operation of a rocket engine is the safety. Some propellants are more dangerous than others. Therefore, propellants selection is fundamental in the safety issues. Not only the propellants itself can be dangerous but also its combustion products. In the next section, a description of the most commons hazards that the propellants handling involves is done.

1.3. Handling propellants hazards

Before discussing the performance properties of liquid propellants, it is necessary to understand the risks involved by the use of some propellants. The risks detailed in this section do not apply to all propellants but such risks must be taken into account when the propellants selection is done. When a propellant is selected, the risk that involves store, handle and burn it into an engine must be carefully understood. A detailed description of these risks can be found in the reference [1], here only some key items are denoted.

1.3.1. Health Hazards

The health risks for the personnel responsible for handling propellants include the possibility of intoxication and poisoning. Some substances are very toxic even in small concentration and can haul severe consequences to the health. The contact with the toxic substance can occur in one of the following ways: ingestion, direct skin contact, inhalation of vapors or gases, or any combination of the above. For example, the inhibited red fuming nitric acid (IRFNA), a well known rocket engine oxidizer, in direct contact with any part of the human body destroys tissues. Also its vapors are highly toxic to the respiratory tract. Generally, the exposure to vapors and gases of a toxic substance can be dangerous to the personnel in one of two following ways. First, a short time exposure to a high concentration of toxic substance may produce immediate physical reactions. For example, high concentrated fumes of nitrogen tetroxide, another well known rocket oxidizer, produce coughing, choking, headache, nausea, pain in chest and abdomen [4]. The other way of intoxication is the long term exposure. As example, the chronic exposure to low concentration vapors of IRFNA may produce wearing down and decay of the teeth, pulmonary emphysema, and chronic inflammation of the respiratory passages, often with ulceration of the nose or mouth [5]. Some

substances could be carcinogens, as in the case of hydrazine. The United States Environmental Protection Agency (EPA) reports that, although no data are available on the effects in humans, an increased incidence of tumors has been observed in mice exposed to hydrazine by inhalation [6]. Some propellants are powerful oxidizing agents and may cause skin burns. This is the case of the hydrogen peroxide, used as a rocket engine oxidizer in high concentrations, which is toxic whether the vapors are inhaled as if ingested or to the contact (skin or eyes) [7]. Some substances also can ignite spontaneously with air, as case of pentaborane, a rocket engine fuel. Such substance is very toxic and may cause permanent injury or death after very short exposure to small quantities [8].

All substances have exposure limits defined in terms of hours at a constant concentration rate. These limits must be well known and respected to ensure a safety operation. Further, for all propellants there are defined security elements and procedures for a correct storage and handling. The Table 3, extracted from [2], resumes the health hazards discusses above and list the typical risks associated to some selected substances:

Table 3: Handling Hazards of selected propellants.	
Propellant	*Hazard*
Hydrazine	Toxic – Flammable
MMH	Toxic
UDMH	Toxic
Nitrogen Tetroxide	Toxic - Hazardous to skin contact
Highly concentrated Hydrogen Peroxide	Hazardous to skin contact – Flammable
IRFNA	Toxic - Hazardous to skin contact
WFNA	Toxic - Hazardous to skin contact
RP-1	Toxic – Flammable
Pentaborane	Explosive on contact with air – Toxic

Notes: MMH: Mono-Methyl Hydrazine.
UDMH: Unsymmetrical Dimethyl Hydrazine.
IRFNA: Inhibited Red Fuming Nitric Acid.
WFNA: White Fuming Nitric Acid.
RP-1: Rocket Propellant.

1.3.2. Fire and Explosion hazards

Many rocket engine propellants can react with other substances causing fire and explosions risks. In some cases, other cause of ignition may include shocks or overheating beyond the security levels. For example, the hydrogen peroxide may react spontaneously with many organic substances, such as paper, wood or oils. Another propellant that reacts spontaneously with organic materials is the IRFNA. The hydrogen peroxide may ignite when is put in contact with hydrocarbon fuels. Also it violently decomposes on contact with some metals and alloys. Some propellants can produce toxics gases when heated. That is the case of the nitrogen tetroxide, which does not burn, but support combustion of some organic materials [4].

Another risk to take into account is that, as was pointed out in the previous paragraph, some substances (like the pentaborane) ignite spontaneously with air.

Detonations may occur with some unstable propellants like hydrogen peroxide and nitro-methane. Shocks, overheating, propellant impurities and contact with some other materials can cause such detonations. Hypergolic propellants also can ignite if are put in contact accidentally during handling.

1.3.3. Corrosion Hazard

Corrosion is one of the causes that limit the rocket engine components life. Some propellants are extremely corrosive for some materials that can be employed in the manufacturing of engine parts. Furthermore, when the corrosion products contaminate the propellants, its properties could be altered, yielding such substance inappropriate for rocket operation [1]. As example, the nitrogen tetroxide corrodes steel if it is humid but can be stored in steel tank while it remains dry [4].

1.3.4. Leak hazard

The leak hazard must be treating as a separated item because it may be dangerous not only for the responsible staff but also for people living in the affected area and the environment itself. Both, propellant liquids and vapors may be dangerous. The propellants must be correctly identified when transported and, if a leakage occurs, the security protocols must be quickly implemented, first to contain the spill and then to neutralize its effects. Usually, a competent governmental authority provides rules and regulations for the transportation of hazard substances that must be followed when the propellants are moved from one location to another. Also, procedures to apply in case of spills should be known and implemented if necessary at the testing and launch facilities.

II.   CANDIDATE LIQUID PROPELLANTS

The first step for the propellants selection is to make a list of candidates that match with our project requirements.

On the one hand, the employed propellants should be economically affordable and have good availability in the local market. Furthermore, the storage system must to be as simpler and cheap as possible. Also, the materials employed in the feed system (including the feed lines) should be available and affordable. Therefore, for our application, cryogenics propellants like LOX and LH2 are discarded from the list.

On the other hand, for safety issues it is convenient that the substances be as harmless as possible. The same requirement applies to the combustion exhaust gases. Hence, hydrazine and its derivates are also ruled out from the list.

Taking into account the former arguments, several propellants are considered as candidates for the experimental rocket engine. Starting with the oxidizers and following with fuels, in the next subsections a brief description of some of these possible propellants is presented.

2.1. Nitrous Oxide

This substance is used either as an oxidizer in a bipropellant system or as a propellant in a monopropellant system. Also it is used as oxidizer in hybrid systems [9]. The nitrous oxide is a low toxicity, non-flammable, liquefied gas and, for these reasons, recently it received increased attention. Nitrous oxide is soluble in water, ethanol and sulfuric acid. It is stable at moderate temperature but decomposes exothermically by heating above 520 K in nitrogen and oxygen, following the next reaction formula:

$$2N_2O \rightarrow 2N_2 + O_2 + heat \qquad\qquad (2.1.1)$$

The decomposition rate can be accelerated employing a catalyst. The list of catalyst materials is very large. A number of metal oxides can be used as catalyst, for example, cobalt,

copper, nickel and magnesium oxides. The catalyst drastically lowers the reaction energy and thus, decreasing the decomposition temperature is achieved. This substance supports combustion and oxidizes certain organic compounds [10]. It can react violently with combustible materials. When exposed to fire, nitric oxide and nitrogen dioxide fumes can be produced, which are toxic and corrosive substances. Although it is a low toxicity substance, handle this oxidizer may carry some health hazard that must be known. On the other hand, nitrous oxide is a non-corrosive fluid and may be employed with common materials. One advantage of this propellant is its high vapor pressure, which allows the tanks to be self-pressurizing by the propellant. Compared with hydrazine used as a monopropellant, nitrous oxide achieves less specific impulse performance but, it is much less toxic and easy to handle.

The Table 4 provides some general data about nitrous oxide [10]:

Table 4: Nitrous Oxide physical data.		
Property	*Value*	*Unit*
Density (at 1 atm and 288K)	1875	$[kg/m^3]$
Molecular mass	44	[g/mol]
Melting point	182	[K]
Boiling point	184	[K]
Vapor pressure (at 293K)	5850	[KPa]
Heat capacity C_P (at 1 atm and 288K)	38	[J/mol/kg]
Heat capacity C_V (at 1 atm and 288K)	29	[J/mol/kg]
Enthalpy of formation (at 298K)	81.6	[kJ/mol]

Currently, several different approaches are taken to improve the propellant properties of nitrous oxide. As a monopropellant, the nitrous oxide performance can be improved by blending it with a hydrocarbon fuel [11]. When the fluid is passed through a catalyst, the nitrous oxide is decomposed releasing heat and thus reaching a high temperature, so that it easily ignites the hydrocarbon fuel. This allows performances comparable with hydrazine but without its associated toxicity. Further, the lower melting point allows more flexibility in the handling and storage conditions when compared with hydrazine.

Recently, a private company launched a new line of oxidizers based on a mixture of nitrous oxide and liquid oxygen [12]. They call the new oxidizer as "Nytrox", showing a number of outstanding advantages over both, nitrous oxide and liquid oxygen. The manufacturer claims that the new propellant keeps the high performance associated to liquid oxygen but preserving the good properties of nitrous oxide: self-pressurizing capability, higher storage temperature and high propellant density.

The nitrous oxide is compatible with a great variety of commonly available materials. Metals like brass and copper can be employed but they suffer corrosion attack in humid environments [13]. The stainless steel and the aluminum are more proper materials; they do not corrode and can be machined easily. Between the recommended plastic materials it can be cited the PTFE and the PCTFE. At the end of this section, in the Table 10 there are some interesting data compiled about these materials.

2.2. Hydrogen Peroxide

Hydrogen peroxide is transparent, colorless, syrupy liquid with slightly pungent odor [14]. It has appearance of water with slightly greenish tint, but it is more viscous and heavier. Hydrogen peroxide is a well known substance used in a large number of applications, both civil and industrial. The typical applications include paper manufacturing, chemical synthesis, water treatment, and a number of applications in textiles, mining, electronic, food and cosmetic industries [15]. Hydrogen peroxide is a strong oxidizing agent and a weak acid in water solution. It is relative stable chemical which decomposes slowly to a rate of less of 1

percent per year. However, the decomposition rate is highly accelerated by two different ways. First, if the hydrogen peroxide is heated, and second, if is contaminated with transition metals and its compounds. It decomposes violently if is heated over 350K. Also, it decomposes in the presence of metal ions and oxidizable organics materials. When this happens, the hydrogen peroxide breaks down into hot water steam and oxygen, releasing heat. The decomposition follows the next reaction formula:

$$2H_2O_2 \rightarrow 2H_2O + O_2 + heat \qquad\qquad (2.2.1)$$

Therefore, the decomposition products are non toxics compounds, which is an important property. In some cases, a stabilizing substance (as sodium stannate) can be added to the solution to retard the decomposition during storage. As a propellant, hydrogen peroxide is used in aqueous solution at concentrations higher than 70% by mass. The chemical properties of hydrogen peroxide and the performance that can be obtained from it as a rocket propellant are strongly dependent of its concentration in the solution. The following table (Table 5) shows some of its properties for different concentration degrees.

Table 5: Hydrogen Peroxide physical data.				
Property	*70% by mass* [15], [17]	*85% by mass* [16] , [17]	*100% by mass* [18]	*Unit*
Density	1288	1365	1440	[kg/m^3]
Molecular mass	27	30	34	[g/mol]
Melting point	233	255	273	[K]
Boiling point	399	410	423	[K]
Heat capacity C$_P$	82	85	89	[J/mol/kg]
Enthalpy of formation (at 298K)	-233	-213	-188	[kJ/mol]

As a propellant, the hydrogen peroxide has some key properties that make it very suitable for rocket propulsion. One of the most renowned properties is its overall low toxicity, even if the substance itself can be hazardous in the concentrations that are employed as rocket propellant. Later in this report, the risks that involve this chemical handling will be described. However, compared with other commonly used propellants, the hydrogen peroxide has a relative low toxicity. Furthermore, the hydrogen peroxide decomposition produce non toxic product, normally found in the atmosphere, which is a very valuable attribute.

In the present days, the hydrogen peroxide is being considered as candidate oxidizer in a number of new low-cost launch vehicle projects. Besides the low toxicity associated to the hydrogen peroxide there are other properties that make it a good choice for launch vehicles. This propellant combined with a hydrocarbon fuel has a greater density than the combination of the same hydrocarbon fuel with liquid oxygen [19]. A combination of recompiled data from existing booster engines and simulations of a hypothetical booster engine was employed to perform this comparison. The hypothetical engine is propelled with hydrogen peroxide and kerosene and its performance is estimated for the same operation conditions of the existing booster engines. In this paper the author found that, compared with the solid booster employed in the Space Shuttle, a first stage booster propelled by a combination of hydrogen peroxide and kerosene would provide an increment of nearly one third in the payload mass.

The hydrogen peroxide is also employed as oxidizer in hybrid rocket engines. It is preferred over nitrous oxide because of one key point: Both oxidizers offer two characteristics highly valued when the economic resources are limited. They are low toxic substances, which facilitates and reduces the cost of propellant handling operations. In addition, both propellants are non cryogenics, which avoids the use of expensive cryogenic systems. Beyond these shared properties, the key point is the performance of hydrogen peroxide, which outweighs the performance of nitrous oxide, in term of specific impulse for the same operation conditions. This argument is justified by the simulations carried out in [20]. In this work, the specific

impulse obtained for hydrogen peroxide (in concentrations of 90% by mass of more) is greater than for nitrous oxide (always using the same solid fuel and operation conditions). The second argument is that both oxidizers have the characteristic of low toxicity, making the handling and storage operations less dangerous and expensive.

As in the case of the nitrous oxide, the hydrogen peroxide decomposition allows for monopropellant operation. Historically, this propellant was used many times as monopropellant in gas generators devices to propel the turbopump feed systems [21]. The main advantage obtained from the hydrogen peroxide as a gas generator propellant is that the hot gas temperature is near to the physical limits of the typical turbine blade materials. This allows simplifying two design points. First, to save turbine blade cooling systems and also, to avoid the heat exchanger interposed between the gas generator and the turbine. Further, the hydrogen peroxide gas generator architecture is less complex than the typical bipropellant gas generator. This features combined results in a more simple gas generator and turbine design. Moreover, the hydrogen peroxide decomposition temperature can be varied according to its concentration in the water solution. The Figure 1 shows the decomposition temperature as a function of the pressure in the combustion chamber for different concentrations of hydrogen peroxide working as a monopropellant.
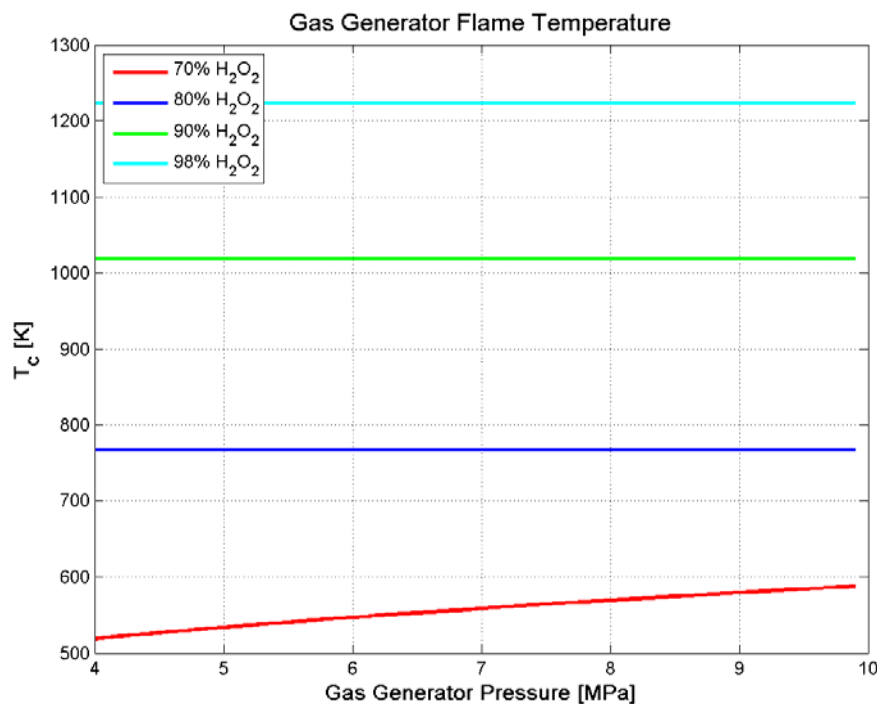
Figure 1: Decomposition temperature of hydrogen peroxide as a function of chamber pressure for a typical range of gas generators working pressure.

In addition to the features mentioned in the previous paragraph there are other properties of hydrogen peroxide that make it suitable to propel the turbopumps. When a bipropellant gas generator is employed, the non-uniform nature of combustion derives into hot spots in the exhaust gas stream that reduces the turbine components life. Furthermore, in order to increase the power extracted from the turbine, it is desirable to get the maximum pressure drop across it. In these conditions, if a hydrocarbon fuel is employed, there exists the possibility of forming soot. The two previous denoted phenomena can be avoided if a hydrogen peroxide monopropellant gas generator is employed. The turbine operating with this propellant shows almost no degradation due to hot gas composition. Additionally, the hydrogen peroxide produces a uniform and moderate temperature steam without hot spots, making the turbine blades temperature stress smoother.

In the section 1.2.1 some hazards related to the hydrogen peroxide handling were described. However, due to the importance of this substance in this work, a more detailed description is presented in the followings paragraphs. The hydrogen peroxide is a high corrosive substance, and the hazards associated with it are due to its corrosive capacity. There are 4 ways of being affected by exposition to this substance [14]. Such ways are: first, the inhalation of its vapors; second, direct contact with eyes; other way is the direct contact with the skin and finally, the ingestion. The consequences and preventive actions that can be adopted are described in more detail in the Appendix of this report.

The hydrogen peroxide is a non combustible substance but it can sustain the combustion of other substances, causing explosions in some cases [22]. That is because heating accelerates the hydrogen peroxide decomposition, thus releasing oxygen. The oxygen released supports the combustion generating more heat and then decomposing more hydrogen peroxide.

The hydrogen peroxide can be stored in tanks for many years if the tank are made from a compatible material and is previously prepared. The materials highly compatible with this propellant are described in [23]. Between the compatible metals it can be mentioned the high purity aluminum alloys which provides the most stable surface for this propellant storage. The aluminum tanks can be repaired, but welding this metal requires some special skills. Another option for hydrogen peroxide storage is the stainless steel with low carbon grades. The low carbon stainless steel alloys offers an excellent surface for long time storage. Although the case of aluminum alloys, the stainless steels can be welded more easily. In all cases, the metal surface must be previously conditioned. It is necessary to clean and degreasing properly with detergent, remove all impurities and the metal surface should be chemically passivated.

In addition, there are other non metallic materials that can be employed for hydrogen peroxide storage. The high density polyethylene is a good example. However, this material is susceptible to high temperature environments and to the attack of UV radiation and thus, the storage time period is decreased to a few years. Moreover, the polyethylene can not be welded and the damaged tank reparation is not possible. On the other hand, this material is cheaper than the previously mentioned metals alloys and it can be used after preparing the surface simply by cleaning. Other materials that can be employed in the hydrogen peroxide handling are PTFE (Teflon®) which has better temperature and shock resistances and PCTFE. The Table 10, at the end of this section, shows some key properties of selected materials employed to handling and storage hydrogen peroxide.

2.3. Catalysts and Stabilizers for Hydrogen Peroxide

As it was said in the preceding section, the hydrogen peroxide can be decomposed through two techniques, heating it over a determinate temperature or putting it in contact with certain catalyst substances. The decomposition reaction is important in the rocket performance. There exist a number of tested and approved methods to decompose the hydrogen peroxide. Here in this section, a description of such methods will be made presenting the most relevant characteristics of each one.

Along time, diverse substances have been employed as catalyst for hydrogen peroxide. Between the most relevant ones it can be mentioned several salts like potassium permanganate and calcium permanganate. The potassium and calcium permanganates are magenta, purple or rose colored when dissolved in water. These substances can be dissolved in the fuel to be afterward injected in the chamber with the hydrogen peroxide. Another way to employ these substances is by coating a chamber with a mud of these salts and then waits to dry. The hydrogen peroxide is injected in the chamber and it decomposes when taking contact with the coated chamber walls. Historically, more common were the beds filled with catalyst coated pellets. As it was mentioned before, also there exist a number of metals that can decompose the hydrogen peroxide. The most usual way to employ these solids substances is to form wire mesh sheets (sometimes also coated with catalyst oxides) that are stacked to form a chamber through which passes the oxidizer. There are a large number of designs based on this approaches, in the Figure 2 schematic diagrams to illustrate them are presented.
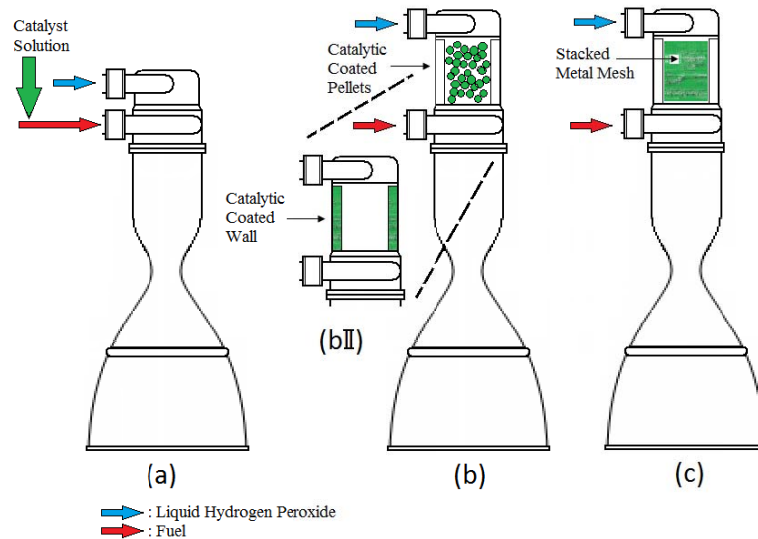
Figure 2: Schematic diagrams of three different approaches for bipropellant hydrogen peroxide rocket engines. In the approach (a) the catalyst substance is dissolved in the fuel. In the approach (b) a separated decomposition bed is filled with catalyst pellets. A variant is shows in (bII) where the chamber walls are coated with a catalyst. In the approach (c) a catalyst formed by stacked metal wire mesh is employed.

In the preceding paragraph several approaches to decompose the hydrogen peroxide were presented. In this paragraph, its advantages and characteristic will be discussed. The first approach to be treated is the injection of a catalyst solution.

In bipropellant engines, the fuel and oxidizer are injected in the combustion chamber together, so this method will be referred as *liquid injection*. This method was employed in rocket propulsion in the times of World War II by Germany and the most prominent example is the turbine drive system of the V2 rocket [24].

For this purpose the permanganate salts like the potassium or calcium permanganate can be employed. The salt is dissolute in water and the decomposition solution is injected together with the hydrogen peroxide. The most remarkable advantage of this approach is that the catalyst is less susceptible to be degraded by the impurities in the hydrogen peroxide solution (i.e. stabilizer salts). This allows employing less refined hydrogen peroxide water solutions. In monopropellant operation the most evident disadvantage is that the engine requires an additional feed system to inject the catalyst solution [24]. This increases notably the hardware complexity which is a marked drawback in this kind of engines.

In a bipropellant engine there exists the possibility of using the fuel to carry the catalyst substance. This requires a fuel that allows dissolving such catalyst, adding an additional engine requirement. Aside from the use of a fuel plus catalyst solution, it must be denoted that there is the option of employing a fuel which is hypergolic with the hydrogen peroxide, like hydrazine. Another disadvantage related to this approach is that the catalyst solution is expelled through the nozzle adding almost nothing to the specific impulse value [24]. Furthermore, the exhaust gases are mixed with the catalyst solution which may degrade some thermochemical characteristics like molar mass.

Historically, the second approach developed was coating solid pellets with a catalyst solution [24]. The catalyst, usually a permanganate salt, is added to a pellet substrate by a dip and bake method. Typically, the pellets size is between 15 and 50 millimeters. Such pellets are then put into a pressure vessel and the hydrogen peroxide is pumped through this vessel during the engine operation. This method can be used in a hybrid rocket engine. The hydrogen peroxide is decomposed in a catalyst bed and then, the exhaust stream pass through the solid fuel grain. The coated pellets scheme allows avoiding the disadvantages inherent to the preceding approach and in addition, the catalyst required mass is reduced. The most evident difference between this approach and the previous is that here there exist a catalyst device. The

mass added to the engine due to the inclusion of this catalyst device is less than the correspondent to a second feed system. Despite the underlined advantages, this approach carry it own drawbacks. First, the pellets are eroded during the engine operation, so that the useful life is reduced to only few minutes. Furthermore, this limited life is even more reduced as the hydrogen peroxide concentration is increased, thus limiting its performance. The erosion generates silting and substrate breakup and thus, some problems in the injection system may occur. It is remarked that a variation of this approach is used in some amateur type rocket engines. As is illustrated in the Figure 2 (bII), the catalyst chamber wall is coated with a permanganate salt instead of by filled with coated pellets.

The third approach implies to replace the pellets in the vessel by screen catalyst [24]. The catalysts are composed by wire meshes made from some catalytic metal and stacked on each other. The wire mesh can be made from a pure catalyst metal or can be plated on a catalyst metal as will be described later. They are the preferred way to decompose the hydrogen peroxide and several reasons for this choice will now treated. First, stacked wire mesh contained into a compact package are robust and better withstand the erosion of hydrogen peroxide during the engine operation. Consequently they have a greater useful life, typically in the order of hours. Also they not present significant silting and breakup increasing the overall engine reliability. Another key feature of the catalyst bed is the high decomposition activity, that is, the hydrogen peroxide amount per time unit that can be decomposed per catalyst area unit. The greater the decomposition activity the smaller the catalyst packs. This allows more compact and light decomposition chamber design. In addition, the oxidizer flow through the catalyst bed becomes more turbulent which in turns enhance the mixing process. This feature is done with a moderate pressure drop which allows to decrease the required pumping power for a given chamber pressure. In spite of its advantages over the catalyst bed, there are some disadvantages that must be considered. The wire mesh is more susceptible to poisoning by fluid impurities and also, only high degree purity hydrogen peroxide (without stabilizer salts) allows a reliable operation. In order to avoid the contamination, the catalyst screens must be maintained inside the vessel and must be handling into a proper environment. In the case of a bipropellant rocket engine, the previously mentioned method can be employed. Basically, the hot exhaust gases generated by the decomposition inside the catalyst bed are sprayed into the combustion chamber where also the fuel is injected. This method will be referred here as *gaseous injection*. The elevated temperature of the hot gas is above the 500K for high concentrations of hydrogen peroxide (see Figure 1), which is sufficient to ignite the fuel.

For bipropellant engines the gaseous and liquid injection approaches, presented in the above paragraphs, will be now discussed.

The first point of comparison is the performance that can be achieved. In the gaseous injection approach, the fuel is injected into a hot gas stream and thus, the propellant atomization and mixing has better quality [25]. Consequently, the combustion efficiency is greater and the effect, from a design point of view, is a direct reduction in the combustion chamber length. This is particularly important when a hydrocarbon fuel is used, because the high mixture ratio needed to reach the optimal performance point, as it is shown in the next graphic (Figure 3).

It can be seen that, even for the highest concentrated hydrogen peroxide, the optimal mixture ratio is not less than 6. Another advantage obtained from the optimal atomization and mixing is that the combustion is less susceptible to show instabilities.

Further, there is another appreciated feature with the gaseous injection approach. The engine, in fact, can operate in a monopropellant mode. This is particularly useful to avoid the hard start transient. In a liquid injection scheme the timing between fuel and oxidizer injection start is very tight and there exist explosion risks if the correct sequence is not achieved (especially in the development phase testing). With a gaseous injection scheme, the engine may be started only using the decomposed hydrogen peroxide and the chamber status can be monitored. Then, the system can be switched to bipropellant operation making the start transient smoother. The optimization in the mixing process also allows to minimizing the start time, which is particularly good feature in the development of thrusters [26].

In addition, employing a catalyst bed to previously decompose the oxidizer provides a hot steam that can be used to power some auxiliary systems. A good example of this feature is

the employ of the decomposed gases to drive the fuel and oxidizer turbopumps. This approach was implemented in the LR-40 engine, that was, in some way, a precursor of the staged combustion closed cycle, the most efficient rocket engine cycle [21].
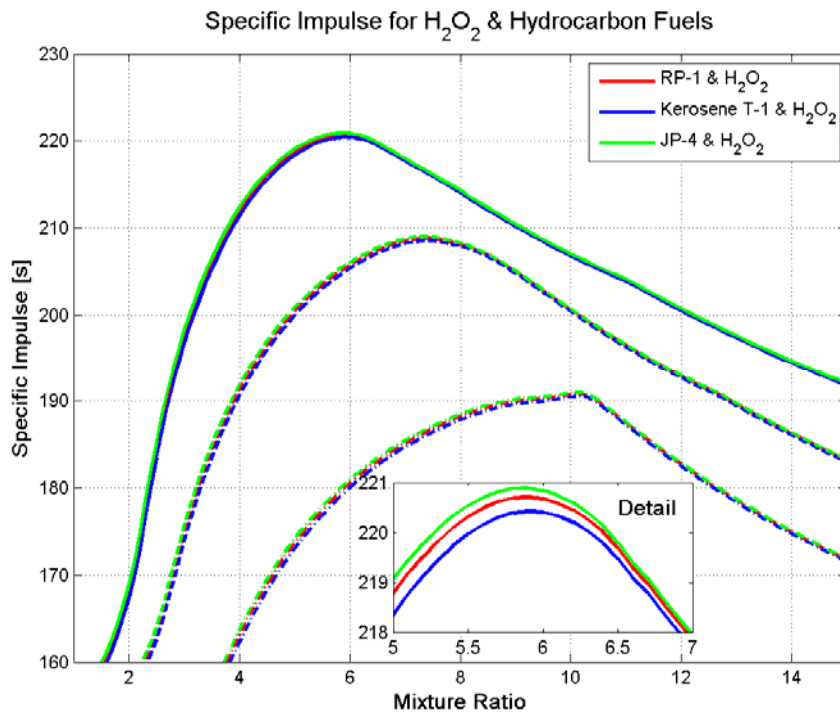
Figure 3: Specific Impulse (Optimal expansion) for hydrogen peroxide and divers hydrocarbon fuels. The solid line correspond to 98% H_2O_2, dashed line to 85% and dotted-dashed line to 70%. The computing conditions are: 1.5MPa chamber pressure, 1atm exit pressure and ideal nozzle. It was predicted using the frozen flow approach (Freeze at the throat).

Furthermore, recent studies have demonstrated that, with a refined design of the catalyst bed, a remarkable reduction in the thrust chamber weight can be achieved [25]. The analytical comparison shows that an engine with a catalyst bed can be lighter than one with liquid injection by a factor of 2.5. This conclusion is not apparent because the addition of a catalyst bed seems to increase the weight. However, a weight reduction is also achieved by the decreasing in the chamber size, which is a consequence of the optimization of the propellant mixing.

The silver is the metal commonly employed to make wire mesh catalyst beds [27]. Several types of catalyst beds employing such metal are available and the following ones can be mentioned:

- Pure silver wire mesh
- Silver plated stainless steel wire mesh
- Ceramic platinum catalyst

The wire mesh catalysts made from pure silver are first treated by oxidizing and later reheated. This allows enlarging the useful contact area. This type of catalyst mesh better resist the abrasion caused by the impact of high energy vapor droplets which are consequence of the complete decomposition. Additionally, it must be taking into account that the hydrogen peroxide is a strong oxidizer and hence it degrades the silver mesh. The pure silver wire mesh can resist this oxidizing attack for longer time. In accordance with these reasons, this type of catalyst mesh should be used at the end part of the catalyst bed.

The silver plated wire mesh has a body of stainless steel which is plated generating a porous silver surface. Such porous surface gives to this type of mesh the highest decomposition capacity. Moreover, the silver layer is very thin (between 20 and 30 μm) leaving this type of catalyst mesh some lower in price. Because of its high decomposition capability, it is recommended to place this meshes at the inlet of the catalyst pack, to quickly decompose the hydrogen peroxide.

The decomposition of very high concentration hydrogen peroxide (above 90%) gives a temperature that might melt the silver mesh. The ceramic platinum catalyst can better withstand the high temperatures involved in the decomposition process. Furthermore, this catalyst mesh has better decomposition capability than the pure silver type and at least, the same capability than the plated silver catalyst mesh. Also, the ceramic mesh type is not poisoned by the stabilizers commonly used in high concentration hydrogen peroxide. Although the significant mentioned advantage, it must be denoted that the total useful life of this mesh type is typically shorter than the silver screen catalyst mesh.

2.4. Ammonium Nitrate solutions

The ammonium nitrate has a moderate performance in term of specific impulse when is compared to other typical rocket propellants. However, it must to be said that this substance has also several characteristics which make it an option to be considered. This chemical compound has a very extensive use as fertilizer in agriculture and so it is highly available at low prices. Another application for this chemical compound is as oxidant agent in explosives like black powder. The ammonium nitrate is a very safe substance, does not burn on its own and is almost not susceptible to friction and shock. These properties make it suitable for storage in large quantities for extended time periods. The ammonium nitrate is highly hygroscopic, experiencing an endothermic reaction that absorbs heat at a rate of 79 calories per gram at room temperature [28]. The usefulness of ammonium nitrate as a propellant lies in its decomposition capability. As in the hydrogen peroxide case, there are two mechanisms that force the decomposition of this substance. The first way is by heating them over 600K approximately and the second one is by putting it into contact with a catalyst substance. Between the most remarkable catalysts there are some chlorides, like sodium chloride (table salt), some chromates, like potassium dichromate and water. The decomposition reaction is quite more complex than the hydrogen peroxide one because it involves two different chemicals process. The first process to be mentioned is an exothermic reaction that follows the next expression:

$$NH_4NO_3 \rightarrow N_2O + 2H_2O + heat \tag{2.4.1}$$

At the same time, an endothermic dissociation reaction occurs through which the ammonium nitrate produce nitric acid and ammonia according to the next expression:

$$NH_4NO_3 + heat \rightarrow HNO_3 + NH_3 \tag{2.4.2}$$

This two process combined contributes to a temperature limited decomposition. At ambient conditions, even if the ammonium nitrate is heated through a very hot source, the decomposition temperature remains moderate because the dissociation reaction absorbs the heat released. However, at elevated pressure, the dissociation reaction is restricted and the decomposition process is accelerated releasing more heat. Some substances can greatly increase the decomposition rate of ammonium nitrate. As example, the sodium chloride can accelerate the decomposition in the order of 1000 times the typical rate at 450K.

The physical properties of ammonium nitrate should be taken into account if this chemical compound is employed as rocket propellant. The Table 6 collects some interesting properties of ammonium nitrate extracted from [18].

At room temperature and standard pressure the ammonium nitrate comes in form of a white crystalline solid, which make it suitable to build solid propellant grains. However at this point there is a disadvantage, the ammonium nitrate shows a crystalline phase change with temperature variation. One of this phase changes happens at 300K approximately and this increment the substance volume in about a 4%. This fact can cause propellant grain breakage problems and carry some storage problems that must be handled.

Table 6: Ammonium Nitrate physical data.		
Property	*Value*	*Unit*
Density (at 1 atm and 288K)	1730	[kg/m^3]
Molecular mass	80	[g/mol]
Melting point	443	[K]
Boiling point	500	[K]
Heat capacity C_P (at 1 atm and 288K)	139	[J/mol/kg]
Enthalpy of formation (at 298K)	-366	[kJ/mol]

As a rocket propellant, the ammonium nitrate is employed shaped like a solid oxidizer cartridge and has some advantages as well as some disadvantages. When this substance is decomposed, the products of such reaction are only in gaseous state. These gaseous products give a low molar mass which contributes to increment the performance (as explained in the section 1.1). However, the specific impulse obtained using this substance as oxidizer and a hydrocarbon fuel is slightly below that those can be obtained employing rocket grade hydrogen peroxide in the same operating conditions.

Handling the ammonium nitrate involve some hazards that must be taken into account. As in the case of hydrogen peroxide, there exist injuries risk if this substance is either inhaled, ingested or take contact with the skin or eyes. The inhalation of this chemical compound may cause irritation to the respiratory tract, sore throat and coughing [29]. As was explained in the preceding paragraphs, the ammonium nitrate decomposes producing nitrogen oxides that, if inhaled, may cause acute respiratory problems.

Although this chemical is stable and non-flammable, it can support the combustion. Ignition also may occur if this chemical is in contact with some combustibles because the heat released. Extremely violent reaction may happen if it is contact with oxidizable substances. Handling the ammonium nitrate involve some hazards that must be taken into account.

The storage of ammonium nitrate must be realized into a moderate to low temperature area; such area must be well ventilated and dry. The containers should remain tightly closed when they are full and they should be well cleaned of any impurity before filled with ammonium nitrate. This substance is incompatible with the most common metals like iron, copper, aluminum and brass between others. In turn, the ammonium nitrate is compatible with some plastic materials like ethylene and propylene rubbers and thus, the containers must be covered with a layer of such materials. In the Table 10, at the end of this section, some properties of these compatible materials are presented.

In the previous paragraph some applications of ammonium nitrate in rocket propulsion as a solid compound, were mentioned.

To be employed in liquid propellants rocket engines it is necessary to dissolve the ammonium nitrate in water. At ambient conditions, the aqueous solution of ammonium nitrate has a very low specific impulse range when is combined with a hydrocarbon fuel. The figure 4 shows the specific impulse profile for both, solid and aqueous solution of ammonium nitrate and, for comparison, the curve of 70% hydrogen peroxide was included.

Although the performance obtained using the ammonium nitrate in an aqueous solution is poor, there exists another application of this chemical compound in liquid propellant rocket propulsion. It can be employed together with hydrogen peroxide to improve this last oxidizer in the way that will be explained in the next section.
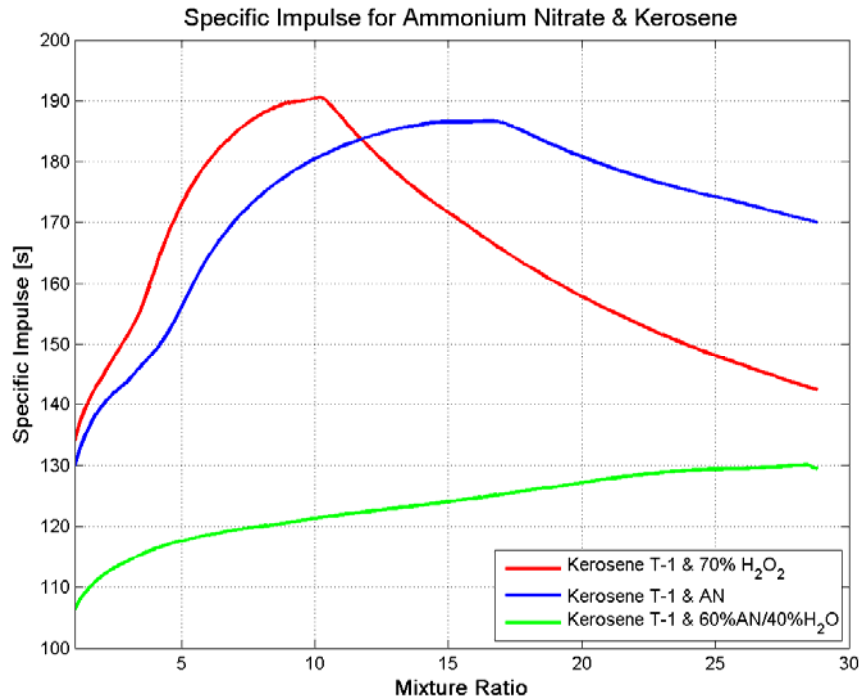
Figure 4: Specific Impulse (Optimal expansion) for ammonium nitrate (AN) and kerosene fuel. The pure solid AN gives performance comparable to 70% H₂O₂. The aqueous solution, however, gives substantial lower performance. The conditions are: 1.5MPa chamber pressure, 1atm exit pressure and ideal nozzle. It was predicted using the frozen flow approach (Freeze at the throat).

2.5. Hydrogen peroxide based solution: PERHAN, PERSOL 1 and PERSOL 2 oxidizers

The first hydrogen peroxide solution that will be considered is the PERHAN. This oxidizer is composed by a combination of water, hydrogen peroxide and hydroxyl ammonium nitrate [30]. This last substance, although is not exactly ammonium nitrate, is a propellant itself that has high oxygen as well as hydrogen and nitrogen content. Due to its composition, it is employed, alone, as monopropellant in rocket engines [1]. Also, combined with solid fuels grains like Hydroxyl-Terminated Polybutadiene (HTPB), it is employed as oxidizer in hybrid rocket engines [9]. However, the HAN is a corrosive and toxic substance, more likely hydrazine than ammonium nitrate, and therefore, it is difficult to handle.

On the other hand, PERHAN is a rocket oxidizer developed to achieve outstanding properties like low cost, high availability and very good handling and storage characteristics, like low corrosivity, low explosion risk and relatively low health hazard [30]. This propellant has also high density and hence, improved chemical energy density. This property is especially interesting in this work. Another important property pointed out by the inventor is the low freezing point, which is particularly interesting in space operated engines. In such cases the low environmental temperatures may cause the formation of solid particles in the propellant flow which, in turn, may cause pumping problems. The two preceding mentioned properties can be adjusted by changing the proportion of components in the solution. This characteristics give to the PERHAN the ability of customize the propellant for a particular application. PERHAN can be used as rocket propellant in the same fashion than the hydrogen peroxide, decomposing it by heating or employing a catalyst bed or catalyst solution.

The second oxidizer to be described is the PERSOL 1, which is a family of substances composed by a mixture of water, hydrogen peroxide and, in this case, ammonium nitrate (AN). Information about PERSOL 1 can be found in [31]. The preparation of such composition can be achieve by mixing its ingredients. The dissolution of the ingredients is generally endothermic,

which make it a relatively safe and simple process. This propellant in non cryogenic and therefore the handling costs are reduced. Its corrosivity is relatively low, which also improves its handling capability. The vapor pressure is very low, which reduces hazards due to toxics vapors. In addition, the components of PERSOL 1 are water soluble and thus, the spills can be contained simply by washing it with water. The final deposition of this propellant is also simple because its components are biodegradable.

In comparison with the PERHAN, a lower cost is obtained by replacing the HAN with the ammonium nitrate (AN). Another advantage of this oxidizer is that the combustion of it with a low carbon fuel should produce nitrogen, water and carbon dioxide, which are non toxic exhaust substances. Likewise, the decomposition of this substance should generate an exhaust plume containing the same species above mentioned plus carbon monoxide and methane among other gases (in minor proportion). Thus, no hydrochloric acid is produced and the exhaust products are less toxic.

From the performance point of view, a comparison with an ammonium nitrate water solution, similar to that done in [31], can be realized using a theoretical thermodynamic equilibrium calculus tool [32]. It is supposed a bipropellant system were the fuel is Kerosene T-1. The chamber pressure is 1.5MPa and the ambient pressure assumed is 1atm. The flow is frozen at the throat and an ideal bell nozzle is considered. With these conditions, the results of such comparison are presented in Table 7.

Another water solution that contains hydrogen peroxide is the PERSOL 2. Promptly, such substance is formed by the following three ingredients: hydrogen peroxide, water and hydrazinium mononitrate. The quantities of each ingredient can vary within a certain range. Detailed data of this chemical compound can be found in [33]. PERSOL 2 can be employed as monopropellant or as oxidizer in bipropellant systems, and it also share several properties with the other two substances yet described in this section. Among this shared properties, it can be mentioned that different compositions can be obtained varying the concentration of each ingredient and this mixing process is relatively simple. PERSOL 2 also has a low freezing point and a high density. All the features obtained from the PERSOL 1 are also expected from PERSOL 2. However, in this case, hydrazinium mononitrate is used and it has some negative consequences [34]. This chemical can explodes above 340K if it is on contact with metals like cobalt, copper and zinc among others and metals compounds like nitrides, sulfides and oxides. Also its decomposition fumes contain nitrogen oxides which are toxics. As the hydrazinium mononitrate is highly toxic and somewhat unstable, the PERSOL 2 is more like PERHAN than PERSOL 1 from the safety point of view and hence, this last mentioned hydrogen peroxide compound is preferred in this work.

Table 7: PERSOL 1 and AN water solution performance comparison.						
Oxidizer formulation [%w/w]			*Combustion performance*			
AN	*H_2O*	*H_2O_2*	*O/F_{opt}*	*T_c [K]*	*I_{sp} [s]*	*c^* [m/s]*
60	40	0	28.4	1073	135	992
50	20	30	14	2064	188	1370
30	20	50	11.5	2224	197	1432

2.6. Liquid Hydrocarbons

Regarding to the rocket fuels, a lot of chemical compounds have been tested throughout history. In this section liquid hydrocarbons will be described because these fuels family have several properties worth to be mentioned. The category treated here includes all those derived from petroleum refining, which belong some of the most widely used fuels in the world, like kerosene, jet fuel and gasoline [1]. The physical properties of these fuels fluctuate depending of several factors like the petroleum source, the refinement process and the accuracy of the manufacture. In the Table 8 the expected properties of few of these propellants are presented.

Table 8: Typical properties of selected hydrocarbon fuels.						
Property	*Unit*	*Jet Fuel*	*Kerosene*	*Av Gas*	*Diesel*	*RP-1*
Density (at 289K)	kg/m^3	0.78	0.81	0.73	0.85	~0.8
Freezing Point	*K*	213	230	213	250	239
Viscosity (at 289K)	*cP*	1.4	1.6	0.5	2.0	16.5(*)
Flash Point (TCC)	*K*	269	331	244	333	316
Reid Vapor Pressure	*KPa*	13 - 21	<6.89	48	0.69	-
Specific Heat	*J/kg/K*	2.10	2.05	2.22	1.97	2.1
Average Molar Mass	*kg/mol*	130	175	90	-	-

Note: The data compiled in this table was extracted from [1].
            * At 239K.

These substances are toxic if ingested and may produce toxic vapors. Although the combustion of hydrocarbon fuels yields theoretically water and carbon dioxide, incomplete combustion may produce also carbon monoxide. Despite its toxicity, compared with other rockets fuels they are relatively easy to handle. Through the recent history, the large number of applications that hydrocarbon fuels have in propulsion and power generation gives them low cost and a high availability.

One of the challenges to overcome when using a hydrocarbon fuel in a regenerative thrust chamber is to avoid, or more exactly to minimize, the carbon deposits in the cooling passages [35]. The carbon deposits are formed due to the fuel thermal instability. As fuel temperature increases, the thermal cracking of the fuel generates carbon compounds that deposit in the cooling passages wall. Also, when a pre-burner or gas generator is employed, the incomplete combustion leads to oxidation of hydrocarbons forming peroxides and eventually deposits in the turbo-machinery.

The RP-1 is a hydrocarbon fuel, similar to kerosene, developed in United States especially for rocket propulsion [37]. It was produces to fulfill the necessity of a clean burning hydrocarbon fuel since the previous tests with jet fuels produces excessive soot and carbon deposits inside several engine components. This propellant has a density and vapor pressure ranges some narrow and hence, the performance prediction is somewhat more accurate. In comparison to hydrogen, RP-1 has much higher density and is cheaper. Although it has explosive hazard is far less dangerous than hydrogen. In addition, RP-1 is storable at ambient temperature which reduces the handling cost. All these characteristics make it a good alternative to hydrogen in first stage rocket engines despite the lower performance, in terms of specific impulse, achieved using this hydrocarbon fuel. The leak in performance is due to the fact that the product of combustion between hydrogen (LH2) and oxygen (LOX) is water which has low specific weight. Additionally, the LH2-LOX engines are fuel rich operated which cause the presence of some hydrogen molecules in the exhaust gas. Such hydrogen molecules are the lightest one. The low weight of the exhaust gas produces a high exhaust velocity and a high specific impulse. In comparison, hydrocarbon fuels produce carbon compounds, like carbon dioxide, into the exhaust gases which have greater molecular weight. Other adverse effect of the presence of CO_2 is that this absorbs some of the combustion energy by generating oscillating modes between the atoms.

A hydrocarbon fuel similar to RP-1, named RG-1 was developed in Russia to propel, in combination with LOX, their first stage engines, like RD-170, RD-180 and NK-33 [35]. The RG-1 (also know as naphthyl) is a type of rocket kerosene denser than the RP-1, with a density range about $0.83kg/m^3$. To increases its density the RG-1 is chilled previously to fill the rocket fuel tank. The LOX tanks are arranged around the fuel tank to keep the RG-1 cold during the vehicle launch. A synthetic (non distillate) hydrocarbon fuel, denominated Syntin, was employed in some upper stages Proton vehicles. Syntin has an increased density of $0.85kg/m^3$ and higher payload ratios are achieved because its improved specific impulse respect to RG-1. In spite of the Syntin better performance, its production was ceased in 1996 because its synthesis was too expensive with respect to other distilled hydrocarbon fuels.

2.7. Liquefiable Gaseous Hydrocarbons

This category involves all the hydrocarbons fuels that are in gaseous state at ambient temperature but, through some procedure, could be liquefied to be stored in the vehicle tanks before being burned. Among the options to be evaluated in this section, there are three hydrocarbon gases that stand out: Methane, Butane and Propane. In the Table 9, the main physical properties of these hydrocarbons are presented. In general, hydrocarbons burn with oxygen following the next ideal reaction formula:

$$C_xH_y + \left(x + \frac{y}{4}\right)O_2 \rightarrow xCO_2 + \left(\frac{y}{2}\right)H_2O + heat \qquad \textbf{(2.7.1)}$$
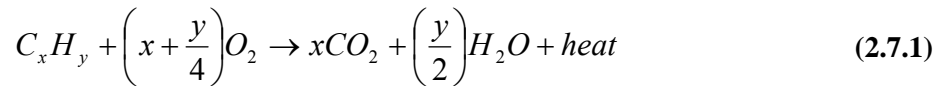
Though the ideal combustion formula shows that this exothermal reaction only yields water and carbon dioxide, incomplete combustion also produces some carbon monoxide. If air is used instead oxygen in the combustion process, the nitrogen content and oxygen excess leads to the production of nitrogen oxides. These are common facts for all the hydrocarbons here analyzed. This section follows with a description of physical properties of selected liquefied hydrocarbons fuels with some comments of their potential applications as rocket propellants.

First, the physical properties of methane are discussed. At standard conditions, it is a colorless, odorless gas that is mainly extracted from natural subterranean reservoirs. It is the main component of natural gas and hence is highly available at relatively low cost. It is the simplest alkane and its molecule is composed by one carbon atom and four hydrogen atoms. Therefore, this gas has the best hydrogen to carbon ratio of all hydrocarbons, which implies that it burns cleaner than other hydrocarbons fuels. As a fuel, methane is non toxic and can be burned with oxygen producing water and carbon dioxide. Therefore, the combustion products and the propellant itself are non toxic. However, it is worth to mention that this gas is a potent greenhouse gas.

Methane gas is usually burned as fuel for gas turbine in electric power generation. Compared to other hydrocarbons fuels, methane produces the least amount of carbon dioxide per unit of released heat. This gas also is used as home heating and cooking gas and in some places, is employed to propel vehicles with internal combustion engines as compressed natural gas (CNG). The CNG is basically methane compressed to a very high pressure (typically above 200 Bar) and stored in heavy spherical or cylindrical tanks [38]. Although its energy density is rather lower than gasoil, its low price has converted to CNG in a good alternative for pick-up, trucks, buses and even trains. As vehicle fuel, the CNG is less harmful to the environment than other fossil fuels. In addition, because it is a gas less dense than air, the spills are less dangerous than liquids fossils fuels. In addition, natural gas contains trace contaminants which makes it a much more sooting fuel than pure methane.

To storage and transport natural gas in large volumes (note that this is primarily methane) it is temporarily liquefied. The liquefied natural gas (LNG) has a very small fraction of the gas volume at standard conditions. The liquefaction process, start with the removal of some impurities like dust, sulfur, other gases, water and heavy hydrocarbons. This is necessary because these substances may cause some difficult in the liquid flow. The purified gas is then condensed to a liquid state at near atmospheric pressure by cooling it to below its boiling point (112 K approximately). The huge volume reduction makes that transporting natural gas to areas without gas pipelines become less expensive. However, less expensive is not cheap: LNG requires super insulation in a pressurized double tank system with a proper venting system [38].

As a rocket propellant, methane is employed as liquefied cryogenic fuel. It has being less exploited than other cryogenic fuels like hydrogen. Compared to this one, methane is denser and although being cryogenic, it has a higher melting point. This last fact implies a tank insulation system with less stringent requirements and hence, a tank system lighter and cheaper. NASA has released tests of an experimental engine that burns methane with oxygen [39]. This

engine incorporates a set of proprietary technologies to achieve high operational reliability and safety [40]. These properties are very important in manned space vehicles.

Moreover, methane may be preferred over hydrogen as fuel in space vehicles because it is abundant in some planets and moons. Therefore, the mission only needs to carry the oxidizer and half the fuel, and may refuel in the remote place. Another engine was tested by the company ATK in a vacuum chamber to prove the viability of employing this engine type in a lunar mission [41]. The company states that this experimental engine has achieved a vacuum specific impulse of 350s. The methane rocket engines are still in experimental phase and more work is needed to achieve the reliability required for a spacecraft engine.

Propane, the second liquefied hydrocarbon to be described, is a colorless odorless gas at standard conditions. Its molecule is formed by three carbon atoms and eight hydrogen atoms. This gas is obtained as a by-product from both, the petroleum refinement and the natural gas processing. Like methane, this chemical compound is widely available at a relatively low cost, making it an option to consider as a rocket propellant. In comparison to methane, propane has the advantage that it becomes to liquid state by only compressing it to a moderate pressure, without the requirement of cooling it to cryogenic temperatures. The combustion of propane with oxygen produces, as in the case of methane, water and carbon dioxide. However, the incomplete combustion also produces carbon monoxide, which is a very toxic gas, and carbon, which are heavy and thus it has an adverse effect in the rocket performance. Unlike methane, propane is denser than air and hence, if a spill occurs, it tends to form a layer around the spill site, instead spreading into the air. This fact supposed an explosion hazard if the concentration of propane is between 3% and 10%. In addition, this gas is non toxic but may produce asphyxia if the concentration in air increases. Some interesting properties of propane are presented in the Table 9, at the end of this section.

Propane is the liquid petroleum gas (LPG) main component, with a concentration of a least 90%, being seconded by butane gas. LPG is used for domestic heating and cooking as well as an alternative fuel in cars and trucks. Because this gas is in liquid state at moderated pressure propane has some advantage over methane as a vehicle fuel. First, the tank construction is less expensive due to that cryogenic temperature requirement is not need. Additionally, the vehicle autonomy with LPG is comparable, although somewhat short, than with gasoline, and its combustion is some clean. Another feature of propane is that, due to its low boiling point, it vaporizes immediately when leave the pressurized system and hence, a vaporization device like carburetor or injector is not needed.

There is a new interest in liquefied hydrocarbon gases as liquid rocket propellants today. Propane is not the exception to this trend. In 2007, the company ORBITEC tested a rocket engine which is propelled with propane and LOX [42]. The propane was initially chosen for this engine as a surrogate fuel for methane, which is currently considered as a hydrogen alternative fuel. Propane is widely available, economical and can be stored at room temperature. Moreover, in comparison with methane, propane has a higher density specific impulse (see Section 3.2). All these facts have been demonstrated that propane is a good rocket engine propellant. In addition to the propane qualities as a propellant, it can be mixed with alcohols fuels, improving the fuel carbon ratio and making it more likely to gasoline. Furthermore, the resulting fuel is auto-pressurized which avoid the utilization of a pressurizing system. Additionally, the combustion process is enhanced because the propane helps to atomize the fuel.

The third liquefied hydrocarbon gas to be considered in this section is butane. Like the other gases described, butane is a colorless odorless gas at standard conditions. Its composition includes four carbons atoms and ten hydrocarbon atoms. Iso-butane or i-butane is the name of a butane isomer, but is worth to mention that the real IUPAC name of such substance is methyl-propane. This gas is obtained from petroleum distillation and is highly available at low cost. The commercial butane actually contains such gas in addition to propane and methyl-propane in less proportion. Although the butane high boiling point makes it unsuitable for transportation by pipelines, because its condensation cause flow problems, this property make it good to be stored in tanks without stringent insulation requirements. This hydrocarbon has a vapor pressure of 2 atm which helps to auto-pressurize the stored butane. Butane is non toxic but is highly volatile and if its concentration in air increases there is an explosion risk. Another health hazard

associated to butane includes somnolence and asphyxia if inhaled. Also, the contact with skin or eyes can cause freezing by the violent expansion. In Table 9, some butane selected properties are shown.

Table 9: Liquefiable Gaseous Hydrocarbon physical data.				
Property	*Methane*	*Propane*	*Butane*	*Unit*
Density (at liquid state)	416	581	600	[kg/m^3]
Molecular mass	16.04	44.1	58.12	[g/mol]
Melting point	91	85	135	[K]
Boiling point	112	231	272.5	[K]
Heat capacity C$_P$	35.7	73.6	140.9	[J/mol/kg]
Enthalpy of formation (at 298K)	-74.6	-103.8	-147.3	[kJ/mol]

Notes: The data compiled in this table was extracted from [18].

Butane is widely employed as fuel for portable heating devices. However, as a rocket propellant, this substance has been less exploited. Taking advantage of its high alcohol solubility, butane can be mixed with ethylic alcohol to auto-pressurize the fuel and, thus, avoid using a tank pressurization system. As in the case of propane, the butane favors the fuel atomization when it is injected in the combustion chamber. The problem associated with the use of these gases as fuels is that, for short burning time, the gas adiabatic expansion can produce a sudden cooling. Such phenomenon may cause local freezing in valves generating blocking of the fuel flow. Even if the blocking is intermittent, the flow fluctuation may have severe consequences that can cause an engine explosion. The cooling can be prevented employing heat exchangers and the blocking can be avoided by using fuel filters.

2.8. Alcohols

Alcohols were used mainly in the rocket early history and, may be, the best known example in this category is the Second War German rocket V-2. Several types of alcohols have been employed as fuels or as fuel additives throughout the history. Methanol, ethanol and to a lesser extent, butanol are the most widely used alcohols as fuel because of two fundamental features. First, they can be synthesized to be produced in large scale and they are compatible with diverse types of combustion engines. The second feature is that all the mentioned alcohols have high octane rates giving a good fuel performance although have less energy density than hydrocarbon fuels like diesel or gasoline. Alcohols can be produced both from petroleum distillation and from biological process. As example, methanol is obtained mainly from processing the natural gas while ethanol is get from biological material fermentation, such sugars fermentation. Alcohols burns with oxygen producing, ideally, carbon dioxide and water. However, incomplete combustion may produce other substances. Anyway, as example, the ideal reaction formula of alcohol combustion is presented:

$$C_nH_{2n+1}OH + \left(n + \frac{n}{2}\right)O_2 \rightarrow nCO_2 + (n+1)H_2O + heat \qquad (2.8.1)$$
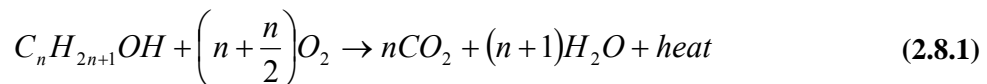
Methanol and ethanol, employed as fuels, have some advantage over other fuels. Due to their high octane these fuels can be employed at high chamber pressure and hence, higher engine performance can be achieved. These alcohols fuels reduce nitrous oxides and carbon monoxide harmful emissions. Due to their lower carbon to hydrogen ratio even the carbon dioxide emissions are reduced. However, these alcohols usually have halide impurities that may cause corrosion problems. To prevent corrosion in engine components, suitable materials must be employed and, additionally, high quality alcohols with very low impurities concentrations

must be used. Alcohols also may have incompatibility problems with some polymers because the carbon-carbon bonds might be broken by the fuel and thus, a reduction in the tensile strength may take place. Methanol is a toxic substance that, if ingested, can produce permanent blindness or even death in higher doses. Due to its volatility, methanol can be dangerous even if not ingested, by contact with skin or by breathing its fumes. In this sense, methanol is as volatile as gasoline and similar safety measures may be employed. Methanol also is a flammable substance that burns invisibly causing a firing detection problem. Despite this drawback, is worth to denote that methanol fires can be extinguished using only water, unlike petroleum fires. Moreover, compared to gasoline, methanol is more difficult to ignite and burns with a lower flame temperature.

Table 10: Selected alcohols physical data.				
Property	*Methanol*	*Ethanol*	*Butanol*	*Unit*
Density (at liquid state)	792	789	810	$[kg/m^3]$
Molecular mass	16.04	44.1	58.12	[g/mol]
Melting point	91	85	135	[K]
Boiling point	112	231	272.5	[K]
Heat capacity C_P	35.7	73.6	140.9	[J/mol/kg]
Enthalpy of formation (at 298K)	-74.6	-103.8	-147.3	[kJ/mol]

Whereas methanol is a very toxic substance, ethanol, in contrast, is less hazardous. The effects of poisoning with this alcohol are better known since it is the beverages alcohol. Beyond the intoxication effects caused by the ingestion of ethanol water solution, pure ethanol also may produce irritation in eyes and skin. Ingestion also, may cause severe damage to the internal organs, leading to pancreatitis, cirrhosis or gastritis. In greater concentrations, the ethanol ingestion may cause death. Ethanol is highly flammable substance and even its vapors can ignite if confined in a closed area [43]. Is worth noting that mixtures with concentrated hydrogen peroxide form powerful explosives. As in the case of methanol, the fire can be extinguished using water.

As rocket propellant fuels, several applications of alcohols have been tested over time. An early application of ethanol as rocket fuel was implemented in the German rocket V-2. In the engine of this weapon the alcohol was burned with oxygen. Later, the North American rocket engines Red Stone and Navaho employ the same propellant combinations but achieving higher performance. Another well known example was the engine that propels the X-1 aircraft which exceeded the sound barrier for first time. In the last decade, a renewed interest in using alcohols as fuels has grown. Recent developments carried out by the private company *XCOR Aerospace* employs alcohols in both primary propulsion engine and low thrust maneuvering rocket applications. An experimental engine propelled with isopropyl alcohol and nitrous oxide serves as demonstrator of a dual cooling approach from which mentions that substantially increase the engine lifetime [44]. This is a key feature in flight control and orbit maintenance maneuvers. Another engine that employs alcohol jointly with liquid oxygen as oxidizer was tested in a flying demonstrator on 2001. In following tests the vehicle reaches burning times over two minutes showing the high reliability of this rocket engine [45]. In conclusion, the renewed interest in alcohols supported by the fact that their have high safety, low cost and price, among other remarkable properties, makes these propellants worth being considered in this work.

Material	Density	Thermal conductivity	UTS	Hardness	Melting Point	Reference
Units	[kg/m^3]	[W/m.K]	[MPa]		[K]	
Aluminum 1060	2705	230	82.7	23 [HB]	919	[46]
Aluminum 5254	2660	125	269	67 [HB]	866	[47]
Stainless Steel 304L	803	16.2	586	80 [RHB]	1673	[48]
Stainless Steel 316L	799	16.2	558	79 [RHB]	1644	[49]
High Density Polyethylene	590	0.2	11.7	55 [SD]	397	[50]
Polytetrafluoroethylene (PTFE) (Teflon®)	460	-	34.5	50 [SD]	590	[51]
Polychlorotrifluoroethylene (PCTFE)	950	0.2	31	80 [SD]	493	[52]
Ethylene-Propylene Rubber	1150	-	13	75 [SA]	-	[53]

Table 11: Propellants compatible materials selected properties.

Abbreviations: HB: Hardness Brinell Scale
                   RHB: Rockwell Hardness – B Scale
                   SD: Shore Hardness – D Scale
                   SA: Shore Hardness – A Scale

III.   SPECIFIC IMPULSE

3.1. Mass Specific Impulse

A complete description of the rocket propulsion theory can be found in specialized books such as those cited in the references [1] and [3]. Here only the most necessary concepts and equations will be presented, in this section a complete analysis of rocket theory is not intended.

To introduce the concept of specific impulse, first some previous definitions should be stated. The *total impulse* (I_t) is the rocket thrust force (F) integrated over the total burning time (t_b):

$$I_t = \int_0^{t_b} F(t)\, dt \qquad\qquad (3.1.1)$$

But, the total impulse does not say anything about the propellant quantity necessary to achieve this thrust force. The propellant mass burned by the engine (m_p) relates to the burning time through the *mass propellant flow rate* ($\dot{m}_p$) concept:

$$\dot{m}_p = \frac{dm_p}{dt} \qquad\qquad \textbf{(3.1.2)}$$

Now it can be introduced the concept of *Specific Impulse* (I_{sp}), which relates the thrust force delivered by the rocket engine with the propellant burned by it. The specific impulse is an important merit figure of rocket performance because, as noted, it allows comparison between engines of different sizes. An expression to compute a time average specific impulse is presented:

$$I_{sm} = \frac{\displaystyle\int_0^{t_b} F(t)\, dt}{g_o \displaystyle\int_0^{t_b} \dot{m}_p\, dt} \qquad\qquad \textbf{(3.1.3)}$$

It is denoted that the specific impulse was arbitrarily defined in function of the propellant mass and then, here it will be referred as specific impulse per unit of mass or simply *specific impulse* (I_{sm}). The subscript *"m"* indicates its relation with propellant mass.

In the case of constant thrust and propellant flow rate the expression 3.1.3 can be simplified as follows:

$$I_{sm} = \frac{F\, t_b}{g_o\, m_p} \qquad\qquad \textbf{(3.1.4)}$$

From the preceding expression, it becomes apparent the dependence of the specific impulse with other key design parameters. As seen, obtaining the highest specific impulse is desirable because that means that the necessary thrust force can be achieved minimizing the propellant mass flow rate. This, in turn, implies a reduction in the required pumping power. In a turbo-pump feed system this has a direct impact in the weight of pumps and turbine. In the electric feed system this means a reduction in the pumps and electric motor weight and, further, this implies to decrease the battery pack size and weight. Furthermore, if a burning time is set, the total propellant mass is minimized for a given mission, thus minimizing the tank size and weight. It should be noted that two objectives are pursued. On one hand, stated a given thrust, an engine as light as possible implicates maximizing the payload. On the other hand, having an engine as small as possible involves a short and narrow vehicle, which implies a reduction in the drag force. The efforts should be focused in the reduction of the propellants tanks size which are, by far, the largest component in the propulsion system.

Besides all the above discussed, the specific impulse is also a function of the propellants and the propellant mixture ratio. Such dependence can not be shown simply through analytical formulae, complex chemical and thermodynamic equilibrium problems should be resolved. Because an analytical expression is not possible to obtain, iterative computing methods were developed to reach a solution to that problem. Today, free computer programs are available to perform these calculations. The results of such calculations are presented in form of table or graphs.

There are two typical approaches to do the thermodynamic analysis: *Frozen Equilibrium Flow* approach and *Shifting Equilibrium flow* approach. The frozen flow approach assumes that not chemical reaction occurs during expansion, thus there are no chemical reactions or phase changes between gases in the chamber and the nozzle exit. Hence, the thermodynamic parameters do not change while the gas flows to the nozzle exit. A conservatively low prediction for specific impulse is obtained with this approach (about 2%) [3]. In the shifting equilibrium flow approach, the reactions occur with infinite speed, so the flow is in equilibrium at any section of the thrust chamber. With this method, the analysis becomes more complex. The specific impulse computed by this approach usually gives optimistic values

(about 3%) [3]. As example, the Table 12 (transcribed from [1]) present the maximum specific impulse expected for selected propellants combinations.

In this report the software *"RPA – Tool for rocket propulsion analysis"* v1.1 (developed by Alexander Ponomarenko) was used to perform the thermodynamic equilibrium calculus [32]. With this tool, a few calculations where made to show the dependence of the specific impulse with some typical design parameter. In addition, the calculations were done for various propellant combinations to remark the different performances that can be achieved.

Table 12: Theoretical Specific Impulses for selected propellants combinations.		
Oxidizer	*Fuel*	*Specific Impulse [s]*
Oxygen	Methane	296
	Hydrazine	301
	Hydrogen	386
	RP-1	300
Fluorine	Hydrazine	365
	Hydrogen	389
Nitrogen Tetroxide	Hydrazine	283
	MMH	278
	RP-1	297
Hydrogen Peroxide	RP-1	297

Notes: Combustion chamber pressure: 6.89MPa – Nozzle exit pressure: 1atm – optimum expansion.
         It's assumed adiabatic combustion and isentropic expansion of ideal gas.
         Mixture ratios are for approximate maximum value of specific impulse.
         Frozen flow approach values are given.
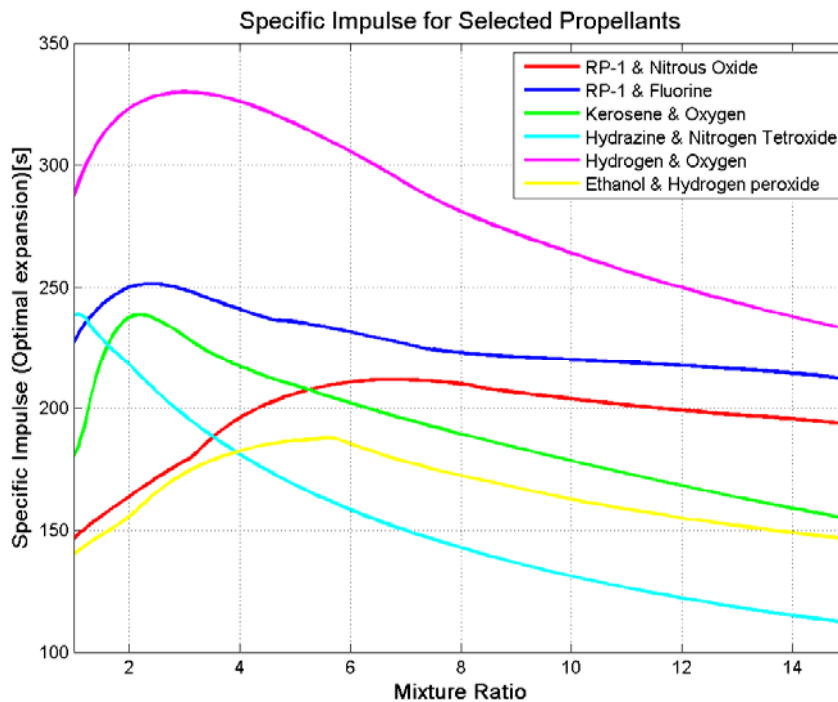
Figure 6: Specific Impulse for selected propellants as a function of the propellant mixture ratio.
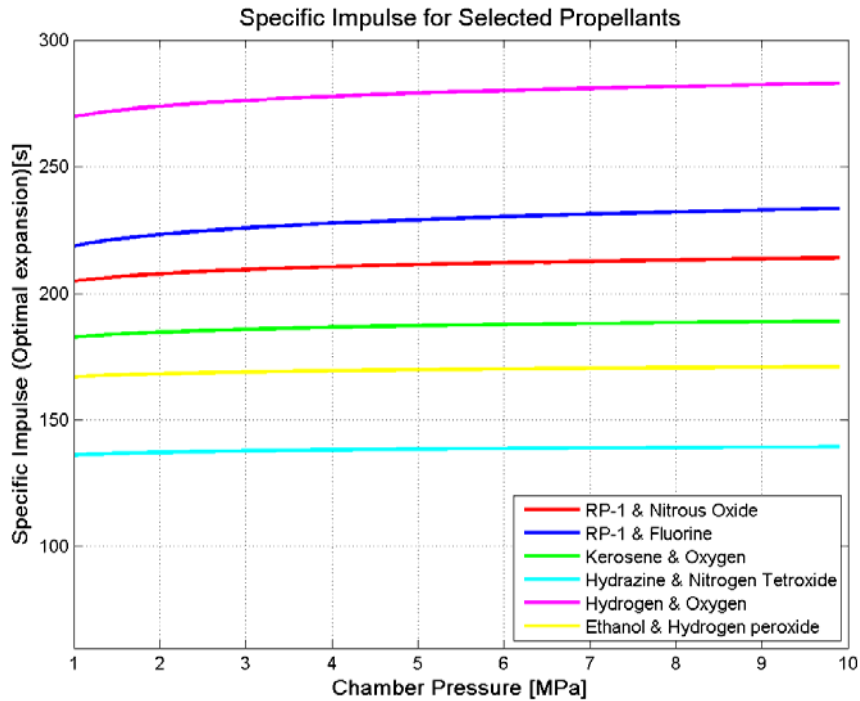
Figure 7: Specific Impulse for selected propellants as a function of the chamber pressure.
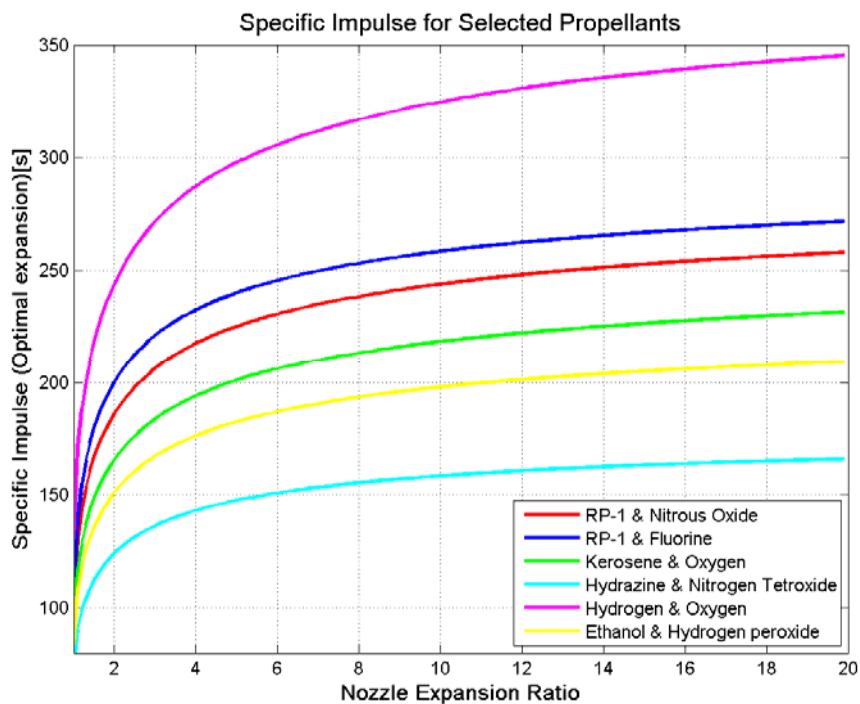
Figure 8: Specific Impulse for selected propellants as a function of the nozzle expansion ratio.

The conditions to perform the estimation are the same for all cases. The chamber pressure is defined in 1.5 MPa and the nozzle selected is a bell nozzle with efficiency of 100%. The approach selected for the calculations is the chemical equilibrium up to the throat with frozen flow further downstream.

3.2. Volumetric Specific Impulse

The specific impulse, defined in terms of the propellant mass flow rate, is a good parameter to perform comparisons between different rocket engines. However, when designing a rocket engine not only the propellant mass is an important issue, the propellant volume is too. So, the density (δ) concept becomes essential, it relates the propellant mass (m_p) and the volume (V_p):

$$\delta_p = \frac{m_p}{V_p} \tag{3.2.1}$$

As in the previous section the mass specific impulse was defined for the propellant mass flow rate, the same can be done for the propellant volume flow rate. This concept will be defined as the *volumetric specific impulse* (I_{sv}) to differentiate it from the *specific impulse* (I_{sm}). Thus, for constant flow rate and constant thrust the following expression is valid:

$$I_{sv} = \frac{F\ t_b}{g_o\ V_p} \tag{3.2.2}$$

It is understood that the I_{sv} is as important as I_{sm} because for a given propellant mass, and thus a given I_{sm}, maximizing the volumetric specific impulse means to minimize the propellants tanks volume and hence, the vehicle size. Therefore, the design efforts should aim to find an optimal compromise between both mass and volumetric specific impulses.

The computer software usually does not deliver theoretical estimations for the herein defined, volumetric specific impulse. So, an analytic expression that allows calculating it from the mass specific impulse is necessary.

It starts by denoting that the total propellant mass is composed by the fuel mass and the oxidizer mass, hence, it can be written:

$$m_p = m_f + m_o \tag{3.2.3}$$

where, m_p: Propellant mass (kg).
   m_f: Fuel mass (kg).
   m_o: Oxidizer mass (kg).

The fuel and oxidizer masses are mixed in the combustion chamber at constant ratio, this ratio is a key parameter denoted as propellant mixture ratio (O/F):

$$O/F = \frac{m_o}{m_f} \tag{3.2.4}$$

From equations 3.2.3 and 3.2.4 the next expressions for fuel mass and oxidizer mass are obtained:

$$m_o = \left(O/F\right) m_f \tag{3.2.5}$$

$$m_f = \frac{m_p}{1 + \left(O/F\right)} \tag{3.2.6}$$

Through the expression 3.2.1 the fuel and oxidizer volumes can be put in terms of its masses:

$$\delta_f = \frac{m_f}{V_f} \tag{3.2.7}$$

$$\delta_o = \frac{m_o}{V_o} \tag{3.2.8}$$

Therefore, the total propellant volume becomes:

$$V_p = V_f + V_o = m_p \left[\left(\frac{1}{1+(O/F)} \right) \left(\frac{1}{\delta_f} + \frac{(O/F)}{\delta_o} \right) \right] \tag{3.2.9}$$

The two expressions for the mass and volumetric specific impulses can be related as follows:

$$I_{sv} = I_{sm} \frac{m_p}{V_p} \tag{3.1.10}$$

Finally, an analytic expression to compute the volumetric specific impulse from the mass specific impulse is obtained combining the equations 3.2.9 and 3.2.10:

$$I_{sv} = I_{sm} \left(\frac{1+(O/F)}{1+\dfrac{\delta_f}{\delta_o}(O/F)} \delta_f \right) \tag{3.1.11}$$

It should be remarked that, in the book cited in references [1] and [2], a similar description is shown. The term between brackets of the above expression is defined as the *average density* or *bulk density*. Moreover, the volumetric specific impulse is defined as "*density specific impulse*".

3.3. Specific Impulse comparison for selected propellants

The propellants presented in the section II will be now compared using the computer program [32]. The complex thermochemical problem that this program resolves has parameters that should be fixed to achieve a solution. Such parameters include those derived from engine operation conditions, engine design and propellant physical parameters. Therefore, first a brief description of the analysis conditions is presented. A chamber pressure of 1.5MPa is adopted for all the calculations. A sea level engine operation is assumed and hence, an ambient pressure of 1atm is adopted. A nozzle that expands the gases to ambient pressure is adopted and, thus, the optimum expansion condition will be achieved at sea level. With the aim of not introducing any nozzle effect in the thermochemical calculus an ideal bell shaped nozzle is adopted. The propellant is kept at ambient temperature, that is, 298K. Regarding to the calculus approach, in the estimations presented, the frozen flow equilibrium approach is adopted and the flow is frozen at the throat level.

According to the propellants described in Section II, many propellant combinations may be considered. Analyzing the performance of all possible propellant combination is not the

objective of the present section, which is only to make a general performance propellant characterization. For this reason, a propellant pre-selection is addressed and presented below.

In this selection procedure, nitrous oxide will be discarded from the list due to two important issues. First, using this oxidizer involves a safety problem. The nitrous oxide is a strong anesthetic and may cause asphyxiation without the victim noticing. In the other hand, nitrous oxide requires high pressure to become to liquid state, and hence, the tank will be heavy penalizing any mass advantage obtained from its relatively high specific impulse. However, this oxidizer can be considered as a reference in performance and is interesting contrast it with hydrogen peroxide. According to this argument, nitrous oxide is included for performance comparison.

As is explained in the Section 2, for rocket applications, hydrogen peroxide is available in water solutions with a concentration range from 70% to 95% or even more. Therefore, in this preliminary performance comparison, 70% and 90% by mass hydrogen peroxide are considered as low concentration bound and as attainable high concentration bound respectively. Further, a PERSOL 1 solution is taking into account as a high density hydrogen peroxide variant. In particular, the total mass of PERSOL 1 solution adopted is composed by 33.7% of ammonium nitrate, 46.4% of hydrogen peroxide and 19.9% of water.

The software employed do not have gasoline within its data base, but still is interesting to estimate the performance achieve when employing this highly available hydrocarbon liquid fuel. Due to that, the hexane is chosen in representation of gasoline because it is its major component.

As described in Section 2, liquefiable hydrocarbon gases are not usually employed as rocket propellant, and only methane is found in some experimental engines. Therefore, this liquefiable gas is considered in the performance comparison. However, it is pointed out that for this project methane is ruled out. This is due to the fact that liquefying this gas requires employing expensive cryogenic equipment. Regarding to alcohol, the most widely employed in propulsion, ethanol and methanol, are selected.

It is worth to mention that this analysis is aimed to upper stage engines, where some propellant combinations are commonly employed. Hence, is interesting to keep present the typical performance achieved by these propellant combinations. There are two oxidizers to consider, although these two oxidizers are discarded from our selection due to their toxicity, but they are included at this point in the comparison as a performance reference. First, the inhibited red fuming nitric acid, which was widely employed until few decades ago and still is considered in some design in South America. In second place, the nitrogen tetroxide, which is today often worldwide employed in storable combinations with hydrazine and its derivatives, is considered. In combination with this last oxidizer, the hydrazine (which is very toxic) is employed as fuel since this combination is hypergolic and due to that, hydrazine is considered here. Although some hydrazine derivatives (i.e. mono-methyl hydrazine or MMH) are more frequently employed than pure hydrazine because they has improved physical properties, pure hydrazine has a higher performance and thus, it is better as a performance reference.

In the Table 13, the performance comparison results are presented. The performance parameter selected is the specific impulse. As explained above, to take into account the propellant density, the volumetric specific impulse is also considered. Two ambient pressures are employed in the calculus, on one hand, the sea level operation is assumed, and due to the nozzle exit pressure condition, the sea level operation matches to optimum expansion operation. On the other hand, the vacuum operation condition, assuming the same chamber pressure and nozzle efficiency as in the first case is used. This allows taking two limits in the engine operation.

By inspecting the Table 13 is apparent that, between the candidates oxidizers presented in section 2, the better performance (in terms of Specific Impulse) is obtained by using nitrous oxide or hydrogen peroxide in concentration of 90%. Compared with the reference oxidizer, red fuming nitric acid, equivalents numbers are reached tilting the balance in favor of the less hazardous candidate oxidizers. A slight difference is seen when they are compared to nitrogen tetroxide and hydrazine. Such fact is a strong argument for choosing this propellant combination

over the rest when a high performance upper stage engine is designed. However, in this work safety is a key issue and, as mentioned above, these propellants are discarded.

Table 13: Computed performance parameters for propellants of Section 2.

Oxidizer	Fuel	O/F	Maximum Specific Impulse [s]		O/F	Maximum Volumetric Specific Impulse [kg.s/m³]	
			Optimum Expansion	Vacuum		Optimum Expansion	Vacuum
Nitrous Oxide	Kerosene RP-1	7.00	208.67	238.28	8.00	338726	387068
	Hexane	7.20	209.72	239.48	10.00	325338	371868
	Methane	8.60	211.27	241.37	15.00	302081	345070
	Methanol	3.40	203.65	232.99	6.20	299955	342794
	Ethanol	4.60	205.33	234.77	6.80	313795	358827
70% Hydrogen Peroxide	Kerosene RP-1	10.20	190.80	218.97	10.20	232504	266833
	Hexane	10.60	191.32	219.54	10.60	226570	260001
	Methane	12.00	191.41	219.52	12.00	211515	242581
	Methanol	4.40	186.81	214.17	4.60	215343	246953
	Ethanol	6.20	188.17	215.83	6.20	221975	254597
90% Hydrogen Peroxide	Kerosene RP-1	6.80	213.79	245.69	7.20	274532	315679
	Hexane	7.00	214.78	246.79	8.00	264875	304672
	Methane	8.20	216.06	248.21	9.60	244005	280582
	Methanol	3.20	207.58	238.52	3.60	247558	284627
	Ethanol	4.40	209.82	241.15	4.80	258132	296862
PERSOL 1	Kerosene RP-1	11.60	189.43	217.22	11.80	249009	285585
	Hexane	12.00	189.89	217.75	12.20	242969	278622
	Methane	13.80	189.93	217.69	14.00	227763	261064
	Methanol	5.20	186.18	213.39	5.20	230445	264129
	Ethanol	7.20	187.19	214.59	7.20	237802	272610
RFNA	Kerosene RP-1	4.40	209.80	240.52	5.00	286781	329054
	Hydrazine	1.40	225.95	258.50	1.40	290756	332640
NTO	Hydrazine	1.10	235.88	269.69	1.20	284380	325350

Notes: Estimated values considering the combustion efficiency.
             Mixture ratios are for maximum value of specific impulse.
             Frozen flow approach values are given.
             RFNA: Red fuming Nitric Acid (85% Nitric Acid – 15% Nitrous Oxide).
             NTO: Nitrogen Tetroxide.

From the Table 13 is expected that the specific impulses achieved when employing PERSOL 1 and hydrogen peroxide in 70% concentration are below the rest. When comparing both oxidizers it can be seen that the volumetric specific impulse is improved using PERSOL 1. Such improvement is detailed below, in this section.

Regarding to the fuels, given one oxidizer, the specific impulse shows no major changes when switch among the different fuels. A slightly poor performance is observed in the case of alcohols but it does not seem so significant. Between methane and liquid hydrocarbon fuels the latter are preferred because the simpler involved hardware.

At this point, performing a more detailed comparison among the candidate propellants is interesting. Regarding to the liquid hydrocarbon fuel, despite the small difference between the gasoline and kerosene, due to its better characteristic as rocket propellant, this last one is selected.

The oxidizer selection is limited to the different hydrogen peroxide solutions. It is particularly interesting to compare the water solution of hydrogen peroxide in concentration of 70% with the denser PERSOL 1. As a reference in performance the hydrazine and red fuming nitric acid combination is included. In the figures 9, 10, 11, 12, 13 and 14 the results obtained are shown.
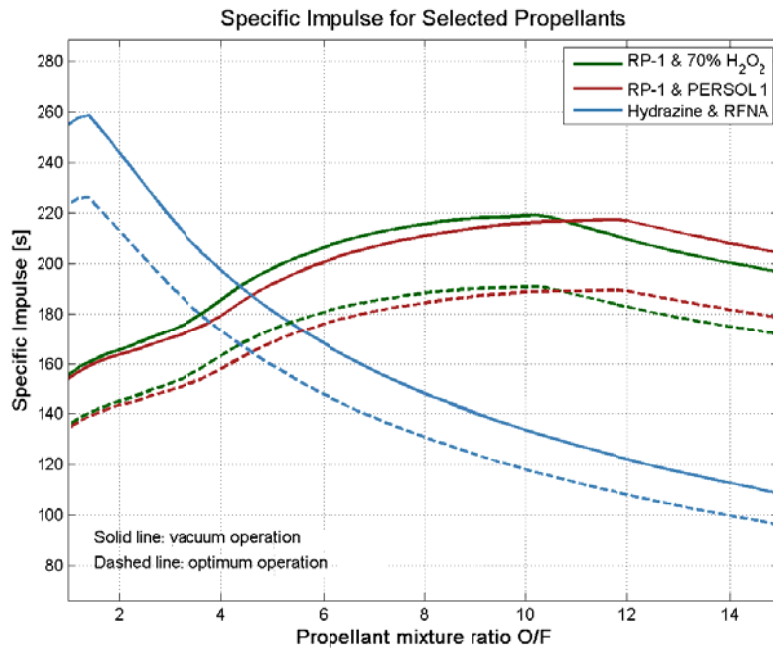
Figure 9: Specific Impulse for selected propellants as a function of the propellant mixture ratio.
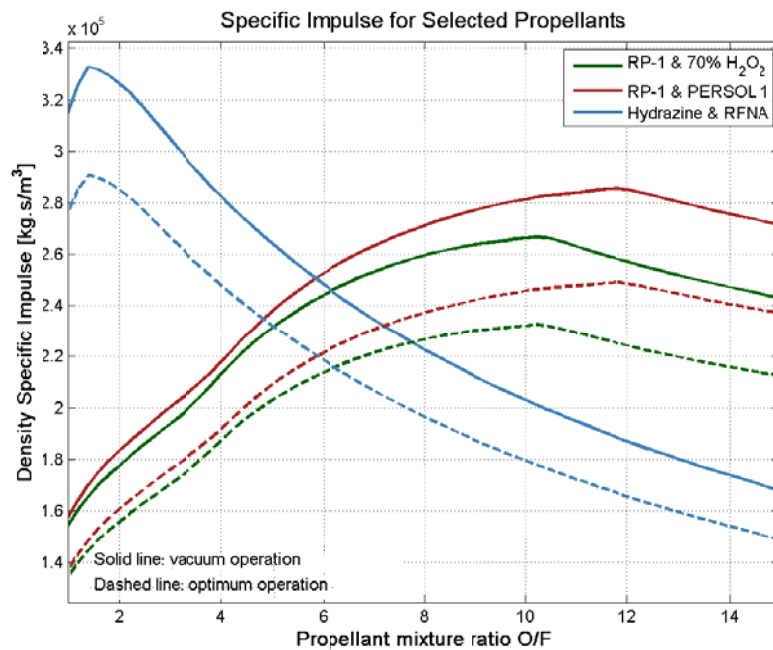
Figure 10: Density or Volumetric Specific Impulse for selected propellants as a function of the propellant mixture ratio.

From figures 9 and 10 is worth denoting that the specific impulse curves of hydrogen peroxide and PERSOL 1 are so similar, showing only a slight shift to higher values in the optimum propellant mixture ratio for this last mentioned oxidizer. Nevertheless, the volumetric specific impulse presented in the Figure 10 shows a clear improvement for PERSOL 1, which implies lower volume propellant tanks.
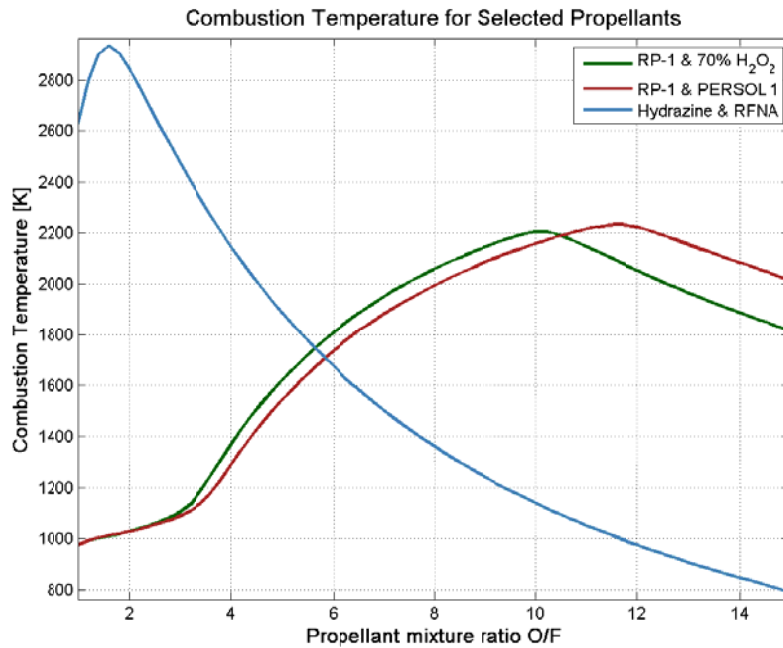
Figure 11: Combustion Temperature for selected propellants as a function of the propellant mixture ratio.
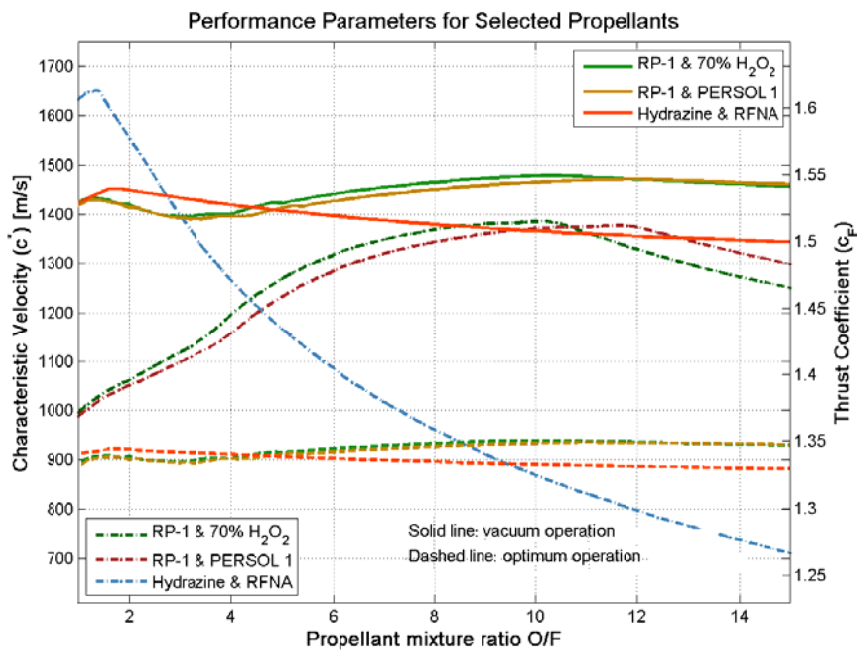
Figure 12: Characteristic Velocity and Thrust Coefficient for selected propellants as a function of the propellant mixture ratio.

Figures 11 and 12 shows that there is not major differences between performance parameters and combustion temperature expected from the two hydrogen peroxide solutions. The plot in Figure 11 indicates that whether one or another oxidizer is employed, the combustion temperature and thus the heat to be released from the combustion chamber remains almost the same. Such fact implies that the same refrigerant scheme may be used when operating the engine with any oxidizer.
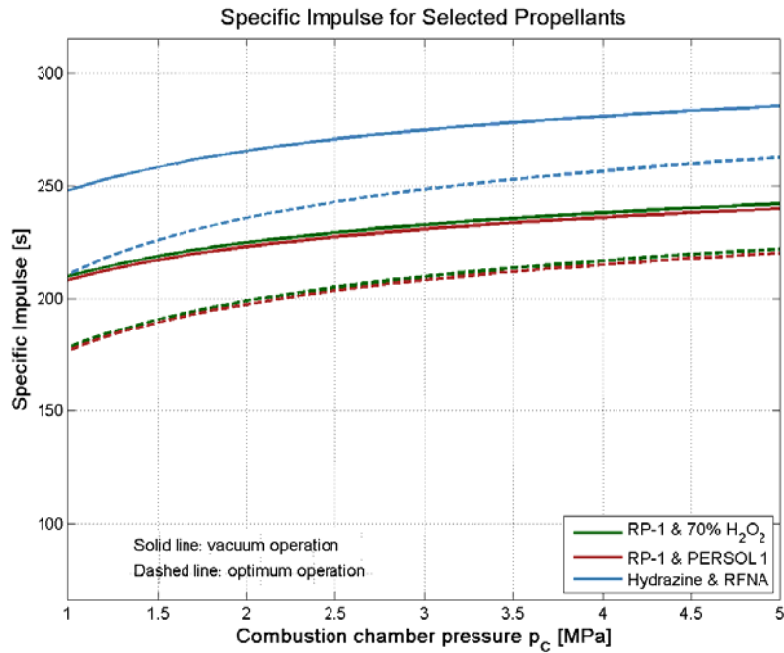
Figure 13: Specific Impulse for selected propellants as a function of the combustion chamber pressure.
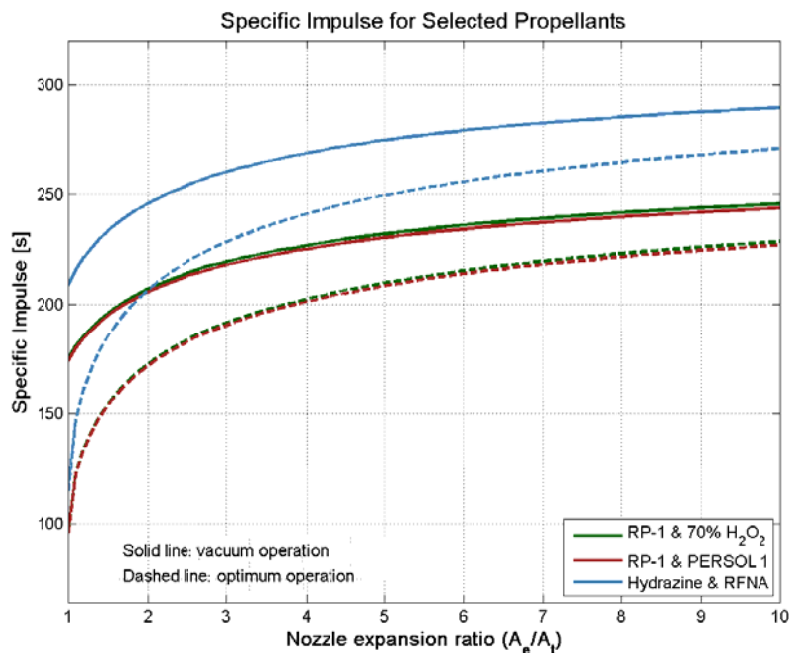
Figure 14: Specific Impulse for selected propellants as a function of the nozzle expansion ratio.

Finally, Figures 13 and 14 reports that no significant changes are expected in specific impulses no matter what hydrogen peroxide solution is employed, whatever pressure chamber or nozzle expansion ratio adopted for the engine.

The density improvement achieved with PERSOL 1 solution allows investigating the possibility of obtain a similar result for the fuel with the aim of minimizing the overall propellant tanks size. In the following section a more detailed analysis of densified propellants are presented.

IV.   DENSIFIED PROPELLANTS

In some cases, additives are mixed into the liquid propellants to improve one or several properties. The properties that are enhanced by the additive can be very diverse, like reducing the freezing point, improving storability, facilitating the ignition, avoiding combustion instabilities and increasing the propellant density. There exist a great number of additives substances that can be employed to get better propellants characteristics. For this particular work the focus is on improving the propellant density. In Section 2, an oxidizer which is a densified solution of hydrogen peroxide, named as PERSOL 1, is described. At this point, few additives for hydrocarbon liquid fuels, taking kerosene as example of this fuel group, are discussed.

Kerosene is chosen as testing fuel due to its high performance, as stated in the preceding section. A metalized propellant, either a fuel or an oxidizer, provides both increased specific impulse and increased volumetric specific impulse. Hence, herein a semimetal and some powdered metals are tested as kerosene additive. For the application studied there are two key properties of such additive. In first place, the metal must be a light substance, is desirable increasing the fuel density without increasing its total mass. On the other hand, a metal that can release a large amount of energy during combustion is desirable. Matching these requirements there are four metals that are proposed: Aluminum, Lithium, Magnesium and Boron. To obtain a uniform mixture, the metal additive particles must be as small as possible and therefore, employing fine metal powder is considered.

In first place a brief description of the proposed metal is given. Aluminum is a strong and lightweight metal widely employed in a lot of applications. More detailed information can be found in [55]. The industrial use of this metal exceed to all other metals with the exception of iron. Aluminum can be used in combination with many other metals to form alloys with very diverse features. In the form of fine powder, as required in this work, aluminum may present some risk to the health. Inhalation of aluminum can cause severe pulmonary fibrosis, especially if the exposure takes place for a long time. To prevent this problem, it is recommended to imbibe it with the fuel previous to any kind of manipulation.

Regarding to lithium, it is denoted that it is highly reactive substance and particularly it reacts with oxygen and water [56]. The reaction with water is exothermal, producing hydrogen gas and lithium hydroxide. It also exothermally reacts with oxygen giving lithium oxide. These two reactions are mentioned because they are present in the combustion with hydrogen peroxide. In fact, if lithium is present in combustion, the fumes contain a high ratio of lithium hydroxide, which is a highly corrosive substance and may represent a major hazard to the environment. Handling lithium requires special care due to its high flammability. Alongside the fire and explosion hazard, exposure to lithium can cause severe health problem due to its high corrosivity. Although these environmental and handling drawbacks, is worth to mention that lithium allows achieving a relatively high increment in specific impulse.

Magnesium is the next metal to consider in this description. It is also very light and due to its capacity to form resistant alloys it is often employed in a number of lightweight metals alloys [57]. Whereas magnesium is a very active substance, reacting with almost non metals and acid, it does not with hydrocarbon, a key property to mixing it in the fuel. As in the case of lithium the reaction with oxygen and water is highly exothermal. Moreover, magnesium is an abundant substance and may be acquired at low cost. This metal is important to human life due to its role in many physiologic processes. Even though this fact, inhalation of magnesium powder may irritate mucous membranes and upper respiratory tract and so, it must be handled carefully. Also there exist a risk of spontaneously ignite due to the violent reaction with the oxygen in air. To avoid these problems is recommended to soak it with the fuel before manipulating it.

Finally, as boron is concerned, it has the common form of a dark powder and remains unreactive with water and oxygen [58]. This is the only non metal among the proposed additives. This substance is founded in the nature only forming chemical compounds with many other elements. While humans are exposed to boron through vegetables, water and air, there exists a limit in the concentration from which it becomes toxic.

Alongside the inclusion of the additive substance, it is necessary incorporating a gelling agent to achieve a proper mixing of the solid metals particles with the liquid fuel. According to reference [59], the silicon dioxide is the gellant adopted in a ratio between 3% and 7%. Although in practice it is necessary, the specific impulse is not greatly affected by the inclusion of the gellant agent in the performance calculation. Thereby, in the performance comparison it is neglected. Regarding to the metal additive, its ratio in function of total fuel mass is kept to 7%, because this mass fraction minimizes the launcher total initial mass [60].

Using the same parameters as in the preceding section some performance calculations are made, in this case, employing only the metalized kerosene as fuel. The Table 14 shows the results of such calculations.

Table 14: Computed performance parameters for densified kerosene.							
Oxidizer	*Fuel*	*O/F*	*Maximum Specific Impulse [s]*		*O/F*	*Maximum Volumetric Specific Impulse [kg.s/m³]*	
			Optimum Expansion	*Vacuum*		*Optimum Expansion*	*Vacuum*
70% Hydrogen Peroxide	Kerosene RP-1	10.20	190.80	218.97	10.20	232504	266833
	Kerosene RP-1 7%w/w Al	9.60	193.36	222.02	9.60	239720	275260
	Kerosene RP-1 7%w/w Li	9.60	192.91	221.44	9.80	233680	268300
	Kerosene RP-1 7%w/w Mg	9.60	192.32	220.82	9.60	236200	271190
	Kerosene RP-1 7%w/w Bo	8.80	197.56	226.70	9.60	280190	243940
PERSOL 1	Kerosene RP-1	11.60	189.43	217.22	11.80	249009	285585
	Kerosene RP-1 7%w/w Al	10.80	191.80	220.05	11.00	256100	293830
	Kerosene RP-1 7%w/w Li	11.00	191.36	219.48	11.20	250060	286870
	Kerosene RP-1 7%w/w Mg	11.00	190.85	218.96	11.00	252570	289760
	Kerosene RP-1 7%w/w Bo	10.00	195.71	224.40	11.20	260250	298660

From the Table 14 is apparent that the specific impulse is improved using additives into the fuel. The best performance in terms of specific impulse and density impulse is obtained by employing boron. Nevertheless, boron is considered in this work as an impractical solution due to its high cost and low availability. Another substance that is ruled out in the selection is lithium. In this case, the reason to exclude this metal is its high toxicity. The lithium powder may cause severe health injuries if inhaled and also the combustion fumes containing lithium are considered toxics. Aluminum and magnesium both have high availability, low cost and moderate handling hazard. Both additives reach almost the same performance but a slight advantage in favor of aluminum is observed. Thereby, a densified solution of kerosene and aluminum is adopted in this work.

At this point, a bit more detailed performance estimation is computed considering two propellant combinations. Kerosene metalized with aluminum is adopted as fuel, whereas a solution of 70% by mass of hydrogen peroxide and a solution of PERSOL 1 are employed as oxidizers. The parameters settled for such performance estimation are identical to those assumed in the previous calculations. In the Figures 15 through 18 the results are shown.
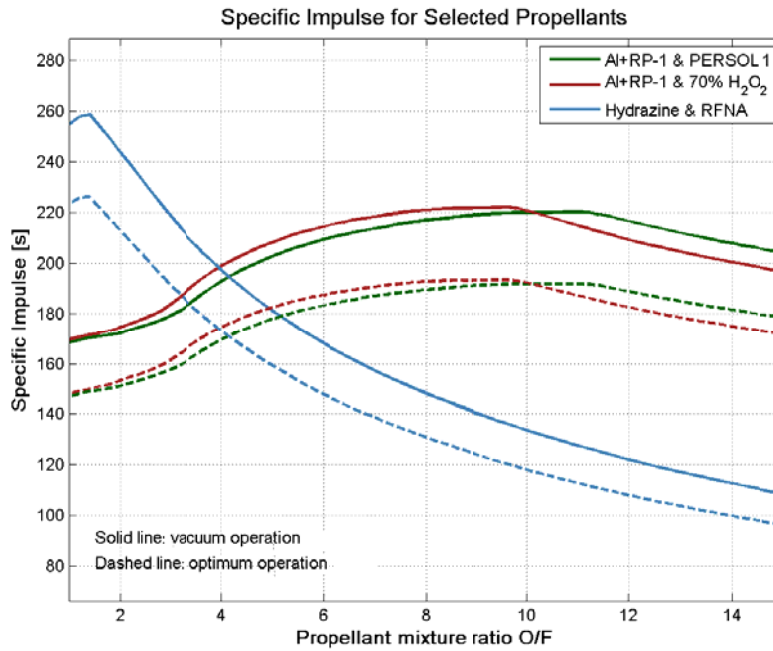
Figure 15: Specific Impulse for selected propellants as a function of the propellant mixture ratio.
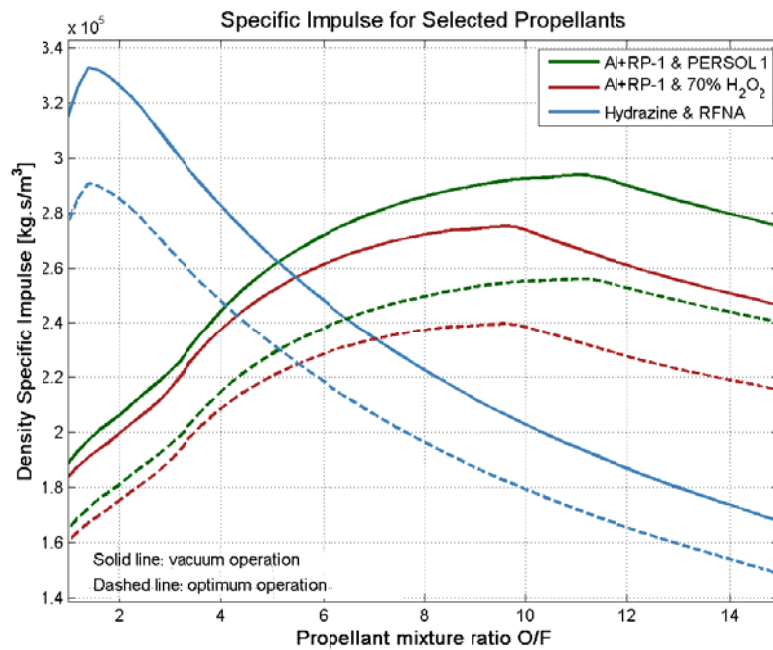
Figure 16: Density or Volumetric Specific Impulse for selected propellants as a function of the propellant mixture ratio.
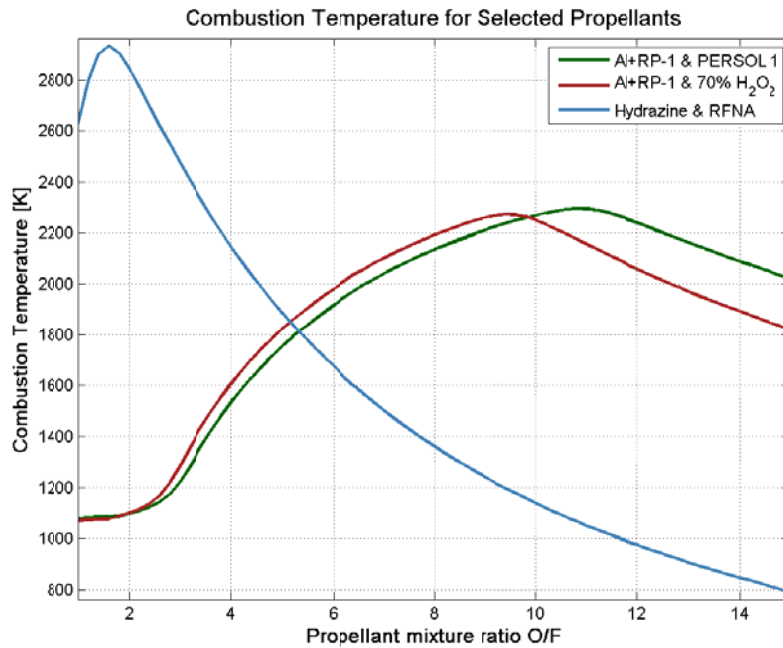
Figure 17: Combustion Temperature for selected propellants as a function of the propellant mixture ratio.
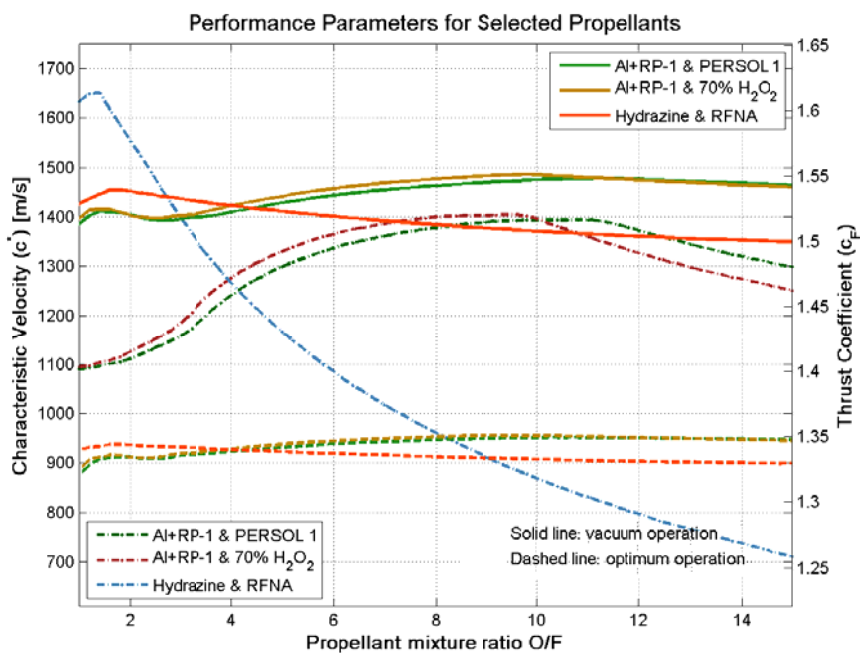
Figure 18: Characteristic Velocity and Thrust Coefficient for selected propellants as a function of the propellant mixture ratio.

V. EXPERIMENTAL ENGINE PROPELLANTS SELECTION

In this section the arguments that support the propellant choice for the experimental engine are presented. As is stated in the foregoing sections, safety and cost are foremost issues to decide the propellants that will be employed in the static testing rocket engine.

The information collected and presented in Section 2 shows that the hydrogen peroxide solutions are available at low cost and have good handling characteristics. Hydrogen peroxide also allows the engine operation in a monopropellant mode that can be useful to perform some tests. The combustion temperature can be easily controlled by shifting the oxidizer water concentration between trials. In Section 3 is denoted that those features are obtained while leading also a good performance. Therefore, those solutions are selected as oxidizing agents and so, it contributes to achieve a versatile test bench. The selection of hydrogen peroxide leads to having to include a catalyst system. From the alternatives mentioned in Section 2.3, is determined that employing wire stacked mesh will be too expensive, despite the high performance achieved. Hence, for this work, the use of a permanganate cake seems a more reasonable option. The combustion chamber inner wall will be covered with such permanganate cake hoping that the short combustion time allows an appropriated decomposition without catalyst cracking.

Focusing on the fuel selection, from the several hydrocarbons fuels evaluated in the preceding sections, the following items are outlined. Working with gaseous hydrocarbons is not good because, in almost all cases, the necessary tanks pressure make it so heavy and difficult to handle. Employing liquid methane is not possible due to the complex hardware needed to manage the cryogenics temperatures. Additionally, if commercials mixtures of propane and butane are burned in the engine, variations in its composition may leads to changes in the performance measures between tests. Meanwhile, alcohols may be considered as fuel, since they are relative safe, inexpensive and can be handled without difficulties. However, when compared to kerosene, alcohols have shown a lower performance and therefore, the latter is considered the best choice.

From these selected propellants an additional feature is obtained. In the previous section a study of the effects of densified propellants in engine performance is presented. There is observed that an enhanced performance in terms of both propellant mass and volume is reached by adding a proper substance to the selected propellants. Therefore, employing aluminized kerosene and PERSOL 1 in the testing engine is considered for a future work. Such fact allows studying the propellant pump system and overall engine behavior when employing those densified propellants. It can be seen that there is only a small change in the propellant mixture ratio whether densified propellants or not densified ones are employed. Such fact allows carrying out tests without major changes in the hardware setup.

VI. CONCLUSIONS

The information collected and analyzed in this report allows extracting several conclusions. In first place, it should be emphasized the influence of the specific impulse in the pumping system sizing. Maximizing the specific impulse implies that for a given thrust, the required propellant mass flow rate is minimized. As was displayed in the previous report, the pumping required power is proportional to the propellant flow rate. Hence, the mass of each pumping component is reduced by decreasing such propellant flow. Meanwhile, the volumetric specific impulse is a key issue in the sizing of both propellant tanks and pumping system. The first have impact in the total propellant tanks mass and the second in the overall pumping system mass. In this particular work, the adopted pumps are of volume displacement type and hence, reducing the volume flow rate implies a direct reduction in the battery pack mass, which, as was stated, is the heaviest component in the electric pumping system. Additionally, a reduction in the tanks volume entails an improvement in the vehicle envelope and thus a reduction in the drag force during ascent. Therefore, a diminution in the required thrust force,

especially for the first stage engine, is obtained which, in turn, reduces the overall vehicle mass. Owing to all the mentioned above, propellants that yield both high specific impulse and volumetric specific impulse are required.

When a single stage vehicle is designed all the previously remarked is very important. A reduction in the specific impulse directly translates into a reduction in the payload mass. Furthermore, the specific impulse is particularly significant in multistage launch vehicles upper stages. The propellant needed in the upper stage is a payload for the other stages and so, a reduction in such quantity is a relief in the thrust requirement for the first stage, which is the largest one. In section 3 the influence of chamber pressure and nozzle expansion ratio in the specific impulse is presented for a set of propellants. The trend shown holds regardless the propellants employed. It may be seen that a high chamber pressure and nozzle expansion ratio is preferred. The achievable nozzle expansion ratio is limited by the ability to extract heat from the throat section and therefore is associated to the limitations in the cooling system design. With a regenerative cooling approach this is directly related to the pumping system through the pressure drop in the cooling passages and the heat transfer characteristics of the cooling propellant. Meanwhile, the pumping power and hence, the pumping system total mass also rely on the chamber pressure. By this means, the proper set of propellants, chamber pressure and expansion ratio ought to be established in order to enhance the pumping system mass.

Regarding to the selected propellants, it should be denoted that the elected ones are "clean" substances. This term refers to the set of three central features. First, they are relatively non toxic substances and can be handled quite easily. Moreover, the combustion of such substances produces non toxic fumes. All the combustion products can be found in the atmosphere and so, breathing in an ambience of non saturated gases is safe for the exposed personnel. The other feature is that the substances itself and its fumes are safe for the environment. This simplifies the disposal operations and facilitates the spills treatment. These facts are valuable not only for the experimental engine but also for whatever future upper stage engine design that will be addressed.

According to section 4, densifying only the oxidizer, that is by employing PERSOL 1 instead 70% by mass hydrogen peroxide and water solution, have almost not impact on the specific impulse but allows achieving an increment of around a 7% in the volumetric specific impulse. On the other hand, the increment in volumetric specific impulse is somewhat lower by densifying only the fuel. In this case, a slight improvement in the specific impulse also is noted but is not significant and may be masked by other performance losses. The best situation is attained by densifying both fuel and oxidizer, achieving an increment in volumetric specific impulse of around 10%. The change of densifying metal does not enhance the specific impulse too much. Thereby, aluminum powder is preferred due to its high availability, low cost and relatively safe handling. The erosion effect of such metals particles into the several engine components will be a study object.

In conclusion, all the preceding arguments allows to think that the selected propellants may be more easily acquired and handled in comparison with all other the proposed option, without compromising too much performance. Such fact adds versatility to the engine test bench and allows reducing the time between tests. In addition, the study over densified propellants shows a promising improvement in the electric pumping system mass. Thereby, although the specific impulse obtained with the selected "clean" propellants is below the attainable with the often employed combinations (i.e. hydrazine derivatives as fuel and tetroxide nitrogen as oxidizer), the reduction in the engine mass suggest the possibility of produce a rocket propulsion system lighter than the classic approach of pressurized tank system feeding high performance and toxicity propellants. However, this last supposition must be studied in a future work before establish that as a conclusion.

VII.   REFERENCES

[1] Sutton, G. P. and Biblarz, O.: *Rocket Propulsion Elements*, 7th ed., Wiley, New York, 2001.

[2] Huzel, D. K. and Huang, D. H.: *Modern Engineering for Design of Liquid-Propellant Rocket Engines*, 1st ed., AIAA, Washington DC, 1992.

[3] Humble R. W. Henry, G.N. and Larson, W. J.: *Space Propulsion Analysis and Design*, 1st ed., McGraw-Hill, New York, 1995.

[4] NOAA, *Chemical Datasheet: Nitrogen Tetroxide*, (http://cameochemicals.noaa.gov/chemical/4075).

[5] Chemical Propulsion Information Agency*, "Liquid Propellants" Hazards of Chemical Rockets and Propellants*, Vol. III, September 1984.

[6] U.S E.P.A., *Technology Transfer Network, Hydrazine Hazard Summary*, (http://www.epa.gov/ttnatw01/hlthef/hydrazin.html).

[7] NOAA, *Chemical Datasheet: Hydrogen Peroxide Solution (>52%)* (http://cameochemicals.noaa.gov/chemical/892).

[8] NOAA, *Chemical Datasheet: Pentaborane* (http://cameochemicals.noaa.gov/chemical/1285).

[9] Chiaverini, M. J. and Kuo, K. K.: *Fundamentals of Hybrid Rocket Combustion and Propulsion,* 1st ed. AIAA, Reston, Virginia, 2007.

[10] School of Aerospace, Tsinghua Space Center, Space Propulsion, *Nitrous Oxide Background*, Nov 2005 (http://hy.tsinghua.edu.cn/teacher/index_files/Page335.htm).

[11] Patent description, *Nitrous Oxide Fuel Blend Monopropellants*, (http://www.faqs.org/patents/app/20090133788).

[12] Space Propulsion Group, *Nytrox® Product description,* January 2011 (http://www.spg-corp.com/nytrox-propellants.html).

[13] Air liquide Gas Encyclopedia, *Nitrous Oxide Datasheet*, January 2011, (http://encyclopedia.airliquide.com/encyclopedia.asp).

[14] School of Aerospace, Tsinghua Space Center, Space Propulsion, *Hydrogen Peroxide Background*, Nov 2005 (http://hy.tsinghua.edu.cn/teacher/index_files/Page653.htm).

[15] Chemical Land 21*, Hydrogen Peroxide datasheet*, January 2011 (http://www.chemicalland21.com/industrialchem/inorganic/HYDROGEN%20PEROXIDE.htm).

[16] Peroxide Propulsion, *P85 product datasheet*, January 2011 (http://www.peroxidepropulsion.com/article/3).

[17] RPA Thermodynamic Database, Jan 2011, (http://software.lpre.de/thermo_data.htm).

[18] Lide, D. R.: *CRC Handbook of Chemistry and Physics*, 76th Ed, Taylor and Francis, Boca Raton, FL, 2006.

[19] S. S. Pietrobon: *High density liquid rocket boosters for the Space Shuttle,* Journal of the British Interplanetary Society, vol. 52, May/June 1999, (http://www.sworld.com.au/steven).

[20] Tsohas, J. Droppers, L. J. and Heister, S. D.: *Sounding Rocket Technology Demonstration for Small Satellite Launch Vehicle Project*, 4th Responsive Space Conference, April 2006.

[21] Ventura, M. Wernimont, E. and Dillard, J.: *Hydrogen Peroxide - Optimal for Turbomachinery and Power Applications*, Joint Propulsion Conference & Exhibit, July 2007.

[22] Solvay Chemical, *Hydrogen Peroxide Safety and Handling Datasheet*, January 2011, (http://www.solvaychemicals.us/services/resourcelibrary/hydrogenperoxide/0,,40001-2-0,00.htm#3).

[23] Solvay Chemical, *Materials of Construction for the Storage of Hydrogen Peroxide - Technical Datasheet*, January 2011, (http://www.solvaychemicals.us/services/resourcelibrary/hydrogenperoxide/0,,40001-2-0,00.htm#3).

[24] Wernimont E. J. and Mullens P.: *Capabilities of Hydrogen Peroxide Catalyst Beds*, 36th AIAA/ASME/SAE/ASEE Joint Propulsion Conference and Exhibit - July 2000.

[25] Wernimont E. J.: *Hydrogen Peroxide Catalyst Beds are Lighter than Liquid Injectors*, 41st AIAA/ASME/SAE/ASEE Joint Propulsion Conference & Exhibit Tucson, AZ, July 10-13, 2005.

[26] Wernimont E. J. and Durant D.: *Development of a 250lbfv Kerosene – 90% Hydrogen Peroxide Thruster,* 40th AIAA/ASME/SAE/ASEE Joint Propulsion Conference and Exhibit 11 - 14 July 2004, Fort Lauderdale, Florida.

[27] Peroxide Propulsion, Decomposition Catalysts, February 2011, (http://www.peroxidepropulsion.com/article/38).

[28] Richard Nakka, Experiments with Ammonium Nitrate / Aluminum based Propellants Formulations, February 2001, (http://www.nakka-rocketry.net/anexp.html).

[29] Rocket Motor Components Inc., Ammonium Nitrate Material Safety Datasheet, February 2011, (http://www.rocketmotorparts.com/).

[30] Wagaman K. L.: *United State Patent No: US 6328831 B1 "Gas-Generating Liquid Compositions (PERHAN)"*, Assignee to the United States of America as represented by the Secretary of the Navy (Washington, DC), Dec 11 2001.

[31] Wagaman K. L.: *United State Patent No: US 6165295 A "Gas-Generating Liquid Compositions (PERSOL 1)"*, Dec 26 2000.

[32] Ponomarenko A.: *RPA – Tool for rocket propulsion analysis*, version 1.1, (http://www.propulsion-analysis.com/index.htm).

[33] Wagaman K. L.: *United State Patent No: US 6331220 B1 "Gas-Generating Liquid Compositions (PERSOL 2)"*, Assignee to the United States of America as represented by the Secretary of the Navy (Washington, DC), Dec 18 2001.

[34] Guide Chem – The Online Trading Guide, Hydrazinium Nitrate, March 2011, (http://www.guidechem.com/dictionary/13464-97-6.html).

[35] Edward T.: *"Liquid Fuels and Propellants for Aerospace Propulsion"*, Journal of Propulsion and Power, Vol. 19 No. 6, Nov-Dec 2003.

[36] National University of Singapore, *Kerosene Safety Datasheet*, (http://www.ece.nus.edu.sg), March 2011.

[37] Braeunig R. A.: *Rocket and Space Technology*, March 2011, (http://www.braeunig.us/space/index.htm).

[38] Envocare Ltd, *"Liquefied Petroleum Gas (LPG), Liquefied Natural Gas (LNG) and Compressed Natural Gas (CNG)"*, April 2011, (http://www.envocare.co.uk/lpg_lng_cng.htm).

[39] The Future of Things article, "NASA test methane rocket engine", April 2011, (http://thefutureofthings.com/pod/228/nasa-tests-methane-rocket-engine.html).

[40] XCOR Aerospace Company, "XR-5M15, LOX/Methane Main Engine", March 2011, (http://www.xcor.com/products).

[41] Space Travel article, "*ATK Test Fires Liquid Oxygen-Methane Rocket Engine in Vacuum*", April 2011, (http://www.space-travel.com/reports/ATK_Test_Fires_Liquid_Oxygen_Methane_Rocket_Engine_In_Vacuum_999.html).

[42] Hobby Space article, *"Orbitec tests vortex rocket engine"*, April 2011, (http://www.hobbyspace.com/nucleus/index.php?itemid=3765).

[43] NOAA, *Chemical Datasheet: Ethanol,* (http://cameochemicals.noaa.gov/chemical/667).

[44] XCOR Aerospace Company, *"XR-3B4, 50 lbf N2O/alcohol NRO Engine"*, March 2011, (http://www.xcor.com/products).

[45] XCOR Aerospace Company, *"XR-4A3, 400lbf LOX/Alcohol EZ-Rocket Engine"*, March 2011, (http://www.xcor.com/products).

[46] Matweb Material Property Data, *Aluminum 1060 H12 Datasheet*, (http://www.matweb.com).

[47] Matweb Material Property Data, *Aluminum 5254 H32 Datasheet*, (http://www.matweb.com).

[48] Matweb Material Property Data, *AK Steel 304L Datasheet*, (http://www.matweb.com).

[49] Matweb Material Property Data, *AK Steel 316L Datasheet*, (http://www.matweb.com).

[50] Matweb Material Property Data, *HDPE Blow Molding Grade Datasheet*, (http://www.matweb.com).

[51] Matweb Material Property Data, *DuPont PTFE 7A Datasheet*, (http://www.matweb.com).

[52] Matweb Material Property Data, *Daikin PCTFE Datasheet*, (http://www.matweb.com).

[53] Matweb Material Property Data, *Seals Eastern 7045 EPR Datasheet*, (http://www.matweb.com).

[54] Resins Online QC, *Aluminum Powder Safety Datasheet*, (http://www.resins-online.com), June 2011.

[55] Lenntech Water Treatment Solutions, *Aluminum datasheet*, June 2011, (http://www.lenntech.com/periodic/elements/al.htm).

[56] Lenntech Water Treatment Solutions, *Lithium datasheet*, June 2011, (http://www.lenntech.com/periodic/elements/li.htm).

[57] Lenntech Water Treatment Solutions, *Magnesium datasheet*, June 2011, (http://www.lenntech.com/periodic/elements/mg.htm).

[58] Lenntech Water Treatment Solutions, *Boron datasheet*, June 2011, (http://www.lenntech.com/periodic/elements/b.htm).

[59] Natan, B. and Rahimi, S.: *The Status of Gel Propellant in the Year 2000*, *Combustion of Energetic Materials*, Kuo, K.K. E DeLuca, L., edistors, Begel House, Boca Raton, 2001.

[60] Luca, S.: *B.Sc. thesis - Impiego di propellenti densificati storable per un piccolo lanciatore*, Facoltà di Ingegneria, Università di Roma "La Sapienza", 2008.

APPENDIX

SELECTED PROPELLANTS HANDLING HAZARDS AND SAFETY PROCEDURES

In this appendix only a brief description of the hazards and safety measures that should be carried out when manipulating the selected propellants is intended. For a more detailed description of the handling equipments, clothes and suggested procedures it is strongly recommended that the safety datasheet of each substance be read. It is observed that since the first aid measures are very similar in all cases, an additional feature is obtained from the selected substances. The equipment needed to handle and to counter eventual hazardous exposures is reduced to common parts thus reducing operatives cost.

A.1.- Hydrogen peroxide

There are four types of hazards relates to the hydrogen peroxide handling. In this appendix a more detailed description of such risks is made, including some basic guidelines to properly handle this substance. The first hazard type associated to this oxidizer are the inhalation of its vapors, which cause irritation of the respiratory tract (from the nose to throat) and, in some cases, sore throat, nosebleeds and suffocation. If this type of exposition is prolonged or repeated in time there are chronic bronchitis risks. More severe consequences of exposure to inhalation include pulmonary edema. The casualty should be moved to fresh air and kept at rest, for more detailed guidelines in first aids refer to [22]. If high concentrations of hydrogen peroxide are handled, air respirator masks must be supplied to cover completely the face, to prevent vapors inhalation.

The second way of hazard exposure to hydrogen peroxide is the direct eyes contact. It carries severe eye irritation, watering, redness and swelling of the eyelids. In the most severe cases there are risk of permanent eye lesions and blindness. Such damages can be delayed and the ulcerations do not appear until a few days later [22]. The first aids associated to this exposure type must include thoroughly wash with abundant water for a least 15 minutes. To prevent this type of exposure it should wear protective goggles in the hazard zone.

The other way of hazard related with the contact is the direct skin contact. In this case, skin burns of diverse degrees may occur. If the exposure is mild, some skin itching and bleaching may occur but the effects fadeout after a few hours. This type of exposure typically happens when the clothes are wet with the hydrogen peroxide solution. The first thing to do is remove the wet clothing and then wash the affected skin area with abundant running water. The prevention of direct contact is carried out wearing gloves of a suitable material like PVC. If also there are splashing risks in the working zone, then chemical resistant clothes and boots should be used.

Finally, the fourth type of hazard exposure to the hydrogen peroxide is the ingestion. This is the most severe form of exposure. The symptoms may include paleness and severe irritation of the digestive tract. There are risk of burn and perforation of the gastrointestinal track (ulcers). Other symptoms are stomach bloating, nausea, belching and bloody vomiting. The first aid includes in all case immediately go to the hospital. If the subject is conscious immediately rinse the mouth with water and drink large amount of water to dilute the stomach content, do not induce vomiting. If the subject is unconscious, never give anything by mouth and lay the subject to their left side.

A thoroughly description of the safety equipment and procedures that should be taken, when handling hydrogen peroxide, are made in [22]. All places where the hydrogen peroxide is handled must be equipped with safety systems as the mentioned below. Showers and eyewash stations must be installed nearby the handling zone to perform the first aid. Also, hoses and water sources should be placed to provide high volume of water to flush hydrogen peroxide spills.

Although hydrogen peroxide is a non flammable substance it may reacts spontaneously when is in contact with some substances. As such reaction release oxygen, it further may support the combustion of other chemical compounds. Therefore, particularly care must be taken when handling it, especially in this work, where its will be handled together with the easily flammable kerosene. The spills of this oxidizer may be fought by washing with abundant water since hydrogen peroxide is soluble in it. As a prevention measure, all the unneeded personnel should be evacuated from the affected area and the staff devoted to contain the spill should use respiratory mask.

A.2.- Ammonium Nitrate

This substance is not very toxic or dangerous but some risks related with it handling should be known. Here a brief description is addressed and it is recommended that, if more detailed information is needed, the reader refers to the material safety datasheet [29]. The first aid that must be imparted if inhalation occurs includes removing the affected personnel to a fresh air area and get medical attention if respiratory difficulties are presented. The ingestion of this chemical may causes weakness, vomiting, abdominal pain, bloody diarrhea and even convulsions. In small doses, chronic exposure to ammonium nitrate may cause weakness, depression, headache and mental impairment. In this case, as a first aid measure, the affected personnel must ingest large amounts of water. Do not induce vomiting and, in all cases, give medical attention to the casualty. The contact with the skin produces irritation with redness and itching. Also redness and irritation may happen when this substance is in contact with the eyes. In case of direct contact, remove any contaminated clothe and wash with abundant water.

As ammonium nitrate is a strong oxidizer its reaction with reducing agents may cause explosion or fire risks. Furthermore, it can support the combustion in an existing fire. Since ammonium nitrate is water soluble, it may be employed to fight fire. Such kind of fires should be extinguished using an adequate media to combating the surrounding fire cause.

A.3.- Kerosene

The four mechanisms of hazard contact that are mentioned for hydrogen peroxide also apply to this fuel. The first way, vapors inhalation, may cause irritation on the respiratory tract, nausea and even loss of coordination and disorientation, as explained in [36]. Special care must be taken in closed or poorly ventilated spaces. As a first aid measure, the casualty must be removed to a place with fresh air. If breathing is difficult, qualified personnel may administer oxygen and immediately give medical attention to the victim [36].

Unlike the oxidizer case, this fuel presents not so severe consequences if is in direct skin contact. However, if the exposure is prolonged, for example by wearing wetted clothes, may cause more severe irritation, redness and swelling. In the case of chronic exposures to this fuel, the effect over the skin may be aggravated due to its irritating property. Almost he same effects are observed when eyes direct contact. The first aid measures to take in relation to direct skin contact include wash the affected zone with plenty water and soap. In the case where dressed cloths are contaminated is mandatory to remove it. If the eyes are affected, it is recommended that the same measures as with the hydrogen peroxide case are taken.

The most severe intoxication way with this fuel is through ingestion. The most commonly found effect of such intoxication includes abdominal discomfort and pain, nausea and diarrhea. Additionally, if inhalation occurs while swallowing, there exists the possibility of lung damage. The same may occur when induced vomiting and therefore it is very important appeal to other evacuation methods if required. Such procedures must be taken by trained personnel and hence it is recommended that the casualty be carried to a hospital.

This substance is highly flammable and therefore special attention must be placed while handling it. In case of fire using water fog, dry powder, foam and carbon dioxide is possible, as recommended in [36]. Water may be used to cool fire exposed containers and other hot structures. Another hazard associated to the manipulation of this fuel is the spills risk. In these cases, it is important to remove any source of sparks as any electric or electronic system or combustion machine. Also is necessary ventilating the affected area and evacuating all the unneeded personnel. Avoid breathing its toxic vapor, to do this it is recommended using air breathing mask. Remove the spill by employing an adequate inner absorbent.

A.4.- Aluminum powder

Handling aluminum powder is not so hazardous if a few measures are taken. Again, the same four mechanism of contact risk are present, here a brief description of the handling hazards and first aids is made, for more detailed information its safety datasheet may be consulted [54]. In case of skin contact, wash off with plenty water and soap and also remove all the contaminated clothes. If contact with the eyes take place, these must be thoroughly washed with water for at least 15 minutes. In case of inhalation, the casualty must be moved to a fresh air zone and, as the powder may cause lung damage, should consult a physician immediately. The most serious risk when handling this powder is that it is a highly flammable substance and particularly, in contact with water, very flammable gases are released. Therefore, if a fire break outs, the use of water jets is forbidden. Only dry sand or special powder against metal fires must be employed and so, there is important to have safety equipments in the facilities. As a prevention measure to counter leaks, it is necessary to keep away any source of ignition and ventilate the area, avoiding the dust formation. The affected area should be promptly cleaned by using a vacuum cleaner or a scoop.

REPORT Nº 3

SIZING AND DESIGN OF A LIQUID PROPELLANTS ROCKET ENGINE

Pablo RACHOV

LABORATORIO DE CONTROL DE ACCIONAMIENTOS, TRACCIÓN Y POTENCIA
(LABCATYP)
Departamento de Electrónica
Facultad de Ingeniería
UNIVERSIDAD DE BUENOS AIRES

Directors:
        Prof. Hernán TACCA, University of Buenos Aires, Argentine
        Prof. Diego LENTINI, University of Roma "La Sapienza", Italy

Buenos Aires, December of 2011.

CONTENTS

I.   INTRODUCTION

1.1. Liquid Propellant Rocket Engine Types

Any type of rocket engine operates generating thrust from the momentum exchange between the engine and the propellant mass expulsed by itself [1]. In a liquid propellant rocket engine, the ejected mass is the product of the chemical reaction, that take place into the combustion chamber, from one or more propellants. Typically, such chemical reaction may involve either the decomposition of a single substance (called a *monopropellant* engine) or the combustion of a fuel and an oxidizer (called a *bipropellant* engine). The rocket engine upon which this work is developed is from the second type. Regarding to the liquid propellants rocket engines, they may be classified according to the method from which the propellants are injected in the combustion chamber. From such classification the following feed system are often employed:

Pressurized gas propellant feed system: In this engines type, the propellant is expelled from tank due to the high tank pressure. This is achieved by the introduction of a high pressure gas inside the propellant tank. Thereby, the propellant tanks are part of the feed system. The Figure 1 shows a simplified schematic diagram of this feed system where the major components are denoted. With the tankage* inclusion, it can be seen further the great number of valves necessaries to control the engine. Such valves are also necessary in the pumping feed system described below. The pressurized gas feed system is employed mainly in low thrust engines, like those used to control the altitude in space vehicles [2]. This feed approach is the simplest and therefore the most reliable. A notable advantage is the restart ability during the mission. The most important disadvantage is its high inert mass when compared with other feed systems.
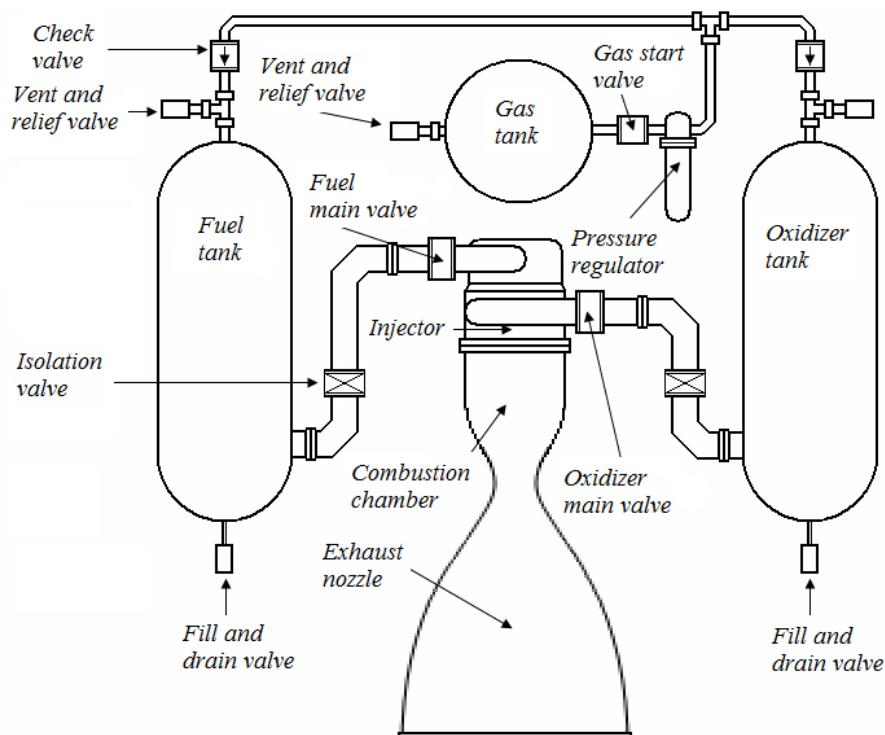
Figure 1: Scheme of a engine with pressurized gas propellant feed system.

---

* It refers to the capacity or contents of all the rocket's tanks.

Pumping propellant feed system: With this system, the propellants are extracted from the tanks using pumps. Thereby, the propellants are stored to a notable lower pressure. In the Figure 2, a simplified scheme of an engine which employs this feed system is presented. This feed approach is employed mainly where both, large propellant mass and high thrust, are required [1]. It is a considerable more complex method, as it involves a great number of mechanical parts. In contrast, the total inert mass is much less than in the previously described feed system. Typically, in this engine type, the pumps are driven by one or more turbines which are powered from a portion of the same propellants that feeds the engine. In this work, the development of an alternative approach, based on employment of electrical pumps instead turbo-pumps, is proposed.
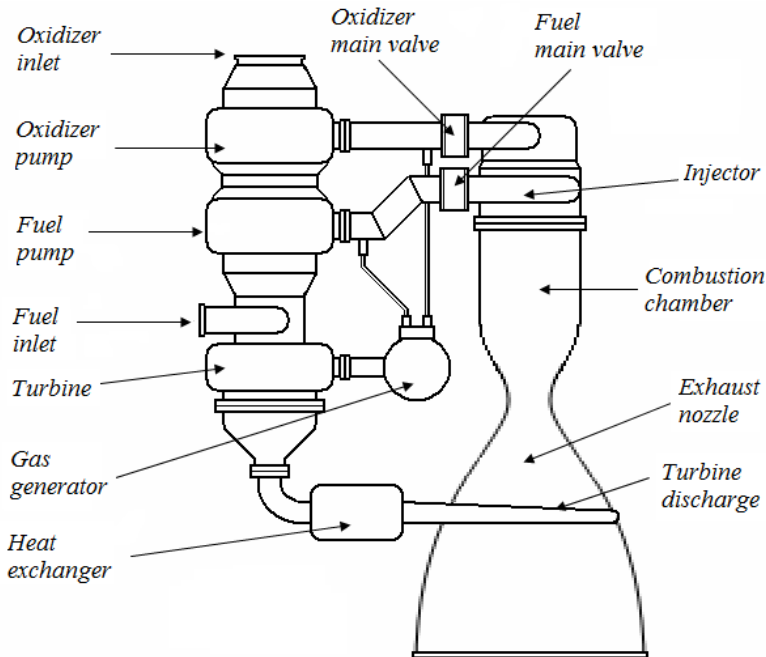
Figure 2: Scheme of an engine with turbopump propellant feed system.

1.2. Pumping fed rocket engine general description

A liquid propellant rocket engine has several subsystems that play specifics functions before and during the engine operation. To understand with more detail the operation of such engine type, in this subsection, a brief description of the systems that compose the rocket engine and the functions that they carry out are presented.

1.2.1. Propellant storage

In a liquid propellant rocket engine, the propellants are stored into solid tanks. These tanks provides to the propellants chemical and mechanical insulation from the outside. Additionally, if cryogenics propellants are employed, the tanks also must provide thermal insulation. The same kind of insulation is necessary in upper stages, where the ambient temperature is below the propellant freezing point. In such cases, an additional heating system is included to the tanks. The materials that they are build must to be chemically compatible with the substances that they contain. Such compatibility means that neither the propellant nor the tank can be degraded by the chemical interaction between them.

1.2.2. Tanks pressurization

In a rocket engine always it is necessary pressurizing the propellants tanks. Even with a pumping feed system keeping a somewhat elevated tank pressure is convenient. Therewith, the propellants are more easily expelled from the tanks even when they are almost empty, which often happens nearly the burnout. Moreover, ensuring an appropriated pressure in the pumps inlet is necessary to avoid cavitation.

1.2.3. Propellants feeding

The feeding system is designed to carry the stored propellants from the tanks to the main combustion chamber at a pressure and flow rate convenient for achieving the optimum engine operation. In a pumping feed system there are at least three principal components that may be distinguished: the propellant pumps, the pump drive device and the pumping system power source.

The propellant pumps often employed in rocket engines are either centrifugal or axial type. Those pumps have several advantages that are exploited and drawbacks that must be resolved during the development phase. When comparing it with other pumps types, the centrifugal and axial pumps are lighter and compact, reaches high efficiency values at high rotational speed and also, it efficiency increased in function of the propellant density. However, the design of such pumps is more expensive in both, time and technical resources. The pump efficiency drop significantly when the rotational speed decreases, which make it impractical to throttling the engine thrust through by adjusting the pump speed. The great mechanical stress generated by the high rotational speed implies that expensive materials and manufacture processes ought to be used. If low density propellants are employed, hydrogen is a good example of this, the pump efficiency drops considerably.

Among the pump drive devices the most widely employed in liquid propellants rocket engines is the turbine. It is elected due to its compact size and low weight. In addition, it reaches high efficiency at high rotational speed, which is convenient if it is coupled to an axial or centrifugal pump. Moreover, its use is encouraged because any rocket engine has a high energy gas source to drive the turbine. Between the disadvantages may be mentioned that, as in the case of the pumps, the high rotational speed has the same negative impact in the deployment resources. Additionally, the gases high temperature complicates the turbine design and makes prohibitive employing some cheap materials. If the turbine and pump are mounted over the same case and shaft, flux insulation problems occur, making the development more complex. In addition, if cryogenics propellants are employed, the temperature gradient in the turbo-pump assembly is so big that the design is complicated even more.

The employed energy source depends on the selected engine cycle. It can be either the high temperature gases obtained from the combustion of the stored propellant, the flux of one of them heated by the main combustion chamber or the decomposition of one of the propellant, typically, the oxidizer.

1.2.4. Thrust chamber

This system function is to convert the thermochemical energy that the propellants contain in kinetic energy, and hence, in thrust. The thrust chamber is composed by the injection head, the combustion chamber and the engine nozzle.

The injection head have the functions of introducing the propellants in the combustion chamber, atomizing, vaporizing and spreading the mixture so that the proper combustion occurs. An injection head is composed by two inlet ports, one for the fuel and other for the oxidizer, a face filled with a set of output holes (injection elements) which is disposed toward the combustion chamber inside and a number of internal ducts which connect both parts. The details

of the most commonly employed injector types and its operation can be found in [1], [2] and [3]. In this work, a simple construction and design injector head will be employed from which a more detailed description can be found in the correspondent section.

The combustion chamber is the enclosure where the chemical reaction happens. The combustion chamber sizing is critical to ensure a proper engine operation. Such chamber should be large enough to maintain optimum combustion efficiency but not too much because the dynamics losses reduce the efficiency and the mass and size increases overmuch. Typically, a cooling system is necessary to avoid material failures due to the thermal stress that the combustion chamber must withstand as long as the engine is operated.

In the exhaust nozzle the combustion gases are expanded, reaching high velocities and reducing its pressure. There exist several nozzle types and the selection of either type always involves a compromise between the performance and the design complexity. In some cases, the nozzles can include a cooling system as the employed in the combustion chambers.

1.2.5 Ignition system

When the propellants employed in a rocket engine are non-hypergolic, it is necessary disposing of an ignition system. These systems are composed by an igniter, an ignition detection device and an igniter actuator. The often employed igniters include pyrotechnical igniter devices, spark plugs and spark torch igniters. Among the detection devices it can be mentioned the pyrometers, the pressure sensing devices and the optical detection devices. A detailed description of such devices can be found in [3].

1.2.6. Cooling system

The main function of this system is to maintain the combustion chamber temperature in a range that ensures an engine operation without excessive thermal stress. For short time combustion periods a simple heat sink approach may be employed, where the heat is absorbed by the chamber walls that acts as heat sink [3]. However, if longer combustion times are required, a more complex steady state cooling approach must be considered. Several methods are commonly used in liquid propellants rocket engines, among the most denotable are: regenerative cooling, ablative cooling, radiation cooling and film cooling. If a regenerative cooling system is considered, a secondary function of such system may be used. The coolant propellant may be further employed to drive the turbopumps and so, increasing the overall engine efficiency. It must to be denoted that such improvement at the expense of increasing also the hardware complexity.

1.2.7. Electronics control system

The overall engine behavior is sensed and controlled by a complex electronics system. During the start and stop transients an events set must be occur in a stringent sequence. These events can be a valve opening or closing, the heating of some component over a given temperature or the achieving the speed regimen of the turbine [3]. The sequence and the time between events ought to be carefully executed.

Another main function that the electronic provides is the fly control system. Thereby, the thrust magnitude and direction may be set up as the vehicle performs its mission. At the time, the electronic provides communication with the command location to monitor the engine operation.

The electronics allows implementing safety mechanisms to avoid or minimizing the consequences of possible failures that may occur during the engine operation. Emergency shutdown system and component insulation from propellant flow may be included as engine safety method.

Finally, the electronic allows the data recollection during the engine tests and even during the vehicle fly. These recollected data can be converted into experience and thus be applied to the development of new engines or the improvement of the existing ones.

1.2.8. Pipes and Valves

These devices are present in all the rocket engine. The valves can be classified according to its function in: propellants control valves, drain valves, filling valves, vent valves and safety valves [2]. As a description of them all is beyond the scope of this report, only the types employed in this project are described in the corresponding section.

On the other hand, the pipes lead the engine fluids (i.e. propellants and pressurizing gas) between the different engine components. As in the case of the propellant tanks, they must be chemically compatible with the carried substances and must be properly sized to withstand both the mechanical stress and the temperatures of a typical operation.

1.2.9. Structural mountings

The engine has several mounting points that allow fixing it to the vehicle structure. The design of such fixing elements should include factors like the vibrations, the acceleration loads and the extreme operation temperatures. The mounting must hold up all the thrust produced by the engine while remains a weight as lower as possible. In some cases, hydraulic actuators are included to the mounting, thus allowing the control of the direction of thrust [3].

II.   PROJECT OBJETIVES

To understand the decisions adopted during the course of the project, before it is necessary to know the project objectives and the scope. The same are briefly listed below:

- Study the application possibilities of liquid propellants rocket engine feed systems based on electric pumps.
- Investigate the viability of employing volume displacement pumps in feed systems.
- Study the probable combustion instabilities product of flow and pressure fluctuations in the pumps outlet.
- Investigate the possibility of a pressure drop minimization across the injector plate.
- Study possible alternatives of Low Cost Access to Space.

To carry out these objectives, assembling a test bench for a low thrust rocket engine is intended. Such test bench will employ a feed system having two volume displacement pumps coupled to an electric motor. The whole test bench will be electronically controlled. Therefore, all the data obtained from each test will be stored for it subsequent analysis. At this point, taking into account the proposed goals, the rocket engine and test bench design begins.

III.   ROCKET ENGINE REQUIREMENTS

Before starting with the design of each test bench component, it is mandatory to give general design parameters. Therefore, the first step in the engine design should be establishing the requirements and defining the global specifications. Then, the next step is to complete the preliminary design and finally, the design of each part can be addressed.

3.1. Engine Requirements

At the beginning of any engineering project is important giving a conceptual framework to the whole development. The diverse necessities to satisfy by the project are documented in the requirements. Therefore, the initial requirements set bring the context and give a guidance to take the decisions during the whole project development. While the design progresses, the several solutions that are studied must be contrasted by the requirements. It allows deciding if the objectives are satisfied by such solutions or it is necessary another iteration in the design to find a proper solution. Nevertheless, these requirements should not be considered as fixed and inflexible. To get started and with the purpose of ordering ideas, the total requirements list is classified as follows:

- Cost.
- Envelope[†] and mass.
- Safety and reliability.
- Performance.
- Functionality and operability.
- Maintenance.

This classification is arbitrary and serves as guidance to elaborate the requirements. As discussed later in this report, some requirements can be located in more than one of the listed categories. In the next subsections the requirements for this project are treated.

3.1.1. Performance requirements

In this project, the performance requirements are conditioned by other requirements (i.e. cost and safety). A high performance and large size engine is not required, but rather, it is necessary to achieve the objectives while maintaining the cost as low as possible. Thereby, in the design of the engine components employing exotics materials is avoided. Moreover, utilizing complex systems is prohibitive, such as a regenerative cooling system in the thrust chamber.

Here, it can be seen an example of how a performance design decision impacts in other requirement category. The thrust level and chamber pressure requirements define the size and weight of the combustion chamber and thus, the overall engine envelope and mass. On one hand, a rocket engine with a too low thrust does not probe that the proposed fed system works on an engine aimed to propel a vehicle. On the other hand, if the thrust is excessively large, all the systems in the rocket engine will be also too. Particularly, the batteries will be too large (which are expensive, heavies and difficult to import). An adequate thrust level estimation is around the 500N, in this range the required pumping power matches with the available commercial batteries. However, in this work, the final exact thrust magnitude will be determined by other design parameter, the propellant flow rate.

The thrust chamber pressure is another important design parameter. In a general sense, given a performance in terms of specific impulse, the selection of a combustion chamber pressure magnitude higher or lower implies a compromise between the combustion chamber size and the pumping system size. In this project, employing a very low chamber pressure means using electric motors with very low power densities. Furthermore, as was denoted in the first report, the lower the chamber pressure, the smaller the advantage of the proposed feed system over the pressurized gas feed system. Meanwhile, too high pressures are very difficult to handle using commercial components, and therefore, special parts ought to be manufacture increasing the engine total cost. Further, if an explosion happens during a test, with high

---

[†] It refers to a roughly estimation of the engine dimensions as is explained in [3].

pressures the consequences could be more dangerous. Having into account the preceding arguments and the available commercials pumps, a chamber pressure range of 1 MPa to 1.5 MPa is suggested.

The propellant flow rate that can be employed in the rocket engine is limited by the available commercial pumps. The smallest models are available from a determined flow rate that is a function of the pump rotational speed [5]. Hence, the minimum fuel flow rate is established and, through the definition of the propellant mixture ratio, the oxidizer pump size is determined. By relieving the commercial pumps, the propellant flow rate is estimated around the 20 l/min. Then the exact value is determined, after the propellant mixture ratio adoption.

The engine run duration, often named as engine burning time defines a number of issues in most of the engine systems, as example may be mentioned the cooling system approach and the propellant tanks size. On the one hand, the burning time should be long enough for testing operation cycles proper of a rocket engine intended to vehicle propulsion. However, excessive long run durations might pose insolvable cooling requirements. First, a heat sink cooling system approach is prohibitive forcing to rely on the development of a more complex cooling system. Further, the electric feed system becomes more expensive due to the bigger batteries required. For a future flight demonstrator, a burning time of around 12 s is considered adequate and thus, the fire tests in the test bench will be of approximately such duration. Therefore, a running time values range of 10 s to 20 s is considered. By decreasing the burning time the amount of stored propellant in the tanks is also reduced, which is convenient from the safety point of view.

Finally, as noted in the previous report, the propellant selection deserves a separated discussion. Herein, only it is remembered that, for the testing engine, a solution of PERSOL 1 and kerosene will be employed, having into account the possibility of a future study over some densified solutions based on these propellants.

3.1.2. Cost requirements

This category is one of the most important either in this work or in any other engineering project. Particularly, the cost requirement is directly associated with the project objective of studying possible alternatives of *Low Cost Space Access*. Therefore, using any expensive component or material in the manufacture of whichever engine part is unacceptable. The availability plays a key role in the parts cost and thereby, while it may be possible all the engine parts will be acquired locally.

3.1.3. Safety requirements

The safety requirements are not only limited to the tests stage but also include the initial engine assembly stage and the storage of both the hardware and the chemical substances. Intermediate tests are necessary to validate the functionality of every part of each engine system. During these tests the safety must be taken as seriously as in any final test. The first engine tests will be carried out by replacing the propellants with some non reactive substance, such water. These tests are denominated *cold tests* due to the fact that there is no combustion. Such tests are necessary to evaluating, inter alia, the absence of leakage in the fed lines, the correct operation of injectors and the pressure and flow rate levels in each point of the fed system. During these tests exists the risk of severe failures, as is the case of a short circuit failure due to a fluid spill. When the cold tests phase is successfully completed starts the next tests stage denominated *hot tests*. In this phase the propellants are employed, and hence, the problems associated to the high temperatures and the presence of combustion products in the ambient appears. During this testing phase there exist risks of catastrophic failure that may finish in a fire or explosion. Consequently, the facilities where the tests will be concreted must ensure the personnel safety above eventually accidents. The accidents hazards are also present when the propellants are handled. For this reason, all the recommended safety equipment and safety procedures must be

employed each time it is handle. Further, a precise storage procedure ought to be followed to ensure the safety while the engine is stored.

3.1.4. Weight and envelope requirements

Whatever be the rocket engine, the dry weight is one of the most stringent requirements, as the engine is intended to be installed in a flying vehicle. However, as the engine of this work is not aimed to fly, it will be fixed in a test bench. Alongside this, the low cost requirement discards most lightweight alloys. Despite these facts, the small engine size makes easy handling the engine components.

Although the projected engine will has low thrust and hence, a bounded envelope, there exist some portability requirements that ought to be fulfilled. The test bench must be transported to a test facility when the testing phase begins. Thereby, there are two evident requirements. First, the overall test bench size might be kept to a transportable size. Also the weight must be restricted to a magnitude that allows moving it without recurring to additional machinery. Moreover, it can be envisage the option of disassembling and easily reassembling some engine parts to facilitate the carrying.

Table 1: Summary of project requirements.	
Performance requirements	Chamber pressure range: 1 MPa to 1.5MPa
	Burning time: 10s to 20s
	Thrust level: ~500N
	Propellant mass flow rate: ~20l/min
	Propellants: PERSOL 1 (oxidizer)
	Kerosene (fuel)
Cost requirements	Non expensive materials ought to be employed
	Commercial parts ought to be used
Safety requirements	Safety procedures must to be elaborated and respected at the intermediate component testing phase
	Safety procedures must to be elaborated and respected at the cold testing phase
	Safety procedures must to be elaborated and respected at the hot testing phase
	Safety procedures must to be elaborated and respected to storage the whole test bench
Weight and envelope requirements	The test bench ought to be easy to transport
	Each engine part ought to be easy to handle

IV. PRELIMINARY DESIGN

In the preliminary design phase fall all the decisions which define the general engine architecture and its performance. Therefore, at the end of this section, a general engine picture is proposed as input information for the following detailed design of each engine part.

A good preliminary design allows detecting design errors early, before the hardware be manufactured, in a way that the design cost in term of both, time and resources, decreases considerably. To achieve a good preliminary design the prior experience is a key concern and therefore, it will be considered by employing subsystems previously tested to advance quickly.

4.1. Engine System Configuration

The basic configuration of the projected engine is shown schematically in the Figure 3. There, the tanks are pressurized via a high pressure gas stored in a proper gas tank. The

pressurant gas fed to the propellants tank through a pressure regulator and an opening valve. The propellants pumps are coupled to the DC brushless motor through a reduction gears properly sized. In the scheme, also it can be seen the current inverter and the batteries pack. The thrust chamber has a pre-chamber to allows the oxidizer decomposition before it be introduced to the main combustion chamber together with the fuel. The electronic sensing and control lines allow the monitoring and data capturing while the test is running. The engine operator is interfaced to the hardware via a PC based computer program.
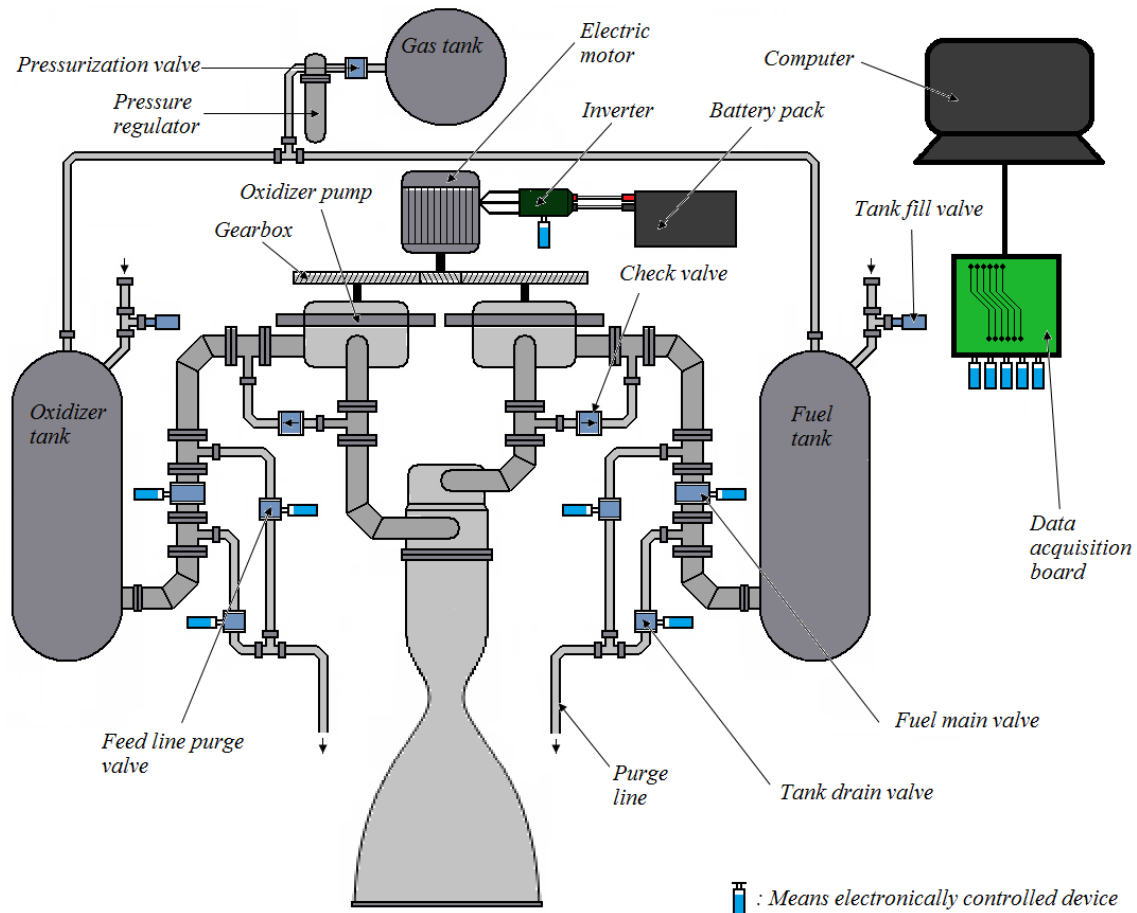
Figure 3: Scheme of the proposed test bench. Light blue lines denote the controlled devices. The sensors are omitted for simplicity.

The Figure 3 shows that both pumps are driven by a single electric motor. This design decision has the advantage of saving the cost of one electric motor. However, in this case, the oxidizer to fuel mixture ratio becomes fixed by the pump pumping characteristic and the gear ratio. Although this feature relieves some flexibility to the test bench limiting it to use optimally only the design selected propellants, it is thought that at this time and as a first trial, varying the propellant mixture ratio is not necessary to achieve the main goals of this project and then, the cost saving is prioritized.

At this point in the preliminary design a separated decomposition chamber is suggested but, it should be considered employing a decomposition chamber included in the same main combustion chamber volume. In the combustion chamber detailed design section the alternatives are evaluated.

Although in the shown scheme only a few control and monitoring lines are traced for the sake of simplicity, in the real test bench the number of variables to sensing and control are greater. Firstly, all the valves and the electric motor must to be controlled. As long as possible, the valves will be controlled manually simplifying the development and reducing the costs. The manually operated valves are those that ought to be actuated only when a test non critical phase is happens. Among the valves included in this category may be mentioned the gas start valve

and the propellants tanks filling valves, which are used in the initial test setup. Nevertheless, the remainder valves and the electric motor will be remotely controlled to ensure a safe operation. The electronic drive valves include the propellant main valves that are actuated at the start and end transient of the engine test running. Moreover, drain valves are foreseen to be used if a safe propellants tank emptying is necessary to abort a test. The Table 2 summarizes all the controlled devices considered to be part of the test bench.

Table 2: Summary of controlled devices.		
Device	*Function*	*Control type*
Electric motor	Drive the propellants pumps	Electronic
Oxidizer main valve	Open and close the main oxidizer line	Electronic
Fuel main valve	Open and close the main fuel line	Electronic
Check valves	Avoid pump overpressures	Automatic
Tanks drain valves	Evacuate the remaining propellants after burnout or in a emergency cutoff	Electronic
Tanks fill valves	Fill the tanks before the tests and	Manual
Pressurization valve	Pressurizes the propellant just before the test start	Manual

Table 3: Summary of monitored variables.		
Variable	*Monitoring device*	*Observations*
Engine thrust level	Load cell	Compression type with electric transducer
Combustion chamber pressure	Pressure transducer	Optionally an indirect method may be used
Injector head inlet pressure	Pressure transducer	Absolute pressure type with transducer
Propellants tanks pressure	Indirect measure	Via gas tank pressure regulator working pressure
Pumps rotational speed	Tachometer	Coupled to the motor shaft
Pump Torque	Dynamometer	Made using strain gauges
Required electric power	Indirect measure	Sensing simultaneously motor current and voltage
Propellants flow rate	Indirect measure	Via pump flow characterization and motor speed sensing
Thrust Chamber evacuated heat	Indirect measure	Through a calorimeter
Exhaust gas exit temperature	Thermocouple	Tentative measure, subject to technical viability

To get a complete picture of what happens during the test there are a number of variables to monitoring. All of the considered variables are listed in the Table 3. To monitoring the whole variables either sensing devices are needed, therefore, alongside to the monitored variable in Table 3 a sensing device is proposed. The magnitude of some variables can not be obtained directly from a measure and thus an indirect calculus method should be adopted. The

detailed description of the approach that will be employed to sensing each variable is done in the corresponding detailed design Subsection. At this point it is evident that the hardware complexity has been quite increased.

4.2. Thrust chamber

As stated in the Section 1, the thrust chamber is a system constituted by three major components: the injector head, the combustion chamber and the exhaust nozzle. In this preliminary design phase some decision over its architecture are taken.

Starting by the nozzle, the several shapes are well studied in the bibliography [1, 2, 3]. The Table 4 lists the often used nozzle shapes and its most notable features. As was denoted above, choosing either nozzle shape involves a tradeoff between nozzle performance and construction simplicity. The four last nozzle types shown in Table 4 (concepts "d" to "g") have some altitude compensation, useful attribute to keep the nozzle performance while the vehicle is ascending. The projected engine will have to operate at sea level and thus, such altitude compensation is not needed. As in this work a high performance engine is not aimed, and instead a low development cost is a requirement, employing a conical nozzle is preferred.

| Table 4: Summary of candidate nozzle shapes concepts.			
Nozzle shape	*Possible Drawback*	*Outstanding features*	*Conceptual Scheme*
(a) Conical Nozzle	•Lower performance	•Simplest production •Widely used in small rockets	
(b) Bell Nozzle (Full length)	•Complex construction	•Good efficiency •No altitude compensation •Large length	
(c) Shortened Bell Nozzle	•Complex construction	•Good efficiency •No altitude compensation •Compact design	
(d) Dual Bell Nozzle	•Complex cooling •Complex construction •Large envelope	•Altitude compensation •Similar performance than multi-position nozzle but lighter	
(e) Expansion – Deflection Nozzle	•Complex cooling •Complex construction	•Good altitude compensation •Short length	
(f) Multi-position Nozzle	•High mass •Complex construction	•Altitude •compensation	
(g) Aerospike	•High mass •Complex cooling •Large diameter	•Good altitude compensation •Short length	
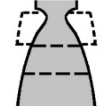
Notes: The data compiled in this table was extracted from [1, 2, 3].

In some cases, the combustion temperature is extremely high and hence, the exhaust gas temperature is consequently high too. Such conditions force to the use of a nozzle cooling system similar to the employed in the combustion chamber. As the engine running time is short and the estimated combustion temperature is relatively low (see Report 2) a heat sink cooling approach is adopted for the nozzle.

Regarding to the combustion chamber, the selection of materials and cooling approach largely defines the durability of its structure. In this project a reusable rocket engine is wanted, allowing a large number of test repetition and thus, the accumulated engine running time and the number of thermal cycles will be large. The approach adopted to deal with such requirements involves to minimize the engine running time and to extend the interval between tests quite enough so that set the thermal stress to be acceptable. Thereby it is expected that the durability requirements will be fulfill employing a low cost steel alloy in the manufacture of the whole thrust chamber. With respect to the combustion chamber shape, the bibliography proposes three basic configurations: the spherical, the near spherical and the cylindrical chamber [3]. From these options, the cylindrical thrust chamber is selected because it is a very proven design and moreover, it is the easiest to manufacture.

In the previous report, it was stated that the oxidizer decomposition will be carried out through a permanganate layer coating the chamber wall. Hence, in the combustion chamber sizing it should be taken into account the extra diameter needed to accommodate such layer. The size of the combustion chamber is estimated in the detailed design section.

Table 5: Summary of candidate injection elements concepts.

Injection scheme	Possible Drawback	Outstanding features	Conceptual Scheme
(a) Spray Former	•Triggered combustion instabilities or poor combustion if is not well designed	•Good combustion •Simple manufacture	
(b) Shower Head	•Poor combustion efficiency	•Very simple design	
(c) Like impinging doublet	•Complex manufacture •Poor combustion efficiency if not well constructed	•Good combustion efficiency	
(d) Pintle injector	•Complex design •Complex manufacture	•Good combustion •Throttling capability	
(e) Coaxial Element	•Large flow velocity difference needed between fuel and oxidizer to achieve good combustion	•Simple design • Good combustion stability	
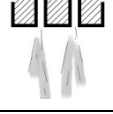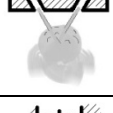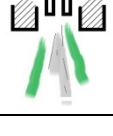
Notes: The data compiled in this table was extracted from [1, 2, 3].

A particularly stuff must to be attended with respect to the injector head design. As hydrogen peroxide will be employed, which will be previously decomposed, the injector design should embrace the fact that the fuel must to be injected into a hot steam flow. Consequently, one of the injection elements configurations proposed in the Table 5 and described in the bibliography [1, 2, 3] can be chosen, but a liquid-liquid injection scheme using unlike impinging injectors should no be selected.

From the several concept displayed in Table 5, employing a spray injection is suggested as the best choice. Such decision is based on the fact that available commercial off the shelf industrial spray injectors may be purchased, saving time and resources in injector design. The use of any other injection element concepts implies facing some design or manufacture problems requiring testing several prototypes before achieving a satisfactory quality injector.

There are not commercially available models for the other injection schema.

4.3. Engine Pressure levels

Devising the pressure distribution over the engine is one of the most critical issues in rocket engine design. Once established the combustion chamber pressure and the propellant flow rate, the pressure distribution allows sizing the tankage and feed system. Generally, the engine pressures are determined from the chamber to the tanks. In a rocket engine development oriented to propel a space vehicle, the typical approach would start by setting the engine thrust needed to accomplish the mission requirements. Then, with the selected propellants, it follows estimating a chamber pressure that gives a reasonable relationship among propellant flow rate and throat area (thrust chamber size). Herein this method should be reformulated as the chamber pressure value is strongly limited by the arguments exposed in the performance requirement discussion, thus turning such parameter so much restrictive than the thrust requirement. The Figure 4 (adapted from [1]) depicts schematically the pressure distribution for a rocket engine with pumping feed system (only one feed line shown for simplicity). This scheme, although not represent a closely real pressure distribution, lets denote the several points where define the pressure is a chief issue.
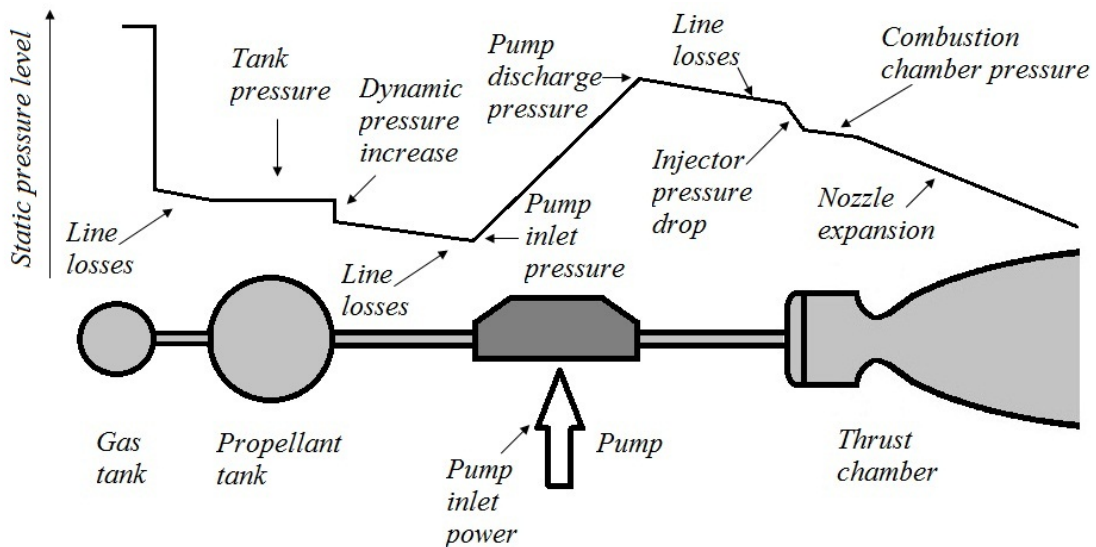

Figure 4: Scheme of pressure distribution in a pumping fed rocket engine.

In this work the pressure distribution designation start with the definition of the combustion chamber pressure. As a high value allows, among other advantages reducing the engine size, from the range suggested in the requirements the upper boundary of 1.5 MPa is adopted.

At this point the pressure at the thrust chamber inlet can be estimated by only adopting a feasible value of injector pressure drop. This pressure drop is necessary to isolate the chamber pressure from the feed system thus decreasing the probability of trigger combustion instabilities and oscillation due to propellant flow fluctuations [1]. The range of admissible values for injector pressure drop should be about 20% to 30% of chamber pressure for unthrottled and throttled engines respectively. As in this work the employed pumps show some flow fluctuation in normal operation, a conservative assumption of 30% of combustion chamber pressure is made. Thereby a value of 450 kPa is fixed for this parameter and the thrust chamber inlet pressure yields 1.95 MPa.

Whichever pressure drop in the feed lines is an unwanted effect. From a qualitative point of view, the shorter the feed line, the lower the pressure loss, so feed lines as short as possible are desirable. However, in a practical design, the lower length limit will be established by the way in which the hardware will be disposed. In this section a computed value is not needed and instead a conservative value of 50 kPa is adopted, according the proposed limits in [1].

The discussion about pump pressure is delayed as it is required known first the propellant tank pressure. The propellant tank mass is increased as its pressure increases and so, a tank pressure not excessively large is preferred. On the other hand, if the tank pressure is set too low it may be cavitation problems at the pump inlet. Meanwhile, although the industrial pumps that will be employed operate over a wide pressure range (typically from 100 kPa to 20 MPa) the industrial seal usually supports as much as 200 kPa before present a leak. Accordingly a value of 200 kPa is suggested, expecting that such value ensures enough pressure at the pump inlet.

Another issue about tank pressure to take into account is that inasmuch the propellant leaves the tank its velocity raises up to the nominal flow velocity. As the dynamic pressure increases, the static pressure must decreases to maintain the total pressure constant [1]. Therefore, a pressure drop occurs in the pipe line near to the tanks exit. To account it the Bernoulli's equation can be employed:

$$\Delta p = \frac{1}{2} \rho_p v_p^2 \qquad \textbf{(3.2.1)}$$

where, Δp: Dynamic pressure drop (Pa).
   ρ_p: Propellant density (kg/m^3).
   v_p: Propellant flow velocity (m/s).

The flow velocity estimation may be quite tricky and hence adopting a typical value of 10 m/s is preferred (as recommended in [1]). By applying the expression 3.2.1 a dynamic pressure drop of 41 kPa for the fuel and 65 kPa for the oxidizer are adopted.

Regarding to the pumps the pressure raise alongside with the propellant flow rate will define the required pumping power. As a result, both the pump discharge pressure and the pump inlet pressure must to be determined. The first is defined by the sum of the pressures adopted hitherto. Consequently, a pump discharge pressure of 2 MPa is adopted to account the possible pressure losses in the pipeline. The pump inlet pressure is estimated as the propellant tank pressure less the pressure drops due to dynamic pressure raise and pipe line losses. Therefore, an inlet pressure of about 110 kPa and 90 kPa are expected in the fuel and oxidizer pump respectively. For the sake of simplicity a lower boundary value of 50 kPa is assumed.

Finally, a discussion about the pressurant system is addressed. In this project the used pressurant will be air from the ambience pressurized via a compressor with a pressure regulator. (Thereby, the actual value of gas tank pressure is not needed as only is necessary obtaining a pressure of at least 200 kPa at the pressure regulator output). The flow velocity and the density of the pressurized gas are expected to be low and thus the pressure loss in the line from the gas tank to the propellant tank is neglected.

Table 6: Summary of estimated pressure distribution.	
Engine device pressure	*Value [MPa]*
Combustion chamber pressure	1.5
Thrust chamber inlet pressure	1.95
Pump discharge pressure	2
Pump inlet pressure	0.05
Propellant tank pressure	0.2
Pressure regulator pressure	0.2

4.4. Rocket engine performance characterization

In the Report 2 and in the subsection 3.1 some of the most important engine performance parameters are presented. Following with the preliminary design it is needed to

define a performance profile for the projected rocket engine as it allows further sizing each engine subsystem.

It should be started by defining the mixture ratio at which the engine will operate. Herein, the rocket performance is analyzed using the specific impulse as chief figure of merit. Hence, the selected propellant mixture ratio should be which maximizes the specific impulse for the selected propellants combination. The software employed to perform the thermochemical calculus in Report 2 also outputs complete performance estimation, including data which is useful herein. The Table 7 summarizes the most relevant data outputted by the calculus software that serves as starting point for the characterization intended here. The complete output is annexed to this report in the Appendix 1, making it available to the reader.

Table 7: Summary of chief performance parameters.

Propellant specification

Component	Density [kg/m³]	Temperature [K]	Mass fraction	Molar fraction
RP-1	810	298.1	0.0786391	0.1744734
PERSOL 1	1388	298.1	0.9213609	0.8255266
O/F	11.7163171 (optimum performance)			

Thermodynamic properties

Parameter	Injector	Nozzle Inlet	Nozzle Throat	Nozzle Exit	Unit
Pressure	1.5000	1.5000	0.8536	0.1013	MPa
Temperature	2232.3118	2232.3118	2062.5026	1448.0505	K
Gas constant	0.3796	0.3796	0.3788	0.3784	kJ/(kg·K)
Molecular weight	21.9030	21.9030	21.9510	21.9700	kg/kmol
Isentropic exponent	1.1625	1.1625	1.1751	1.2150	-
Density	1.7701	1.7701	1.0927	0.1849	kg/m³
Area ratio	0.0000	0.0000	1.0000	2.9307	-
Mass flux	0.0000	0.0000	1046.9587	357.2402	kg/(m²·s)

Estimated delivered performance

Parameter	Sea level	Optimum expansion	Vacuum	Unit
Characteristic Velocity	0.0000	1377.6700	0.0000	m/s
Specific impulse	189.4500	189.4500	217.2600	s
Volumetric Specific impulse	248985	248985	285534	kg.s/m³
Thrust coefficient	1.3486	1.3486	1.5465	-

Although the engine is designed to running at maximum specific impulse, it is useful to know what the volumetric specific impulse in such conditions is. From Report 2 it is apparent that the propellant mixture ratios that maximize both the mass and volumetric specific impulses are very nearly to each other. Through the corresponding equations developed in such Report, the estimated volumetric specific impulse is computed and attached in Table 7.

Given these performance parameters the first stuff to address is finding a convenient propellant flow rate. To accomplish that job, two major issues must be observed. On one hand, the propellant flow rate will be limited by the maximum flow rate attainable by the industrial positive displacement gear pumps. On the other hand, as explained in the previous report, given a specific impulse, the thrust level is defined by the propellant flow rate. Therefore, the adequate propellant flow rate should meet the thrust requirement. Having into account the previously exposed arguments, it is clear that the most stringent constraint will define the sought parameter. The propellant flow rate value that gives the required thrust level can be computed using the following expression:

$$I_{sp} = \frac{F}{g_o \, \dot{m}_p}$$

(3.2.3)

where, I_{sp}: Estimated specific impulse (s).
F: Required thrust level (N).
g_o: gravity constant (m/s^2).
$\dot{m}_p$: Propellant mass flow rate (kg/s).

For a required thrust level of 500N, by applying the equation 3.2.3, the resulting flow rate is 0.27 kg/s. Besides this estimated value, it is needed to check that the pumps may deliver that flow rate level. Assuming a pump rotational speed of around 4000 rpm, it is observed that a volumetric flow range of 20l/min is feasible and taking into account the propellants densities yields a propellant flow rate level enough to cover the thrust level requirement. For a more detailed description of the pump capabilities, the available data may be consulted in references [5, 6].

With the estimated propellant flow rate the engine size can be sketched by calculating the throat area, for which the following expression is useful:

$$A_t = \frac{\dot{m}_p \, c^*}{p_C}$$

(3.2.4)

where, A_t: Engine throat area (m^2).
c^*: Characteristic velocity (m/s).
p_C: Combustion chamber pressure (Pa).

Hereby the estimated throat area throws a value of 2,5cm^2 and thus, a throat diameter of 1.8cm.

Following with the engine characterization, at this point it is convenient to fix the engine running time. The required range is among 10 s and 20 s with special interest in a running test of 12s because that time is expected to be used in a future fly demonstrator. So, the selected test engine running time is 12s. The oxidizer mass and volume as well as the fuel mass and volume may be now determined by using the next equations:

$$\dot{m}_p = \frac{m_p}{t_b}$$

(3.2.5)

where, t_b: Engine running time (s).
m_p: Propellant mass (kg).

$$m_o = m_p \frac{O/F}{1 + O/F}$$

(3.2.6)

$$m_f = m_p \frac{1}{1 + O/F}$$

(3.2.7)

where: m_o: oxidizer mass (kg).
m_f: fuel mass (kg).

$$\rho_o = \frac{m_o}{V_o}$$

(3.2.8)

$$\rho_f = \frac{m_f}{V_f} \qquad\qquad \textbf{(3.2.9)}$$

where: V_o: oxidizer volume (m³).
$\quad\quad\quad V_f$: fuel volume (m³).
$\quad\quad\quad \rho_o$: oxidizer density (kg/m³).
$\quad\quad\quad \rho_f$: fuel density (kg/m³).

The Table 8 summarizes the parameters computed with the expressions 3.2.5 to 3.2.9 for a group of running time values that fall within the required interval. Further, this table provides quick data access to set the test bench if the test time should be modified.

Table 8: Summary of estimated propellants parameters.					
Engine running time *[s]*	*Propellant mass* *[kg]*	*Fuel mass* *[kg]*	*Oxidizer mass* *[kg]*	*Fuel volume* *[l]*	*Oxidizer volume* *[l]*
10	2.69	0.21	2.48	0.261	1.79
12	3.23	0.26	2.98	0.314	2.15
14	3.77	0.30	3.47	0.366	2.50
16	4.31	0.34	3.97	0.418	2.86
18	4.85	0.38	4.47	0.471	3.22
20	5.39	0.42	4.96	0.523	3.58

Having the total pressure raise in the pumps and the propellant flow rate in both fuel and oxidizer lines, now it is possible to estimate the pumping required power. As it is proposed in the Report 1, neglecting the mechanical losses in the gear box, the required motor power may be computed with the following expression:

$$P_{oem} = \Delta p_{pu} \left(\frac{m_f}{\rho_f \eta_{puf}} + \frac{m_o}{\rho_o \eta_{puo}} \right) \frac{1}{t_b} \qquad\qquad \textbf{(3.3.10)}$$

where, P_{oem}: Electric motor mechanical output power (W).
$\quad\quad\quad \Delta p_{pu}$: Pump pressure raise, difference between pump discharge and inlet pressures (Pa).
$\quad\quad\quad \eta_{puo}$: Oxidizer pump efficiency.
$\quad\quad\quad \eta_{puf}$: Fuel pump efficiency.

Together with the mechanical power, the power density and efficiency of each electric component allows sizing the electric pump system. Such densities and efficiencies can be computed from the manufacturer's datasheets [8, 9, 10]. The Figure 5 shows a set of typical performance plots for a gear pump similar to those that will be employed in this project [7]. As far as the efficiency concerns, it can be seen from the upper right graph, that adopting a value of 75% as lower performance bound is a very conservative assumption regardless the adopted pressure raise. The electric motor and inverter values of power densities and efficiencies were presented in Report 1. Here, a set of values representing the expected performance are used. Regarding to the battery, a lithium-polymer technology will be adopted due to its high availability. While its parameters are not needed to compute the electric required power, they are included herein to present all the electric parameters together. For the sake of simplicity, the whole data needed to sizing the electric pumping feed system is put all together in the Table 9.

Table 9: Summary of electric drive system power densities and efficiencies.				
Component	*Parameter*	*Value*	*Unit*	*Reference*
Oxidizer pump	Efficiency	0.75	-	[7]
	Power density	3.50	kW/kg	[6]
Fuel pump	Efficiency	0.75	-	[7]
	Power density	0.68	kW/kg	[6]
Electric motor	Efficiency	0.8	-	[8]
	Power density	4.8	kW/kg	[8]
Inverter	Efficiency	0.85	-	[9]
	Power density	70.5	kW/kg	[9]
Battery	Power density	6	kW/kg	[10]
	Energy density	130	Wh/kg	[10]

With the motor mechanical power, now it is possible to compute the electrical power and the energy needed from the batteries by applying the equations pair 3.3.11 and 3.3.12:
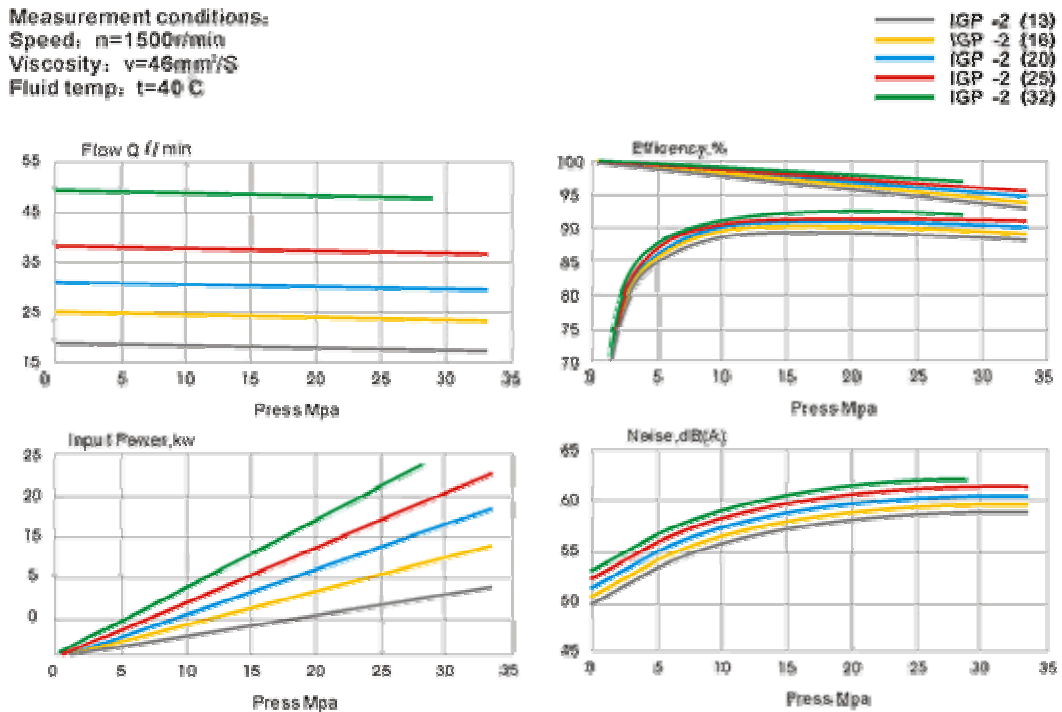
Figure 5: Typical performance plots of gear pumps. They are extracted from [7].

$$P_{bat} = \frac{P_{oem}}{\eta_{em}\,\eta_{inv}}$$ (3.3.11)

$$W_{bat} = \frac{P_{oem}}{\eta_{em}\,\eta_{inv}}\,t_b$$ (3.3.12)

where, P_{bat}: Battery required electric output power (W).
W_{bat}: Battery required electric Energy (Wh).
η_{em}: Electric motor efficiency.
η_{inv}: Inverter efficiency.

From both preceding equations plus the data in Table 9, the electric drive system can be characterized. Two parameters are needed, the mechanical motor power and the electrical power

required from the batteries. In the next section, a more detailed estimation enables selecting commercial parts for the test bench. At this point, such powers are enough to accomplish the preliminary design.

4.5. Start and stop sequences sketching

Following a rigorous start sequence ensures a safety and reliable transition from the ready state to the main-stage operation. The electronic control and monitoring system becomes essential, controlling the start transient and thus given a reliable and repeatable engine startup providing a safety switching off maneuver in case of engine failure. During both start and stop transients, the most severe pressure and temperature peaks typically occurs over the different engine components. Therefore, good start and stop sequences allows maximizing the rocket engine reliability and the engine parts life.

The proposed start sequence is displayed in the Figure 6. After the start signal, the pyrotechnic igniter is triggered, providing a hot flame source inside the combustion chamber which is maintained until the propellants entrance. This action is followed by the opening of the main propellant valves which feed the propellant pumps with the required positive pressure. Almost immediately after the valves are opened, the pumps are driven with an increasing velocity ramp in a way that the propellant flow rate continuously raises until the nominal required flow.
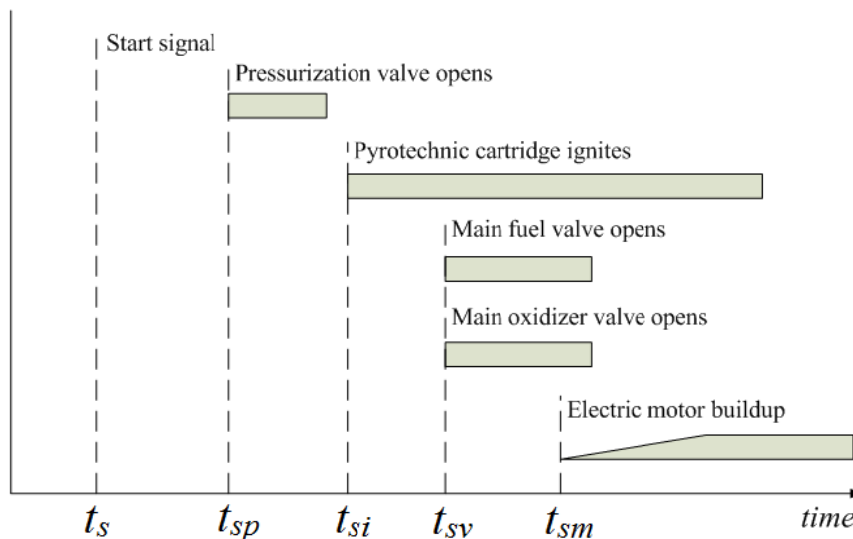

Figure 6: Proposed start sequence diagram.

The engine cutoff sequence must provide rapid and safe engine shutdown, in normal test mode operation as well as in emergency case. For a normal test end operation, the cutoff sequence is presented in Figure 7. Commonly the rocket engines cutoff is done in a fuel rich fashion (other way, the oxidizer may attack seriously the chamber interior). However, in this experimental engine, a cutoff sequence employing an oxidizer excess is preferred, since the hydrogen peroxide is not as corrosive as other oxidizers (i.e. nitric acid or nitrogen tetroxide). This approach has the advantage that unburned fuel residues over the hot engine are avoided. Otherwise, such circumstance may leads to serious fire risk . Therefore, after the stop command is asserted, the fuel valve is closed first and then the oxidizer valve is closed too. While the cutoff transient, the pumps remain running and hereby, cleaning the propellant feed lines. Once the main valves be completely closed and after a guard time, the feed lines purge valves will be opened allowing the feed lines be totally purged by the air suctioned from the purge line. Finally, the propellant tanks are drained by opening its drain valves using the tank pressure to expel the propellant remainder.
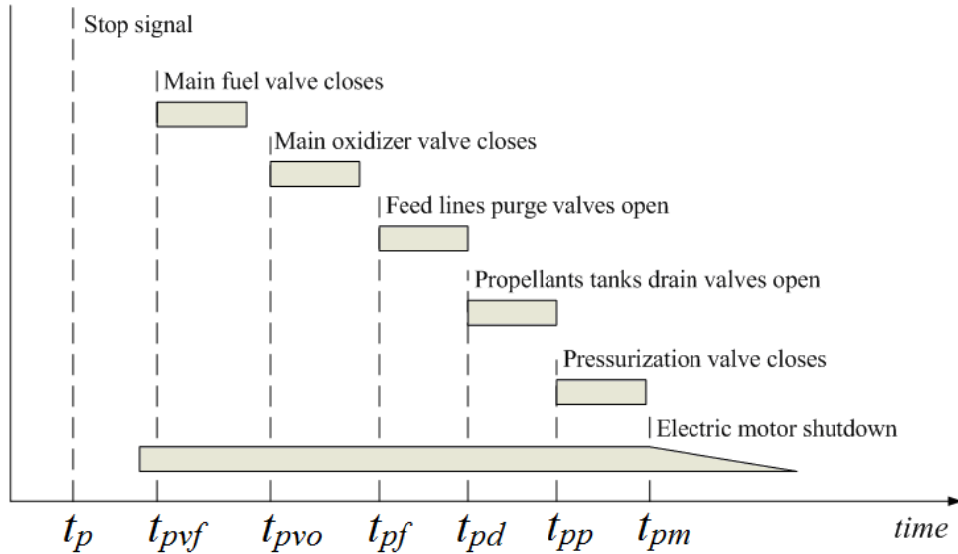
Figure 7: Proposed stop sequence diagram.

The emergency cutoff sequence is slightly different from that employed in normal operation. Both propellants valves are closed simultaneously since as faster as possible thrust decay is prioritized over an engine soft thermal transient. Immediately the feed lines are purged with air and the propellant tanks are evacuated by opening each propellant tank purge valve. Both, propellant tanks drain and feed lines purge valves are opened at the same time for a rapid system purge and depressurization. Once the tanks are already empty, the pressurization valve is closed.
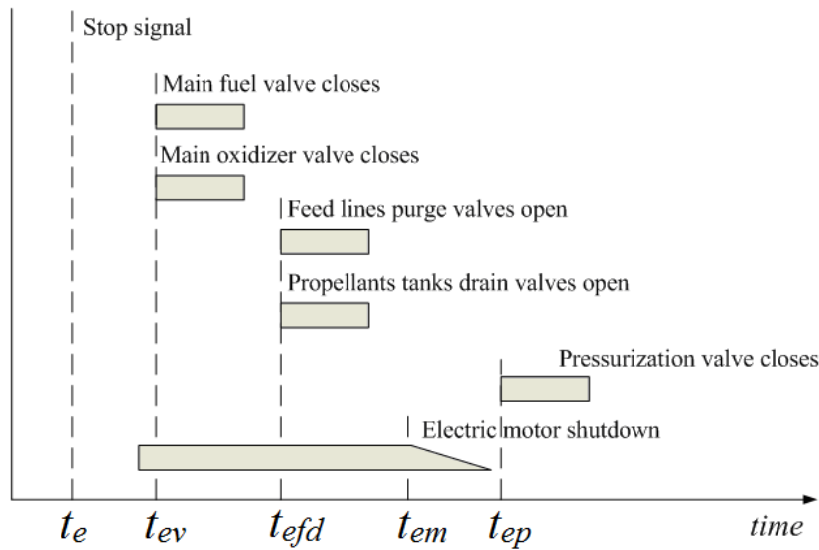
Figure 8: Proposed emergency stop sequence diagram.

4.6. Test bench material selection

Whereas in a flying intended rocket engine the mass requirement leads the decision of material selection, in this project the low cost requirement has the higher priority. Therefore, the rocket components material selection will be addressed with the idea of keeping the cost as low as possible.

Regarding to the thrust chamber, the selected material also must withstand the high combustion temperature at the working pressure. A high melting point metal alloy is considered to be the constituting material of the whole thrust camber, including the injector plate, the nozzle and the calorimeter jacket. Between the many options, a stainless steel alloy is preferred

due to its high corrosion resistance feature. In Report 2, a stainless steel 316 is proposed as compatible material and herein it is used to address the preliminary design. It is denoted that the particular stainless steel alloy employed in the test bench may vary according to the availability but not significant differences in its properties are expected.

With respect to the pumping system, the gear pumps are oriented to hydraulic drivers in industrial application and thereby, they will be made from steel alloy. The electric motor proceeds from the scale radio-controlled vehicles industry. As it is intended to drive a flying model, it is made from a metal lightweight alloy. The material composition of the batteries is, of course, defined by its technology.

The pipelines, the valves and sensors employed in the propellant lines ought to be made from a material chemically compatible with the selected fuel and oxidizer. Such chemical substances are very compatible with the most materials available. Therefore, the pipelines and valves may be made from steel as such the used to conduct water or oil.

Finally, as far as the propellant tanks are concerned, the kerosene and the PERSOL 1 are chemically compatible with the polyethylene polymer. Therefore, as not great volume capabilities are required, simply high density polyethylene (HDPE) bottles may be employed in propellant tanks. Such material withstand the required propellant tank pressure and thereby it may be employed also in the low pressure feed lines.

All the rocket engine, including the control and monitoring lines and devices must be mounted over a bench. The only part that is not contained in such bank is the computer, used to control the engine and process data from the tests. The bench must withstand the vibrations and temperatures produced while the engine is running. Additionally, the safety requirements force to make it from an inflammable material. For that reasons, a steel alloy is proposed to be the major constituent material of the bench. A typical machine tool bank is considered as a good point to start the design of the rocket testing bench.

Table 10: Summary of preliminary design output parameters.

Engine component	Parameter	Value	Unit
Thrust chamber	Specific impulse	190	s
	Volumetric specific impulse	248840	$kg.s/m^3$
	Thrust (Sea level)	500	N
	Propellant mixture ratio	11.6	-
	Nozzle area expansion ratio	2.9307	-
	Throat area	2,5	cm^2
	Throat diameter	1.8	cm
Fuel pump	Flow rate	1.6	l/min
	Pressure raise	1.95	MPa
	Fuel density	810	kg/m^3
	Rotational speed	4000	rpm
	Efficiency	0.75	-
	Required power	50	W
Oxidizer pump	Flow rate	11	l/min
	Pressure raise	1,95	MPa
	Oxidizer density	1388	kg/m^3
	Rotational speed	4000	rpm
	Efficiency	0.75	-
	Required power	350	W
Electric motor	Required mechanical power	535	W
	Efficiency	0.8	-
Battery	Technology	Li-Po	-
	Required electrical power	785	W
	Required electrical energy	2.61	Wh

V.   DETAILED DESIGN

With the guidelines of the preliminary design, on this point it is possible dividing the test bench design into separated sections. This approach allows focusing on each part at time, dividing the entire design problem into small ones so that, the complexity of the whole development becomes lower. However, it should not lose sight that each component is related with the rest and the definitions made in its design affects the other components design. Therefore, a global outlook should be maintained and each part design should be contrasted with the overall design to validating it.

5.1. Combustion chamber sizing

The first step to size the combustion chamber is already made with the estimation of the throat area in the preceding Section. The actual thrust chamber size should be determined in function of the characteristics of the combustion process that will be carried out within it. This process is very complex and any attempt to understand it involves a hard labor. Furthermore, typically the most reliable information about it proceeds from empirical experiences. Herein, the labor is limited to shows the design procedure leaving aside the details of such process, (however, the basic bibliography may be consulted to have a more detailed picture).

The Figure 9 shows a thrust chamber scheme where the presented basic dimensions allow configuring the thrust chamber layout.


lc: Chamber length.
rc: Chamber radius.
tc: Chamber wall thickness.
θc: Chamber contraction angle.
rt: Throat radius.
lN: Nozzle length.
rN: Nozzle radius.
θN: Nozzle half angle.

1.- Fuel inlet port.
2.- Oxidizer inlet port
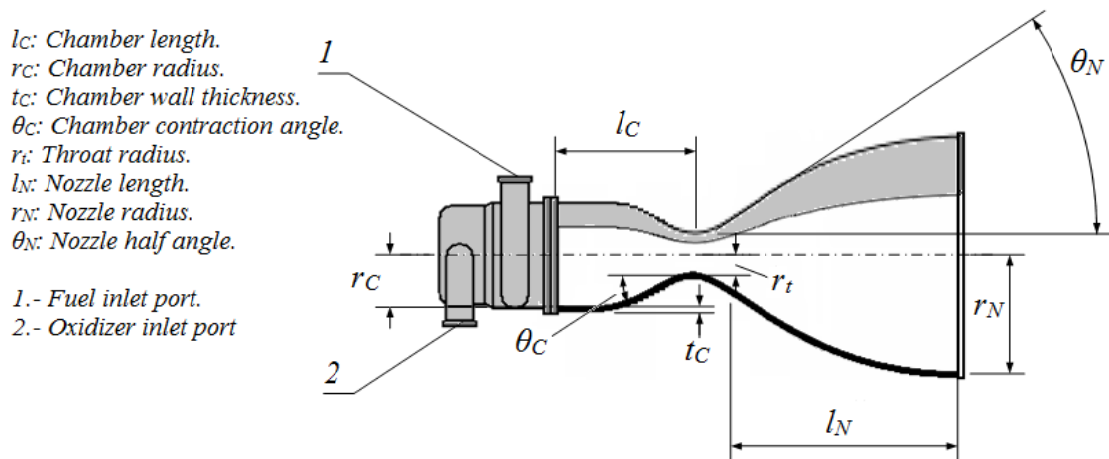
Figure 9: Thrust chamber cutaway scheme showing its main dimensions.

The combustion chamber volume must provides the space to properly mixing and combusting the propellants. Accomplishing such steps requires a time period that is very dependent of the involved propellants and the physical conditions in which the combustion occurs. Such period is commonly named *stay time* and is strongly related to the required combustion chamber volume. There exists another useful parameter which relates the concepts of stay time with the required chamber volume and it is denominated *characteristic length (L*)*. It must be denoted that, as with the stay time, the determination of characteristic length is an experimental issue. As the characteristic velocity notices the effective energy level of the combustion products is a good parameter for evaluating the quality of combustion chamber design. Therefore, it is reasonable analyzing the relationship between characteristic velocity (chamber performance) and characteristic length (chamber size). A typical trend is presented in Figure 10 where it may be observed that exists an *L** value which optimizes the combustion process. A tests series may be carried out to raise a similar curve, representative of the selected propellants and the engine operation conditions adopted. If a too lower characteristic length value is adopted, then the chamber volume will be insufficient to properly mixing, vaporizing and combusting the propellants and thus, the engine performance will be affected. On the other

hand, a too higher value gives to excessive thermal and frictional losses, also reducing the performance. Additionally, in flying intended engine designs, large values of characteristic length give to a very large and heavy chamber and hence, the engineers usually adopt a minimum value that gives the expected performance.
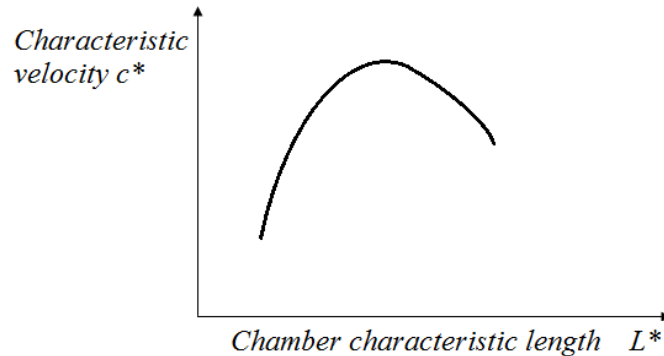

Figure 10: Effect of *L** on *c** for an experimental thrust chamber (Based on data extracted from [3])

Commonly, such election requires of further tests for validating it. Herein, such tests can not be realized and therefore, the estimation of the characteristic length must rely on the data available [3]. Although, there is no data available about the adopted propellant combination, the proposed range for hydrogen peroxide and RP-1, presented in Table 11, may be used. The characteristic length is chosen from this range hopping that such selection gives no significant degradation of characteristic velocity. It must be noted that, for the case of hydrogen peroxide, the length that is occupied by the catalyst is included in the estimation of the *L** range. As in this project an extra chamber diameter is needed to account the needed space for the permanganate layer, the additional length estimated via the *L** assumption is turned into the necessary diameter. From the proposed range in Table 11, choosing a small value of *L** implies a small engine but giving the chance to combustion insufficiency. On the other extreme, the larger the *L** value the larger the engine, but ensuring a good combustion process. As the total weight is not a major issue in this work, the conservative highest value of 1.78m is preferred. However, for the purpose of performing calculations, it may be used both the high and low boundaries and the average value between they, so that the effect of *L** in chamber sizing may be observed.

Table 11: Proposed *L** range for some propellant combinations.			
Oxidizer	*Fuel*	*Characteristic Length [m]*	
		Maximum	*Minimum*
Hydrogen peroxide	RP-1	1.78	1.52
Oxygen	RP-1	1.27	1.02
Oxygen	Hydrogen	1.02	0.76
Nitrogen tetroxide	Hydrazine	0.89	0.60
Nitric acid	Hydrazine	0.89	0.76

Note: Data extracted from [1].

Once adopted an *L** value, the combustion chamber volume may be calculated by applying the equation 5.1.1.

$$V_C = A_t \, L^*$$ **(5.1.1)**

where, V_C: Combustion chamber volume (m^3).

It must be noted that the calculated volume through 5.1.1 includes both the volume of the cylindrical section and the cone convergent section from the chamber cylindrical section to the throat section. Therefore, fully sizing the combustion chamber requires knowledge of the magnitude of the contraction angle. This magnitude is very particular from each design, varying from 20° to even 45°. Herein, having no other data that allows determinate the best value, a yardstick of manufacturing simplicity is taken setting such angle to 45°.

Having determined the chamber volume it is necessary computing both the chamber diameter and length to univocally define the combustion chamber size. At this point it may be followed two different approaches, one based on the analytical study of the propellant combustion thermo-chemical behavior and other supported by the historical data [1, 3]. It is interesting to contrast the results achieved when both approaches are applied to engine sizing.

First, the analytical approach is presented. It is desired that the Mach number associated to the gases inside the combustion chamber gets lower because in this way the combustion chamber pressure nears the stagnation pressure. For small engines a conservative assumption is forcing a Mach number of about 0.1 [1]. At the moment, there is no way of knowing if such value is convenient for the designed engine. The only criterion that may be followed is that the ratio among chamber length and diameter would be kept into the 0.5 to 2.5 range, based on historical data [1]. An excessive high Mach number value gives a chamber too long and narrow whereas a too small value yields to a too short and wide chamber. Hereby, when performing calculations with this approach, a Mach number magnitude of 0.1 is adopted for starting the process and it is iterated until an acceptable chamber length to diameter ratio being obtained. Having said that, the ratio between the chamber cross sectional area and the throat area, named *contraction ratio*, may be computed employing the following expression:

$$\varepsilon_C = \frac{A_C}{A_t} = \frac{1}{M_C}\left[\left(\frac{2}{\gamma+1}\right)\left(1+\frac{\gamma-1}{2}M_C^2\right)\right]^{\frac{\gamma+1}{2(\gamma-1)}} \tag{5.1.2}$$

where, ε_C: Combustion chamber contraction ratio.
γ: Isentropic parameter.
M_C: Combustion chamber Mach number.

On the other hand, it may be possible searching for data available about dimensions of proven engine designs and compiling all it, without discrimination of engines that burn cryogenic, hypergolic or storable propellant, to trace plots as the presented in the bibliography [1, 3]. The data in reference [3] may be useful as starting point, with particular interest on which represent engines that employs a combination of gaseous and liquid injection and chamber pressure of around 3MPa (among 400 psi and 500 psi). Such conditions fit better to the engine that is designed herein. Regarding to the contraction ratio, in reference [1] it is proposed an analytical expression which fits to the data in [3], which is transcribed here for simplicity:

$$\varepsilon_C = \frac{A_C}{A_t} = 4\,d_t^{-0.6} + 1.25 \tag{5.1.3}$$

Regarding the combustion chamber length, no analytical expression is proposed but a similar procedure to the one used in [1] may be adapted. Taking the data in [3], by applying a model similar to the employed in 5.1.3 and employing a numerical fitting method likely expressions may be obtained. The equations 5.1.4 and 5.1.5 show the results of this procedure:

$$\varepsilon_C = \frac{A_C}{A_t} = 0.95\,d_t^{-0.52} + 1 \tag{5.1.4}$$

$$l_C = 1.07 \, d_t^{0.88} + 0.07 \qquad\qquad\qquad \textbf{(5.1.5)}$$

For validating all these expressions it is useful plotting they together with the historical data proposed in [3]. The resulting graphs are presented in Figure 11 where it should be interesting to note that the estimated curve fits better than the proposed in [1]. It may be due to the fact that the analytical expression here estimated take into account only the relevant data and the proposed curve may respond to a fitting model which account with all the information presented in [3].

Having presented the two proposed approaches for combustion chamber sizing, at this point it is possible computing all the needed dimensions. It should not lose sight that the inputs for the calculation are the throat area and the adopted characteristic length whereas the searched dimensions are the chamber length and diameter. With the first method, the chamber Mach number is supposed to be 0.1 to start the calculation and it is iterated until reasonable ratio of length to diameter is attained. Meanwhile with the second method the analytical expression 5.1.4 and 5.1.5 are employed. The equations presented below result useful to perform the calculation. Finally, the estimated dimensions are presented in Table 12.

$$l_C = \frac{A_t}{A_C} L^* = \frac{L^*}{\varepsilon_C} \qquad\qquad\qquad \textbf{(5.1.6)}$$

$$r_C = \sqrt{\frac{A_t \, \varepsilon_C}{\pi}} \qquad\qquad\qquad \textbf{(5.1.7)}$$

$$l_{cs} = \frac{r_C - r_t}{tg\theta_C} \qquad\qquad\qquad \textbf{(5.1.8)}$$

$$V_{cs} = \frac{\pi \, l_{cs}}{3}\left(r_C^2 + r_t^2 + r_C r_t\right) \qquad\qquad\qquad \textbf{(5.1.9)}$$

where, l_{cs}: Chamber conical section length (m).
$\quad\quad\; V_{cs}$: Chamber conical section volume (m³).
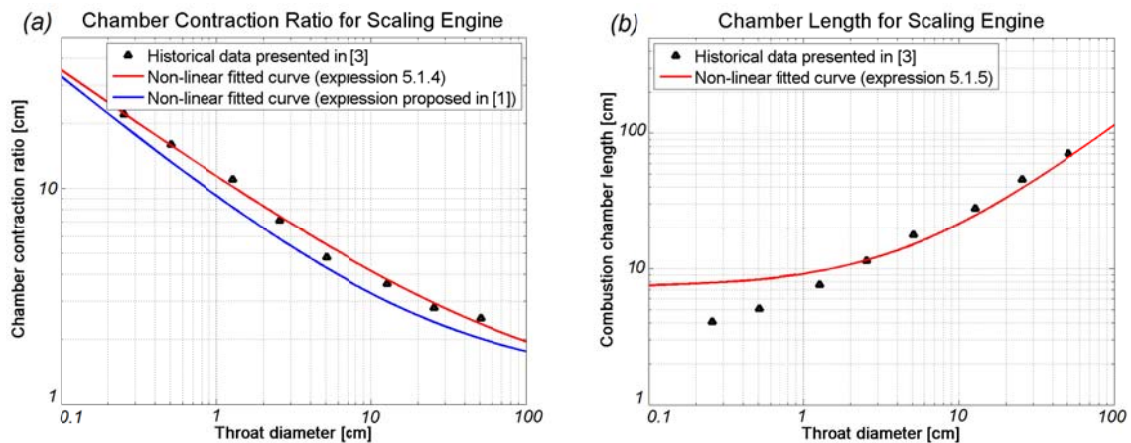
Figure 11: Useful relationship for engine scaling. Plot *(a)* shows chamber contraction ratio as function of throat diameter and plot (b) shows chamber length as function of the same parameter.

Dimension	Mach number approach			Curve-fit approach	Unit
Table 12: Summary of estimated combustion chamber dimensions.					
Characteristic length	1.52	1.65	1.78	0.83	*m*
Chamber Mach number	0.04	0.04	0.04	-	-
Chamber volume	376	408	440	205	*cm³*
Chamber length	11.6	12.5	13.4	10.4	*cm*
Chamber conical section length	2.5	2.5	2.5	1.7	*cm*
Chamber diameter	6.9	6.9	6.9	5.2	*cm*
Throat diameter	1.8	1.8	1.8	1.8	*cm*
Chamber contraction angle	45	45	45	45	*degree*
Chamber contraction ratio	14.9	14.9	14.9	8.7	-
Chamber length to diameter ratio	1.70	1.83	1.95	1.32	-

At the first glance, the engine estimated through the historical data approach seems to be significant smaller than the expected using the other approach. It should be explained if it is considered that the L^* proposed in the first estimation method account for the catalyst volume, while with the second method the employed data takes account only for combustion chambers volumes, without any catalyst device. Such argument seems supported by the resulting L^*, calculated for the second approach using the expression 5.1.1. Notice that the combustion chamber volume needed to burn only the propellants is around a half of the one needed if the decomposition of hydrogen peroxide is considered. Such information may be useful as starting point for a future project (providing that a rocket engine with separated catalyst chamber be designed).

As in this engine the catalyst will be located at the chamber wall instead longitudinally over the fuel injector face, the volume needed to properly decomposes the oxidizer is immediately toward the center of the catalyst surface and the combustion takes place in the central portion of the chamber volume. Therewith, in this particular design seem to be necessary employing a wider than predicted thrust chamber but at the same time no so long. At this point, in the absence of experimental data, the proposed chamber concept is explained in the following paragraph.

The volume needed to accomplish the propellant combustion process computed by the curve fit (empirical) approach is supposed to be sufficient for the experimental engine. Therefore, in no case, the chamber length and diameter should be smaller than the calculated with this method. The total chamber volume, that is the needed to decompose the oxidizer and make the propellant combustion, is supposed to be equal to which computed using the Mach number (analytical) approach. From the three result columns obtained with such approach, the corresponding to the most conservative value of L^* is selected. As the chamber dimensions computed with this approach are larger than the estimated with the empirical approach, the same are adopted as starting point. Having taken all these decisions, the dimensions of the combustion chamber may be already computed.

The permanganate layer should be thick enough to withstand the loads that may occur during engine running at the operating pressure and temperature. Any grain cracking may result in throat clogging which in turn may lead to a catastrophic failure. Therefore, a catalyst thickness of 1cm is considered sufficient, based on the information founded in [12]. Such thickness must be added to the chamber diameter computed with the analytic method.

Regarding to the chamber wall thickness, the mechanical tension that this wall must withstand is directly proportional to the chamber pressure and the chamber shape. Besides this, the thickness is inversely proportional to the material wall tensile strength which in turns is a function of the material temperature. Although the tensile strength is not typically defined for a temperature range as those the combustion chamber reaches when engine is running, most stainless steels have values of ultimate tensile strength well above 500 MPa. Hence, such value is adopted for the wall thickness estimation and, by using the expression 5.1.10 presented below,

chamber wall thickness may be computed. The included safety factor must accounts for the possible stress concentration and for any withdrawal from the assumed material tensile strength. Therefore, a value of 5 is considered enough in the thickness estimation.

$$e_C = \kappa_{sw} \frac{p_C \; r_C}{\sigma_C}$$

(5.1.10)

where, e_C: Combustion chamber thickness (m).
κ_{sw}: Safety factor.
σ_C: Ultimate tensile strength of chamber wall material (Pa).

Table 13: Summary of defined combustion chamber dimensions.		
Dimension	*Adopted value*	*Unit*
Characteristic length	2.86	*m*
Chamber volume	700	*cm³*
Chamber length	13	*cm*
Chamber conical section length	2.5	*cm*
Chamber diameter	9	*cm*
Throat diameter	1.8	*cm*
Chamber contraction angle	45	*degree*
Chamber contraction ratio	25	-
Chamber length to diameter ratio	1.5	-
Chamber thickness	0.1	*cm*
Chamber catalyst thickness	1	*cm*

Finally, it must be denoted that since an extra volume is needed to allocate the catalyst layer, all the combustion chamber parameters should be recalculated for its final characterization. In this way, the proposed chamber dimensions for the experimental engine are presented in Table 13 and a conceptual sketch is displayed in the Appendix at section A.2.

5.2. Exhaust nozzle sizing

As a preliminary design choice the conical nozzle is preferred for the experimental rocket engine, leaving others more complex designs for futures works. As a result, only a few dimensions must to be adjusted to complete the design. A conceptual sketch of the proposed nozzle configuration is shown in the Figure 12. The nozzle exit area is already defined since the nozzle expansion ratio and throat area have been established from the preliminary design section. So, the nozzle exit area and then, its radius and diameter, can be calculated by applying the expression 5.2.1.

$$\varepsilon_N = \frac{A_N}{A_t}$$

(5.2.1)

where, ε_N: Nozzle expansion ratio.
A_N: Nozzle exit area (m²).

θ_N: Nozzle divergent half angle.
l_N: Nozzle length.
r_N: Nozzle exit radius.
r_t: Throat radius.
r_a: Nozzle contour circular arc radius.
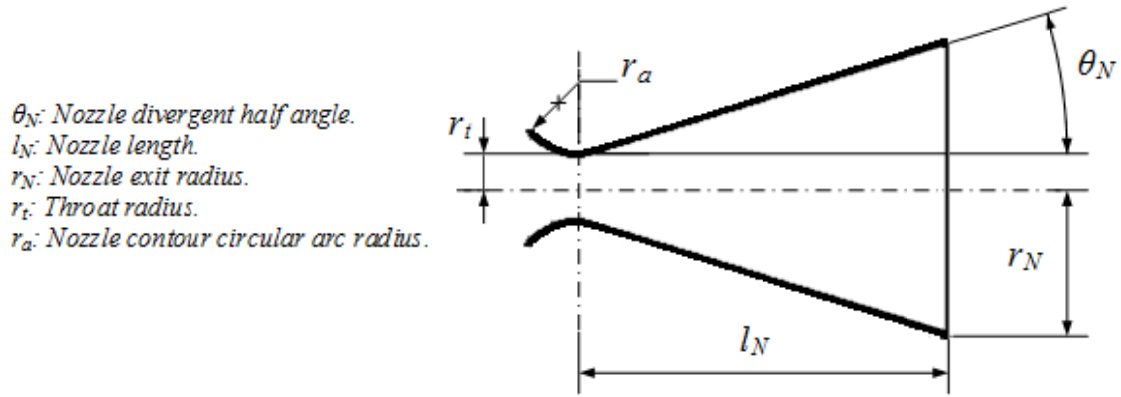
Figure 12: Conical nozzle sketch showing its main dimensions.

Meanwhile, the adoption of either value for nozzle divergent angle involves a tradeoff among nozzle performance and nozzle size and weight. For the proposed nozzle shape, divergent half angle values are typically around 12° to 18°. In this particular design a mid-range value of 15° is adopted because it comprises a good relationship among size and performances. The performance losses that happen in a conical nozzle due to the non axial component of the exhaust gas velocity affect the original thrust coefficient estimation. To adjust such parameter which was initially computed supposing an ideal nozzle, a correction factor *"λ"* is proposed. Since this performance loss is directly related to the divergent half angle, the correction factor can be computed by applying the expression 5.2.2. Having established the divergent angle the nozzle length is given by the expression 5.2.3, which is presented below:

$$\lambda_N = \frac{1 + \cos\theta_N}{2} \tag{5.2.2}$$

$$l_N = \frac{r_N - r_t}{tg\,\theta_N} \tag{5.2.3}$$

Since the pressure and temperature along the nozzle are lower than in the combustion chamber, the thickness needed is smaller than the one settled in the preceding section. For this reason, the same thickness as in the chamber is adopted to simplify the thrust chamber manufacture. Finally, only the nozzle contour circular arc radius is yet to be defined. Typical values for this dimension are proposed in [3], ranging between 0.5 and 1.5 times the throat radius. With no other information source, the same throat radius value is adopted for it. The Table 14 summarizes all the computed nozzle dimensions for the experimental engine.

Table 14: Summary of estimated nozzle dimensions.		
Dimension	*Value*	*Unit*
Nozzle thrust coefficient	1.3257	
Nozzle expansion ratio	2.93	*-*
Nozzle exit diameter	3	*cm*
Thrust correction factor (λ)	0.983	*-*
Nozzle length	2.4	*cm*
Nozzle divergent half angle	15	*degree*
Nozzle wall thickness	0.1	*cm*
Nozzle throat contour radius	0.9	*cm*

5.3. Calorimeter sizing

Accounting for future measurements of the heat released by the rocket engine, a calorimeter is designed. This device consists of a jacket covering the whole thrust chamber and a water flow is forced to pass through. It works in the same way as a heat exchanger, where the rocket heat is transferred to the water which proportionally will increase its temperature, giving a rough measure of the heat transferred through the chamber walls. The Figure 13 depicts a scheme of the calorimeter, showing its jacket rounding the thrust chamber assembly and also presents the three sections on which the thermal analysis proposed in this section is aimed.
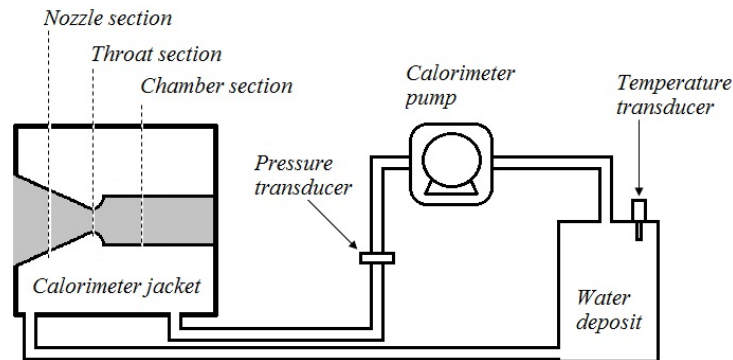

Figure 13: Calorimeter scheme.

To tackle the calorimeter design first it is necessary finding, approximately, the heat transferred from the combustion process to the thrust chamber. The first issue to address is the adoption of a proper theoretical model. The thrust chamber heat transfer characteristic depends mainly on the heat transfer properties of each material employed in its manufacture. As in the combustion chamber section, the wall will be covered by a catalyst layer, its heat transfer characteristics will be different from those in the throat and nozzle sections. The Figure 14 shows a simplified scheme of the heat transfer interfaces for these three different thrust chamber sections. The heat transfer model adopted to perform the calorimeter sizing is the same employed for the design of regenerative cooling thrust chamber as in both cases it is a heat flow between two moving fluids through a boundary layer.

To carried out the calorimeter sizing, herein is utilized the same procedure described in [1, 2, 3]. At this point, it is convenient remarking some assumptions used when this theoretical model is applied. Regarding to the heat flux estimation, although the engine running time will be short, the engine size is small enough to assume that the start and stop transients can be neglected. In fact, it is a steady state heat transfer model, supposed valid since the transient time is insignificant when it is compared to the total running time. Another simplification may be done by employing a short running time. The combustion with hydrocarbons fuels commonly leaves soot and carbon deposits over the chamber wall. However, in this case the effect of such deposits will be neglected in the chamber wall heat transfer coefficient estimation. Also, it is expected that the hydrogen peroxide, interacting with the catalyst layer, decreases even more the effect of carbon deposits by hampering its adherence to such layer. On the other hand, it is mentioned that both, the hot gases flow inside the chamber and the coolant flow, are supposed to be turbulent. The correlation expressions employed for computing the heat transfer coefficient are based on the assumption of the existence of a turbulent boundary layer nearly to the inner chamber wall. Such assumption seems to be not completely right for the throat and nozzle section [13]. Herein, for the sake of simplicity, the turbulent flow assumption will be assumed valid over all the thrust chamber sections considered in the analysis. At the same time, the calorimeter flow is supposed to be turbulent too, due to the way that it will be injected and extracted from the thrust chamber jacket.

Finally, it is denoted that any discontinuity effect among the divers sections will be neglected. A one dimensional model developed over the radial direction is applied.
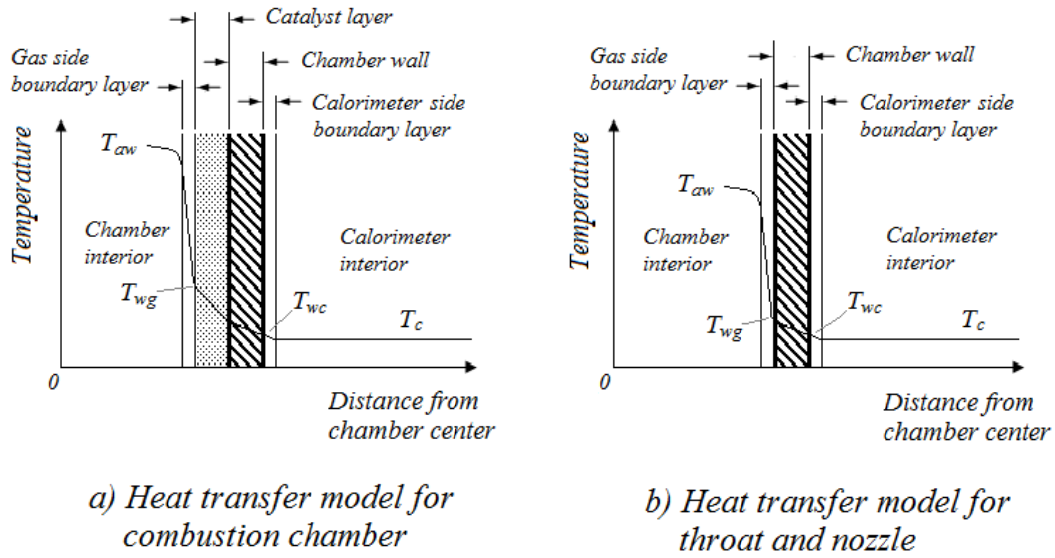
Figure 14: Heat transfer schemes for calorimeter sizing (Adapted from [3]).

Having mentioned the foregoing assumptions, it begins with the heat flux estimation from the combustion gases to the thrust chamber wall which is performed by forced convection. The specific heat flux, that is, the amount of heat crossing the chamber wall per surface unit and per time unit is computed using the next expression:

$$\dot{q} = h_g \left(T_{awX} - T_{wgX} \right) \qquad (5.3.1)$$

where, $\dot{q}$: Specific heat flux rate (W/m^2.s).
h_g: Gas side heat transfer coefficient (W/m^2-K).
T_{awX}: Chamber wall adiabatic temperature at estimation point (K).
T_{wgX}: Chamber wall gas side temperature at estimation point (K).

In a general sense, this equation is valid for forced convection regarding of chamber treated section. Hence, the *"X"* suffixes denote that the heat flux will vary according to the chamber section upon which it is estimated.

Meanwhile, the adiabatic wall temperature at any given location of the thrust chamber is lower than the stagnation temperature. This is due to the effect of heat radiated back to the free gas stream since the great temperature difference between the chamber wall and the hot gas stream [1]. To account for such effect a parameter named *recovery factor* is introduced. Therefore the adiabatic wall temperature can be computed from equation 5.3.2.

$$T_{aw} = T_C \left(\frac{1 + r \dfrac{(\gamma_X - 1)}{2} M_X^2}{1 + \dfrac{(\gamma_X - 1)}{2} M_X^2} \right) \qquad (5.3.2)$$

where, T_C: Combustion temperature (K).
r_X: Local recovery factor (Local means: at the X chamber section).
γ_X: Local isentropic parameter (Local means: at the X chamber section).
M_X: Local Mach number (Local means: at the X chamber section).

The local recovery factor depends largely on the combustion gas mixture and is normally determined from tests. As no experimental data is available in this case, it is needed to

estimate the value of such parameter. Experimental results for typical rocket propellants and fluid flows up to Mach 4 shows that $r = 0.91$ is a good approximation [1]. Also, the following empirical correlations may be used to verify such value:

$$r_X = Pr_X^{0.5} \tag{5.3.3}$$

$$r_X = Pr_X^{0.33} \tag{5.3.4}$$

where, Pr: Prandtl number

The expression 5.3.3 should be applied if laminar flow is considered whilst the expression 5.3.4 will be valid in case of turbulent flow. Further, the Eucken's formula, presented below, can be employed for estimating the Prandtl number, needed in the preceding correlations:

$$Pr_X = \frac{4\gamma_X}{9\gamma_X - 5} \tag{5.3.5}$$

To determinate the heat flux in the considered nozzle section it is necessary estimating the gas side heat transfer coefficient. It is function of fluid properties and flow characteristics, becoming its determination a rather complex problem. Therefore, empirical estimations are preferred over analytical inference.

The heat transfer at the boundary layer of the hot gas is produced by two mechanisms, that is, mainly convective transfer occurs but also it is present a conduction heat transfer mechanism. Hence, it is useful to introduce the Nusselt number, which gives the ratio of convective to conductive heat transfer coefficients. Such dimensionless number adopts the following form:

$$Nu = \frac{h\,\mathcal{L}}{k_f} \tag{5.3.6}$$

where, Nu: Nusselt number.
  h: Convective heat transfer coefficient (W/m²-K).
  $\mathcal{L}$: characteristic length of the analyzed interface (m).
  k_f: Conductive heat transfer coefficient (W/m-K).

As it said above, when a boundary of turbulent hot gas inside a rocket nozzle is analyzed, the heat transfer coefficient shows a strong dependence of the flow and fluid properties and by this way, the Nusselt number can be also expressed by the following empirical correlation:

$$Nu = C\left(Re\right)^{0.8}\left(Pr\right)^{0.34} \tag{5.3.7}$$

where, C: Experimental constant.

By combining the expression 5.3.6 and 5.3.7 Bartz developed an experimental correlation to estimate the heat transfer coefficient in a rocket nozzle. Such correlation is proposed in [3] to estimate such coefficient over the whole thrust chamber:

$$h_g = 0.026\left(\frac{p_C}{c^*}\right)^{4/5}\left(\frac{c_P\,\mu_0^{2/5}}{Pr_0}\right)\left(\frac{1}{r_a\,2r_t}\right)^{1/10}\left(\frac{A_t}{A_X}\right)^{9/10}\sigma_{bl} \tag{5.3.8}$$

where, c_P: Stagnation specific heat of exhaust gas (J/kg.K).

μ_0: Stagnation dynamic viscosity of the hot gas (kg/m.s).

Pr_0: Stagnation hot gas Prandtl number.

r_a: Nozzle contour circular arc radius (m).

A_X: Chamber area at the estimation point (m^2).

σ_{bl}: Correction factor for property variations across the boundary layer.

It must be denoted that the above equation is valid at any point of the thrust chamber by setting the valid parameters at the corresponding chamber section. As seen on such equation, there is a correction factor that accounts for the heterogeneous nature of the boundary layer gas flow. The expression 5.3.9, presented below, is used for estimating this factor on every analyzed point. Therefore, these correlations will be employed in the analysis of each chamber section.

$$\sigma_{bl} = \left(\frac{T_{wg}}{2T_C} \left(1 + \frac{\gamma_X - 1}{2} M_X^2 \right) + \frac{1}{2} \right)^{-0.68} \left(1 + \frac{\gamma_X - 1}{2} M_X^2 \right)^{-0.12} \tag{5.3.9}$$

The exhaust gas viscosity varies along the thrust chamber and again, it depends on the combustion characteristics. The expression 5.3.10 should be used to obtain an approximate result [3]. It is noted that the units are in the American System and therefore transformation constants are required to get correct results.

$$\mu_X = 46.6 \cdot 10^{-10} \, \mathrm{M}_X^{1/2} T_X^{3/5} \tag{5.3.10}$$

where, $\mathfrak{M}_X$: Exhaust gas molecular weight at the estimation point (lb/mol).

T_X: Exhaust gas temperature at the estimation point (°R).

μ_X: Exhaust gas molecular weight at the estimation point (lb/in.s).

The above equation set allows determining the heat flux derived from the combustion process. This heat passes entirely through the chamber wall by conduction, which means that no heat losses across the propellant manifold and injector are considered. Therefore, the estimated heat flux remains constant over all the considered interfaces. Herein a simple, steady state model is proposed for obtaining an approximation of the temperature at which the chamber wall will stay after the engine burnout. By applying the Fourier's Law to an axisymmetric cylindrical configuration, the following expression may be derived:

$$\dot{q} = -k_w \frac{dT}{dr} = k_w \frac{T_{wgX} - T_{wcX}}{r_X \ln\left(1 + \frac{e_C}{r_X} \right)} \tag{5.3.11}$$

where, k_w: Chamber wall material thermal conductivity (W/m.K).

T_{wgX}: Chamber wall gas side temperature at estimation point (K).

T_{wcX}: Chamber wall calorimeter side temperature at estimation point (K).

r_X: Thrust chamber radius at the estimation point (m).

The preceding expression is attained by assuming that there is not heat transferred to the outside. In the test engine such assumption will be no totally true since the heat effectively will be transferred to the calorimeter. However, this assumption serves to figure a worst-case situation allowing thus, adjusting the thickness of the chamber wall to achieve a proper coolant side wall temperature. Such an issue is needed to avoid the calorimeter water being to be boiled which, in turns, brings practical problems. For the thrust chamber dimensions, the simplification

of a planar instead cylindrical interface throws a minimum error and hence is adopted in the calculations. Thereby, the following simplified expression is presented:

$$\dot{q} = \frac{k_w}{e_C} \left(T_{wgX} - T_{wcX} \right)$$
(5.3.12)

If the combustion chamber section is analyzed, a similar conduction equation may be derived, but this time the catalyst layer must be considered. By making an analogy with an electrical circuit model, the catalyst layer presents a thermal resistance added in series to which is proper of the chamber wall. Hence, the next expression, which accounts the conduction through the two materials, is applied in the combustion chamber section:

$$\dot{q} = \left(\frac{k_w}{e_C} + \frac{k_{cl}}{e_{cl}} \right) \left(T_{wgX} - T_{wcX} \right)$$
(5.3.13)

where, k_{cl}: Catalyst layer thermal conductivity (W/m.K).
e_{cl}: Catalyst layer thickness (m).

The forced convection mechanism that occurs in the calorimeter side of the thrust chamber wall reduces still more the temperature. When analyzing this interface the goal is to find an adequate water flow rate which ensures that it is kept at liquid state. Herein, a steady state model similar to those applied in the hot gas side of the chamber is proposed. This model supposes that the water that leaves the calorimeter is not re-circulated toward it, which allows adopting a constant inlet flow temperature. Depending on the total water mass needed, practical issues may forces employing a re-circulating flow approach and the preceding supposition may not be fulfilled. Therefore, the adopted value for the calorimeter inlet temperature must be high enough to provide a safety margin. Thereby, in the performed analysis an inlet water flow temperature of 330K is assumed.

The flow regime for a given case is characterized by the Reynolds number [14]. The expression 5.2.14 brings a definition valid for a fluid passing through a tube. Reynolds numbers below 2000 results in a stable laminar flow. On the other hand, Reynolds numbers above 10000 characterize turbulent flow for heat transfer calculations. In the experimental engine calorimeter, the inlet an outlet ports will be close together since the jacket will be as long as the thrust chamber is. For this reason, laminar flow is not expected to occur and then, a Reynolds number value of 10000 is adopted for the estimations.

$$Re = \frac{d_{hy} \, \rho \, v}{\mu}$$
(5.3.14)

where, Re: Reynolds number.
d_{hy}: Hydraulic diameter of the tube (m).
μ: Dynamic viscosity (kg/m.s).
ρ: Fluid density (kg/m^3).
v: Flow velocity (m/s).

The calorimeter diameter can be roughly estimated by adapting an expression used in heat exchanger design [15] to the herein analyzed situation. For the sake of simplicity, the thrust chamber outside diameter is considered constant throughout calorimeter jacket and equal to the combustion chamber outside diameter, since it is the widest section. Consequently, the chamber outside area is approximated to the area of a cylinder of the same length that the calorimeter jacket and a diameter that equals the thrust chamber outside diameter. Therefore, the resulting equation is presented below:

$$d_c = 0.7963 \sqrt{\frac{A_o\, d_o}{l_o}} \qquad\qquad \textbf{(5.3.15)}$$

where, d_c: Calorimeter diameter (m).
  A_o: Thrust chamber outside area (m^2).
  d_o: Thrust chamber outside diameter (m).

As in the analyzed case, when dealing with non cylindrical tube geometries the hydraulic diameter is commonly used to estimate the Reynolds number [16]. In the designed engine, the thrust chamber and the calorimeter jacket can be approximated to a set of coaxial cylindrical tube sections, among which the water flows. In such case, the definition of hydraulic diameter gives the following expression, useful to compute it:

$$d_{hy} = 4\frac{A_{tube}}{P_{wetted}} = d_c - d_o \qquad\qquad \textbf{(5.3.16)}$$

where, A_{tube}: Cross-sectional area of the tube (m^2).
  P_{wetted}: Wetted perimeter of the tube (m).

Another useful quantity is the Prandtl number which is defined for the next expression for the flow conditions imposed in the calorimeter section:

$$Pr = \frac{c_P\, \mu}{k} \qquad\qquad \textbf{(5.3.17)}$$

The Colburn correlation results useful for estimating the heat transfer coefficient of the calorimeter side convection interface [17]. Such correlation is particularly suitable for turbulent flow, it approximates to experimental coefficient values when the forced convection is the main heat transfer mechanism. Studying such situation is complicated due to some phenomena like boundary layer separation. In the calorimeter case, the water flow will be in the direction of the thrust chamber axis. This simplification allows applying the Colburn correlation, originally aimed to flow parallel to a plane surface. This correlation is proportional to the Reynolds number, the Prandtl number and a fitting constant. The heat transfer coefficient is given in the following expression:

$$h_c = 0.036\left(\frac{c_{Pc}\dot{m}_c}{A_c}\right)\left(\frac{d_{hy}\,\rho_c\, v_c}{\mu_c}\right)^{0.55}\left(\frac{c_{Pc}\,\mu_c}{k_c}\right)^{\!\frac{1}{3}} \qquad\qquad \textbf{(5.3.18)}$$

where, h_c: Calorimeter side heat transfer coefficient (W/m^2-K).
  c_{Pc}: Specific heat of water (J/kg.K).
  μ_c: Dynamic viscosity of water (kg/m.s).
  $\dot{m}_c$: Water mass flow rate (kg/m^3).
  A_c: Calorimeter cross-sectional area (m^2).
  d_{hy}: Calorimeter hydraulic diameter (m).
  ρ_c: Water density (kg/m^3).
  v_c: Water flow velocity (m/s).
  k_c: Water thermal conductivity (W/m.K).

The heat flux equation employed in the boundary calorimeter side interface is analogous to that employed in the hot gas side interface. By assuming that the heat is conserved, as in the

case of chamber wall interface, the expression 5.3.19 brings the relationship between the previously estimated parameters and the sought water flow rate value.

$$\dot{q} = h_c \left(T_{wcX} - T_c \right)$$ (5.3.19)

where, T_c: Calorimeter water bulk temperature (K).

Since many parameters of the water are needed to perform calculations, the Table 15 summarizes all the required data.

Table 15: Summary of water physical properties.

Property	Value	Unit
Density (at 1 atm and 333K)	983	[kg/m³]
Molecular mass	18.015	[kg/kmol]
Melting point	273	[K]
Boiling point	373	[K]
Critical temperature	647	[K]
Vapor pressure (at 333K)	19.93	[KPa]
Heat capacity C$_P$ (at 1 atm and 333K)	75.38	[J/mol.kg]
Viscosity (at 333K)	0.000467	[kg/m.s]
Thermal conductivity (at 333K)	0.654	[W/m.K]

Notes: The data compiled in this table was extracted from [18].

The pressure drop in the calorimeter jacket has several sources among which the most remarkable are: pressure losses in the inlet and outlet ports, pressure drop associated to the flow acceleration, pressure losses due to the change in the cross-sectional area at the throat section and frictional losses on the calorimeter jacket. If all these sources are considered, the pressure drop estimation becomes a rather complex problem. Herein, a simplified analysis is done by concerning only the flow equation for an incompressible fluid, as is proposed in [19]. Moreover, only the frictional losses are taken into account and a liquid phase flow is assumed. Following this approach the next equation is obtained:

$$\Delta p_c = \frac{f_c \, d_c}{2 \, \rho_c \, d_{hy}} \left(\frac{\dot{m}_c}{A_s} \right)^2$$ (5.3.20)

where, Δp_c: Calorimeter jacket pressure drop (Pa).
          f_c: frictional loss empirical factor.
          l_c: Calorimeter jacket length (m).
          A_s: Difference between thrust chamber and jacket cross-sectional areas (m²).

The friction factor needed in the above equation may be computed by using the next factor correlation, which includes the entrance and exits losses. The formula is valid only for Reynolds number from 3000 to 5x10⁶ [15].

$$f_c = e^{0.576 - 0.19\ln(Re)}$$ (5.3.21)

Meanwhile, the calorimeter jacket wall thickness can be computed by the same way that the chamber wall thickness and thus, the expression 5.3.22 can be derived. If the thickness computed with this expression is too small then, for practical reasons, the same thickness that for the combustion chamber may be used.

$$e_c = \kappa_{swc} \frac{\Delta p_c \, d_c}{2 \sigma_c} \tag{5.3.22}$$

where, e_c: Calorimeter jacket thickness (m).
κ_{swc}: Safety factor for the jacket thickness estimation.
σ_c: Ultimate tensile strength of calorimeter jacket wall material (Pa).

The required pumping power is proportional to its pressure raise (needed to counteract the jacket and pipes pressure drops) and the water flow rate. Additionally, a margin factor is included to proper sizing the calorimeter pump. It is considered that by doubling the required power a good estimation is achieved and so, a value of 2 is adopted for such factor. Together with the pump sizing it is needed setting the water tank volume. It is simply attained by multiplying the water flow rate by the total engine burning time. Finally, it is noted that the calorimeter design parameters are summarized in Table 15.

$$P_{pc} = \kappa_{spc} \frac{\Delta p_c}{t_b} \tag{5.3.23}$$

where, P_{pc}: Calorimeter pumping power (W).
κ_{swc}: Safety factor for the pumping power estimation.

Table 15: Summary of estimated calorimeter parameters.

Parameter	*Value*	*Unit*
Calorimeter jacket length	16	*cm*
Calorimeter jacket diameter	13	*cm*
Calorimeter jacket thickness	0.1	*cm*
Calorimeter jacket pressure drop	46.6	*KPa*
Water flow	54.4	*kg/s*
Pumping power	5.2	*kW*
Required Water volume	660	*l*

As a final note to this section, the required water volume is too large to consider using a water tank of such dimensions. This indicates that the water must be recirculated through the calorimeter. Consequently, maybe some heat exchanger (i.e. water cooler radiator) should be considered to lower the water temperature before it being pumped again toward the rocket engine.

5.4. Injector head design

The injector design typically is a very complex problem which requires several validating tests before the requirements being fulfilled. Commonly problems that must be overcome are: combustion instabilities, injection efficiency, propellant mass distribution over the injection area and mixture ratio distribution. In this work, however, to aim a rigorous design is not the goal. Leaving aside some requirements as combustion efficiency will simplify the design process. In addition, due to the small size of the engine it is not expected that combustion instabilities and propellants distributions becomes serious problems.

The designs start by adopting an appropriated injector pressure drop. Such pressure drop is needed to isolate the combustion chamber from pressure oscillations in the feed system that further may trigger combustion instabilities. In the experimental engine this issue is particularly important since the employed pumps have a significant propellant flow ripple. Also, must be denoted at this point that the engine is projected to have thrust throttling capability. For this

engine type the bibliography recommends that the pressure drop in the injector being around 30% of the combustion chamber pressure. Such recommendation is adopted to start the design.

The next step in the injector design is choosing a convenient number of injection orifices. A small number leads to increase the propellant mass flow that passes through each orifice. This gives a lower injector flow velocity which in turn, penalizes the droplets formation. Such issue can be compensated by increasing the propellants stay time, that is, by enlarging the combustion chamber. On the other hand, the injector manufacture becomes more complex when the number of orifices increases. Due to the small space available for the injector head it is expected that no more than one central fuel injector and at most six surrounding oxidizer injectors can be allocated. Thereby, the number of injection orifices is selected according to such requirement. To perform the calculation, the following expression is useful:

$$A_{inj} = \frac{\dot{m}_i}{N_i} \sqrt{\frac{\kappa_{inj}}{2\rho_i \Delta p_{inj}}} \qquad (5.4.1)$$

where, A_{inj}: Injector hole exit area (m^2).
N_i: Number of injection orifices.
ρ_i: Propellant density (kg/m^3).
Δp_{inj}: Injector pressure drop (Pa).
κ_{inj}: Head loss coefficient.

If the combustion efficiency is proved to be very deficient, a future work should be consider one of the following possible solutions. First, the propellants mass flow rate could be decreased. Although this improves the combustion efficiency, also has a negative impact in engine performance, particularly lowering the engine thrust. Another solution should contemplate that the injector pressure drop can be increased. The preceding equation shows that the injector diameter decreases but this solution also requires a larger pumping power and therefore batteries mass. Finally, increasing the combustion chamber size, promptly its diameter, allows allocating a greater number of injector elements. Even though this will increases the engine mass, in this case such issue is not a main constraint.

The head loss coefficient is introduced to account for all the nonreversible pressure losses. It is desirable that the entire injector pressure drop can be used to increases the flow velocity. However, the nonreversible pressure losses which are in a range from 20% to 70% of the dynamic pressure needed (according the injector geometry [1]), forces increasing the injector pressure drop to attain the desired injection velocity. The value of such coefficient, for the selected injectors, could be determined through tests by measuring pressure drop and flow rate.

Since industrial spray injectors will be employed, the proper model may be selected considering only the pressure drop, flow rate and number of injection elements. As it is previously mentioned, the injection head will have a single central fuel injector surrounded by 6 oxidizer injectors. Having into account the foregoing paragraphs the calculations are performed and the results are presented in the Table 16.

Table 16: Summary of estimated injector parameters.			
Propellant	*Parameter*	*Value*	*Unit*
Fuel	Mass flow rate	0.021	*kg/s*
	Mass flow rate	1.57	*l/min*
	Flow velocity	30.43	*m/s*
	Number of injection elements	1	-
Oxidizer	Mass flow rate per injection element	0.041	*kg/s*
	Mass flow rate per injection element	1.79	*l/min*
	Flow velocity	23.25	*m/s*

Number of injection elements	6	-

In this engine, the fuel injector will be placed in axial direction but, in contrast, the oxidizer injectors will be pointed to the chamber wall. Since the catalyst layer is allocated over the chamber wall, it is expected that such configuration enhances the decomposition efficiency. The right angle for the oxidizer elements depends on the injector spray angle. The spray boundary should not be above the catalyst layer upper limit. This idea is depicted in the conceptual drawing presented in Figure 15.

θ_{spray}: Injector spray angle
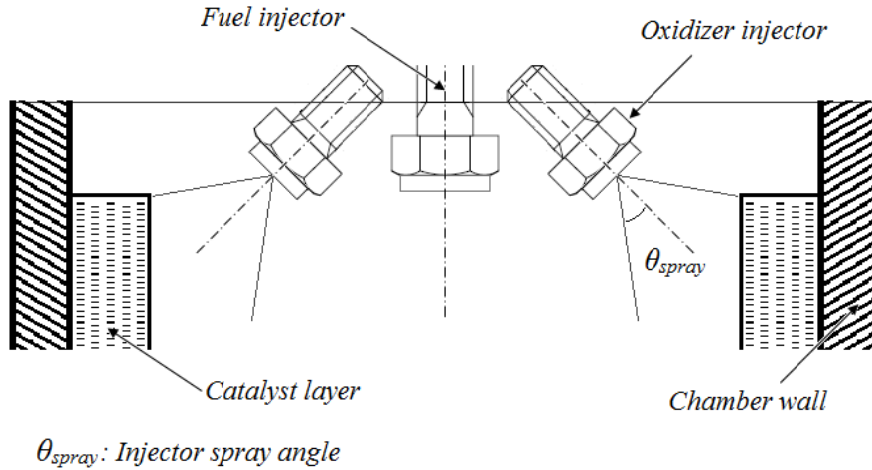
Figure 15: Injector head simplified layout scheme.

Having determined the injector main parameters, at this point is possible selecting a set of industrial spray injector for the rocket engine. By relieving several sources, the injectors set presented in Table 17 are chosen. For more detailed information, the corresponding reference should be consulted [20]. As the required flow rate per injection unit and pressure drop are very similar in both propellant lines, it will be employed the same injector nozzle model. The available injector nozzle, which is characterized by the data in Table 17, has a lower pressure drop for the required flow rate. For this reason, in the cold test phase the pressure and flow ripple will be carefully measured to ensure an acceptable operation.

Table 17: Selected injector nozzle data.			
Parameter		*Value*	*Unit*
Model		1/8 PZ2490 QZ2	-
Main dimensions	A	6.5	
	B	12	
	L	19.5	
	R	1/8	
Volumetric flow rate @0.1MPa		1.52	*l/min*
Volumetric flow rate @0.2MPa		2	*l/min*
Volumetric flow rate @0.4MPa		2.65	*l/min*
Volumetric flow rate @0.5MPa		2.89	*l/min*
Spray angle		90	*degree*
Technical Drawing			

Notes: The data compiled in this table was extracted from [20].

5.5. Propellants pumps sizing

The main parameters of the pumps are defined in the preliminary design section and, as in this work industrial pumps will be employed, only remains to select the proper model. Such issue is accomplished from manufacturers' datasheets [6]. Looking at the datasheet, it can be see that the lowest specific displacement obtainable from these pumps are in 0.6cm^3 per revolution, which in turns, leaves to a greater than required flow rate for the given pump speed in the preliminary design section. At this point it is clear that the pump rotational speed should be reduced. Such issue may be done through one of two different ways. On one hand, lowering the motor speed may brings a near acceptable flow rate but this involves to oversize the motor. On the other hand, the gear ratio may be adjusted to gives a near optimal speed relation and therefore, this is the preferred way. The expressions 5.5.1 and 5.5.2, presented below, are used to calculate the pump rotational speed, yielding:

$$\dot{m}_f = \frac{\rho_f \, r_{df} \, n_f}{60} \tag{5.5.1}$$

$$\dot{m}_o = \frac{\rho_o \, r_{do} \, n_o}{60} \tag{5.5.2}$$

where, $\dot{m}$: Propellant mass flow rate (kg/s).
n: Pump rotational speed (rpm).
r_d: Pump specific displacement (cm^3/rev)
ρ: Propellant density (kg/cm^3).

According to the foregoing mentioned, the selected fuel pump has the smallest specific displacement available, and by applying the expression 5.5.1 the pump rotational speed is calculated. The oxidizer pump is chosen so that the oxidizer flow rate requirement is fulfilled. There are two pump models that fit the flow requirement: the Model 35 and the Model 04. If the bigger pump is chosen, the rotational speed of both pumps results nearly equal and so, for simplification of the gear box development, such model is adopted. Having determined the pumps models, the most relevant data is transcribed from the datasheet to the Table 18 and a technical drawing is annexed to the report Appendix.

Table 18: Selected propellant pumps data.				
Parameter		*Value*		*Unit*
Model		0S	04	-
Displacement		0.6	4.1	*cm^3/rpm*
Pressure	*Continuous*		21	*MPa*
	Maximum		25	*MPa*
Speed	*Minimum*		600	*rpm*
	Maximum		4000	*rpm*
Dimensions	*Length*		120	*mm*
	Width		102	*mm*
	Height		84	*mm*
Weight			1.37	*kg*
Ports	*Inlet*		UNF-8	-
	Outlet		UNF-6	-

Notes: The data compiled in this table was extracted from [6].

Having defined the pumps to be used in the testbench, it follows the determination of the pump rotational speeds, through expressions 5.5.1 and 5.5.2. In the next subsection, this allows the gearbox sizing. Besides the preceding speed determination, it is also necessary to find the required mechanical power. By assuming that the power losses in the gearbox may be neglected, such power ought to be delivered by the electric motor. Having into account the pump pressure raise, the propellant flow rate and with the datasheet help, the power is estimated. Since in the datasheet there are no data for the Model 0S, the estimation is made from the immediately large model pump (Model 01), which in turns, allows accounting with a relative safety margin in the estimations. Note the discrepancy in the estimated values with respect to the estimation in the preliminary design section. Such deviation is attributed to the fact that, in the preliminary design, the pump efficiency is arbitrarily assumed while herein more reliable characteristic curves support the estimation.

Table 19: Summary of estimated pumps parameters.

Propellant	Parameter	Value	Unit
Fuel	Flow rate	1.57	*l/min*
	Pump rotational speed	2600	*rpm*
	Pump required mechanical power	200	*W*
Oxidizer	Flow rate	10.73	*l/min*
	Pump rotational speed	2600	*rpm*
	Pump required mechanical power	600	*W*

5.6. Electric motor, gearbox and inverter sizing

This subsection starts with the selection of the electric motor. From the preliminary design it is known that the employed motor will be of synchronous brushless type. Furthermore, the electric power is the sum of both pumps required powers. In the Report 1, several options were presented, from which can be seen that a gear reduction must be included since the motor speed far exceeds the pump required speed.

As in the case of the pumps, cost and availability rule the electric motor selection and thereby a Hyperion Z Series is preferred. From this series, the Z4045-12, which the technical data are presented in Table 20, fits well the requirement and therefore is selected. Notice that such motor can handle powers well over the estimated in the preceding section (providing large safety margin).

Table 20: Summary of electric motor technical data.

Parameter		Value	Unit
Manufacturer		*Hyperion*	-
Model		Z4045-12	-
Power range	*Continuous*	$1000 - 1800$	*W*
	Maximum	2200	*W*
Current	*Continuous*	$35 - 50$	*A*
	Maximum (30 seconds)	63	*A*
I_o		1.63	*A*
k_V		275	*Rpm/V*
R_i		0.0313	*Ω*
Dimensions	*Length*	70	*mm*
	Diameter	48	*mm*
	Shaft Length	30	*mm*
	Shaft Diameter	6	*mm*
Weight		0.553	*kg*

Notes: The data compiled in this table was extracted from [8].

The motor working voltage may be determined so that the maximum allowable power is obtained for the maximum allowable current. The expression 5.6.1 yields the relationship between power and voltage while accounting for the electric losses in the internal winding. Such losses are proportional to the nominal current and the internal winding resistance. Since the motor will be powered from Li-Po batteries, its input voltage should be expressed as the Li-Po cell nominal voltage times the number of cell in series. By applying such equation it is found that a Li-Po battery array of 10 cells (named as 10S packs) can satisfy the power requirement.

$$P_m = i_{im}\left(V_{im} - i_{im}\ r_m\right)$$ **(5.6.1)**

where, P_m: Electric motor mechanical power (W).
  V_{im}: Electric motor input voltage (V)
  i_{im}: Electric motor input current (A).
  r_m: Electric motor internal winding resistance (Ω).

With the data consigned in the preceding table, the motor speed may be computed. To do that it is necessary, again, to account the power losses in the internal winding. The parameter named herein speed coefficient is delivered by the manufacturer and allows relating the motor speed with their electrical characteristics. Thus, the following expression may be useful:

$$n_m = k_V\left(V_{im} - i_{im}\ r_m\right)$$ **(5.6.2)**

where, n_m: Electric motor speed (rpm).
  k_V: Speed coefficient (rpm/V).

At this point the gearbox may be sized. The configuration employed involves a drive gear, which is mounted over the electric motor shaft, coupled to other gear mounted on each pump shaft. Therefore the gear ratio must match both the motor speed with the pump required speed. For manufacture simplicity and taking advantage of the near equal pumps speeds, the same ratio will be adopted for both pumps and then it is allowed that some dispersion from the theoretical flow rate may be present.

The inverter, also named electronic speed controller (ESC), is chosen according to the power demanded by the electric motor. In this way, any inverter that accomplishes the specifications of working power and voltage could be employed. Considering cost, weight and availability, the Phoenix ICE HV 80 was selected (its main features are presented in Table 21).

Table 21: Summary of inverter technical data.			
Parameter		*Value*	*Unit*
Manufacturer		*Castle Creations*	-
Model		ICE HV 80	-
Voltage	*Continuous*	50	*V*
	Maximum	50	*V*
Current	*Continuous*	80	*A*
	Maximum	80	*A*
Switching rate (programmable)		11 − 22 − 41	*kHz*
Resistance		0.001	*Ω*
Dimensions	*Length*	71	*mm*
	Width	33	*mm*
	Height	23	*mm*
Weight		0.06	*kg*

Notes: The data compiled in this table was extracted from [9].

5.7. Batteries pack selection

From portable computers to small electric vehicles, there exist a large number of applications for Li-Po batteries. The main difference of Li-Po batteries over its direct predecessors (Li-Ion) is that the lithium salt electrolyte is held in a solid polymer compound, giving them lower manufacture cost, higher ruggedness and the possibility of widely adapt the packaging shape. The allowable voltage of the Li-Po cell varies from 2.7V to 4.23V. Overcharging the cell belong the upper limit may result in an explosion or fire. Therefore, the battery charger must include a protection circuit against overload. Meanwhile, if the cell is deeply discharged (below 3V) is possible that it no longer accept a full reload. Further, it may present problems maintaining its nominal voltage under load condition. Due to that reasons, an electronic circuit ought to be placed between the battery and the load to prevent the cell voltage drops below 3V. Modern Li-Po batteries have exceptional discharge and recharge capabilities. The first feature allows maximum discharge current in a range extending from 15 to 30 times the nominal cell capability. The second feature allows the cell to be quickly recharged. Another outstanding feature of Li-Po cells is the large number of reload cycles that it may withstand until its capacity drops below a useful limit. In addition to all these features, the good power density, which was studied in the Report 1, make the Li-Po batteries a good option to power the electric feed system of a rocket engine. Therefore, this battery technology is adopted for the testbench.

The Li-Po cell commonly is characterized in terms of its nominal capacity through the "C" rating. Such evaluation parameter refers to the current capability as a multiple of its nominal capacity. It may result confuse since the cell capacity is expressed in Amperes per hour (Ah) while the current is in Amperes. However, expressing the current capability of the cell in this way is very usual.

The batteries pack employed in the testbench should be chosen according to the requirements imposed by the electric motor. Since the motor is adopted from the ones aimed for RC modeling, it is reasonable to search among batteries packs created for this kind of application which fit the motor requirements. In this application field, the Li-Po cells arrays are often named with an "S" letter which is preceded by a number indicating the amount of Li-Po cells in series. In this way, a 4S Li-Po pack refers to a battery pack containing 4 cells in series.

Without delving too in the diverse options, in this section a brief description of the requirement needed to acquire the batteries pack is made.

The electric motor manufacturer recommends that the battery voltage be within the range of the 8S to 10S packs. Therefore, in this work it is decided acquiring two Li-Po packs 5S which will be put together in series for reaching the required voltage. Typically, the RC modeling Li-Po packs nominal capacity varies from 1800 mAh to even more than 5000 mAh. Herein, both the nominal capacity and the continuous discharge rate must be high enough to ensure the constant current needed to feed the electric motor, while the battery voltage remains in the required range. As a reference, in the Table 22, it is presented the technical data of two typical Li-Po batteries that may fulfill the electric motor requirements.

Table 22: Summary of batteries technical data.				
Parameter		*Value*		*Unit*
Manufacturer		*Thunder Power RC*		-
Model		TP2250-5SP30	TP2700-5SPL25	-
Capacity		2250	2700	*mAh*
Voltage	*Nominal*	18.5	18.5	*V*
	Cutoff	15[(*)]	15[(*)]	*V*
Discharge current	*Continuous*	67.5 (30C)	67.5 (25C)	*A*
	Maximum (3sec burst)	135 (60C)	135 (50C)	*A*

Charge current	Maximum	11.25 (5C)	13.5 (5C)	*A*
	Standard	2.25 (1C)	2.7 (1C)	*A*
Cycle life			600	*Cycles*
Dimensions	Length	102	102	*mm*
	Width	35	34	*mm*
	Height	41	42	*mm*
Weight		0.292	0.292	*kg*
Reference		[10]	[11]	-

Notes: (*) The value is estimated from the presented Li-Po general information.

5.8. Propellants pipelines sizing

As it is mentioned in the preliminary design section, one of the goals when designing the pipelines is keep the pressure drop between 35kPa and 50kPa. To meet this feature, the propellant flow velocity should be about 10 m/s [1]. To calculate a flow channel that gives this flow velocity the next expression can be employed:

$$\dot{m}_p = \rho_p vA \tag{5.8.1}$$

where, ρ_p: Flow channel cross-sectional area (m^2).

Meanwhile, the required pipeline wall thickness is proportional to the propellant pressure and the mechanical features of the pipeline material. The Laplace equation can be applied, as in the preceding cases, supposing a pipeline cylindrical section and taking a conservative safety factor. In the case that the wall thickness estimated by this method results excessively thin, a commercial standard pipe will be adopted. Since high density polyethylene has the lower tensile strength, it is adopted as a reference material for both low and high pressure lines. Any commercial pipeline that withstands the same operating conditions that the herein calculated should be selected.

In the case of the high pressure lines, the proximity to the thrust chamber imposes a demanding thermal stress. Therefore, stainless steel pipelines are considered in the estimation. As the pressurized gas does not comply with the hypothesis assumed for the flow velocity, the equation 5.8.1 can not be directly applied. However, the compressed air at 0.2 MPa can be handled with a standard hose for such application. In fact, the compressor acquired for the testbench has such hose. In the Table 23 the different pipes are divided according to its function and its mechanical properties are summarizes.

Table 23: Summary of pipelines estimated data.							
Parameter	Value						Unit
Working fluid	Low pressure propellant		High Pressure propellant				-
Material	HDPE		HDPE		Stainless Steel		-
Propellant	Ox.	Fuel	Ox.	Fuel	Ox.	Fuel	-
Minimum flow channel diameter	5	2	5	2	5	2	*mm*
Minimum wall thickness	0.1	0.1	1.2	1.2	0.1	0.1	*mm*

The values in the preceding table represent lower bounds that must be respected; they are established through the foregoing technical criteria. Certainly, commercial pipelines which far exceed these requirements also can be employed.

5.9. Monitoring peripherals selection

Each engine parameter that is needed to known must be measured through a proper method. In the preliminary design section all these parameters are summarized and in this section are given the arguments that justify the measurement devices selection.

It begins with the rocket engine heat measurement. The calorimeter implemented allows computing the heat dissipated through the walls by simultaneous measure of water flow and temperature. The instantaneous volumetric water flow can be measured using a plate- orifice. Both the initial and final water temperature by themselves does not matter but the difference between them is proportional to the produced heat. Therefore, two thermocouples will be employed, one installed into the water tank to take the initial water temperature and other at the calorimeter jacket outlet, to account for the temperature of the water releasing the engine.

For the characterization of the electric feed system measuring several electrical and mechanical variables is needed.

In first place, the electric motor, inverter and batteries set must be characterized separately from the rest of the engine, obtaining curves of the motor efficiency as a function of its speed.

For the electric motor characterization, the output couple can be calculated from a blocked rotor test, employing a load cell and a calibrated arm. A tachometer will be attached to the electric motor shaft, thus allowing the real time measure of the rotational speed.

Based on the blocked rotor test, the electrical input motor power could be estimated from the mechanical power on the shaft, and since the battery electric power can be directly computed from the measurements of its voltage and current, the inverter efficiency should be estimated too.

The propellant volumetric flow can be estimated through the pump characteristic displacement (which is function of the pump speed), the electric motor speed and taking the gear ratio as a fixed parameter. The pump displacement may be confirmed with a separated test performed with water.

Another important stuff in the electric feed system characterization is the measurement of the pressures profile. The propellants tanks pressure will be settled by the pressure regulator attached at the output of the gas tank. Such pressure will be assumed to be equal to the pump inlet pressure since, as it is confirmed in the previous section, the pressure drop in the pipelines can be neglected. The pump outlet pressure, which will be assumed to be the same as the inlet thrust chamber pressure, will be directly measured through a pressure transducer. Meanwhile, the injector should be characterized performing separated tests, particularly the pressure drop as a function of the input propellant flow is required. Furthermore, the chamber pressure may be estimated using such injector characterization and the measure of the pump outlet pressure. However, the thrust chamber will be provided with a port for the installation of a capillary. In the future, the same will be employed for extracting hot gases from the chamber, cooling it in the calorimeter jacket, and then taking its pressure with a proper pressure transducer for a direct thrust chamber pressure measure.

It is desired measuring the exhaust gas temperature but it involves a significant problem. The first aim to perform a direct measure is by employing a thermocouple attached to the nozzle exit. However, the nozzle flow is reversible, essentially isentropic flow process and therefore, any obstruction in the supersonic flow at the nozzle exit convert back the gas kinetic energy into thermal energy, increasing the local temperature near the stagnation temperature [2]. This effect not only avoids a right temperature measurement, but also may overheat the thermocouple causing a failure. Another approach could involve employing an infrared thermometer, but these devices are expensive and therefore its utilization should be carefully evaluated. In any case, experimental tests must be carried out for determination of a proper measure method.

VI. DESIGN OF A 70% H$_2$O$_2$ ROCKET ENGINE

Although until this point the addressed design concerns to a rocket engine which employs PERSOL 1 as oxidizer, this propellant may present some additional problems. Among such problems, the expertise grade in preparing the hydrogen peroxide and ammonium nitrate solution seems to be the more complex one. The chemical issues that may appear from the experimentation with this propellant can not be beforehand estimated. It is important that this issue should not affect the testbench development, which is the principal goal of this work. Therefore, the design of a rocket engine that works with 70% hydrogen peroxide is considered, since it allows leaving the PERSOL 1 problems for a later work. In fact, the same design criteria and guidelines holds for the new engine and only the thermochemical input parameters (derived from Report 2) must be corrected. The latter avoids having to rewrite the preceding sections since the arguments employed remains the same. As a result, in this section only the computed parameters corresponding to the preliminary and detailed design are presented into several tables. At the end of this section, three tables which contains the engine input parameters, the preliminary design output and the detailed design parameters respectively are presented.

By relieving these tables, it is observed that only some minor changes are necessary in the new design respect to the foregoing established. An important thing to highlight is that calorimeter, thrust chamber and electric drive systems remain unchanged. Actually, the more remarkable change is about the oxidizer pump, since the oxidizer to fuel ratio is slightly decreased. Therefore, oxidizer pump is replaced in this engine by the smaller Model 35 from the same manufacturer, which has a specific displacement of 3.5cm^3 per revolution. This modification allows maintaining both pumps running with the same gear box, both at the same speed, with only a mild deviation from the theoretical oxidizer propellant flow rate. Such deviation is expected to have a small impact in the engine performance, which has to be tested empirically. Furthermore, the specific impulse curve (see Report 2) for this propellants combination is nearly flat around the maximum value which suggests that the effect of such deviation will be kept restrained.

Table 24: Summary of chief performance parameters.

Propellant specification

Component	Density [kg/m^3]	Temperature [K]	Mass fraction	Molar fraction
RP-1	810	298.1	0.0893117	0.1585799
70% Hydrogen Peroxide	1288	298.1	0.9106883	0.8414201
O/F	10.1967352 (optimum performance)			

Thermodynamic properties

Parameter	Injector	Nozzle Inlet	Nozzle Throat	Nozzle Exit	Unit
Pressure	15.000	15.000	0.8548	0.1013	MPa
Temperature	2205.65	2205.65	2040.74	1444.52	K
Gas constant	0.3881	0.3881	0.3873	0.3870	kJ/(kg·K)
Molecular weight	21.4217	21.4217	21.4650	21.4823	kg/kmol
Isentropic exponent	1.1597	1.1597	1.1712	1.2087	-
Density	1.7522	1.7522	1.0814	0.1812	kg/m³
Area ratio	0.0000	0.0000	1.000	2.950	-
Mass flux	0.0000	0.0000	1040.53	352.67	kg/(m²·s)

Estimated delivered performance

Parameter	Sea level	Optimum expansion	Vacuum	Unit
Characteristic Velocity	0.00	1386.12	0.00	m/s

Specific impulse	190.8	190.8	218.97	*s*
Volumetric Specific impulse	233450	233450	267910	*kg.s/m³*
Thrust coefficient	1.3499	1.3499	1.5492	-

Table 25: Summary of preliminary design output parameters.

Engine component	Parameter	Value	Unit
Thrust chamber	Specific impulse	191	*s*
	Volumetric specific impulse	233450	*kg.s/m³*
	Thrust (Sea level)	500	*N*
	Propellant mixture ratio	10.2	-
	Nozzle area expansion ratio	2.95	-
	Throat area	2,6	*cm²*
	Throat diameter	1.8	*cm*
Fuel pump	Flow rate	1.8	*l/min*
	Pressure raise	1.95	*MPa*
	Fuel density	810	*kg/m³*
	Rotational speed	4000	*rpm*
	Efficiency	0.75	-
	Required power	60	*W*
Oxidizer pump	Flow rate	11.3	*l/min*
	Pressure raise	1,95	*MPa*
	Oxidizer density	1288	*kg/m³*
	Rotational speed	4000	*rpm*
	Efficiency	0.75	-
	Required power	370	*W*
Electric motor	Required mechanical power	570	*W*
	Efficiency	0.8	-
Battery	Technology	Li-Po	-
	Required electrical power	835	*W*
	Required electrical energy	2.79	*Wh*

Table 26: Summary of detailed design output parameters.

Dimension	Adopted value	Unit
Combustion chamber		
The same configuration as in the preceding engine can be employed		
Exhaust nozzle		
The same configuration as in the preceding engine can be employed		
Calorimeter		
Calorimeter jacket length	16	*cm*
Calorimeter jacket diameter	13	*cm*
Calorimeter jacket thickness	0.1	*cm*
Calorimeter jacket pressure drop	43.9	*KPa*
Water flow	53.9	*kg/s*
Pumping power	4.8	*kW*
Required water volume	665	*l*
Injector head		

		The same configuration as in the preceding engine can be employed	
Pumps			
Fuel pump	Flow rate	1.77	*l/min*
	Pump rotational speed	3000	*rpm*
	Pump required mechanical power	200	*W*
Oxidizer pump	Flow rate	11. 34	*l/min*
	Pump rotational speed	3300	*rpm*
	Pump required mechanical power	720	*W*
Electric pump drive system			
The same set of electric motor, inverter and batteries pack can be adapted to this engine by adjusting the engine speed.			
Pipelines			
The same devices as in the preceding engine can be employed			
Engine Monitoring system			
The same devices as in the preceding engine can be employed			

VII.   CONCLUSIONS

The elaboration of this report leaves some concepts and ideas that worth be commented as conclusions.

Throughout the diverse engine design phases, on many occasions became present the fact that the rocketry is a very experimental science.

The design process will be refined as the practical experience increase and more experimental data is obtained. Therefore, for this first rocket engine it can not be expected achieving a high degree in design accuracy. There will be certainly many things to adjust in practice so the final design could divert from those proposed in this report. Despite the above mentioned, as much as possible, the calculations are made considering a wide error margin. The data recollected along all the tests that will be made with this testbench allows future more refined engines design, on the way of getting a rocket engine capable of propelling a flying demonstrator.

One of the more relevant issues where the lack of experimental data is reflected regards to the thrust chamber design. Whatever the approach adopted, the calculations are based either on experimental information about the combustion process or previous successful rocket engine designs. In the consulted bibliography this kind of information is very limited since the propellants combinations employed in this work have not been widely used throughout history, with the exception of one or two rocket programs. For this reason, it will be interesting to evaluate the rocket engine performance and contrast it with the theoretical estimated performance. The results of such evaluation will give progressively experimental data about the combustion of the employed propellants. The thrust chamber design adopted decisions, therefore, give a probably larger and heavier than needed thrust chamber, unsuitable for a fly demonstrator, but satisfying for getting experimental data from an initial static testbench.

Another issue that is treated in a very biased way here but which will require especial attention in the practical tests is the engine ignition. Again, the lack of information about engines which operates with these propellants forces to leave the igniter design to the tests phase and to adopt an approach in a fashion of trial an error method. The major problem with the ignition of these propellants resides in the relatively low chemical energy, which makes its ignition a hard stuff. The adoption of an ignition cartridge allocated into the combustion chamber seems to be the best choice since it is capable of maintain a combustion process with

associated high temperatures by itself for a prolonged time. However, some practical problems, as the expulsion of the cartridge particles after the engine start, must be resolved.

One of the key features in the testbench design is its flexibility. As example it may be taken the thrust chamber design. Its very simple design helps counteracting the fact that its dimensions are not probed to be optimal. Such optimization, which requires practical experience as previously stated, can be carried out by manufacturing several thrust chamber while slightly varying its dimensions. The simple design makes such manufacture becoming a relatively inexpensive process. Then, firing tests for each of such chamber will allow trace performance curves as those employed herein to sizing the combustion chamber.

The calorimeter design proved to be a very complex issue. In its particular design section a number of simplifications had to be undertaken with the objective of avoids having to employ a computer assisted numerical analysis tool. However, this approach enforces realizing a series of practical test for validating the calorimeter design. Among the simplifications herein adopted one of the less realistic is the assumption of one phase liquid. Actually, to keep the water temperature below its boiling point one of two irrationals approaches should be used. First, the chamber wall thickness could be increased to a value that the thermal gradient established in the wall material yields an adequate cold side wall temperature, but the required thickness is well over a couple of meters. Another approach that could be used would be increasing the calorimeter flow rate to the point that the water leaving the calorimeter jacket did not gains so much thermal energy as to increases the temperature over its boiling point. However, the required water flow rate and consequently the required pumping power should be so excessive. As a result, two phases heat transfer fluid is expected and hence, the calculation model can not adjust to reality. Moreover, the model employed in the calorimeter design is a steady state approach whilst the testbench reality is that the running time is as small enough as only transients operation is allowed. This also imposes a bias from the theoretical estimation but, in this case, is projected that the total real heat will be below the expected. As a future work, the possibility of developing a numerical approach for the analysis of transient thermal behavior in thrust chambers can be considered. In any case, the calorimeter must be validated performing several compliance tests.

The electric feed system also is designed with aim of simplicity and flexibility. Even if the oxidizer composition is changed (as proposed in the preceding section), which is a hard conditioning for a rocket engine design, the engine can be adapted with only minor changes. This further allows performing tests with different solutions of hydrogen peroxide and ammonium nitrate, which will be useful for a full oxidizer characterization. By changing the concentration of hydrogen peroxide in water, however, moves the optimum oxidizer to fuel ratio considerably so that a reconfiguration of the gearbox will be mandatory to adjust the testbench. Even in that case, the hardware modification should be minimal, which suggest the wide application field of this rocket engine testbench in the hydrogen peroxide based propellants characterization.

The main feature of this pump system is the propellant flow rate variation, which will allow experiencing several soft start strategies. In addition, such feature opens the possibility of studying diverse issues, as the effect of thrust throttling on engine performance. Furthermore, both pumps running to the same speed may allow simplifying the transmission by mounting both in the same axis in a future design. Regarding to the start and stop operations, the flow regulation capability brings new opportunities in the development of ignition systems. As an example, the engine could be started with a pyrotechnic cartridge by burning propellants only at a small rate and when the combustion becomes steady, the propellant flow rate can be gradually increases to its nominal value. This fact perhaps enables using an igniter smaller than the needed in the case of a full flow start operation, minimizing the risks of throat clogging.

VIII.   REFERENCES

[1] Humble R. W. Henry, G.N. and Larson, W. J.: *Space Propulsion Analysis and Design*, 1st ed., McGraw-Hill, New York, 1995.

[2] Sutton, G. P. and Biblarz, O.: *Rocket Propulsion Elements*, 7th ed., Wiley, New York.

[3] Huzel, D. K. and Huang, D. H.: *Modern Engineering for Design of Liquid-Propellant Rocket Engines*, 1st ed., AIAA, Washington DC, 1992.

[4] NASA SP-8112, *Pressurization Systems for Liquid Rockets* , October 1975.

[5] Bucher Hydraulics Catalog, Gear Pumps, reference: 200-P-991218-E-02. September 2007.

[6] Honor Pumps Catalog, 1A Series gear pumps. July 2011.

[7] Chap Group Co., *Internal Gear Pumps Products Folder*, August 2011, (http://www.chap-china.cn/products/Internal_gear_pump1769.htm).

[8] Hyperion HK Ltd., Hyperion ZS 4045-10 datasheet, (www.hyperion-world.com).

[9] Castle Creations Inc., Phoenix ICE HV ESC data sheets, (www.castlecreations.com).

[10] Thunder Power Li-Po Battery Data Sheet, 2250mAh, 5-Cell/5S (18.5V 30C/60C), October 2011, (http://thunderpowerrc.com).

[11] Thunder Power Li-Po Battery 6G Family Data Sheet, 2700mAh, 5-Cell/5S (18.5V 25C/50C), October 2011, (http://thunderpowerrc.com).

[12] System Solaire, *SS67B-1 Construction procedures*, 2nd ed., 1997.

[13] DeLise J.C. and Naraghi M. H. N.: *Comparative Studies of Convective Heat Transfer Models for Rocket Engines*, AIAA 95-2499 31st AIAA/ASME/SAE/ASEE Joint Propulsion Conference and Exhibit, July 1995.

[14] Wolverine Tube Inc., *Wolverine Engineering Data Book II*, (http://www.wlv.com/products/), September 2011.

[15] Department of Mechanical Engineering, School of Engineering and Technology, Purdue University, *Shell & tube heat exchanger design*, (http://www.engr.iupui.edu/me/).

[16] Computational Fluid Dynamics Online, *Hydraulic diameter*, (http://www.cfd-online.com/), September 2011.

[17] Wikipedia - The Free Encyclopedia, *Heat Transfer Coefficient*, September 2011.

[18] Lide, D. R.: *CRC Handbook of Chemistry and Physics*, 76th Ed, Taylor and Francis, Boca Raton, FL, 2006.

[19] D.Q. Kern: *Process Heat Transfer*, McGraw-Hill, 1950.

[20] Ideal Spray Technology, Normal Full Cone Nozzles Catalog, September 2011, (http://www.idealspray.cn/product.asp?keyfid=pro3).

APPENDIX

A.1. RPA software performance calculus output file

Table A-1: Summary of output parameters.

Propellant specification

Component	Temperature	Mass fraction	Molar fraction
RP-1	298.1	0.0786391	0.1744734
70% by mass H_2O_2	298.1	0.6108623	0.7052410
Ammonium Nitrate (IV)	298.1	0.3104986	0.1202856
Propellant formula		(H)2.232 (O)1.456 (N)0.241 (C)0.174	
O/F		11.7163171 (optimum performance)	
O/F		11.9225667 (stoichiometric)	

Table A-2: Summary of output parameters.

Thermodynamic properties

Parameter	Injector	Nozzle Inlet	Nozzle Throat	Nozzle Exit	Unit
Pressure	1.5000	1.5000	0.8536	0.1013	*MPa*
Temperature	2232.3118	2232.3118	2062.5026	1448.0505	*K*
Enthalpy	6848.3535	6848.3535	7307.3398	8714.8747	*kJ/kg*
Entropy	11.7729	11.7729	11.7729	11.7729	*kJ/(kg·K)*
Specific heat (c_p)	2.9530	2.9530	2.6535	2.1390	*kJ/(kg·K)*
Specific heat (c_v)	2.5360	2.5360	2.2563	1.7605	*kJ/(kg·K)*
Gas constant	0.3796	0.3796	0.3788	0.3784	*kJ/(kg·K)*
Molecular weight	21.9030	21.9030	21.9510	21.9700	*kg/kmol*
Isentropic exponent	1.1625	1.1625	1.1751	1.2150	*-*
Density	1.7701	1.7701	1.0927	0.1849	*kg/m³*
Sonic velocity	992.5378	992.5378	958.1485	815.9727	*m/s*
Velocity	0.0000	0.0000	958.1485	1932.1083	*m/s*
Mach number	0.0000	0.0000	1.0000	2.3679	*-*
Area ratio	0.0000	0.0000	1.0000	2.9307	*-*
Mass flux	0.0000	0.0000	1046.9587	357.2402	*kg/(m²·s)*

Table A-4: Summary of output parameters.

Theoretical (ideal) performance

Parameter	Sea level	Optimum expansion	Vacuum	Unit
Characteristic Velocity	0.0000	1432.7200	0.0000	*m/s*
Specific impulse	1932.1100	1932.1100	2215.7400	*m/s*
Specific impulse	197.0200	197.0200	225.9400	*s*
Thrust coefficient	1.3486	1.3486	1.5465	*-*

Estimated delivered performance

Parameter	Sea level	Optimum expansion	Vacuum	Unit
Characteristic Velocity	0.0000	1377.6700	0.0000	*m/s*
Specific impulse	1857.8600	1857.8600	2130.6000	*m/s*

Specific impulse	189.4500	189.4500	217.2600	*s*
Thrust coefficient	1.3486	1.3486	1.5465	-

Table A-3: Summary of output parameters.

Mass fractions of the combustion products

Species	Injector	Nozzle Inlet	Nozzle Throat	Nozzle Exit
CO	0.0067768	0.0067768	0.0045323	0.0035917
CO_2	0.2369814	0.2369814	0.2405081	0.2419859
H	0.0000065	0.0000065	0.0000027	0.0000013
H_2	0.0005993	0.0005993	0.0004439	0.0003880
H_2O	0.6417919	0.6417919	0.6438569	0.6446453
H_2O_2	0.0000008	0.0000008	0.0000002	-
HO_2	0.0000016	0.0000016	0.0000004	-
N_2	0.1084015	0.1084015	0.1085641	0.1086296
NO	0.0005725	0.0005725	0.0002245	0.0000843
NO_2	0.0000004	0.0000004	-	-
O	0.0000268	0.0000268	0.0000067	0.0000017
O_2	0.0027028	0.0027028	0.0009337	0.0002673
OH	0.0021373	0.0021373	0.0009264	0.0004047